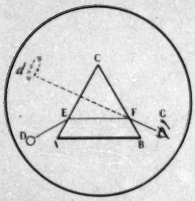

optics and spectroscopy

volume vii
number 6
december 1959

OPTICAL SOCIETY OF AMERICA

RUSSIAN EDITORIAL STAFF

Editor: S. E. FRISH

Assistant Editor: P. P. FEOFILOV
Corresponding Secretary: L. S. SAZONOV

Associate Editors:

M. M. GUREVICH M. A. EL'IASHEVICH A. A. LEBEDEV V. P. LINNIK
S. L. MANDEL'SHTAM I. V. OBREIMOV V. K. PROKOF'EV
N. N. SOBOLEV A. N. TERENIN A. I. TUDOROVSKII

Translated on the Initiative of
THE OPTICAL SOCIETY OF AMERICA, INC.
With a Grant-in-Aid from
THE NATIONAL SCIENCE FOUNDATION

TRANSLATION EDITORIAL STAFF

Scientific Editors

FRED W. BEHNKE, *Perkin-Elmer Corp.*

CYRUS FELDMAN, *Oak Ridge National Laboratory*

GEORGE HERRMAN, *Columbia University*

Administrative Editor: PATRICIA R. WAKELING, *OSA*

Published monthly by the Optical Society of America, Inc. Executive office: 1155 Sixteenth Street, N.W., Washington, D.C. Subscriptions for one year to members of the Society: Associates $13.00; Regular members and Fellows $17.00. Subscriptions for non-members of the Society: One year U. S. and Possessions, $25.00; Foreign $28.00. Back numbers: $3.00 per copy. Subscriptions, changes of address and undeliverable copies should be referred to the Executive offices in Washington, D.C. The office of publication is 2500 South State Street, Ann Arbor, Michigan. Second class postage paid at Ann Arbor, Michigan.

Printed in the U.S.A. by Edwards Brothers, Inc., Ann Arbor, Michigan.

STUDY OF THE CONTOUR OF THE CADMIUM RED LINE USING AN ATOMIC BEAM

F. A. Korolev, B. A. Kozlov, and A. I. Odintsov

Received 2 March 1959

The contour of the red cadmium line, λ6438 A, was studied using an atomic beam and a Fabry-Perot interferometer with a 15 cm spacer. The contour was found to be markedly asymmetric. The half-width of the line was measured to be $(11.8 \pm 0.5) \times 10^{-3}$ cm^{-1} (this includes the instrumental half-width). A theoretical interpretation of the contour obtained was attempted.

The red cadmium line, λ6438 A, is the primary standard of wavelength. This line is widely used in metrology for interferometric measurements of length. Consequently, the determination of the line's contour, which is defined by the hyperfine structure and the natural width of the line, is very important.

A number of papers have been written concerning the shape of the red cadmium line in various light sources.[1-3] Reliable data on the half-width and form of the natural contour of the line could not be obtained, due to the presence of the Doppler broadening of the line in various sources (including the hollow cathode source). In 1935, Minkowski and Bruck used an atomic beam light source (which they constructed) for the study of the red cadmium line.[4] They found the half-width of the line to be 16.4×10^{-3} cm^{-1}, which greatly exceeded the sum of the instrumental and Doppler half-widths. Thus, it was established that the red cadmium line is a complex line and has an appreciable half-width.

Minkowski and Bruck assumed that the complex structure of the line can be explained as a shift of the components of different isotopes*; they also estimated the magnitude of the shifts. The authors were unable to completely remove the influence of Doppler broadening on the form of the line because the low intensity of their source forced them to use insufficiently collimated beams. In addition to this, their Fabry-Perot etalon had insufficient resolving power.

*Natural cadmium has the following isotopic composition (in %): Cd^{106} - 1.2, Cd^{108} - 0.9, Cd^{110} - 12.4, Cd^{111} - 12.8, Cd^{112} - 24, Cd^{113} - 12.3, Cd^{114} - 28.8, and Cd^{116} - 7.6.

The investigation of the red cadmium line using an atomic beam was repeated by Meissner and Luft and, comparatively recently, by Errou in Meggers' laboratory.*

*The authors express their appreciation to Professor Meggers for communications concerning this work. (This may possibly refer to work done elsewhere by H. Arroe (translator's note).)

The results of these studies were never published.

In 1953, Batarchukova, Kartashev and Ramonova,[5] using monoisotopic light sources, measured the shifts between the red lines of the isotopes Cd^{112}, Cd^{114}, and Cd^{116}. The shifts were 3.1×10^{-3} cm^{-1}.

The present work is an attempt to improve on the resolution achieved by Minkowski and Bruck and to obtain as accurately as possible a measure of the contour of the red line of natural cadmium.

EXPERIMENTAL PART

The atomic beam equipment used in this investigation was described in a previous paper by one of the authors.[6] The collimation used was 1 : 14.5 and 1 : 22.

In order to have a high resolving power, a Fabry-Perot interferometer with a 15 cm spacer between the plates was employed. The coefficient of reflection of the interferometer's dielectric mirrors was 90%. The instrumental half-width of the etalon was experimentally determined to be 1.5×10^{-3} cm^{-1}. (For comparison, we cite Minkowski and Bruck, who used a Fabry-Perot etalon 11 cm thick. Their instrumental half-width was 3×10^{-3} cm^{-1}.) The contrast of the etalon was found to be 290 ± 20. Contrast was defined as the ratio of the maximum ring intensity to that of the background between the orders.*

*The half-width of the etalon and the contrast were determined using interference spectrograms of the red cadmium line, which were taken with etalons having 0.3, 0.5, and 1.0 mm thicknesses. In this case, the width of the line itself may be considered negligible compared with the instrumental half-width of the etalon. The instrumental half-width of the 15 cm etalon was determined by assuming that it varies inversely as the thickness of the etalon.

An ISP-51 spectrograph with a UF-84 camera (f = 800 mm) served as a monochromator. Several interference spectrograms were also taken with the UF-85 camera (f = 1300 mm). The etalon was placed in the parallel beam between the prisms of the spectrograph and the camera. "Agfa" "Rot rapid," photographic plates were used. Exposure time varied from 2 to 8 minutes. Calibration marks were put on each plate with a step-filter.

The interference spectrograms were measured with a MF-2 microphotometer. Several orders were measured on both sides of the center of the interference fringes. The orders closer to the center were used to construct the profile of the line. The contour given in Fig. 1 is derived from the reduction of four interference spectrograms. The contours obtained from dif-

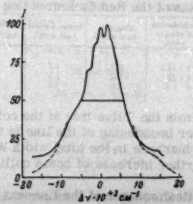

Fig. 1. The contour of cadmium red line λ6438 A in an atomic beam (the thickness of Fabry-Perot etalon is 15 cm). The wings of the line, which were obtained by the 10 cm etalon, are represented by dotted lines.

ferent plates coincided well with each other. An important difference was found only in the upper double peak, where the form of the peaks and the depth of the valley between them varied greatly from one spectrogram to another. Figure 1 gives the form of the peaks as the mean of the four spectrograms investigated. On some of the plates, no division of the peak could be seen. It is possible that the indicated deviations can be explained as being caused by an accidental variation of resolution and also by the grain of the photographic plates.

Figure 1 shows that the red cadmium line has a marked asymmetry. The form of the line also shows definite indications of unresolved structure. The half-width of the line is $(11.8 \pm 0.5) \times 10^{-3}$ cm^{-1}.

The wings of the profile are considerably distorted by the superposition of the orders of the Fabry-Perot etalon. To avoid this superposition, some interferometric spectrograms were taken with an etalon 10 cm thick. In Fig. 1, the wings of the line obtained from these spectrograms are given by dotted lines. Due to the decrease in resolving power, these half-widths (14.2×10^{-3} cm^{-1}) are considerably greater than those produced by the 15 cm etalon.

DISCUSSION OF THE RESULTS

The value obtained for the half-width of the contour of the red cadmium line (11.8×10^{-3} cm^{-1}) differs substantially from the value 16.4×10^{-3} cm^{-1} obtained by Minkowski and Bruck. This smaller half-width can be explained by the greater resolution achieved in our work.

For the theoretical evaluation of the resolution, the following formula given by Buerger and van Cittert[7] can be used:

$$W^2 = (a + \gamma)^2 + 2.15\ \omega^2. \qquad (1)$$

where a is the instrumental half-width of etalon, γ is the natural half-width of the line, ω is the Doppler half-width,* and W is the total half-width of the contour.

*The dimensions of the slit which defined the atomic beam were such that the line emitted by the beam had a Doppler contour.[8]

The table gives values of W calculated by formula (1) for the two degrees of collimation of the atomic beam used in the present investigation. For comparison, similar values from Minkowski's and Bruck's work are also given in this table. The natural half-width of the red cadmium line, according to published data,[4] was taken to be 2.6×10^{-3} cm^{-1}.

The Half-Widths of the Red Cadmium line (10^{-3} cm^{-1})

	Collimation of atomic beam	Doppler half width	Instrumental half width	Natural half width	Total half width
Our data	1 : 14.5	0.9	1.5	2.6	4.3
	1 : 22	0.6	1.5	2.6	4.2
Data of reference 4	1 : 5.5	2.0	3.0	2.6	6.3

It is seen from the Table that at the collimations used, the Doppler broadening of the line in the beam leads to only a small increase in the total width W of the line. Therefore, a further increase of beam collimation is not advisable.

The theoretical contour of the line was constructed (Fig. 2) for comparison with the experimental one. The profiles for the separate isotopes were found by combining the Doppler and natural widths of the lines, and the instrumental function of the etalon according to Buerger and van Cittert.[7] For the construction of the wings, numerical integration was used to calculate a few points. The following instrumental function of the etalon[9] was used:

$$I(p) = \frac{I_0}{1 + (C-1)\sin^2 \pi p}, \qquad (2)$$

where p is the order of interference and C is the experimentally determined contrast of the etalon. Equation (2) accounts for the periodicity of the instrumental function. In Fig. 2, the superposition of orders was accounted for in the theoretical contour. The theoretical contour can be directly compared with the experimental one. The displacement between the components due to neighboring even isotopes, according to data of Batarchukova, Kartashev, and Romanova,[5] was taken as 3.1×10^{-3} cm^{-1}. The even isotope components and the centers of gravity of the odd isotope components Cd^{111} and Cd^{113} are equidistant. The intensities of different components were taken to be proportional to the percentages of the corresponding isotopes in natural cadmium. The value of 12.6×10^{-3} cm^{-1}, which is equal to the splitting of the lower 6^3P_1 level,[10] was used for the hyperfine splitting of the components of the isotopes Cd^{111} and Cd^{113}. The splitting of the upper level 7^3D_2 is not known, but one can expect that it is much smaller than the splitting of 6^3P_1.

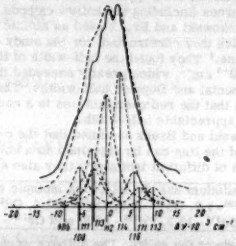

Fig. 2. The comparison of the experimental contour of the red cadmium line (solid curve) with the theoretical one (dotted curve).

It is seen from Fig. 2 that the theoretical contour constructed in this way differs somewhat from the experimental one. Much better agreement can be reached by shifting the odd isotope components in the theoretical curve. If 16×10^{-3} cm^{-1} is accepted as the value of the hyperfine splitting for the odd isotope components in the theoretical contour, the theoretical and the experimental curves are in good agreement. The two contours coincide even better if the centers of gravity of the odd isotope components are moved ~ 0.7×10^{-3} cm^{-1} toward lower frequencies.

Comparison of the experimental and the theoretical contours shows that the spacing between the even isotope components of the red cadmium line is close to 3×10^{-3} cm^{-1}, and that the heavy isotope components are displaced in the direction of higher frequencies. This conclusion is in complete agreement with the data compiled by Batarchukova, Kartashev, and Romanova.[5]

The great natural width of the components of the red cadmium line restricts the theoretical limit of resolution to the value 2.6×10^{-3} cm^{-1} (which is unattainable in practice). This value is just a little smaller than the distance between neighboring components. Therefore, it follows that it is practically impossible to obtain really satisfactory resolution of the structure of the red line of natural cadmium.

REFERENCES

1. A. Perard. Rev. opt. 7, 1 (1928).
2. H. Nagaoka and V. Sigiura. Sci. Papers Inst. Phys. Chem. Research, (Tokyo) No. 10, 263 (1929).
3. M. F. Romanova and A. A. Ferkhmin. Doklady Akad. Nauk SSSR, 2, 55 (1933).
4. R. Minkowski and H. Bruck. Z. Physik 95, 284 (1935).
5. N. R. Batarchukova, A. I. Kartashev, and M. F. Romanova. Doklady Akad. Nauk SSSR 90, 153 (1953).
6. A. I. Odintsov. Opt. i Spektr. 6, 398 (1959).
7. H. C. Buerger and P. H. van Cittert. Z. Physik 44, 58 (1927).
8. F. A. Korolev, B. A. Kozlov, and A. I. Odintsov. Opt. i Spektr. 6, 576 (1959).
9. S. Tolansky. "Spektroskopiya vysokoi razreshaiushchei sily." (High Resolution Spectroscopy), Moscow, 1955.
10. N. P. Heydenberg. Phys. Rev. 43, 640 (1933).

THE TRANSPARENCY OF A DISCHARGE IN XENON AT VERY HIGH PRESSURES

R. E. Rovinskii and G. P. Razumtseva

Received 13 May 1959

By means of procedures used previously for the measurement of the transparency of the discharge in mercury vapor, the transparency of a xenon discharge in the visible was measured at very high pressures as a function of the discharge power per unit length. On the basis of the data obtained and the measured geometrical depth of the discharge, values were calculated for the absorption coefficient $\overline{\kappa}$.

It has been concluded from experimental data[1-4] that a discharge column in xenon at high pressure can be considered as a gray emitter, and that it can be characterized by a mean absorption coefficient $\overline{\kappa}$. The experimental determination of this coefficient and its dependence on discharge power is of considerable interest both for the verification of several theoretical assumptions, and for the solution of practical problems in the construction of xenon lamps operating at very high pressures.

The purpose of the present study was to find values of the mean absorption coefficient in the visible part of the spectrum for a high pressure xenon discharge at various discharge powers. The absorption coefficient $\overline{\kappa}$ was determined indirectly by measurement of the transparency of the discharge:

$$\alpha = e^{-\overline{\kappa}l}, \tag{1}$$

where l is the geometric depth of the discharge. The optical depth of the discharge $\tau = \overline{\kappa}l$ can then be determined. If the value of l is known, the absorption coefficient $\overline{\kappa}$ can also be determined.

For determining the transparency of the xenon discharge, a procedure was used which was previously applied by Fabrikant and Pulver[5] for determining the transparency of a mercury discharge.

A sketch of the experimental setup is shown in Fig. 1.

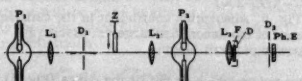

Fig. 1. Experimental setup for measurement of the transparency of discharge.

A slightly magnified image of the discharge gap of a spherical xenon lamp P_1 was projected by lens L_1 onto screen D_1, which had an opening in its center. The opening defined a definite section of the discharge. With the aid of lens L_2, this section was projected onto the plane of the discharge of a second spherical xenon lamp P_2. The parameters of the optical system were selected so as to make the latter image 0.3 mm in diameter. Lamp P_2 could be continuously shifted along both the vertical and horizontal axes perpendicular to the optical axis of the apparatus.

This arrangement permitted the beam from the lamp P_1 to be transmitted through various portions of the discharge of lamp P_2. An image of the discharge plane of lamp P_2, magnified 2.5 times, was then projected onto screen D_2. This screen contained an opening, behind which, in a special tube, were a frosted glass and a selenium photoelement E, together with a correcting filter. Between lamps P_1 and P_2 there was a shutter Z which could be opened or closed at will.

The measuring procedure consisted of the following steps: After adjusting the optical system, we measured the combined intensity B'_{12} of the beam of lamp P_1 and the section of the discharge of lamp P_2 through which the beam of lamp P_1 passed. Then the shutter Z was closed, and the intensity of this section of the discharge of lamp P_2 was measured. Next, shutter Z was opened, lamp P_2 switched off, and the intensity B_1 of the beam from P_1 was measured after it had passed through the glass envelope of lamp P_2. These three measurements permitted a determination of the transparency of the discharge. Denoting the transparency of lamp P_2 by α, the transparencies of the front and back walls of the envelope of lamp P_2 by α_1 and α_2, respectively, and the intensities of the first and second lamps without absorption by B_1 and B_2, the results of these three consecutive measurements can be expressed thus:

$$B'_{12} = \alpha \cdot \alpha_1 \cdot \alpha_2 \cdot B_1 + \alpha_2 B_2, \tag{2}$$

$$B'_2 = \alpha_2 B_2, \tag{3}$$

$$B'_1 = \alpha_1 \cdot \alpha_2 \cdot B_1 \tag{4}$$

Then

$$\frac{B'_{12} - B'_2}{B'_1} = \alpha. \tag{5}$$

This method makes it unnecessary to take account of the absorption and scattering of light by the walls of lamp P_2.

The lamps P_1 and P_2 used for these measurements were of the same type, and were operated under the same conditions. Furthermore, the discharge column of lamp P_2 was traversed by the light beam from a corresponding

section of the discharge column of lamp P_3; for the measurement in the cathode spot of the lamp P_3, the light from the cathode spot of lamp P_1 was used.

The main measurements were made with the spherical direct current xenon lamps of the type DKsSh-3000 in the power range 600 w to 3 kw. For comparison, similar measurements were made with OSRAM lamps, types XBO-1001 and XBO-2001, in the power range 570 w to 1.5 kw. The operating pressure in all these lamps was about 20–23 atm.

The results of the measurements in the discharge column are shown in Fig. 2, where the absorption $a = 1 - \alpha$ is given as a function of the discharge power per unit length W_p/d (the discharge power is equal to the lamp power minus the electrode losses).

It can be seen from the figure that the degree of absorption in the column increases fairly rapidly at relatively low powers; the rate of increase is smaller above 2.5 kw/cm. This behavior is connected with the widening of the discharge channel at higher power. The degree of absorption in the column can be considered approximately equal to the optical depth $\tau = \kappa l$ of the discharge. Both factors of this expression should increase with increasing power. However, at relatively low powers, the broadening of the discharge column can be disregarded, and the increase of τ is not hindered. At relatively high power, however, the increase of l reduces the rate of increase of κ, and this retardation has a greater effect than the increased broadening of the discharge channel. Indeed, the absorption coefficient, according to Kramer's formula, depends exponentially on temperature, which is in turn a function of the specific power of the discharge (that is, the power per unit discharge volume). Assuming the discharge column to be a cylinder, we obtain for the specific power a value proportional to W_p/l^2. Consequently, the increase of l with power will retard the rate of increase of the specific power, the retardation being proportional to l^2; the resulting reduction of the rate of increase of the discharge temperature strongly affects the rate of increase of κ, because these quantities are connected exponentially. These general considerations lead to the expectation that the rate of increase of absorption will decrease with increasing power, because of the broadening of the discharge channel.

Figure 3 shows the dependence of the degree of absorption in the cathode spot on the discharge power per unit length. The concentration of power is much higher in the cathode spot than in the discharge column, and for the same values of the discharge power, a higher degree of absorption is observed in the cathode spot than in the column. The broadening of the cathode spot with power is slight, and the dependence of absorption in the cathode spot on power remains approximately linear.

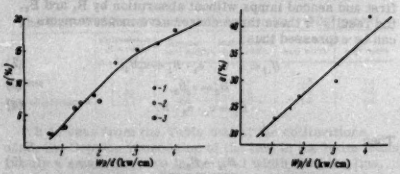

Fig. 2

Fig. 3

Fig. 2. Absorption in the xenon discharge column vs. discharge power per unit length. 1—DKsSh-3000 lamp; 2—XBO-1001; 3—XBO-2001.

Fig. 3. Absorption in the cathode spot of the xenon discharge vs. discharge power per unit length.

For the estimation of the dependence of absorption in the discharge on the wavelength, absorption was measured for three wavelengths: 483, 530, and 608 mμ. The measurements were made in the middle of the discharge column at 4.1 kw/cm using interference light filters having an absorption band 12 mμ wide. The absorption was found to be the same (18%) for all three wavelengths, which agrees well with the previously found value for the mean absorption in the visible range at the same discharge power.

The absorption coefficient $\bar{\kappa}$ can be determined from the above absorption data if the geometric depth of the discharge is known. In our case, the latter was obtained from the intensity distribution curves taken at the discharge locations and power values at which the absorption measurements were made. The geometric depth was assumed to be equal to the distance between the two points of the discharge cross section at which the intensity was 0.25 of the maximum value for that cross section. This definition was suggested by the fact that this drop of intensity corresponds to the beginning of the steep drop in the temperature of the discharge channel. The value chosen for the geometrical depth includes the part of the channel in which the temperature is fairly uniform, and excludes the narrow border areas characterized by sharply dropping temperatures.

Figure 4 shows the dependence of the absorption coefficient $\bar{\kappa}$ in the discharge column on the discharge power per unit length; Fig. 5 shows the same relation in the cathode spot. The general form of this relationship is the same as for absorption (See Figs. 2,3).

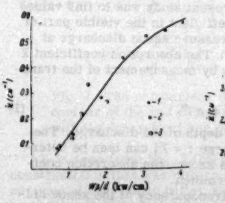

Fig. 4

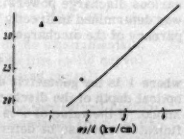

Fig. 5

Fig. 4. Absorption coefficient in the xenon discharge column vs. discharge power per unit length. 1—DKsSh-3000 lamp; 2—XBO-1001; 3—XBO-2001.

Fig. 5. Absorption coefficient in the cathode spot of the xenon discharge vs. discharge power per unit length.

Two points which do not fit the curve (Fig. 5) belong to the values of $\bar{\kappa}$ in the cathode spot of the OSRAM XBO-1001 lamp. Because of certain characteristics of the construction of the cathode, the contraction of the discharge at the cathode in lamps of this type is greater than at the cathodes of DKsSh-3000 lamps, and consequently the temperature in the cathode spot may be considerable, even at a relatively low discharge power.

The authors express their deep gratitude to V. A. Fabrikant for suggesting the problem and procedures for the present paper, for helping with valuable advice on the experimental arrangements, and for discussion of the results obtained.

REFERENCES

1. P. Schulz. Ann. Physik 1, 95 (1947).
2. W. A. Baum and Z. Dunkelman. J. Opt. Soc. Am. 40, 782 (1950).
3. H. Schirmer. Z. Physik 136, 87 (1953).
4. H. Schirmer. Z. Physik 6, 1 (1954).
5. V. A. Fabrikant and V. O. Pulver. Doklady Akad. Nauk SSSR 3, 435 (1934).

EIGENVALUES OF π-ELECTRONS IN A POTENTIAL BOX WITH AN EVEN NUMBER OF N-BARRIERS

S. M. Vazykova

Received 8 April 1959

A general formula was derived for computing eigenvalues for the π-electrons in a periodic field with an even number of barriers. A model of a metallic molecule in an infinitely deep well was utilized. The formula obtained was used to evaluate the electron energy levels for $C_{10}H_{12}$ which is a member of the polyene series.

For some time the metallic model of the molecule was used to compute several basic molecular properties, that is, frequencies of electronic transitions, oscillator strengths,[1-4] polarizations, and the intensities of the Raman spectra.[5,6]

In the case of a complicated model in an infinitely deep well, the potential of the molecular structure can be considered periodic accounting for the incomplete straightness of the single and double bonds in the molecule. Here an attempt was made to use the model of Vaselova and Rekasheva, who calculated the electron spectra of butadiene and hexatriene,[3,4] to derive a general expression for the determination of the eigenvalues of the π-electrons, with an arbitrary even number of n barriers (barriers correspond to the single bonds in molecules with $n > 2$).

The length of a single bond will be denoted by l_1, and that of a double bond by $l_2 a = l_1 + r/2$, where r is a homopolar radius of the extreme hydrogen. The molecular axes of symmetry passes through the center of l_2.

As usual we shall seek a solution of the Schrödinger equation

$$\frac{d^2\psi}{dx^2} + 2(E - U)\psi = 0$$

where

$$\left.\begin{aligned} \psi_j &= A_j e^{i\alpha x} + B_j e^{-i\alpha x} \text{ in the region } U = 0, \\ \psi_k &= A_k e^{i\beta x} + B_k e^{-i\beta x} \text{ in the region } U = U_0, \end{aligned}\right\} \quad (1)$$

U_0 is the barrier height, $\alpha = \sqrt{2E}$, and $\beta = \sqrt{2(E - U)}$. (All calculations will be made in atomic units.) In order to simplify the calculating further we shall introduce the following definitions

$$\left.\begin{aligned} e^{i\alpha a} &= x_1, \quad e^{2i\alpha l_1} = x_2, \quad e^{i\alpha l_2} = x_3, \\ e^{i\beta a} &= y_1, \quad e^{i\beta l_1} = y_2, \quad e^{i\beta l_2} = y_3. \end{aligned}\right\} \quad (2)$$

Matching of the eigenfunctions $\psi_1, \ldots \psi_{2n+1}$ and their derivatives at the boundaries gives $(4n + 2)$ equations. Furthermore, the application of the boundary conditions and molecular symmetry allows separation of $(n + 3)$ dependent equations (these conditions automatically separate the eigenfunctions into even and odd functions).

$$\psi(0) = \psi(L) = 0; \quad \psi_1(x) = \pm\psi_{2n+1}(L - x),$$
$$\psi_2(a + x) = \pm\psi_{2n}(L - a - x),$$

$$\psi_n\left[a + \left(\frac{n}{2} - 1\right)(l_1 + l_2) - x\right] = \pm\psi_{n+2}\left[a + \left(\frac{n}{2} + 1\right)l_1 + \frac{n}{2}l_2 - x\right],$$

$$\psi_{n+1}\left[a + \frac{n}{2}l_1 + \left(\frac{n}{2} - 1\right)l_2\right] = \pm\psi_{n+1}\left[a + \frac{n}{2}l_1 + \frac{n}{2}l_2\right]. \quad (3)$$

From the number of $(3n - 1)$ compatible equations the eigenvalues are evaluated. In order to obtain these equations in a suitable form for calculation we shall separate them from a general system by matching the eigenfunctions at all points in a potential box including the point $n(\psi_n, \psi_{n+1})$ and we shall exclude point $n + 1$; moreover, beginning with point $n + 2$, (ψ_{n+2}, ψ_{n+3}) we match eigenfunctions only.

EVEN EIGENFUNCTIONS

A determinant of the order $(3n - 1)$ can be expressed by means of the Laplace's Theorem as follows

$$\left.\begin{aligned} D^{(e)}_{3n-1} &= D^{(1)}_{2n} D^{(2)}_{n-1}, \\ D^{(1)}_{2n} &= D_{n+1}\Delta_{n-2} - D'_{n+2}\Delta'_{n-2}. \end{aligned}\right\} \quad (4)$$

Determinants Δ_{n-2}, Δ'_{n-2} can be expressed with the following recurrence formulas

$$\left.\begin{aligned} \Delta_{n-2} &= \left[\mu_1\Delta_{n-1} + \mu_2\Delta'_{n-4}\right]\xi_{\frac{n-2}{2}}, \\ \Delta_{n-2} &= \left[\mu_1\Delta_{n-2-2} + \mu_2\Delta'_{n-2-3}\right]\xi_{\frac{n-2}{2}}, \\ \Delta'_{n-2} &= \left[\nu_1\Delta_{n-4} + \nu_2\Delta'_{n-4}\right]\eta_{\frac{n-2}{2}}, \\ \Delta'_{n-2} &= \left[\nu_1\Delta_{n-2-2} + \nu_2\Delta'_{n-2-3}\right]\eta_{\frac{n-2}{2}}, \end{aligned}\right\} \quad (5)$$

where

$$\left.\begin{aligned} \mu_1 &= -(a + \beta), \ \mu_2 = (a - \beta)\ (-1)^{\frac{n-k-2}{2}}, \\ \nu_1 &= -(a - \beta), \ \nu_2 = -(a + \beta), \end{aligned}\right\} \quad (6)$$

$$\left.\begin{aligned} \xi_{\frac{n-k}{2}} &= \left[x_3^{-1}\left(1 - \delta_{\frac{n-k}{2}, 2m+1}\right) + y_3^{-1}\left(1 - \delta_{\frac{n-k}{2}, 2m}\right)\right], \\ \eta_{\frac{n-k}{2}} &= \left[x_3\left(1 - \delta_{\frac{n-k}{2}, 2m+1}\right) + y_3\left(1 - \delta_{\frac{n-k}{2}, 2m}\right)\right]. \end{aligned}\right\} \quad (7)$$

Here

$$\delta_{\frac{n-k}{2},\,2m+1};\quad \delta_{\frac{n-k}{2},\,2m};$$

are the Kronecker symbols, m– are arbitrary numbers 1, 2, 3 ...

Then with the help of Eqs. (5)-(7) Δ_{n-2}, Δ'_{n-2}, can be expressed in terms of Δ_n and Δ'_n

$$\left.\begin{aligned}\Delta_n &= y_2^{-1}[\alpha(x_3-1)-\beta(x_3+1)],\\ \Delta'_n &= y_2[\alpha(x_3-1)+\beta(x_3+1)].\end{aligned}\right\} \tag{8}$$

Determinants D_{n+2}, D'_{n+2} can also be expressed with recurrence formulas as follows:

$$\left.\begin{aligned}D_{n+2} &= \Theta_{\frac{n+2}{2}}\mu_1 D_n + \Omega_{\frac{n+2}{2}}\mu_2 D'_n,\\ D_{n-k+2} &= \Theta_{\frac{n-k+2}{2}}\mu_1 D_{n-k} + \Omega_{\frac{n-k+2}{2}}\mu_2 D'_{n-k},\\ D_{n+2} &= \Theta_{\frac{n+2}{2}}\nu_1 D_n + \Omega_{\frac{n+2}{2}}\nu_2 D'_n,\\ D'_{n-k+2} &= \Theta_{\frac{n-k+2}{2}}\nu_1 D_{n-k} + \Omega_{\frac{n-k+2}{2}}\nu_2 D'_{n-k},\end{aligned}\right\} \tag{9}$$

where

$$\left.\begin{aligned}\Theta_{\frac{n-k+2}{2}} &= \left[x_3^{-1}\left(1-\delta_{\frac{n-k+2}{2},\,2m}\right)\right.\\ &\quad\left.+y_2^{-1}\left(1-\delta_{\frac{n-k+2}{2},\,2m+1}\right)\right],\\ \Omega_{\frac{n-k+2}{2}} &= \left[x_3\left(1-\delta_{\frac{n-k+2}{2},\,2m}\right)\right.\\ &\quad\left.+y_2\left(1-\delta_{\frac{n-k+2}{2},\,2m+1}\right)\right].\end{aligned}\right\} \tag{10}$$

Also, with the help of Eqs. (9) and (10) D_{n+2}, D'_{n+2} can be expressed in terms of D_2 and D'_2

$$\left.\begin{aligned}D_2 &= -\beta(x_1-x_1^{-1})+\alpha(x_1+x_1^{-1}),\\ D'_2 &= \beta(x_1-x_1^{-1})+\alpha(x_1+x_1^{-1}),\end{aligned}\right\}$$

Finally,

$$D^{(2)}_{n-1} = (1-y_2^2)\left(y_2^{-1}-y_2\right)^{\frac{n}{2}-1}. \tag{11}$$

A transcendental equation for determination of the electron levels, corresponding to the even eigenfunctions is obtained by substituting Eqs. (6)-(11) into (4).

The eigenvalues are analogously obtained for the odd eigenfunctions. In this case the determinant of the order (3n – 1) will differ from (4) in the way that it will have additional terms B_n and A_{n+1} in the expression for $D^{(1)}_{3n}$. Also $D^{(1)}_{3n}$ will have a different sign for the carbon in the lower left position. Similarly, another transcendental equation is obtained and instead of (8) we have, with the same definitions,

$$\left.\begin{aligned}\Delta_n^a &= y_2^{-1}[-\alpha(x_3+1)+\beta(x_3-1)],\\ \Delta'^a_n &= y_2[-\alpha(x_3+1)-\beta(x_3-1)].\end{aligned}\right\} \tag{12}$$

Derived formulas can be applied to the case of the $C_{10}H_{12}$ molecule—a member of the polyene series (n = 4). After some trigonemetric transformations a transcendental equation is obtained giving the eigenvalues for the π-electrons which correspond to the even eigenfunctions.

$$\left(1+\frac{\beta}{\alpha}\tan 2\beta l_1\cdot\cot\frac{\alpha l_2}{2}\right)\left[2\frac{\beta^2}{\alpha^2}\tan\alpha a+\left(1+\frac{\beta^2}{\alpha^2}\right)\tan\alpha l_2\right]$$
$$+\frac{\beta}{\alpha}\left(\tan 2\beta l_1-\frac{\beta}{\alpha}\cot\frac{\alpha l_2}{2}\right)\left[2-\left(1+\frac{\beta^2}{\alpha^2}\right)\tan\alpha a\cdot\tan\alpha l_2\right]$$
$$=\operatorname{tg}\alpha l_2\left(\frac{\beta_2}{\alpha^2}-1\right)\sec 2\beta l_1\left[\frac{\beta^2}{\alpha^2}\tan\alpha a\cdot\cot\frac{\alpha l_2}{2}-1\right]. \tag{13}$$

The even eigenfunctions are of the form

$$\left.\begin{aligned}\psi_1 &= A^*\sin\alpha s,\quad 0\leqslant s\leqslant a\\ \psi_2 &= A^*\sin\alpha s\cdot\cos\beta s+\frac{\alpha}{\beta}\cos\alpha s\cdot\sin\beta s,\\ \psi_3 &= A^*(\lambda_1\cos\alpha s-\lambda_2\sin\alpha s),\\ \psi_4 &= A^*\left(\lambda'_2\cos\beta s-\frac{\alpha}{\beta}\lambda'_2\sin\beta s\right),\\ \psi_5 &= A^*\frac{\lambda'_1\cos\beta l_2-\lambda'_2\sin\beta l_2}{\cos\frac{\alpha l_2}{2}}\cos\alpha\left(\frac{l_2}{2}-s\right).\end{aligned}\right\} \tag{14}$$

Substituting cos α(L – s), sin α(L – s), cos β(L – s), sin β(L – s) for cos αs, sin αs, cos βs, sin βs, we note that ψ_6, ψ_7, ψ_8, ψ_9, has a form analogous to ψ_4, ψ_3, ψ_2, ψ_1.

For all even ψs varies in the interval $0 \leqslant s \leqslant l_1$ and for all odd ψ (except for ψ_1 and ψ_4) in the interval $0 \leqslant s \leqslant l_2$, A* = 2iA₁. Similarly, the equations determining the eigenvalues corresponding to the odd eigenfunctions are given below

$$\left(1+\frac{\alpha}{\beta}\cot\frac{\alpha l_2}{2}\cdot\tan 2\beta l_1\right)\cdot\left[\left(1+\frac{\beta^2}{\alpha^2}\right)\tan\alpha l_2\cdot\tan\alpha a-2\right]$$
$$+\frac{\alpha}{\beta}\left(\tan 2\beta l_1-\frac{\alpha}{\beta}\cot\frac{\alpha l_2}{2}\right)\left[\left(1+\frac{\beta^2}{\alpha^2}\right)\tan\alpha l_2+2\frac{\beta^2}{\alpha^2}\tan\alpha a\right]$$
$$=\tan\alpha l_2\left(\frac{\beta^2}{\alpha^2}-1\right)\sec 2\beta l_1\left[\tan\alpha a+\frac{\alpha^2}{\beta^2}\cot\frac{\alpha l_2}{2}\right]. \tag{15}$$

The odd eigenfunctions ψ^a_1, ψ^a_2, ψ^a_3, ψ^a_4 correspond exactly to the even functions in (14).

$$\left.\begin{aligned}\psi^a_6 &= -\psi'_6,\ \psi^a_7 = -\psi'_7,\ \psi^a_8 = -\psi'_8,\ \psi^a_9 = -\psi'_9,\\ \psi^a_5 &= A^*\frac{(\lambda'_1\cos\beta l_1-\lambda'_2\sin\beta l_1)}{\sin\frac{\alpha l_2}{2}}\sin\alpha\left(\frac{l_2}{2}-s\right)\ (0\leqslant s\leqslant l_2).\end{aligned}\right\} \tag{16}$$

The following definitions were made in (14) and (16)

$$\lambda_1 = \sin\alpha a\cdot\cos\beta l_1+\frac{\alpha}{\beta}\sin\beta l_1\cdot\cos\alpha a,$$
$$\lambda_2 = \frac{\beta}{\alpha}\sin\alpha a\cdot\sin\beta l_1-\cos\alpha a\cdot\cos\beta l_1,$$
$$\lambda'_1 = \lambda_1\cos\alpha l_2-\lambda_2\sin\alpha l_2,$$
$$\lambda'_2 = \lambda_1\sin\alpha l_2+\lambda_2\cos\alpha l_2.$$

The numerical value obtained from the above equations gives the long wavelength absorption line λ_{00} = 0.1189 atomic units = 384 kcal (the experimental value for acenaphtene is λ_{00} = 346 kcal).

REFERENCES

1. H. Kuhn. Helv. Chim. Act. 34, 1308, 2371 (1951).
2. N. Bayliss. J. Chem. Phys. 17, 1353 (1949); J. Chem. Phys. 18, 292 (1950).
3. T. N. Rekasheva. Doctoral dissertation, LGU, 1955; Zhur. Fiz. Khim. 28, 1129 (1954).

4. M. G. Veslov and T. N. Rekasheva. Izvest. Akad. Nauk SSSR, Ser. Fiz. 18, 711 (1954).
5. S. M. Vezykova. Doctoral dissertation, Fiz. Inst. Akad. Nauk USSR, 1954.
6. M. N. Adamov and B. I. Orlov, Vestnik LGU, Ser. i Fiz. Khim No. 22, 182 (1958).
7. M. A. Kovner. Opt. i Spektr. 2, 304 (1957).
8. M. V. Volkenshtein and S. M. Yazykova. Doklady Akad. Nauk SSSR, 104, 834 (1955).

INTENSITIES IN RAMAN SPECTRA AND THE METALLIC MODEL OF THE MOLECULE I. POLYENE COMPOUNDS

F. A. Savin and I. I. Sobel'man

Received 20 March 1959

The general method suggested earlier by one of the authors has been used to calculate intensities in the Raman spectra of polyene compounds, with the help of the metallic model. It is shown that the results of the calculation are in satisfactory agreement with a series of experimental data in the literature.

The semiclassical intensity theory based on the additivity of molecular optics (see reference 1) has not been applied to molecules containing conjugated double bonds. At the same time, a number of properties of such molecules are well conveyed by a metallic model. It is therefore of interest to clarify the extent to which the metallic model may be used for calculating intensities in the Raman spectra of such molecules.

The present work is based on the general method suggested by one of the authors[2] (a short account is contained in reference 3).

The principle of the method consists of the following. When scattering takes place, the interaction of the molecules with the light is entirely determined by the electrons, since the contribution of the nuclei to the scattering is negligibly small. The energy of the radiation field is transmitted to the nuclei by means of the electronic system, as a result of the coulombic interaction of the electrons and the nuclei. We shall start, therefore, from the equilibrium configuration of the nuclei, considering the interaction of the electrons with a displacement of the nuclei as a perturbation.

Let the function $\Psi_n(\mathbf{r}, \mathbf{R}) = \Psi_n(\mathbf{r})$ correspond to the equilibrium configuration $\mathbf{R}$ of the nuclei. If the nuclei undergo certain displacements $\delta\mathbf{R}$, this leads to the appearance of an additional potential $W(\mathbf{r}, \delta\mathbf{R})$, which may be interpreted as the interaction of the electrons with the displacement of the nuclei. In the case when the displacement of the nuclei is the result of a vibration of the molecule, one must understand by "interaction energy" not the quantity $W(\mathbf{r}, \delta\mathbf{R})$ but the expression

$$w(r) = \int u_n^{\nu}(Q)\, W(\mathbf{r}, \delta\mathbf{R})\, u_n^{\nu'}(Q)\, dQ. \qquad (1)$$

Here u_n^{ν} are the vibrational functions, Q the normal coordinates of the nuclei, and the indices n and ν characterize respectively the electronic and vibrational states.

Let us consider the Raman scattering of light by a molecule as consisting of the absorption of a photon of frequency ω_0 and polarization $\mathbf{e}_\rho$ (perturbation $V \sim \mathbf{er}\mathbf{e}_\rho = p^\rho$), the emission of a photon ω, $\mathbf{e}_\sigma$ (perturbation $V \sim \mathbf{er}\mathbf{e}_\sigma = p^\sigma$), and the excitation of a vibration of the nuclei (perturbation w). Using the general methods of perturbation theory, it is easy to obtain for the matrix element of this process (in third-order theory) the following expression:

$$M_{\omega_0, n1} \sim (\beta_{\rho\sigma})_{n0, n1} = \sum_{m, k} \frac{(p^\rho)_{nm} (p^\sigma)_{mk} w_{k0}}{(E_n + \hbar\omega_0 - E_m)(E_n - E_k + \hbar\Omega)} \qquad (2)$$

+ terms of the same type, differing in the order of p^ρ, p^σ, and w.

In (2) the summation is carried out over all intermediate electronic states; E_n, E_m, E_k are the energies of the molecule in states n, m, k for the equilibrium configuration of the nuclei; $\hbar\Omega$ is the vibrational quantum. The matrix elements p^ρ, p^σ, and w are evaluated with the help of the functions $\Psi_n(\mathbf{r})$, which do not depend on the vibration. Therefore $(p^\rho)_{nm}$, $(p'^\sigma)_{mk}$ in general do not depend on the vibration, and w_{k0} may be represented as the product of independent factors—"electronic" and "nuclear." In the completely general case, $W(\mathbf{r}, \delta\mathbf{R})$ has the form

$$W(\mathbf{r}, \delta\mathbf{R}) = \sum_i \frac{\partial H}{\partial \mathbf{R}_i} \delta\mathbf{R}_i = \sum_{i, \tau} \frac{\partial H}{\partial \mathbf{R}_i} C_{i\alpha} Q_\alpha; \quad \delta\mathbf{R}_i = \sum_\alpha C_{i\alpha} Q_\alpha \qquad (3)$$

Here H is the Hamiltonian function of the molecule, and the indices i and α number the nuclei of the molecule and the normal coordinates respectively. Using (3), we may represent $\beta^{\nu}_{\rho\sigma}$, which corresponds to the excitation of the vibration Q_μ, in the following form:

$$\beta^{\nu}_{\rho\sigma} = \sum_i \mathbf{B}^i_{\rho\sigma} \delta\mathbf{R}^{\nu}_i = (Q_\mu)_{0\nu} \sum_i C_{i\mu} \mathbf{B}^i_{\rho\sigma}. \qquad (4)$$

Each term of the sum (4) corresponds to the interaction of the electrons of the molecule with the displacement of one of the nuclei. The vector coefficients $\mathbf{B}^i_{\rho\sigma}$ do not depend on the vibration and are fully determined by the structure of the electron clouds of the molecule (for the equilibrium configuration of the nuclei).

In essence, the approach set forth is equivalent to representing the polarizability of the molecule $\alpha(\mathbf{R}_1, \mathbf{R}_2, \ldots \mathbf{R}_N)$, corresponding to some arbitrary nuclear configuration $\mathbf{R}_i$, in the form

$$\alpha = \alpha_0 + \sum_i \left(\frac{\partial \alpha}{\partial \mathbf{R}_i}\right)_0 \delta\mathbf{R}_i, \qquad (5)$$

where α_0 and $(\partial\alpha/\partial\mathbf{R}_i)_0$ are defined by the equilibrium configuration of the molecule. Using the Placzek formula

$$\beta^{\nu}_{\rho\sigma} = \frac{\partial \alpha_{\rho\sigma}}{\partial Q} Q_{0\nu},$$

(4) may be obtained from this. The derivation of (4) set forth above is less easily visualized, but on the other hand it reveals the structure of the coefficients $\mathbf{B}^i_{\rho\sigma}$, which is important for what follows.

We shall first consider polyene compounds on the basis of (3) and (4). We shall represent $\beta_{\rho\sigma}$ as a sum of two parts, $\beta_{\rho\sigma}(\pi) + \beta_{\rho\sigma}(\sigma)$, associated respectively with the π-electrons and with the σ-electron skeleton of the molecule, and we shall carry out the evaluation of $\beta_{\rho\sigma}(\pi)$ within the framework of the metallic model. (We shall confine ourselves to considering planar vibrations of the carbon chain.)

We assume that the electron moves in the field

$$V(\mathbf{r}) = \sum_i V_i(\mathbf{r}),$$

of N identical force centers, arranged as shown in the Figure; for polyene molecules N is an even number and the chain has a center of symmetry. Furthermore, let the motion of the electron be limited by infinitely high

potential barriers ($V(\mathbf{r}) = \infty$ for $z \leqslant 0$ and $z \geqslant L$) and let $L = Nd/2$. $V(\mathbf{r})$ is periodic along z with period d, and therefore the wave function of the electron in this field may be represented in the form

$$\Phi_n(\mathbf{r}) = \frac{1}{\sqrt{N}} u(\mathbf{r}) \sin \frac{n\pi}{L} z; \; u(x, y, z + md) = u(x, y, z). \quad (6)$$

We assume, as is usually done, that the N delocalized π-electrons of the molecule occupy the N/2 lowest levels $n = 1 \ldots N/2$. Then the electrons of the last of the occupied levels, $n = N/2$, play a fundamental role. Independently of the specific form of the potential $V_i(\mathbf{r}) = V_i(\mathbf{r} - \mathbf{R}_i)$, it may be asserted that $\partial V_i/\partial R_i$ is different from zero only in the small region $|\mathbf{r} - \mathbf{R}_i| \leqslant d/2$. Taking this circumstance into account and confining ourselves in (2) to a single term, corresponding to a transition to the nearest level, we obtain for the components β_{zz},*

*The transverse dimension of the region of localization of the electron ~d/2, and therefore the matrix elements of the x and y components of the dipole moment will be less by a factor of approximately d/2L than the matrix element of the z component. For this reason, it is precisely β_{zz} which is of fundamental interest. Furthermore, within the framework of the metallic model, $z_{n, n+1}$ is approximately one order larger than the remaining nonzero matrix elements $z_{n, n+2}$, $z_{n, n+3}$, etc., which permits us to confine ourselves to one term in the sum (2).

$$\beta_{zz} = \sum_i \beta'_{zz}; \; \beta'_{zz} = F(N)\, w^i_{\frac{N}{2}; \frac{N}{2}+2};$$

$$F(N) = \frac{e^2}{N} \frac{4z^2_{\frac{N}{2}, \frac{N}{2}+1} z^2_{\frac{N}{2}+1, \frac{N}{2}+2} \left(E_{\frac{N}{2}} - E_{\frac{N}{2}+1}\right)}{\left(E_{\frac{N}{2}} - E_{\frac{N}{2}+2}\right)\left[\left(E_{\frac{N}{2}} - E_{\frac{N}{2}+1}\right)^2 - \hbar^2\omega_0^2\right]}, \quad (7)$$

$$w^i_{\frac{N}{2}; \frac{N}{2}+2} = \hbar R_i \int |u(\mathbf{r})|^2 \frac{\partial V_i(\mathbf{r} - \mathbf{R}_i)}{\partial R_i} \sin \frac{N\pi}{2L} z \sin \frac{(N+4)\pi}{2L} z\, d\mathbf{r}. \quad (8)$$

If we introduce the variable

$$\xi \left(z = Z_i + \xi = \frac{d}{4} + (i-1)\frac{d}{2} + \xi\right),$$

then after a series of trigonometric transformations (8) takes the form

$$w^i_{\frac{N}{2}; \frac{N}{2}+2} = \hbar R_i \left\{\cos(2i-1)\frac{\pi}{N}\left[I_1 + \frac{1}{2}(-1)^{i-1} I_2 + \frac{1}{2}(-1)^{i-1} I_3\right] - \sin(2i-1)\frac{\pi}{N}\left[I_4 + \frac{1}{2}(-1) I_5 - \frac{1}{2}(-1) I_6\right]\right\}$$

$$\left.\begin{aligned} I_1 &= \int |u|^2 \frac{\partial V_i}{\partial R_i} \cos\frac{4\pi}{Nd}\xi\, dx dy d\xi; \\ I_2 &= \int |u|^2 \frac{\partial V_i}{\partial R_i} \sin\frac{2\pi}{d}\xi \cos\frac{4\pi}{Nd}\xi\, dx dy d\xi; \\ I_3 &= \int |u|^2 \frac{\partial V_i}{\partial R_i} \cos\frac{2\pi}{d}\xi\, dx dy d\xi; \\ I_4 &= \int |u|^2 \frac{\partial V_i}{\partial R_i} \sin\frac{4\pi}{Nd}\xi\, dx dy d\xi; \\ I_5 &= \int |u|^2 \frac{\partial V_i}{\partial R_i} \sin\frac{2\pi}{d}\xi \sin\frac{4\pi}{Nd}\xi\, dx dy d\xi; \\ I_6 &= \int |u|^2 \frac{\partial V_i}{\partial R_i} \cos\frac{2\pi}{d}\xi \cos\frac{4\pi}{Nd}\xi\, dx dy d\xi \end{aligned}\right\} \quad (9)$$

If we consider the nuclei of the upper set alone or of the lower one alone, it is easy to show that the integrals (9) do not depend on the position of the nucleus in the set. This is connected with the periodicity of the chain here considered and can be in error only for the end nuclei, which is of little significance. If we allow further for the symmetry of the chain and take into consideration the selection rule $\beta_{zz} = 0$ for vibrations antisymmetric with respect to the center of the chain, we can establish a connection between the integrals (9) for nuclei of the upper and the lower sets. Since the molecule possesses a plane of symmetry, in which all its atoms lie, all the y components of these integrals equal zero. We give the final expression for β_{zz}:

$$\beta_{zz} = F(N)\left\{B_1(N)\sum_{i=1}^{N}(-1)^{i-1}\cos(2i-1)\frac{\pi}{N}\hbar R_i - B_2(N)\sum_{i=1}^{N}\sin(2i-1)\frac{\pi}{N}\hbar R_i\right\}; \quad (10)*$$

*In reference 3 the number of delocalized electrons was erroneously taken as equal to 2N. Consequently, formula (8)[3] is incorrect and should be replaced by formula (10) of the present work.

$$\left.\begin{aligned} B_1(N) &= \int |u|^2 \left\{e_x \frac{\partial V_i}{\partial X_i}\cos\frac{4\pi}{Nd}\xi + \frac{1}{2} e_z \frac{\partial V_i}{\partial Z_i}\sin\left(1+\frac{2}{N}\right)\frac{2\pi}{d}\xi\right\} dx dy d\xi, \\ B_2(N) &= \int |u|^2 \left\{-e_x \frac{1}{2}\frac{\partial V_i}{\partial X_i}\cos\left(1+\frac{2}{N}\right)\frac{2\pi}{d}\xi + e_z \frac{\partial V_i}{\partial Z_i}\sin\frac{4\pi}{Nd}\xi\right\} dx dy d\xi. \end{aligned}\right\} \quad (11)$$

According to (10) and (11), the magnitude of β_{zz} for any of the planar vibrations of the chain is determined by 4 parameters. The values of these parameters, generally speaking depend on N; i.e., they change from molecule to molecule. However, this dependence is significant only for small values of N. For $N \gg 1$ (long chains), one can obtain from (11)

$$\left.\begin{aligned} B_1(N) \to B_1 &= \int |u|^2 \left\{e_x \frac{\partial V_i}{\partial X_i} + e_z \frac{1}{2}\frac{\partial V_i}{\partial Z_i}\sin\frac{2\pi}{d}\xi\right\} dx dy d\xi, \\ B_2(N) \to B_2 &= -e_x \frac{1}{2}\int |u|^2 \frac{\partial V_i}{\partial X_i}\cos\frac{2\pi}{d}\xi\, dx dy d\xi. \end{aligned}\right\} \quad (12)$$

Three parameters, B_{1x}, B_{1z}, and B_{2x}, do not depend on N and are the same for any chain of the form here

considered, independent of the number of nuclei which enter into it. These parameters depend only on the form of the function $u(\mathbf{r})$ and the potential $V_1(\mathbf{r} - \mathbf{R}_1)$; i.e., they are determined by the character of the force field for the π-electrons. The dependence on N is concentrated, in general, for all vibrations in the factor F(N). This factor may be evaluated on the basis of experimental data concerning the electronic spectrum of the molecules. In comparing the intensities within the spectrum of a single molecule, this factor may simply be included in the parameters B_1 and B_2.

In the derivation of (10), it was implicitly assumed that the vibration does not change L. This restriction can easily be removed. Any arbitrary displacement of the nuclei can be represented as a superposition of two displacements: a nuclear displacement $\delta\mathbf{R}'_l$, which is associated with a uniform extension of the chain without distortion of its periodic structure, and a nuclear displacement $\delta\mathbf{R}''_l$, for which the length of the chain remains unchanged:

$$\delta\mathbf{R}_l = \delta\mathbf{R}'_l + \delta\mathbf{R}''_l. \tag{13}$$

In the same way as (13), β_{zz} is also composed of two parts, $\beta'_{zz} + \beta''_{zz}$. β''_{zz} is determined by formula (10), while β'_{zz} may be expressed as the derivative of the polarizability $\alpha_{zz}(\pi)$ with respect to L:

$$\beta'_{zz} = \frac{\partial \alpha_{zz}}{\partial L}\,\delta L.$$

It is not difficult to evaluate the quantity $\partial\alpha_{zz}/\partial L$ within the framework of the metallic model.[4] Thus, finally,

$$\beta = \beta'(\pi) + \beta''(\pi) + \beta(\sigma). \tag{14}$$

The part of the tensor associated with the σ-electrons might be evaluated on the basis of additivity. This would introduce into our considerations a series of additional parameters, for the evaluation of which reliable and extensive data on intensities in Raman spectra of polyenes would be necessary. Inasmuch as such data do not exist at present, we shall carry out the calculation according to a rougher approximation by separating out the principal terms in (14).

We shall assume that, for vibrations of the carbon chain, the terms associated with the π-electrons will predominate in (14). Such an assumption is justified, since the data on the dependence of the intensities in Raman spectra of polyenes on the frequency of the exciting light show that this dependence is determined by the first electronic absorption band, which is associated with excitation of the π-electrons.[5] Furthermore, it may be shown that B_{1x} and $B_{2x} \ll B_{1z}$ (for a linear chain $B_{1x} = B_{2x} = 0$). Consequently, we obtain

$$\beta_{zz} \cong \beta'_{zz}(\pi) + \beta''_{zz}(\pi)$$

$$= F(N)\,B_{1z} 2 \sum_{i=1}^{N/2} (-1)^{i-1} \cos(2i-1)\frac{\pi}{N}\,\delta Z''_i + \frac{\partial \alpha_{zz}}{\partial L}\,\delta L. \tag{15}$$

Here we have taken into consideration the fact that for vibrations which are symmetric with respect to the center of the chain

$$\sum_{i=1}^{N} (-1)^{i-1} \cos(2i-1)\frac{\pi}{N}\,\delta Z''_i = 2 \sum_{i=1}^{N/2} (-1)^{i-1} \cos(2i-1)\frac{\pi}{N}\,\delta Z''_i. \tag{16}$$

On solving the vibrational problem for purely stretching vibrations,* assuming that all the bonds of the molecule are alike and have one and the same force constant K, we obtain (see references 1, 7, 8)

$$\left.\begin{aligned} &\omega_j^2 = 2\varepsilon K\left\{1 - \frac{1}{2}\cos\frac{j\pi}{N}\right\};\quad \delta s_{jp} = \alpha_j \sin p\frac{j\pi}{N};\\ &\alpha_j = \sqrt{\frac{4\varepsilon}{N}\left(1 - \frac{1}{2}\cos\frac{j\pi}{N}\right)}\,\frac{4}{\sqrt{\omega_j\ \text{см}^{-1}}}\,10^{-8}\ \text{см}\quad (j = 1 \ldots N-1). \end{aligned}\right\} \tag{17}$$

Here ε is m_H/m, where m_H is the spectroscopic mass of hydrogen and m is the mass of the force center (we include the masses of the hydrogen atoms in the mass of the center, and therefore m equals the mass of the CH_2 group for the end centers and the mass of the CH group for the others; we shall roughly consider all the masses the same), and ω_j and δs_{jp} are respectively the vibration frequency and the change in the length of the pth bond in the jth normal vibration; according to (17), larger ω_j's correspond to larger j's. For vibrations which are symmetric with respect to the center of the chain (only they are active in the Raman spectrum), j is odd. We can further obtain

$$\delta L(j) = \frac{\sqrt{3}\,\alpha_j}{2\tan\frac{j\pi}{2N}};\quad \delta Z''_i(j) = -\frac{\sqrt{3}\,\alpha_j}{4\sin\frac{j\pi}{2N}}\left\{\cos(2i-1)\frac{j\pi}{2N} - \cos\frac{j\pi}{2N} + 2\,\frac{i-1}{N-1}\cos\frac{j\pi}{2N}\right\}. \tag{18}$$

$$S(N, j) = \sum_{i=1}^{N/2} (-1)^{i-1} \cos(2i-1)\frac{\pi}{N}\,\delta Z''_i(j)$$

$$= -\frac{\sqrt{3}\,\alpha_j}{8\tan\frac{j\pi}{2N}}\left\{\frac{2\cos\frac{\pi}{N}}{\cos\frac{j\pi}{N} + \cos\frac{2\pi}{N}} - \frac{N}{N-1}\,\frac{1}{\cos\frac{\pi}{N}}\right\}. \tag{19}$$

For β_{zz}, consequently, we have

$$\beta_{zz} = F(N)\,B_{1z} S(N, j) + \frac{\partial \alpha_{zz}}{\partial L}\,\delta L(j). \tag{20}$$

The quantities F(N) and $\partial\alpha_{zz}/\partial L$ may be evaluated on the basis of a basically planar metallic model, using the experimental values for the frequencies of the electronic absorption bands of polyenes.

Experimental data are lacking for the intensities in Raman spectra of long molecules, for which $L \gg d$. Therefore, in order to compare the results of our calculation with experiment, we are obliged to use experimental data referring to molecules for which $L > d$ (by a small factor), but the condition $L \gg d$, generally speaking, is not fulfilled. Analysis of the formulas obtained above shows that in this case we may expect qualitative agreement between the results of calculation and experiment.

Let us consider the molecules of butadiene (N = 4), hexatriene (N = 6), and octatetraene (N = 8). Let us assume $\varepsilon = 0.08$ (an average between the values of ε for the CH and CH_2 groups), and let us take the value of K equal to the value of K in benzene (11.4×10^5 cm^{-2}).[9] The frequencies of the ultraviolet absorption bands for the molecules under consideration equal 47,700 cm^{-1} for butadiene, 39,750 cm^{-1} for hexatriene, and 33,100 cm^{-1} for octatetraene.[10, 11] The frequency of the exciting line equals 22,938 cm^{-1} (λ4358 A). The results of the calculations according to formula (20) are entered in the table. In this

*Generally speaking, the method here considered is applicable to the calculation of intensities for any vibrations of the carbon chain, but, since the force constants for the molecules under consideration are unknown, we are forced to confine ourselves to this approximation for the solution of the vibrational problem (the same approximation was used in references 4 and 6).

N	J	ω_J cm^{-1}	$F(N)D_{1J}$	$2B(N,J)$ cm	β^2_{11} cm^2	$\frac{\partial a_{11}}{\partial L}$	$L(J)$ cm	β^2_{11} cm^2	$I_{expt.}$	$I_{calc.}$
4	1	1200	83 A cm^2	$-0.32 \cdot 10^{-10}$	$25.5\,A \cdot 10^{-10}$	20 B cm^2	$5.8 \cdot 10^{-10}$	$116\,B \cdot 10^{-10}$	~0.4 [12]	0.4
	3	~1600		$2.32 \cdot 10^{-10}$	$192\,A \cdot 10^{-10}$		$1.19 \cdot 10^{-10}$	$23.8\,B \cdot 10^{-10}$	1 [12]	1
6	5	~1600	404 A cm^2	$1.96 \cdot 10^{-10}$	$780\,A \cdot 10^{-10}$	65 B cm^2	$0.64 \cdot 10^{-10}$	$41.5\,B \cdot 10^{-10}$	~10 [12] *	18
8	7	~1600	1370 A cm^2	$2.02 \cdot 10^{-10}$	$2770\,A \cdot 10^{-10}$	210 B cm^2	$0.41 \cdot 10^{-10}$	$86\,B \cdot 10^{-10}$	—	200

*The determination refers to the allocinene molecule. We may suppose that the intensities of the ~1600 cm^{-1} lines in hexatriene and in allocinene are of the same order.

table A and B are constants, the same for all polyene molecules. Starting from the experimental fact that the ~1600 cm^{-1} line in butadiene is about 2.5 times as intense as the 1200 cm^{-1} line, we conclude that in each case B does not significantly exceed A. Therefore, for the 1600 cm^{-1} vibration, the first term makes the principal contribution to the intensity.* For the intensity ratio of corresponding lines in the molecules of butadiene, hexatriene, and octatetraene, we obtain

$$I_{but.} : I_{hex.} : I_{oct.} \approx 1 : 16 : 200,$$

which agrees with experiment (for the ratio $I_{but.}/I_{hex.}$ see the 10th column of the table; as for $I_{hex.}/I_{oct.}$, although there are no quantitative experimental data, an increase in intensity of the same order as given by calculation has been qualitatively observed in going from hexatriene to octatetraene).

*In references 4 and 6 it was assumed that the extension of the chain plays the fundamental role in the intensity of the 1600 cm^{-1} line. This was associated with the fact that the 1600 cm^{-1} frequency was erroneously assigned to the totally symmetric vibration of the chain which consists in the simultaneous equal extension of all its bonds, without disturbance of the periodicity of the chain.

For all the other vibrations of the carbon chain, our approximation for the solution of the vibrational problem is inapplicable, since in this case one may not neglect the change in the valence angles between the C—C bonds and the participation of the CH groups in the vibrations. Considering, however, that the increase in the line intensities in a series of polyenes takes place for the most part on account of an increase in the electronic factors $F(N)$ and $\partial a_{11}/\partial L$ (see columns 4 and 7 of the table), we may expect a strong increase in the intensity for these vibrations as well.

If the term $\beta_{11}(\pi)$ makes the fundamental contribution to the intensity, as has been assumed above, the degree of depolarization, ρ, of the lines for all vibrations of the chain—valence and deformation—must be $\rho \leq 0.5$, while for long chains $\rho \to 0.5$. (We call to mind that, for additive compounds within the framework of the zeroth approximation of the semiclassical theory, $\rho = 0$ for deformation vibrations[1]). Experiment gives $\rho \cong 0.35$ for the ~1600 cm^{-1} line in compounds with two double bonds, whereas for compounds with one double bond $\rho \sim 0.1$.[14]

The trans-form of the polyenes was assumed above. If we do not make this assumption and confine ourselves to consideration of a one-dimensional metallic model, the fundamental results remain the same even for chains of a different form.

It is possible to carry out the calculation of intensities for benzene and other aromatic compounds (see reference 15) to the same approximation as for polyene molecules. In this case one can obtain formulas analogous to formulas (10) and (20). It is extremely significant that the force centers of the benzene ring are like those in the polyene compounds. It appears possible to establish a connection between the parameter B_{1t} in the polyenes and the corresponding parameter for benzene. This permits us to calculate the ratio of the intensities of the ~1600 cm^{-1} line in hexatriene and the 1586 and 1606 cm^{-1} lines in benzene. The calculation gives

$$I_{hex.} : I_{benzene} \cong 85,$$

which agrees with the experimental value of ~50.[15]

We thank P. A. Bazhulin for his interest in the work and discussion of the results.

REFERENCES

1. M. V. Vol'kenshtein, M. A. El'yashevich, and B. I. Stepanov. "Kolebaniya molekul." (Molecular Vibrations), GITTL, 1949.
2. I. I. Sobel'man. Sbornik trudov pamyati akad. G. S. Landsberga. (Collection of works in memory of academician G. S. Langsberg), Izd. Akad. Nauk, SSSR, 1959.
3. I. I. Sobel'man. Izvest. Akad. Nauk SSSR, Ser. Fiz. **22**, 1026 (1958).
4. S. M. Yazykova. Kand. diss. (Dissertation), Fiz. Inst. Akad. Nauk SSSR, Moscow-Leningrad, 1954; M. V. Vol'kenshtein and S. M. Yazykova. Doklady Akad. Nauk SSSR **104**, 834 (1955).
5. P. P. Shorygin and L. Z. Osityanskaya. Doklady Akad. Nauk SSSR **98**, 51 (1954).
6. M. D. Zepe. Kand. diss. (Dissertation), Riga, 1952.
7. F. R. Gantmakher and M. G. Krein. "Ostsillyatsionnye matritsy i yadra i malye kolebaniya mekhanicheskikh sistem." (Oscillation Matrices and Kernels and Small Vibrations of Mechanical Systems), GITTL, 1950.
8. L. I. Vidro and M. V. Vol'kenshtein. Doklady Akad. Nauk SSSR **85**, 1243 (1952).
9. M. A. Kovner. Zhur. Eksp. i Teoret. Fiz. **26**, 598 (1954).
10. W. C. Price and A. D. Walsh. Proc. Roy. Soc. **185A**, 182 (1946).
11. K. W. Hausser. Z. techn. Phys. **15**, 10 (1934).
12. A. Dadieu and K. W. F. Kohlrausch. Ber. **63**, 1657 (1930).
13. P. P. Shorygin. Izvest. Akad. Nauk SSSR, Ser. Fiz. **12**, 578 (1948).
14. M. M. Sushchinskii and V. I. Tiulin. Doklady Akad. Nauk SSSR **95**, 505 (1954).
15. F. A. Savin and I. I. Sobel'man. Opt. i Spektr. **7**, 740 (1959).

INTENSITIES IN RAMAN SPECTRA AND THE METALLIC MODEL OF THE MOLECULE
II. AROMATIC COMPOUNDS

F. A. Savin and I. I. Sobel'man

Received 20 March 1959

The method previously worked out by one of the authors has been used to calculate intensities in the Raman spectra of aromatic compounds, with the help of the metallic model. From the examples of benzene, toluene, and deuterobenzene, it is shown that the theory is in satisfactory agreement with a series of experimental data.

In the present work, the relative intensities in the Raman spectra of aromatic compounds are evaluated on the basis of the method proposed in references 1 and 2 (for the application of this method to polyene molecules, see reference 3, hereafter denoted by I).

In the same way as was done in I, we shall represent the Raman tensor $\beta_{\rho\sigma}$ for lines corresponding to vibrations of the benzene ring in the form of a sum of two parts $\beta_{\rho\sigma}(\pi) + \beta_{\rho\sigma}(\sigma)$, associated respectively with the π-electrons and with the σ-electron skeleton of the ring, and we shall carry out the evaluation of $\beta_{\rho\sigma}(\pi)$ within the framework of the metallic model by the same method as in I. Just as was done in I, we may divide any displacement of the nuclei during the vibrations into two displacements—a nuclear displacement $\delta\mathbf{R}_i'$, in which the radius of the benzene ring changes without distortion of its symmetry (totally symmetric expansion of the ring), and a nuclear displacement $\delta\mathbf{R}_i''$, in which the length of the ring remains unchanged but its symmetry is distorted; i.e.,

$$\delta\mathbf{R}_i = \delta\mathbf{R}_i' + \delta\mathbf{R}_i''. \tag{1}$$

In the same way as (1), $\beta_{\rho\sigma}(\pi)$ is divided into two parts:

$$\beta_{\rho\sigma}(\pi) = \beta'_{\rho\sigma}(\pi) + \beta''_{\rho\sigma}(\pi). \tag{2}$$

Let us consider an electron moving in the field

$$V(r) = \sum_{i=0}^{5} V_i(r),$$

of 6 potential centers, arranged as shown in the Figure, a. The circumference is kept equal to the perimeter of the benzene ring, $2\pi r_0 = 6a$, where a is the length of the C—C bond in benzene. $V(r)$ is periodic over ϕ with the period $\pi/3$, and therefore the wave function of the electron may be represented in the form

$$\Phi_l(r) = u_l(r)\, e^{il\varphi}; \quad u_l\left(r,\ z,\ \varphi + m\frac{\pi}{3}\right) = u_l(r,\ z,\ \varphi); \quad s = \varphi r_0. \tag{3}$$

Let us assume, as is usually done, that the 6 delocalized π-electrons of the benzene ring occupy the lowest energy levels $l = 0$; ±1 (the ±1 levels are degenerate according to the sign of the moment). Then the transitions permitted by the selection rules from the last occupied level, $l = \pm1$, to the next unoccupied one, i.e., to the level $l = \pm2$, will play a fundamental role in Raman scattering. Repeating the same reasoning as in the derivation of Eq. (10) in I, we obtain in the given case (see, for example, reference 4) from the general formula (2) in I:

$$\beta''_{xx} = -\beta''_{yy} = F_b \cdot B_s^b \cdot \sum_{i=0}^{5} \delta S_i'' \sin\frac{2\pi i}{3}, \tag{4}$$

$$F_b = -\frac{2(E_2 - E_1)(er_0)^2}{(E_2 - E_1)\left[(E_2 - E_1)^2 - \hbar^2\omega_0^2\right]}, \tag{5}$$

$$B_s^b = \int_{-\frac{a}{2}}^{\frac{a}{2}} |u_1(s)|^2 \frac{\partial V_i}{\partial S_i''} \sin\frac{2\pi s}{3a}\, ds, \tag{6}$$

$$\beta''_{zz} = 0. \tag{7}$$

For convenience in the further calculations we introduce the symbols

$$\sum_{i=0}^{5} \delta S_i'' \sin\frac{2\pi i}{3} = Q; \quad F_b B_s^b = \sqrt{A}; \quad \beta''_{xx} = -\beta''_{yy} = \beta''. \tag{8}$$

The second part of the tensor $\beta_{\rho\sigma}(\pi)$ is evaluated by the same method as in I:

$$\beta'_{xx} = \beta'_{yy} = \beta' = \frac{\partial\alpha_{yy}}{\partial L} \cdot \delta L = \sqrt{C}\,\delta L, \tag{9}$$

$$\beta'_{zz} = \frac{\partial\alpha_{zz}}{\partial L} \cdot \delta L. \tag{10}$$

To the first approximation, we may consider that the potentials $V_i(r)$ for the π-electrons of the benzene ring are the same as in polyene molecules. This permits us to establish a connection between the parameter B_s^b and the corresponding parameter for the π-electrons of polyene molecules. For this purpose let us consider a linear polyene chain in which the force centers are arranged as shown in the Figure, b. The wave function of the electron in such a field may be represented in the form

$$\Phi_n(r) = \frac{1}{\sqrt{N}}\, u_2(r) \sin\frac{n\pi}{L} z, \quad u_2(x,\ y,\ z + ma) = u_2(x,\ y,\ z) \tag{11}$$

Calculations analogous to those conducted in I give

$$\beta_{zz} = F(N)\, B_s^p \cdot \sum_{i=1}^{N} (-1)^{i-1} \cos(2i-1)\frac{\pi}{N} \delta S_i'' + \frac{\partial\alpha_{zz}}{\partial L}\,\delta L, \tag{12}$$

$$F(N) = \frac{e^2}{N} \frac{4\sin\frac{N}{2}; \frac{N}{2}+1; \frac{3}{2}\frac{N}{2}+1; \frac{N}{2}+2\left(E_{\frac{N}{2}} - E_{\frac{N}{2}+1}\right)}{\left(E_{\frac{N}{2}} - E_{\frac{N}{2}+2}\right)\left[\left(E_{\frac{N}{2}} - E_{\frac{N}{2}+1}\right)^2 - \hbar^2\omega_0^2\right]}, \tag{13}$$

$$b_s^p = \frac{1}{2}\int_{-\frac{a}{2}}^{\frac{a}{2}} |u_2(s)|^2 \frac{\partial V_i}{\partial S_i} \sin\frac{\pi s}{a}\, ds. \tag{14}$$

Formulas (12)-(14) coincide with the formulas which were used in I for the final calculations. Comparing (11) with (3), we may obtain a connection between the functions $u_1(s)$ and $u_2(s)$, since these functions are determined by the properties of the force centers $V_i(r)$, which are the same, in the approximation here considered, for the carbon chains of polyenes and for the benzene ring. Taking the normalization of functions (11) and (3) into account, we obtain

$$u_1(s)^2 = \frac{1}{12} u_2(s)^2. \tag{15}$$

From this we obtain a connection between the parameters B_s^b and B_r^p:

$$B_s^b = \int_{-\frac{\pi}{2}}^{\frac{\pi}{2}} u_1^2 \frac{\partial V_i}{\partial S_i} \sin \frac{2\pi s}{3a} ds \approx \frac{1}{9} B_r^p. \tag{16}$$

The electronic factors $F(N)$ and F_b may be evaluated in the same way as in I on the basis of the metallic model, using experimental data on the electronic spectra of the molecules under consideration. Using (4)-(10), (12)-(14), and also (16), we can evaluate the relative magnitudes of $\beta_{\rho\rho}(\pi)$ for polyene and aromatic compounds. It is known that the intensity of the ~1600 cm^{-1} line in hexatriene is about 50 times as great as the intensity of the 1596 and 1606 cm^{-1} lines in benzene. From (4), (12), and (16) it follows that, for the 1600 cm^{-1} frequency,

$$I_{hex.} : I_{benz.} \simeq 85. \tag{17}$$

Thus there exists good agreement between calculation and experiment.

Let us proceed to the evaluation of the relative intensities in the Raman spectra of benzene and its substitution products. We shall consider only that part of the Raman tensor which is associated with the π-electrons, neglecting the contribution of the σ-electrons. Apparently it is not permissible to consider that, in aromatic compounds, the π-electrons play the predominant role in Raman scattering as they do in polyene molecules (see I). The fact that in aromatic compounds the intensity of the lines which correspond to vibrations of the benzene ring are of the same order as the intensities of the lines associated with vibrations of the σ-bonds, and at the same time are significantly less than the intensities of lines corresponding to vibrations of the carbon chain in polyene molecules (see formula 17), indicates that the contribution of the σ-electrons to the intensity of these lines is not negligible. It is necessary to take account of this circumstance in interpreting the results of the calculation.

On the basis of (4), (9), and (10), we obtain the following expression for the Raman tensor:

$$\beta_{\rho\rho} = \begin{pmatrix} \beta' + \beta'' & 0 & 0 \\ 0 & \beta' - \beta'' & 0 \\ 0 & 0 & \beta'_{zz} \end{pmatrix}. \tag{18}$$

The value of β'_{zz} may be estimated in the following way. For the benzene vibration with the frequency 992 cm^{-1}, $\beta'' = 0$. The degree of depolarization of the 992 cm^{-1} line is $\rho = 0.11$. Hence we have two possible values for β'_{zz}:

$$(\beta'_{zz})_1 = 0.268\beta'; \quad (\beta'_{zz})_2 = 2.44\beta'.$$

Considering that $\beta'_{zz} < \beta'$, we choose the value $\beta'_{zz} = 0.268\,\beta'$. We note that taking account of β'_{zz} in (18) has only an insignificant effect on the calculated values for the line intensities.

We obtain as our result for the quantity $S = 5b'^2 + 7g'^2$

$$S = 5b'^2 + 7g'^2 = 21AQ^2 + 29.4C\,(\delta L)^2. \tag{19}$$

here b' is the trace and g' the anisotropy of the tensor.

Using the normalized forms obtained by Kovner[4] for the vibrations of the benzene and deuterobenzene molecules, it is not difficult to obtain the values of Q and δL during the vibrations of these molecules. For the toluene molecule, the nuclear displacements during the vibrations were recently evaluated by Bogomolov.[5] (For other aromatic molecules, such data are lacking at present.) The results of the evaluations are brought together in the table (the experimental values $S_{expt.}$ for the first seven lines were taken from reference 6, those for the last three from reference 7). Since there are some discrepancies among the values of $S_{expt.}$ presented in the works cited, the last three values of $S_{expt.}$ are actually expressed on a somewhat different scale. It can be seen from the table that the calculation gives the correct sequence of $S_{calc.}$, using the two parameters determined from experiment. Actually the determination of only one parameter from experiment is necessary, since the second parameter is a "scale factor" and serves to reduce $S_{calc.}$ to a predetermined scale. It can be seen from the table that the calculation gives low values for $S_{calc.}$; that is, $S_{calc.} < S_{expt.}$. This is natural, since we did not take account of the contribution of the σ-electrons to the intensity of the lines.

No.	Molecule	ν cm^{-1}	$S_{calc.}$	$S_{expt.}$
1	Benzene	992	4.85	4.85
2	Toluene	1004	1.8	2.54
3	Benzene	1596; 1606	0.64	1.56
4	Toluene	786	0.4	1.07
5	Toluene	1030	0.3	0.71
6	Benzene	606	0.28	0.28
7	Toluene	520	0.1	0.34
8	Deuterobenzene	945	4.35	4.04
9	Deuterobenzene	1560	0.54	0.98
10	Deuterobenzene	577	0.34	0.15

In principle, the contribution of the σ-electrons may be taken into account by means of the additivity scheme. In doing so, a series of additional parameters enters into the expressions for the line intensities. We have not carried out such calculations, since the aim of our work was to show the possibility of taking account of the π-electrons within the framework of the metallic model.

We thank P. A. Bazhulin for his interest in the work and for discussion of the results, and also A. M. Bogomolov, who made available to us the results of his calculations of the forms of the vibrations.

REFERENCES

1. I. I. Sobel'man. "Sbornik trudov pamyati akad. G. S. Landsberga." (Collection of works in memory of academician G. S. Landsberg), Izd. Akad. Nauk SSSR, 1959.
2. I. I. Sobel'man. Izvest. Akad. Nauk SSSR, Ser. Fiz. 22, 1026 (1958).
3. F. A. Savin and I. I. Sobel'man. Opt. i Spektr. 7, 733 (1959).
4. M. A. Kovner. Dokt. diss., Minsk, 1958.
5. A. M. Bogomolov. Kand. diss. Saratovsk. gos. univ. (Dissertation, Saratov State University), 1959.
6. N. I. Rezaev. Kand. diss., MGU (Dissertation, Moscow State University), 1958.
7. G. Allen and H. I. Bernstein. Can. J. Chem. 33, 1137 (1955).

BAND SHAPE IN THE INDUCED ROTATIONAL AND VIBRATIONAL SPECTRA OF DIPOLELESS MOLECULES

E. E. Nikitin

Received 18 February 1959

In a quasi-classical approximation, the shape of induced rotational and vibrational absorption bands has been computed and their half-widths determined for dipoleless molecules undergoing binary collisions. The theoretical and experimental values for the half-width of the bands agree satisfactorily with each other. The analogy between induced absorption (emission) spectra and electronic absorption (luminescence) spectra of complex molecules is briefly considered.

Infrared spectroscopy of induced vibrational and rotational absorption of dipoleless molecules has been intensively developed in recent years. This absorption is dependent on the fact that, during molecular collisions, there arises a dipole moment whose presence leads to the appearance of vibrational and rotational transitions in one of the colliding molecules.

As experiment shows (see, for example, references 1 and 2), in the density range up to a few tenths of an Amagat unit only binary collisions are significant for absorption. In a number of works,[3-6] a calculation of the integrated intensity of the binary vibrational and rotational absorption spectrum of hydrogen has been presented. The calculated and experimental values of the integrated absorption coefficients coincide satisfactorily. Theoretical predictions of the temperature dependence of the integrated intensity have also been confirmed by experiment.[6]

It may be expected that the shape of induced absorption bands will depend to a greater degree on the details of the molecular collisions than will the integrated intensity.[7] In particular, the half-width of the bands must be connected with the radius of action of the exchange forces, the determination of which is of great interest in connection with the study of various relaxation processes in gases.

In the present work, the shape of the induced vibrational and rotational absorption bands of dipoleless diatomic molecules undergoing binary collisions is calculated.

ROTATIONAL ABSORPTION

The rotational absorption spectrum of H_2 colliding with various partners (H_2, He, Ar, N_2, CO) was studied by Colpa and Ketelaar.[1] Their calculation of the integrated intensity[5] confirmed the experimental conclusion that the absorption is fundamentally controlled by the dipole moment induced in the partner by the rotating quadrupole field of H_2. Taking account of the anisotropy of the polarizability of the partner (H_2, N_2) gives only a small correction to the "isotropic" absorption. Accordingly, in calculating the shape of an induced rotational absorption band of a molecule A as a result of A + B collisions, we assume that the polarizability α of the partner B is isotropic. In this case the induced dipole moment of the colliding pair has the form

$$\mu = \alpha F, \tag{1}$$

where F is the quadrupole field of the absorbing molecule A.

The general method for calculating the induced absorption spectrum was given by Kranendonk.[7] We shall not, however, use the general, complicated formulas of reference 7, and in considering the collision process we shall apply a simpler method of quasi-classical approximation. In this case, the differential absorption of coefficient will be proportional to the square of the modulus of the matrix element $(j_1 \,|\mu(\omega)|\, j_2)$ of the Fourier amplitude of the dipole moment $\mu(t)$, the time dependence of which is determined by the relative coordinates of A and B. The frequency ω is taken here from the center of the band ω_0 which corresponds to the rotational transition $j_1 - j_2$.

We must express the field F in an invariant form, correct in any coordinate system. It is convenient to do this by introducing spherical coordinates for the vector $F_m (m = 0, \pm 1)(\sqrt{2}F_{\pm 1} = \pm F_x + iF_y, F_0 = F_z)$ and expanding F_m with respect to the irreducible tensors (see, for example, reference 8). Assuming

$$F = \nabla a \frac{P_2(\cos\theta)}{r^3},$$

where θ is the angle between the vector $r = r_{AB}$ and the axis of the diatomic molecule A, and using the gradient formula[8] we obtain

$$F_m = \left(a\nabla \frac{P_2(\cos\theta)}{r^3}\right)_m = a \sum_n Y_2^{*n}(\theta_1, \varphi_1) \frac{1}{r^4} C \times (1, 3, 2; -m, n+m)\, Y_3^{2+m}(\theta_2, \varphi_2), \tag{2}$$

where $C(l_1, l_2, l_3; m_1, m_2)$ are the Clebsch-Gordan coefficients. Here, and hereafter, all quantities which do not depend on the orientations of the molecules and the corresponding quantum numbers, and hence do not influence the band shape, are symbolized by a; the arguments θ_1, ϕ_1 and θ_2, ϕ_2 of the spherical functions symbolize the spherical angles of the axis of molecule A and of the vector r.

In accordance with what was said above, $\mu(\omega)$ may be written in the form

$$\mu_m(\omega) = a \sum_n Y_2^{*n}(\theta_1, \varphi_1)\, C(1, 3, 2; -m, n+m)\, I_3^{n+m}(\omega), \tag{3}$$

where the quantities $I_3^n(\omega)$ are equal to

$$I_3^n(\omega) = \int_{-\infty}^{\infty} Y_3^n(\theta_2, \varphi_2) \frac{e^{i\omega t}}{r^4}\, dt. \tag{4}$$

In evaluating the matrix element $(m_1, j_1 \,|\mu(\omega)|\, m_2, j_2)$, it is convenient to express all integrals of spherical functions by means of the Clebsch-Gordan coefficients. If then we average $|(m_1, j_1 \,|\mu(\omega)|\, m_2, j_2)|^2$ over the initial quantum numbers m_1 and sum over m_2 and m, we obtain for the band shape $f(\omega)$ the following expression, in which

we neglect the slight dependence on ω of the proportionality coefficient between $f(\omega)$ and $\left|\left(j_1\left|\mu\left(\omega\right)\right|j_2\right)\right|^2$:

$$f(\omega) = a \cdot (2j_2+1)\, C(j_1,\ j_2,\ 2;\ 0,\ 0)^2 \sum_n \left|I_2^n(\omega)\right|^2. \qquad (5)$$

The index n, as can be seen from (3), runs from −3 to +3. From the first factor of expression (5) there follows the selection rule $j_2 = j_1 \pm 2$. For the calculation of the second factor, we assume, as is customarily done, that the interaction between A and B may, to a sufficient degree of accuracy, be considered as central. In this case it is convenient to choose a coordinate system (see, for example, reference 9) whose z = 0 plane coincides with the plane of the trajectory of the relative motion of A and B. Thus the polar angle of the vector r equals $\theta_2 = \pi/2$, and the relationships

$$Y_3^n(\theta_2,\ \varphi_2) = Y_3^n\left(\frac{\pi}{2},\ 0\right) e^{in\varphi} = e^{in\varphi} \begin{cases} \sqrt{\frac{7}{4\pi}}\, \frac{[(3-n)!\ (3+n)!]^{1/2}}{(3-n)!\ (3+n)!}\, (-1)^{\frac{3+n}{2}}, & n = 2p+1 \\ 0, & n = 2p. \end{cases} \qquad (6)$$

hold for the spherical functions.

The vanishing of the functions I_2^n for n = 0, ±2 corresponds to the selection rules $\Delta l = \pm 1,\ \pm 3$ for the moments of the relative motion. It is not difficult to see that the selection rules presented above for j and l correspond to a change in the total moment of the system A + B by ±1, as must be the case for dipolar absorption. Expressions (5) and (4) may now be rewritten in the form

$$f(\omega) = a\,(j_1,\ j_2) \sum_n b_n \left|I_0^n(\omega)\right|^2 \cong a\,(j_1,\ j_2) \sum_n b_n \left|\int_{-\infty}^{\infty} e^{i\omega t + in\varphi(t)}\, \frac{dt}{r^4}\right|^2, \qquad (7)$$

where the dependence of a on j_1 and j_2 is determined by the first factor of expression (5), and the coefficients b_n, on the basis of (6), are equal to

$$b_0 = 0,\ \ b_{\pm 1} = 1,\ \ b_{\pm 2} = 0,\ \ b_{\pm 3} = \frac{5}{3}. \qquad (8)$$

For the evaluation of the integrals in (7), we must find the time dependence of ϕ and r for the classical trajectory. The law of conservation of momentum gives

$$r^2\dot{\varphi} = v\rho, \qquad (9)$$

where v is the relative velocity of the molecules at infinity and ρ the impact parameter. Since, for the inelastic collisions which lead to band broadening, only the region of integration near the point of deflection is significant in the integrals (7), we may consider, as an approximation, that r in (9) does not depend on time. Actually, at the moment of deflection, r is equal to the gas-kinetic radius r_0, which is a few times larger than the radius of action of the exchange forces. Integration and substitution of (9) in (7) gives then

$$I^n(\omega) = \int_{-\infty}^{\infty} \exp\left[i\left(\omega + \frac{nv\rho}{r_0^2}\right)t\right] \frac{dt}{r^4(t)} = I\left(\omega + n\,\frac{v\rho}{r_0^2}\right). \qquad (10)$$

It follows from expressions (7) and (10) that each band of the rotational absorption spectrum consists of four bands similar in shape, the intensity of the outer ones being 5/9 that of the inner ones.

For the integration of (10), we approximate the interaction potential near the point of deflection by an exponential function with a radius of action $1/\alpha$. We shall consider the centrifugal energy term ρ^2/r^2, which changes slowly in comparison with $e^{\alpha r}$, as constant and equal to ρ^2/r_0^2. (Schwartz and Herzfeld's "variable quantum number" method[10]). The classical trajectory in this approximation is determined by the expression

$$e^{-\alpha r} = ch^{-2}\left(\frac{\nu(\rho)\,\alpha t}{2}\right), \qquad \nu(\rho) = v\sqrt{1-\frac{\rho^2}{r_0^2}}. \qquad (11)$$

We may also approximate the integrand function $r^{-4}(t)$ near the point of deflection by an exponential with radius of action $r_0/4$; namely, we assume

$$r^{-4} \sim \exp\left[-\frac{4\,(r-r_0)}{r_0}\right] = \text{const} \cdot ch^{-2y}\left(\frac{\nu(\rho)\,\alpha t}{2}\right), \quad y = \frac{4}{r_0\alpha}. \qquad (12)$$

Substituting (12) in (10), we find

$$I(\omega) = \text{const} \int_{-\infty}^{\infty} \frac{\exp\left[i\left(\omega + \frac{nv\rho}{r_0^2}\right)t\right]}{ch^{2y}\left(\frac{\nu(\rho)\,\alpha t}{2}\right)}\, dt$$

$$= c(\nu,\ \rho)\, B(y + i(x + nx_0),\ y - i(x - nx_0)), \qquad (13)$$

where $c(\nu, \rho)$ is some known function of v and ρ and the symbols $x = \omega/\alpha\nu(\rho)$, $x_0 = v\rho/r_0^2\alpha\nu(\rho)$ have been introduced. Expressing the B-function by means of the Γ-function, we finally obtain

$$f(\omega) = a \sum_n b_n \left|\Gamma(y + i(x + nx_0))\right|^2. \qquad (14)$$

If we consider the intensity of the wings of the $j_1 - j_2$ band we may use, in place of the Γ-function, the asymptotic expansion for $x \gg 1$. After averaging over the relative velocities and approach distances, there is obtained, as one can easily convince oneself, an expression which coincides, to within an unimportant factor, with the formula for the probability of an inelastic molecular collision (see, for example, references[10, 11]). In the rotational spectrum of induced absorption, however, it is impossible to study experimentally the intensity distribution in the wings, in consequence of the strong overlapping of the bands for different $j_1 - j_2$ transitions. The determination of the band width and of its shape near the maximum is more interesting.

We shall show that each band $(j_1 j_2 n)$ may be approximated by a Gaussian curve. In fact, expanding $\ln\Gamma(y + iz)$ in a series with $z = x + nx_0$, we obtain

$$\left|\Gamma(y+iz)\right|^2 = e^{2\mathrm{Re}\ln\Gamma(y+iz)} \cong \left|\Gamma(y)\right|^2 e^{-2\psi'(y)z^2},$$

$$\psi'(y) = \frac{d^2}{dy^2}\ln\Gamma(y), \qquad (15)$$

the band width being defined by the expression

$$\langle z\rangle = \int_{-\infty}^{\infty} \exp\left(-2\psi'(y)\,z^2\right) dz = \sqrt{\frac{\pi}{2\psi'(y)}}. \qquad (16)$$

The exact expression for the width, corresponding to the definition (16), is given by the formula

$$\langle z\rangle = \frac{1}{\left|\Gamma(y)\right|^2} \int_{-\infty}^{\infty} \left|\Gamma(y+iz)\right|^2 dz = \frac{2\pi\left|\Gamma(2y)\right|^2}{\left|\Gamma(y)\right|^4\,\Gamma(4y)}. \qquad (17)$$

Actual comparison of (16) and (17) in the range of y which is of interest to us ($0 \leq y \leq 1$) shows that the difference between these two expressions is entirely insignificant; this justifies the approximation made.

In averaging the function $f(\omega)$ over all approach distances in accordance with the expression

$$\langle f(\omega)\rangle = 2\pi \int_0^\infty f(\omega, \rho)\, \rho d\rho \qquad (18)$$

we may, as an approximation, take out all the factors which vary slowly with ρ from under the integral sign at the point where the integrand is a maximum. The corresponding evaluations give

$$\langle f(\omega)\rangle = a \sum_n \delta_n e^{-\beta V(\rho)\left[x^2 + \alpha x x_0 + \frac{1}{4}\alpha^2 x_0^2\right]} \Phi(x, x_0), \qquad (19)$$

where now $x = \omega/\sigma v$ and $x_0 = 1/r_0\alpha$, and $\Phi(x, x_0)$ is a function which varies slowly in comparison with the exponential. The intensity distribution $I(\omega)$ of the $j_1 \to j_2$ band is obtained after averaging $\langle f(\omega)\rangle$ over the velocities of the colliding molecules. In doing so, the following circumstance must be taken into consideration. In the quasi-classical approximation presented here, the variation in the velocity of the colliding molecules as a result of the inelasticity of the impact is neglected. The quantity v which enters into $\langle f(\omega)\rangle$ is actually some average of the initial and final velocities, $v = v(v_i v_f)$. It is easy to show[11] that one may assume $v = \frac{1}{2}(v_i + v_f)$ and $\bar{v}^2 = \frac{1}{2}(v_i^2 + v_f^2)$ and be accurate up to terms of order $(\hbar\omega/mv^2)^2$. We note that an analogous symmetrization of the probability has also been carried out in the classical calculation of the coulombic rotational excitation of nuclei.[9] It is not difficult to show then that averaging over the thermal distribution leads to the expression

$$I(\omega) = \exp\left(\frac{\hbar\omega}{2kT}\right) \cdot F(\omega), \qquad (20)$$

in which $F(\omega)$ is an even function of ω. The relation (20) is a particular case of the more general relation

$$\frac{I(\omega)}{I(-\omega)} = \exp\left(\frac{\hbar\omega}{kT}\right), \qquad (21)$$

which arises from the principle of microscopic equilibrium. For infrared spectra of induced absorption, the latter relation was verified in reference 2.

The function $F(\omega)$ will have a fairly complicated analytical form. But for the approximate estimation of the half-width of the band, it is sufficient to replace v in (19) by $\bar{v}$. The half-width $\Delta\omega$ of the band is approximately made up of the half-width of the outer band ($n = -3$) and its displacement $\Delta\omega_1$ with respect to the center ω_0. This displacement is determined by the position of the maximum of the outer band ($n = -3$):

$$2\frac{\Delta\omega_1}{a\bar{v}} - \frac{3}{r_0\alpha} = 0, \quad \Delta\omega_1 = \frac{3}{2}\frac{\bar{v}}{r_0}. \qquad (22)$$

On the other hand, the half-width of each band with $n = 1$, $n = 3$, on the basis of (16), equals

$$\Delta\omega_2 = \frac{1}{2}\sqrt{\frac{\pi}{2V(\rho)}} \cdot a\bar{v}. \qquad (23)$$

The half-width $\Delta\omega$ is the sum of these expressions:

$$\Delta\omega = \frac{\bar{v}}{2}\left[\frac{3}{r_0} + \sqrt{\frac{\pi}{2V(\rho)}} \cdot \alpha\right]. \qquad (24)$$

To estimate $\Delta\omega$ according to this formula, we assume $r_0 \approx 3$A and $m = 2$ (the reduced mass of A and B), which corresponds to the collision of H_2 with a heavy atom or molecule (Ar or N_2). The radius of action of the exchange forces, $1/\alpha$, may be approximately estimated on the basis of the well-known Morse potential curves for diatomic molecules, and may be taken as 0.5×10^{-8} cm. A similar value is also obtained in the determination of α from vibrational relaxation experiments.[10] The value taken for α corresponds to the value $y = \frac{2}{3}$. Substituting these values in (24), we get

$$\Delta\nu = \frac{\Delta\omega}{2\pi c} \simeq 7.3\sqrt{T}\ \text{cm}^{-1}. \qquad (25)$$

The experimental value of the half-width of the ($j_1 = 1 \to j_2 = 3$) band for the induced rotational absorption of H_2-Ar is $\Delta\nu = 8.15\sqrt{T}$ cm^{-1}.[3] Considering the inexact values of the quantities entering into (24), such agreement may properly be considered satisfactory.

In the rotational induced absorption spectra of hydrogen presented in reference 1, one may discern an asymmetry of the bands like that noted in the vibrational absorption spectra.[3] This asymmetry may be described by introducing two half widths $\Delta\nu_+$ and $\Delta\nu_-$, corresponding to positive and negative frequencies ω. Approximating the function F by a square curve and using (16) and (20), it is easy to evaluate $\Delta\nu_+$ and $\Delta\nu_-$. In doing so, one should simultaneously take account of the fact that actually $F(\omega)$ must also contain a factor $(\omega_0 + \omega)$, omitted in expression (5). For $T \simeq 300°$K, evaluation gives $\Delta\nu_+/\Delta\nu_- \simeq 1.5$-2, which corresponds qualitatively to the spectra presented in reference 1.

VIBRATIONAL ABSORPTION

The induced vibrational absorption of hydrogen in the region of the fundamental vibration frequency has been studied by a number of authors (see, for example, references 2-4). As may be concluded from these works, the Q-band of the spectrum is fundamentally connected with the dipole moment which arises when the wave functions of the colliding molecules overlap significantly. As might have been expected on the basis of purely qualitative considerations about the deformation of the electron cloud as the A + B pair approach each other, the induced dipole moment is directed along the collision line r_{AB}.[3] The spherical components of the dipole moment in this case equal.

$$\mu_m = f(r)\exp(im\varphi), \quad m = \pm 1; \quad \mu_0 = 0. \qquad (26)$$

The function $f(r)$ must diminish exponentially as r increases, with the same radius of action as characterizes the exchange interaction. Just the same conclusion is reached in an actual calculation based on the approximate wave functions of the system A + B.[3]

The angular dependence of μ_m leads to the appearance of two strongly overlapping bands (Q_P and Q_R bands), which were discovered during the study of the H_2 spectrum.[3] In our approximation, the distance $\delta\omega$ between the maxima of the Q_P and the Q_R bands equals

$$\delta\omega = \frac{\bar{v}}{r_0} \simeq \sqrt{\frac{3kT}{mr_0^2}}, \qquad (27)$$

which corresponds approximately to the rotational frequency of the rigid rotator A-B. A similar interpretation of the splitting was given in reference 2, where the temperature dependence of the splitting was also verified experimentally. We may determine the half-width $\Delta\nu$ of the Q band with the help of (24):

$$\Delta\nu = \frac{1}{2\pi c} \cdot \frac{\bar{v}}{2}\left[\frac{1}{r_0} + \sqrt{\frac{\pi}{2V(\rho)}}\,\alpha\right]. \qquad (28)$$

Assuming here $\alpha = 2 \cdot 10^8$ cm^{-1}, $y = 1$, $r_0 \simeq 3$A, $m = 2$, we find, at $T = 300°$K, $\Delta\nu \simeq 120$-130 cm^{-1}. The experimental value for the half-width of the Q band in the induced absorption of hydrogen is $\Delta\nu = 160$ cm^{-1}.[12] Such agreement

between the calculated and experimental values may be considered satisfactory.

As for the P and R bands of the vibrational spectrum, which are rotational satellites of the Q band, then, as calculation shows,[7] the corresponding dipole moment arises both as a consequence of the overlap of the electron clouds during collision (exchange interaction) and as a result of the polarization of the hydrogen molecule by the quadrupole field of its partner. For the latter case, the selection rule for l will be the same as in the case of rotational absorption. Estimation of the half-width of the P and R bands must be made by simultaneously taking account of the exchange and quadrupole interactions of the molecules.

If we had considered not induced absorption but induced emission of dipoleless molecules, then it is easy to see that we should have obtained for the intensity distribution, to within an unimportant factor, the same expression (20), with the difference, however, that ω would be replaced by $-\omega$. This indicates that the bands of induced rotational (vibrational) absorption and emission are symmetrical with respect to the corresponding rotational (vibrational) frequencies. This symmetry is analogous to the symmetry of the absorption and luminescence bands of the electronic spectra of complex molecules. Actually, a significant interaction of electronic and nuclear motions in complex molecules corresponds in our case to an interaction of the rotations or vibrations of the molecules with their translational motion; rapid establishment of a distribution equilibrium among the vibrational states during electronic excitation of complex molecules corresponds to a Maxwell distribution of the colliding molecules with respect to velocity; and, finally, equality of the matrix elements of the dipole moment for the transitions $i \to j^*$ and $j \to i^*$ (i and j are sets of quantum numbers for the ground state, i^* and j^* for the excited state), which leads to the mirror symmetry of the absorption and luminescence bands, also holds for induced absorption. Furthermore, the broadening of the absorption and luminescence bands, and also their "expansion" when the temperature is raised, find a qualitative analogy in induced absorption spectra. In this connection, one may suppose that theoretical consideration of the regularities in induced infrared absorption at high pressures, when the asymmetry of the absorption bands increases, may be of interest also for the study of the electronic spectra of complex molecules.

REFERENCES

1. J. P. Colpa and J. A. A. Ketelaar. Mol. Phys. **1**, 15 (1958).
2. D. A. Chisholm and H. L. Welsh. Can. J. Phys. **32**, 291 (1954).
3. J. Van Kranendonk and R. B. Bird. Physica **17**, 969 (1951).
4. R. F. Britton and M. F. G. Crowford. Can. J. Phys. **36**, 761 (1958).
5. J. P. Colpa and J. A. A. Ketelaar. Mol. Phys. **1**, 343 (1958).
6. J. Van Kranendonk. Physica **24**, 347 (1958).
7. J. Van Kranendonk. Physica **23**, 825 (1958).
8. M. Rouz. "Polya mul'tipolei." (Multipole Fields), IL, Moscow, 1957.
9. K. Alder, A. Bohr, T. Huus, B. Mottelson, and A. Winther. Revs. Modern Phys. **28**, 432 (1956).
10. R. N. Schwartz and K. F. Herzfeld. J. Chem. Phys. **22**, 767, (1954).
11. E. E. Nikitin. Opt. i Spektr. **6**, 141 (1959).

VIBRATIONAL SPECTRA OF AROMATIC COMPOUNDS VI. CALCULATION AND INTERPRETATION OF THE VIBRATIONAL SPECTRA OF O-XYLENE

M. A. Kovner and A. M. Bogomolov

Received 10 April 1959

A calculation of the frequencies and forms of the vibrations of the o-xylene molecule has been carried out. A set of fundamental frequencies of the molecule has been established and their assignment to symmetry types and to vibrations of bonds and valence angles has been given. A correlation of the frequencies and forms of the o-xylene and benzene vibrations has been established.

We take "interpretation of the vibrational spectra of an alkylbenzene" to mean the solution of four problems.

1. The subdivision of the observed frequencies into fundamental and combination; the estimation of fundamental frequencies which, for various reasons, are not observed in the spectra (prohibition of lines by the selection rules, merging of lines, the presence of very weak lines or masking of weak lines by intense neighbors, the presence of low-frequency lines which are difficult to observe in the infrared spectrum); the setting up of a complete set of $3N - 6$ fundamental frequencies of the molecule (N is the number of atoms) and, finally, their assignment to the irreducible representations (symmetry types) of the symmetry group to which the molecule belongs.

2. The assignment of the fundamental frequencies of each given symmetry type to the vibrations of one or more bonds, one or more valence angles; in particular, the assignment of frequencies to vibrations of the ring and of the alkyl groups.

3. The establishment of a correspondence between the ring vibrations in the alkylbenzene and in benzene itself, and between the frequencies of these vibrations.

4. The assignment of the composite frequencies to linear combinations of the fundamental frequencies.

In our previous articles of the present series, only the first and fourth problems were completely solved. For their solution, it proved sufficient to complete the solution of the secular equations by the method of stepwise diagonalization and to compare the calculated and observed frequencies, as well as to match the intensities (I) and depolarizations (ρ) with the selection rules and the general theoretical concepts of the properties of I and ρ in Raman spectra and of I in infrared spectra. The solution of the second and third problems has been of only

an orienting and conditional character, since it demands knowledge of the vibrational form coefficients (v. f. c.), to which we have repeatedly referred in previous articles.

In the present work all four problems have been fully solved. This has proved possible because the v. f. c.*

*The v. f. c. matrices are very unwieldy, and we cannot include them in this article.

have been calculated by one of us (A. M. Bogomolov) for all frequencies of the o-xylene molecule, according to a special program worked out as a method[1] of making the roots of secular equations more precise and determining the v. f. c. (the eigenvectors of the matrix of the secular equations).

For the o-xylene molecule, three geometric models A, B, C may be offered.[2] Calculation of the repulsion energy between the hydrogen atoms of the two methyl groups according to the approximate formula of Van Vleck and Cross[3] leads to the values 0.22, 0.34, and 0.85 ev for models A, B, and C. The minimum repulsion energy corresponds to model A, shown in the figure, and consequently the calculation of the frequencies and v. f. c. was carried out for this model. However, our check calculations show that the differences in the calculated frequencies for all three models lie within limits which would have no effect on the interpretation.

The o-xylene molecule belongs to the symmetry group C_{2v}, and the classification of its 48 frequencies according to symmetry types has the form: 16 A_1 + 15 B_1 + 9 A_2 + 8 B_2. Symmetry type A_1 includes 11 ring vibrations and 5 methyl group vibrations. Correspondingly, B_1 has 10 and 5; A_2, 5 and 3; B_2, 4 and 3. Symmetry types A_2 and B_2 each include one twisting vibration which was not taken into consideration in the calculation. The symbols for the internal vibrational coordinates of the planar vibrations of the ring and the vibrations of the methyl groups are shown on the figure. Besides these, there were introduced coordinates of type ρ, describing the movement of the C—H and C—C bonds from the plane of the ring, and of type κ, describing the nonplanar vibrations of the carbon skeleton of the ring.

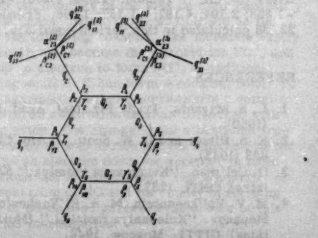

For the solution of the second and third problems, the entire calculation was carried out in two sets of ring-vibration symmetry coordinates: (1) in a set of coordinates with the approximate symmetry D_{2h},[4] in which the calculation of the frequencies and v. f. c. for C_6H_6 and C_6D_6 was carried out,[5,6] and (2) in a set of coordinates with the exact symmetry C_{2v}, which are sums and differences of pairs of the equivalent coordinates shown in the figure, and of pairs of coordinates of types ρ and κ. Only Q_2, Q_3, κ_{12}, and κ_{45} appear as single symmetry coordinates. In both cases, the same symmetry coordinates were introduced to describe the vibrations of the methyl groups; namely, coordinates with the approximate symmetry C_{3v},[4] for which the ethane force constants were assumed. During calculations in set (1), the force constants found in references 5 and 6 were used directly, except for the force constants of the coordinates with the symmetry $B_{2u}D_{2h}$, concerning which we make the following remark. In reference 7 there were described and discussed two variants (Nos. 1 and 2) of these force constants, while in the interpretation of the spectrum of m-xylene,[7*] and also of octadeuterotoluene[8] the advantageous character of variant No. 2 was shown.[9,10] The latter leads to better agreement of the calculated and observed frequencies in the case of o-xylene as well. Consequently, in the present work, we give the results of the calculations carried out with this variant, which includes, beside the B_{2u} force constants, the values $k_\gamma(CCC) = 1.1 \times 10^5$ cm^{-2} and $m_\delta = m_\beta = 0$.

*See correction at end of this article.

For the calculation of the force constants in set (2), the coordinates with the exact symmetry C_{2v} were expressed by means of coordinates with the symmetry D_{2h} on the basis of the laws for the resolution of symmetry types:

$$C_{2v}\left\{\begin{array}{l} 11A_1 \to 2A_{1g} + 2B_{2u} + 3E_u^{-I} + 4E_g^{+I} \\ 10B_1 \to A_{2g} + 2B_{1u} + 3E_u^{-II} + 4E_g^{+II} \\ 5A_2 \to 2B_{2g} + 2E_u^{+II} + E_g^{-II} \\ 4B_2 \to A_{2u} + 2E_u^{+I} + E_g^{-I} \end{array}\right\} D_{2h}. \qquad (1)$$

The formulas (1) differ from the analogous formulas for m-xylene or toluene and from those given in reference 11 since in o-xylene the twofold axis does not pass through a C atom but bisects a C—C bond. Formulas (1) make it possible to express the force constants in C_{2v} coordinates by means of D_{2h} force constants[5-8] and, furthermore, they already establish some correlation between the frequencies of o-xylene and benzene; i.e., they contain a partial solution to the third problem, if the first problem is solved. However, a solution to the third problem is usually considered complete if to each ring-vibration frequency of the alkylbenzene there is matched some definite vibration frequency of benzene. Such a solution is possible only on the basis of matching the v. f. c., calculated in both sets of coordinates, (1) and (2), with each other and with the v. f. c. of benzene itself. The latter are known from references 5 and 12.

In the table are presented the frequencies observed in the Raman and infrared spectra of o-xylene by various authors and assigned by us, on the basis of calculation and of experimental data, as fundamental frequencies. For the Raman spectra $I_\perp$ and ρ from reference 13 are given. There are also included in the table the vibration frequencies found from the analysis of the vibrational structure of luminescence[11,14] and absorption[15] spectra. In the same table are presented the calculated frequencies, which in most cases agree sufficiently well with the experimental ones, and their assignment to symmetry types is given. These columns of the table exhaust the first problem. The solution of the second and third problems is based on the following conclusions, which come from the analysis of the v. f. c. and of the table itself.

1. The peculiarity of the vibrations of benzene and its derivatives consists in the fact that many vibrations are not at all localized in separate bonds or angles, but are vibrations in which all the CC bonds, the internal CCC angles, and the CCH angles take part to a significant degree. This delocalization of the vibrations is apparently connected with the delocalization of the bonds themselves, as a result of the delocalization of the π-electrons. Therefore, assignment of the ring frequencies to separate

bonds or angles is possible only in some cases, for which this assignment is given in the table (Nos. 2-4, 6, 23, 24, 43-46). For the rest of the ring vibrations, there is given only the type of vibrational coordinate which is principally represented in the given vibration.

2. The vibration frequencies of the CH_3 group (Nos. 14, 16, 18, 19, 27, 28, 30-33, 37-42) show a high degree of localization.

3. Frequencies Nos. 2-4, 6, 23, 24 are vibrational frequencies which have no analog in benzene, since they correspond to new structural elements, namely the external CCC angles and single C—C bonds. Therefore, no benzene frequencies are given for them in the last column of the table, in which the benzene frequencies are listed with their accepted numbering.

4. In many cases (Nos. 5, 8, 9, 13, 15, 17, 20, 22, 25, 26, 29, 34-36, 43-46) the forms of the ring vibrations in benzene and in o-xylene are fairly close and a regularity appears to vibrations which are similar in form. In the two molecules there correspond values of the frequencies themselves which are also fairly close.

Observed and Calculated Fundamental Vibration Frequencies of the o-Xylene Molecule and their Assignment to Symmetry Types, to Vibrations of Bonds and Valence Angles, and to Vibrations of the Benzene Molecule

No.	Experiment						Calculation			
	Ram.[13,14,19]			I.R.[20-22]		Lum. [11, 14]				
	ν	I_{est}	ρ	ν	I	ν	ν	Symmetry	Bonds, angles	C_6H_6 frequencies
1	180	220	0.78	—	—	180	183	A_2	τ	405; 16 b
2	—	—	—	—	—	—	211	A_1	$\beta_2 + \beta_3$ (CCC)	—
3	250	230	0.75	250	m.	256	238	B_2	ρ (C—C)	—
4	406	w.	—	406	w.	—	370	B_2	$\beta_2 - \beta_3$ (CCC)	—
5	433	w.	—	436	s.	—	425	B_1	τ	405; 16 a
6	—	—	—	—	—	—	486	A_2	ρ (C—C)	—
7	508	210	0.85	505	w.	506	508	B_1	τ	606; 6 b
8	582	320	0.30	580	w.	582	564	A_1	τ	606; 6 a
9	710	w.	—	694	m.	—	704	A_2	τ	703; 4
10	735	740	0.12	—	—	733	729	A_1	CC, CCC, CCH	—
11	—	—	—	720	s.	740	746	B_2	ρ (C—H)	849; 10 a
12	830	w.	—	830	w.	833	803	B_2	τ	1010; 12
13	862	39	—	860	w.	862	869	A_2	ρ (C—H)	849; 10 b
14	931	w.	—	940	m.	—	927	A_1	β^s (CH_3)	—
15							946	B_2	ρ (C—H)	970; 17 a
16	986	140	0.10	980	m	987	977	B_1	β^s (CH_3)	—
17							978	A_2	ρ (C—H)	985; 5
18	1022	w.	—	1022	m.	—	1025	B_2	β^s (CH_3)	—
19							1034	A_2	β^s (CH_3)	—
20	1052	450	0.10	1060	m.	1054	1084	A_1	CCH, CC	1037; 18 b
21	1118	w.	—	1120	s.	1118	1114	B_1	CCH	1178; 9 b
22	1150	170	0.54	1160	w.	1156	1154	A_1	CCH	1152; 15, 1178; 9 a
23	1223	430	0.11	1221	m.	1233	1227	B_1	$q_4 - q_7$ (C—C)	—
24							1239	A_1	$q_4 + q_7$ (C—C)	—
25							1275	B_1	CCH	1326; 3
26	1290	w.	—	1300	m.	1287	1306	A_1	CCH, CC	1309; 14
27							1380	A_1	β^A (CH_3)	—
28	1384	260	0.35	1380	s.	1381	1380	B_1	β^A (CH_3)	—
29							1447	B_1	CCH	1482; 19 a
30	1448	190	0.68	1460	vs.	1448	1454	A_1	α^s (CH_3)	—
31							1463	B_2	α^s (CH_3)	—
32	1480	w.	—	1480	vs.	—	1484	A_2	α^s (CH_3)	—
33							1497	B_2	α^s (CH_3)	—
34	—	—	—	1500	s.	—	1517	A_1	CCH	1482; 19 b
35	1583	230	0.57	1584	w.	1584	1610	A_1	CCH, CC	1596; 8 a
36	1609	430	0.62	1610	m.	—	1616	B_1	CCH, CC	1596; 8 b
37	2878	28	—	—	—	—	2898	A_1	γ^A (CH_3)	—
38	2919	w.	—	—	—	—	2898	B_1	γ^A (CH_3)	—
39	2971	w.	—	—	—	—	2975	A_1	γ^s (CH_3)	—
40							2975	B_1	γ^s (CH_3)	—
41							2975	A_2	γ^s (CH_3)	—
42	2983	w.	—	—	—	—	2975	B_2	γ^s (CH_3)	—
43	3030	w.	—	—	—	—	3052	A_1	$q_1 + q_4$ (CH)	3056; 7 a
44	3045	s.	—	—	—	—	3054	B_1	$q_2 - q_5$ (CH)	3056; 7 b
45	3079	m.	—	—	—	—	3068	A_2	$q_2 + q_5$ (CH)	3064; 20 b
46							3071	B_1	$q_1 - q_4$ (CH)	3064; 20 a

Notes: Symbols: Ram.—according to Raman spectra; I.R.—according to infrared absorption spectra; Lum.—according to luminescence spectra. Units: frequencies in cm^{-1}; intensities: s—strong, m—medium, w—weak, vs—very strong; I_{est} in units in which I_{est} of the 802 cm^{-1} line of cyclohexane equals 600. In the last column are the accepted numbers of the benzene frequencies.

5. Vibrations Nos. 1, 7, 11, 12, 21 suggest by their form the benzene vibrations listed in the table. However, these forms of vibration are somewhat distorted by the influence of the substituents, which are heavy compared to hydrogen, and this increase in weight brings about a marked lowering of the frequency.

6. Vibration No. 10 shows special properties. According to the values of I_{est} and ρ, it might have been assigned to the fully symmetrical benzene vibration with the frequency 992 cm^{-1}. However, with respect to its form, this o-xylene vibration has nothing in common with the benzene vibration cited. Almost all the CC bonds of the ring, the CCC and CCH angles, and also the vibrations of the C—C bonds which interact with them take part in it.

We have completed the interpretation of all 46 fundamental frequencies.

The fourth problem is easily solved (combination frequencies in cm^{-1}): 360[22]: 180 × 2; 619[22]: 180 + 436; 660-675[18-19]: 180 + 506, 250 + 433; 910[20]: 180 + 735; 1190[20, 21]: 180 + 1020, 250 + 940. In all cases these lines are observed to be very weak.

In conclusion we note that the interpretation of frequencies Nos. 11, 13, 14, 17, 20-22, 26, 29, 34-36 agrees completely with that proposed in referencec 24 and 25, where these frequencies were related to the characteristic frequencies of ortho-disubstituted benzenes. A special article of this series will be devoted to the characteristic frequencies of alkylbenzenes of all substitution types.

CORRECTION TO REFERENCE 7

In reference 7 on p. 303 in the first line, the Latin letter q should be replaced by the Gothic $\mathfrak{q}$, which is used to symbolize the coordinates of the ring CC bonds. The same substitution should be made throughout Tables 1 and 2 in lines 15, 25, 28, 32, 37, and 38 of Table 3.

Ten force constants of symmetry type A_1, namely those for the coordinate pairs q_1q_1, q_2q_2, q_2q_3, $q_2\Gamma_3$, $q_2\Gamma_4$, q_2q_5, $q_3\Gamma_3$, $q_3\Gamma_4$, $\Gamma_3\Gamma_3$, $\Gamma_3\Gamma_4$, $\Gamma_4\Gamma_4$ in variant No. 2 equal respectively (10^5 cm^{-2}): 13.233; −1.699; 2.568; −1.994; 13.233; −1.858; 2.704; 4.187; −1.737; 4.596. Frequencies Nos. 9, 22, 36 calculated in this variant equal 515, 1002, 1503 cm^{-1}.

REFERENCES

1. L. S. Mayants. Trudy Fiz. Inst. Akad. Nauk 5, 65 (1950).
2. K. S. Pitzer and D. W. Scott. J. Am. Chem. Soc. 65, 803 (1943).
3. G. Gel'man. "Kvantovaya khimiya." (Quantum Chemistry), ONTI, 1937.
4. M. V. Vol'kenshtein, M. A. El'Yashevich, and B. I. Stepanov. "Kolebaniya molekul." (Molecular Vibrations), GITTL, Moscow, 1949.
5. M. A. Kovner. Zhur. Eksp. i Teoret. Fiz. 26, 598 (1954).
6. M. A. Kovner. Doklady Akad. Nauk SSSR 97, 65 (1954).
7. M. A. Kovner and A. M. Bogomolov. Opt. i Spektr. 4, 301 (1958).
8. M. A. Kovner and G. V. Peregudov. Opt. i Spektr. 5, 134 (1958).
9. F. A. Miller. J. Chem. Phys. 24, 996 (1956).
10. S. Brodersen and A. Langseth. Kgl. Danske Videnskab Selskab, Mat.-fys. Skr. 1, 1 (1956).
11. P. P. Dikun and B. Ya. Sveshnikov. Zhur. Eksp. i Teoret. Fiz. 19, 1000 (1949).
12. M. A. Kovner and B. H. Snegirev. Opt. i Spektr. 5, 239 (1958).

13. G. S. Landsberg, P. A. Bazhulin, and M. M. Sushchinskii. "Osnovnye parametry spektrov kombinatsionnogo rasseyaniya uglevodorodov." (Fundamental parameters of Raman Spectra of Hydrocarbons). Izd. Akad Nauk SSSR, 1956.
14. P. Pesteil and A. Zmerli. Ann. Phys. 10, 1079 (1955).
15. C. D. Cooper and H. Sponer. J. Chem. Phys. 20, 1248 (1952).
16. Catalog of Raman spectral data. N. J., 1949.
17. M. R. Fenske, W. G. Braun, R. V. Wiegand, and D. Q. R. H. McCormick. Analyt. Chem., 19, 700, 1047.
18. E. G. Treshchova and V. M. Tatevskii. Doklady Akad. Nauk SSSR, 61, 841 (1948).
19. A. Ray. Indian J. Phys. 26/35, 226 (1952).
20. R. Barnes, R. C. Gore, U. Liddel, and V. Williams. "Infrared Spectra." N. J., 1944.
21. Zh. Lekont. "Infrakrasnoe izluchenie." (Infrared Radiation), GIFML (Fizmatgiz), 1958.
22. E. K. Plyler. Discussions Faraday Soc., No. 9, 100 (1950).
23. H. L. McMurry and V. Thornton. Analyt. Chem. 24, 318 (1952).
24. D. H. Whiffen. Spectrochim. Acta 7, 254 (1955).
25. R. R. Randle and D. H. Whiffen. "Molecular Spectroscopy." Inst. Petrol., 1955.

INFRARED SPECTRA OF NITRIC OXIDE ADSORBED ON TRANSITION METALS, THEIR SALTS AND OXIDES

L. M. Roev and A. N. Terenin

Received 18 June 1959

Infrared spectra of nitric oxide adsorbed on transition metals, their salts, and oxides were investigated. A series of absorption bands was observed in the region 1600-2000 cm^{-1}, with positions and intensities essentially dependent on the nature of the absorbent and on the experimental conditions. A detailed interpretation of the experimental data is given.

In recent years there has been increasing use of infrared absorption spectra in the investigation of adsorption phenomena. In the present work this method has been used to study nitric oxide adsorbed on transition metals, their salts and oxides. Since the transition metals and their oxides are widely used as catalysts in chemical reactions, the investigation of these substances is of particular importance. The study of adsorption on salts of the transition metals had the ancillary purpose of consolidating the interpretation of the spectra obtained with the metals and oxides; however, the study has also an independent interest from the point of view of the effect of the filling of the d-orbits of the ions on their capability of forming complexes. Nitric oxide was chosen as the adsorbate for the following reasons. The molecule easily gives up an electron to become the nitrosyl ion NO^+, and easily takes up an electron to form NO^-; in addition, while remaining neutral, it can form a covalent bond. To each of these aggregations there corresponds a definite shift of the infrared absorption band as compared with gaseous nitric oxide. The change in the vibrational frequency can be used as a criterion for the behavior of the NO molecule as an electron donor or acceptor in molecular interactions and in adsorption.[1] The simplicity of the infrared spectrum of NO and its faculty of forming various types of bonds also governed the choice of this molecule for the investigation.

EXPERIMENTAL DETAILS

(a) Preparations of the Dispersed Metal Samples

Chemically prepared samples of the transition metals are not suitable for infrared studies because of their low transmissivity. Considerably greater transmissivity can be obtained in samples in which the metal is deposited on the surface of a carrier with a relatively low weight percentage of the metal. In this case the size of the metallic particles, which form islands on the surface of the carrier, does not exceed 500 A.[2]

Alumina gel was used as the carrier; this has a large surface area, of the order of 300 m^2 per gm, and is transparent in a wide region of the infrared. The method used in depositing the dispersed metal on the carrier involved the adsorption of the corresponding metal carbonyl followed by the thermal decomposition of the carbonyl at a temperature of ~150°C. Samples of dispersed iron, nickel, and chromium were obtained in this way. We had previously used this technique of producing a dispersed metal in an investigation of the adsorption of carbon monoxide on nickel.[3]

In the case of nickel metallic samples were prepared also by the reduction of the oxide in an atmosphere of hydrogen. A comparison of the absorption of nitric oxide showed identical results for the two methods of preparation. However, the reduction method was impracticable for oxides which are difficult to reduce as, for example, chromic oxide.

(b) Preparation of Samples of Salts of the Transition Metals

As a consequence of their small surface areas, salts in the crystalline form cannot be used for adsorption studies by infrared spectra. It was therefore necessary to deposit the salts on a carrier of large surface area, just as in the case of the metals. The carrier chosen was aluminium oxide gel with a surface area of 300 m^2 per gm. The aluminium oxide was immersed in a solution of the salt in question for a period of 5-10 hr and afterwards dessicated at ~100°C. The last traces of water were removed by conditioning in a vacuum, as will be described below. The technique of depositing the salt from solution permitted the preparation of samples with a definite ratio by weight of salt to absorbent. In the samples used the salt content varied from 5 to 20% by weight.

(c) The Oxide Absorbents

The samples of ferric and chromic oxides were gel-like absorbents with a specific area of ~100 m^2 per gm. In the case of chromic oxide the spectra of NO adsorbed on the gel-like absorbent and on a sample prepared by

burning ammonium bichromate were compared; no differences in the spectra were observed.

Samples of nickel monoxide were obtained by the thermal decomposition of $Ni(NO_3)_2$. Nickel monoxide, freshly prepared in this way, had a satisfactorily large surface area.

After preparation by the methods described above the samples were coated on a fluorite plate. The thickness of the samples gave a weight per unit area of ~5-15 mg per cm^2. With thicknesses of this order the transmission of the samples in the region of 2000 cm^{-1} did not normally exceed 5-8%. This relatively low transmission of the samples necessitated the use of spectral slit widths of 10-20 cm^{-1}. An IKS-11 spectrometer was used for the measurements in the region 1000-2300 cm^{-1} with an NaCl prism. The curves reproduced below give the ratio I/I_0, where I_0 and I are the intensities transmitted by the sample before and after adsorption, respectively. Each spectrum was recorded several times with good reproducibility.

The conditioning of the surface of the samples was carried at ~150°C over a period of several hours in a vacuum of 5×10^{-5} mm Hg. The sample was then cooled down and a comparison spectrum recorded. The adsorption was carried out at ~20°C and a pressure of 20 mm Hg; the pressure varied a little from experiment to experiment. The spectrum of the sample with adsorbed nitric oxide was then recorded. Adsorption on ferric and chromic oxides was carried out also at ~150°C; comparison with the adsorption at room temperature showed no differences.

EXPERIMENTAL RESULTS

(a) Adsorption on the Metals

The spectrum of NO adsorbed on dispersed iron is reproduced in Fig. 1. A very intense absorption band at 2008 cm^{-1} and a series of weak bands at 1805, 1735, 1698, 1660, and 1625 cm^{-1} were observed. Pumping off the gas to a pressure of 10^{-4} mm Hg at 20°C over a period of 30 min led to the total disappearance of the band at 2008 cm^{-1} but left the rest of the bands practically unaltered (curve 2). Heating to 150°C with continuous pumping over a period of an hour led to the disappearance of the bands at 1735 and 1805 cm^{-1}. The bands at 1698, 1660, and 1625 cm^{-1} disappeared only with pumping and heating up to 350°C.

Figure 2 shows the spectra of NO adsorbed on nickel (curve 1) and on chromium (curve 2). Both spectra were obtained after adsorption for 10 min at 20°C. Just as in the case of iron, bands at 1735, 1698, 1660, and 1625 cm^{-1} were observed; within the limits of error of the measurements the frequencies are the same for all three absorbents. In the region of frequencies higher than 1800 cm^{-1} the spectra show marked differences from that of NO adsorbed on iron. For the adsorption on nickel there is an intense band at about 1850 cm^{-1}, and for chromium a series of bands of approximately equal intensities at about 1830, 1905, and 2010 cm^{-1}. After prolonged pumping at 20°C the band at 2010 cm^{-1} disappeared and the intensities of the bands at 1905 and 1830 cm^{-1} decreased for the adsorption of NO on chromium. These bands, and also the band at 1850 cm^{-1} for nickel, disappeared completely when the specimen was heated slightly.

(b) Adsorption on the Oxides

Spectra were obtained for NO adsorbed on ferric, chromic, and nickel oxides, as well as on the oxides, Al_2O_3 and SiO_2, which were used as the substrate for the adsorption of NO on the metals. A detailed discussion of the spectra observed will be given using ferric oxide as an example; the results for the other oxides will be summarized in a schematic diagram.

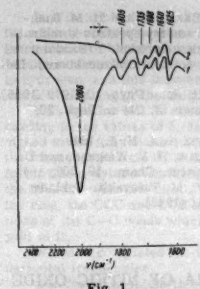

Fig. 1

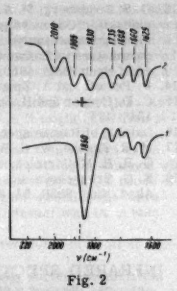

Fig. 2

Fig. 1. Infrared absorption spectrum of NO adsorbed on iron deposited on the surface of Al_2O_3. Curve 1—with the gas present; curve 2—after desorption at 20°C.

Fig. 2. Infrared absorption spectrum of NO adsorbed on (1) nickel and (2) chromium.

The spectrum of NO adsorbed on ferric oxide gel is reproduced in Fig. 3. A comparison of curves 1 and 2 shows that increasing the time of contact of the gas with the absorbent had no effect on the number of the bands, but led to an increase in the intensities of the bands at 1865, 1806, and 1770 cm^{-1}. Pumping out the gas without heating led to the disappearance of the bands at 1865 and 1770 cm^{-1} and to a decrease of the relative intensities of the bands at 1806 and 1738 cm^{-1} (curve 3). Curve 4 shows the spectrum after desorption at 150°C. The dotted

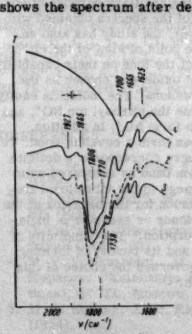

Fig. 3

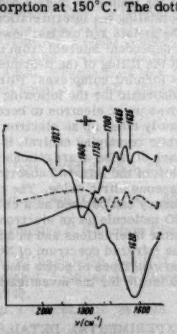

Fig. 4

Fig. 3. Infrared absorption spectrum of NO adsorbed on ferric oxide gel. Curve 1—adsorption at 20°C, 30 min interval; curve 2—adsorption at 20°C, 12 hr interval; curve 3—desorption at 20°C, 1 hr interval; curve 4—desorption at 150°C.

Fig. 4. Effect of admission of oxygen on the infrared absorption spectrum of NO adsorbed on ferric oxide gel. Curve 1—before admitting oxygen; curve 2—after admitting oxygen; curve 3—after evacuation at 20°C.

lines under the curves indicate the positions of the absorption bands of the N_2O_2 dimer (4). Figure 4 shows the change in the spectrum of the adsorbed NO molecule as a result of the admission of oxygen; the bands at 1927 and 1806 cm^{-1} disappeared and a very wide intense band appeared at about 1620 cm^{-1}. Pumping off the oxygen led to the spectrum shown in curve 3.

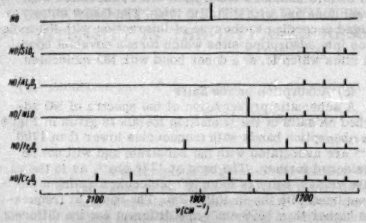

Fig. 5. Schematic presentation of the spectra of NO adsorbed on various oxides.

Figure 5 gives a schematic representation of the spectra of NO absorbed on the series of oxides which were studied. It can be seen from the diagram that the bands at 1625, 1660, and 1698 cm^{-1} coincide for all the absorbents within the limits of the experimental error and do not appear to be characteristic of the chemisorption of nitric oxide. The absorption bands at frequencies higher than 1800 cm^{-1} occur only for the oxides of the transition metals, their number and positions varying for the different oxides. In the transition from NiO to Cr_2O_3 the number of bands increases as the number of d-electrons in the atom of the metal decreases.

(c) Adsorption on the Salts

The group of salts studied was selected so that the number of d-electrons in the metal ion would change from salt to salt. Unfortunately, it was not possible to study ions with 1, 2, and 4 electrons, respectively, in the d-shell since these compounds are unstable. The type of anion had no effect on the NO absorption, since the spectra of NO adsorbed on the sulfates and nitrates of nickel and chromium showed no differences. The spectra obtained for NO adsorbed on the salts are shown schematically in Fig. 6. The configuration of the d-shell of the corresponding ion is given on the right of each spectrum. The absorption bands at frequencies lower than 1800 cm^{-1} were observed for all the salts studied; within the limits of the experimental accuracy their positions coincide. The

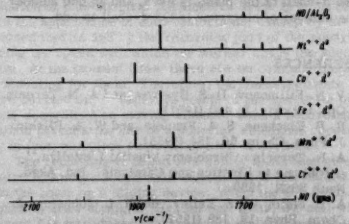

Fig. 6. Schematic presentation of the spectra of NO adsorbed on salts of various transition metals.

bands at frequencies higher than 1800 cm^{-1} change markedly from absorbent to absorbent. An examination of the diagram shows that the number of absorption bands higher than 1800 cm^{-1} is equal to unity if the number of d-electrons in the ion is even, and equal to three if the number of d-electrons is odd. A comparison of the relative intensities of the bands for Co^{++} and Mn^{++} shows that, of the three bands occurring higher than 1800 cm^{-1}, two predominate. The changes in the spectra on desorption were as follows: the bands at frequencies higher than 1900 cm^{-1} disappeared quickly after pumping at 20°C, those in the region 1800-1900 cm^{-1} required very slight heating (~50°C) for their disappearance, and those at frequencies lower than 1800 cm^{-1} disappeared only on heating higher than 150°C.

DISCUSSION OF THE RESULTS

The absorption band of gaseous nitric oxide has a frequency near 1876 cm^{-1}. When the nitrosyl ion NO^+ is formed the vibrational frequency shifts to the short wavelength region of the spectrum as a consequence of the removal of the single antibonding electron in the N=O bond.[5] A similar shift in the frequency should be observed for the following possible types of bonding of the NO molecule with the surface:

1) M^-NO^+ (ionic bond),

2) $M^- \ldots \overset{N}{\underset{O^+}{\|}}$ or $M^- : N \equiv O^+$.

In the second case the electron is only partially removed, and the NO frequency will be shifted towards the shorter wavelength region somewhat less than in the case of bond 1.

The formation of a covalent bond between NO and the surface can presumably occur according to the following schemes:

1) $M-N=O$, 2) $M^- = N^+ = O$, 3) $M : NO$.

For these types of bond the vibrational frequency could occur in the 1870-1700 cm^{-1} region, where the vibrational frequency of the double bond between nitrogen and oxygen in a series of compounds is known to lie.[7,8] On formation of the NO^- ion the NO vibrational frequency shifts into the 1000-1100 cm^{-1} region.[5] No absorption bands were observed in this region for NO adsorbed on the metals or on the salts and oxides.

(a) Adsorption on the Metals

The adsorption bands lower than 1700 cm^{-1}, observed in the spectra of NO on the metals, are due to the presence of the substrate and will be considered in the discussion of the oxides. The adsorption of NO on iron takes place for the most part according to the schemes:

$$M^- NO^+ \quad \text{or} \quad M^- \ldots \overset{N}{\underset{O^+}{\|}},$$

since the position of the predominant band at 2008 cm^{-1} (Fig. 1) is characteristic of NO^+, and the ease with which the band is removed indicates a comparatively weak bond with the surface. In addition to this bond other types also exist, as is indicated by the presence of the bands at 1805 and 1735 cm^{-1}, which are characteristic of the double bond between nitrogen and oxygen. Since these same bands are observed in the case of adsorption on ferric oxide, it can be assumed that the NO adsorption had taken place on oxidized iron. The technique of preparing the dispersed iron from the carbonyl excludes any possibility of oxidation of the metal from the outside. It is therefore

possible that the oxidation could have occurred with oxygen furnished by the substrate.

In the adsorption of NO on nickel, covalent or coordination bonds are formed for the most part, since the positions of the bands at 1735 and 1850 cm^{-1} are characteristic of the double bond between nitrogen and oxygen.

In the case of chromium (Fig. 2) various types of bonds between the NO molecule and the metal occur. The presence of the band at 2010 cm^{-1} indicates the formation of the nitrosyl ion. The bands at 1905 and 1830 cm^{-1} can be attributed to the following schemes:

$$M^- : NO^+; \quad M^- \cdots \overset{N}{\underset{O^+}{\|}}; \quad M^- = \overset{+}{N} = O,$$

and the band at 1735 cm^{-1} to the covalent bond M—N=O.

(b) Adsorption on the Oxides

A comparison of the spectrum of NO adsorbed on ferric oxide gel (Fig. 3) with the spectrum of dimer N_2O_2 immediately permits the correlation of the bands at 1865 and 1770 cm^{-1} with the formation of dimers on the surface of the gel. Since the vibrational frequencies of the dimer are not shifted, the bond between the dimers and the surface must be of the Van der Waals type. This is also indicated by the behavior of the bands on desorption.

A comparison of curves 1, 3, and 4 of Fig. 3 shows that the bands can be divided into two groups which behave in different ways on desorption. The bands higher than 1700 cm^{-1} can be eliminated at 150°C, whereas those lower than 1700 cm^{-1} disappear only at 350°C. Similarly, the admission of oxygen affects only the group of bands with frequencies higher than 1700 cm^{-1}. From this it can be concluded that these two groups of bands belong to NO molecules adsorbed on different sites on the surface of the ferric oxide gel.

The bands at 1700, 1665, and 1625 cm^{-1} of the chemisorbed molecules can probably be ascribed to the formation of a covalent bond with oxygen atoms of the absorbent. According to the data of Tarte,[9] the absorption bands of the —O—N=O group do in fact occur in the frequency region 1690-1610 cm^{-1}. Moreover, bands in the same region were observed in the present investigation in the adsorption of NO on a series of oxides with different metallic ions (Fig. 5).

The absorption bands at frequencies higher than 1700 cm^{-1} are observed only for the oxides of the transition metals and change in position from one oxide to another (Fig. 5). It is therefore natural to ascribe them to the adsorption of NO on the metallic ions. The band at 1735 cm^{-1} behaves differently from the others on admission of oxygen and belongs to molecules which are bound relatively strongly to the metallic ions. This bond could be the covalent bond M—N=O. The absorption bands near 1800 cm^{-1} fall in the frequency region of the N=O double bond and could belong to one of the schemes:

$$1)\ M : NO, \qquad 2)\ M^- = \overset{+}{N} = O.$$

However, scheme 2 is very close to the scheme $M^- : NO^+$, and in fact something intermediate between them is realized. Thus, the frequency should be somewhat higher than for scheme 1. It is more likely that the bands close to 1800 cm^{-1} belong to NO molecules bound according to scheme 1.

The band at 1927 cm^{-1} observed in the adsorption of NO on ferric oxide gel belongs to molecules bound to iron ions with formation of the NO^+ ion. The reason for this interpretation is the presence of the frequency, 1925 cm^{-1}, which has been observed in sodium nitroprusside, $Na_2[Fe(CN)_5NO]$,[8] in which the NO is present as the nitrosyl ion.

The bands at 2028 and 2093 cm^{-1} observed in the adsorption of NO on chromic oxide undoubtedly belong to NO^+ ions. The presence of two frequencies in this region can be ascribed either to different adsorption sites or to the bonding of two NO molecules with a single chromium ion, as has been observed for CO adsorbed on rhodium.[10]

Thus, the adsorption of NO on the oxides of transition metals indicates adsorption sites associated with oxygen ions and with metallic ions. The latter in turn are divided according to the type of interaction with NO molecules into adsorption sites which form a covalent bond, and sites which form a donor bond with NO molecules.

(c) Adsorption on the Salts

A schematic presentation of the spectra of NO adsorbed on salts of the transition metals is given in Fig. 6. The absorption bands with frequencies lower than 1700 cm^{-1} are associated with the substrate and will not be considered further. The band at 1735 cm^{-1}, as in the case of the oxides, belongs to an NO molecule forming a covalent bond with the metallic ion. The bands at frequencies higher than 1800 cm^{-1} are different for the different adsorbents.

In contrast to the oxides and the metals for which the electronic configurations of the d-orbits of the metallic ions are not known, each ion in the salts has a known number of d-electrons. For an even number of d-electrons (Fe^{++}, Ni^{++}) one absorption band higher than 1800 cm^{-1} is observed. The spectra of NO adsorbed on CO^{++}, Mn^{++}, and Cr^{++} ions show the same number of bands; each of these ions has an odd number of electrons. Each of the spectra of NO on these ions shows three absorption bands in the region higher than 1800 cm^{-1}. Thus, the nature of the spectrum of adsorbed NO depends basically on whether the number of d-electrons is even or odd. Of the various bonding schemes of NO molecules with ions of the transition metals,

$$1)\ M—N=O, \qquad 4)\ M^- = \overset{+}{N} = O,$$

$$2)\ M : NO, \qquad 5)\ M^- \cdots \overset{N}{\underset{O^+}{\|}}$$

$$3)\ M^- NO^+,$$

only the coordination band (scheme 2) is feasible with the even number of electrons available for the bond and with a frequency higher than 1800 cm^{-1}. On the other hand the number of bond types where the NO molecule furnishes an uneven number of electrons for the bond is equal to three (schemes 3, 4, 5). When the number of observed bands in the spectrum of adsorbed NO molecules is compared with the number of possible bond types, one arrives at the following conclusion: when the NO molecule interacts with the transition metals, it furnishes an even number of electrons for the bond if the number of d-electrons in the d-shell of the metal is even, and an odd number if the number of electrons in the d-shell is odd.

REFERENCES

1. V. N. Filimonov, D. S. Bystrov, and A. N. Terenin. Opt. i Spektr. 3, 480 (1957).
2. R. P. Eischens, S. A. Francis, and W. A. Pliskin. J. Phys. Chem. 60, 194 (1956).
3. A. N. Terenin. "Problemy kinetiki i kataliza." (Problems in Kinetics and Catalysis), Izd. Akad. Nauk SSSR, 1959.
4. A. L. Smith, W. E. Keller, and H. L. Johnston. J. Chem. Phys. 19, 189 (1951).
5. W. R. Angus and A. H. Leckie. Proc. Roy. Soc. A, 149, 327 (1935).

6. L. N. Short. Revs. Pure Appl. Chem. (Australia) 4, 41 (1954).
7. W. G. Burns and H. J. Bernstein. J. Chem. Phys. 18, 1669 (1950).
8. D. W. Magnuson. J. Chem. Phys. 20, 380 (1952).
9. P. Tarte. J. Chem. Phys. 20, 1570 (1952).
10. A. C. Yang and C. W. Garland. J. Phys. Chem. 61, 1504 (1957).

DETERMINATION OF THE ABSOLUTE VALUE OF PARAMETERS CHARACTERIZING INTENSITY IN THE INFRARED ABSORPTION SPECTRUM IN THE CASES OF THE ABSENCE OF TIME DISTORTIONS I

The calculated part of the present work carried out by I. V. Peisakhson, the experimental part by D. N. Shchepkin

V. M. Chulanovsky, I. V. Peisakhson, and D. N. Shchepkin

Received 14 March 1959

A description is given of the method of recording transmission in the infrared spectrum in the cases of the absence of time distortions. Also, three proposals of a method for the determination of spectral parameters (by optical density in the maximum, by integral density and the half width of the band) correcting for distortions brought in by the monochromator's apparatus function.

The obtaining of objective data, free from apparatus distortions and characterizing true intensity distribution in the absorption spectrum, is at the present time an actual methodical problem of molecular spectroscopy in the infrared region. The importance of the solution of this problem is determined not only by the broad utilization of infrared spectroscopy for structural and analytical purposes, but also by the very large number of different classes of substances with which one must work.* In these cases, the making of tables for the value of spectral parameters, correcting for errors brought in by apparatus and therefore suitable for work in any laboratory in practicable apparatus, frees the worker from the necessity of determining them anew, which in practice does not always prove to be possible.

*At the present time, investigations and documentaries on the infrared spectrum of more than 10,000 different organic substances.

The correction of apparatus distortions is particularly essential for infrared absorption bands, whose half-width in liquids ordinarily amounts to from a few up to 20-30 cm^{-1}, i.e., comparable with spectral slit width. Even by considerable increase in practical resolving power (going over from prisms to diffraction gratings) the problem of the determination of the true significances of spectral parameters does not lose its actuality.

In contemporary infrared single beam spectrophotometry, with the best recording, difficulties in the determination of true spectral parameters arise in connection with the appearance of time distortions, caused by increased inertia and by the recording part of the apparatus during the speed with which the worker scans the spectrum. At the present time, there are no common methods of deducting for them. Therefore, our measurements were carried out in separate points of the spectrum by using recordings on moving ribbons. Such a recording method permits the use of a superior automatic recording by, in fact, complete removal of time distortions.

The recording is begun at a closed beam that gives a zero intensity. A cell with solvent (I_0) is introduced into the beam on a sliding device. When the pen stops and begins to draw straight, parallel null lines, the cell with solvent I is introduced into the beam and thereupon the beam is closed again. The recording has the form represented in the drawing. The recording for every point requires only a little longer time than that necessary for overcoming inertia. Gained time is obtained for the calculation of the transmissions of the parts of the spectrum between points which can be taken with different densities in different parts of the spectrum (dependent on its detailed structure). Complementary gained time is given by the greater simplicity (and certainty) of the measurement of the height of the point (I) above the zero line, necessary for obtaining the value of the optical density $k_\nu (k_\nu = \log I_{0\nu}/I_\nu)$. Partial control of the null line saves the necessity of making a control run which is impossible to avoid on a recording of a continuous curve if sure and accurate intensity determinations are necessary.

Example of a recording for discrete points of the infrared spectrum.

During the described working conditions inertial distortions are completely avoided, but distortions brought in by noise may be averaged out comparatively simply.

The influence of the spectral instrument on the investigated curve in this case is completely characterized by the monochromator's apparatus function which is determined as the change of light current (having passed through the exit slit) is displaced with respect to the width of the monochromatic image of the entrance slit.

Let the true spectral distribution of energy entering the instrument be given by the function f(x) (x is expressed in wave number distances from a certain fixed point of the contour band, for example from its maximum). Then the observed distribution is described by the formula

$$F(x_1) = \int_{-\infty}^{\infty} f(x)\, A(x_1 - x)\, dx. \qquad (1)$$

The apparatus function A(x) is normalized thus, in order

$$\int_{-\infty}^{\infty} A(x)\, dx = 1. \qquad (2)$$

The monochromator's apparatus function is deter-

mined by the width of its slit, diffraction phenomena, and aberrations of the optical system. If, calculated according to the fundamental laws of geometrical optics, the width of the figure dispersed in the infinite image of the narrow slit does not exceed the normal slit width, then the instrument can be considered without aberration.[1] That is the condition fulfilled in most monochromators for the infrared region from contributing parabolic mirrors; in particular, it is accomplished in the instrument IKS-11 in the working region with prisms of NaCl and KBr, but at limited slit heights up to 10-12 mm. and also with LiF prisms. Thereby in the case of incoherent illumination of the entrance slit, the apparatus function is the result of the average distribution of illumination in the infinite diffraction image of the narrow slit.

$$\varepsilon(x)=\frac{1}{\Delta\nu_0}\frac{\sin^2\frac{\pi x}{\Delta\nu_0}}{\left(\frac{\pi x}{\Delta\nu_0}\right)^2} \tag{3}$$

With respect to the width of the entrance and the exit slits

$$A(x_2)=\frac{1}{\Delta\nu_2}\int\limits_{x_2-\frac{\Delta\nu_2}{2}}^{x_2+\frac{\Delta\nu_2}{2}}dx_1\,\frac{1}{\Delta\nu_1}\int\limits_{x_1-\frac{\Delta\nu_1}{2}}^{x_1+\frac{\Delta\nu_1}{2}}\varepsilon(x)\,dx. \tag{4}$$

Here $\Delta\nu_0$ is the normal slit width, expressed in wave numbers (limit of the resolution according to Rayleigh), $\Delta\nu_1$ and $\Delta\nu_2$ correspondingly the spectral width of the entrance and the exit slits measured by the difference in wave numbers corresponding to the width of the image of the entrance slit S_1 or the exit slit S_2.

$$\Delta\nu_{1,2}=S_{1,2}\frac{d\nu}{dl}, \tag{5}$$

where $d\nu/dl$ is the difference in wave numbers per unit length of the spectrum.

Formerly, it was shown[1] that at $\Delta\nu_1=\Delta\nu_2=\Delta\nu$ the apparatus function, expressed by the formulas (3) and (4), can be approximately represented by triangular distribution

$$A(x)\approx\frac{1}{\Delta\nu_e}\left(1-\frac{|x|}{\Delta\nu_e}\right)\quad\text{for}\quad |x|\leqslant\Delta\nu_e, \tag{6}$$

whose half-width is

$$\Delta\nu_e=\sqrt{\Delta\nu^2+\Delta\nu_0^2}. \tag{7}$$

In other words, the measured distribution of practical energy does not differ from that distribution which in the absence of diffraction would be given by a monochromator with a slit width $S_e=\Delta\nu_e/(d\nu/dl)$. Hence the value $\Delta\nu_e$ is called the effective spectral slit width. Formula (7) is derived by the approximation of the diffraction distribution by the Gaussian error curve, having that same area as the curve (3). A small error is brought in by this, but expression (7) for $\Delta\nu_e$ at rather narrow slits is accurate, for which the authors offer a series expressed in the form

$$\Delta\nu_e=\Delta\nu+\varphi\Delta\nu_0, \tag{7a}$$

where ϕ is a certain constant.

In the case of partial coherence of illumination of the slit, the half-width of the curve A(x) is a little less than that in completely incoherent illumination.[2] However, the influence of the method of illumination of the slit on the distribution of energy is insignificant, but at $\Delta\nu>2\Delta\nu_0$ it cannot be discounted, if only the objective (lens) of the collimator is completely filled. At slits of five and more times the normal width, the role of diffraction in the widening of the image of the slits is insignificant and generally need not be taken into account.

In the case of significant aberrations of the monochromator's optical system, it is not always possible to express its apparatus function analytically. But, as calculations showed, in this case also the approximation A(x) is allowed in the triangular form (6), if $\Delta\nu_e$ is assumed equal to the half-width of the curve A(x). In this way, the influence of the monochromator's optics on the results of quite complete measurements is characterized by only one quantity, $\Delta\nu_e$—the half-width of the curve of its apparatus function.

The integral equation (1) at the nucleus (6) can be brought into the form

$$F(x_2)=\frac{1}{\Delta\nu_e}\int\limits_{x_2-\frac{\Delta\nu_2}{2}}^{x_2+\frac{\Delta\nu_2}{2}}dx_1\,\frac{1}{\Delta\nu_e}\int\limits_{x_1-\frac{\Delta\nu_1}{2}}^{x_1+\frac{\Delta\nu_1}{2}}f(x)\,dx. \tag{8}$$

As was shown in reference 1, formula (8) is correct and can be expressed by a series containing only even derivatives of the function f(x)

$$F(x)=f(x)+f''(x)\frac{\Delta\nu_e^2}{12}+f^{(IV)}(x)\frac{\Delta\nu_e^4}{360}+\ldots \tag{9}$$

Inversely, the true distribution is expressed, and through observation it is possible to obtain

$$f(x)=F(x)-F''(x)\frac{\Delta\nu_e^2}{12}+F^{(IV)}(x)\frac{\Delta\nu_e^4}{240}-\ldots \tag{10}$$

In those cases when $\Delta\nu_e$ does not exceed the true half-width of the band, three terms of the series (10) are sufficient for the calculation of significant f(x) with accuracy of that same order as the error of photometric measurements. For more narrow slits, two terms of the series are sufficient.

In the application to absorption spectra, f(x) in formula (1) represents the true transmission of the investigated substance, interestingly connected (by us) with the true optical density k(x) by the equation

$$f(x)=e^{-k(x)}.$$

Correspondingly

$$F(x)=e^{-K(x)}$$

for the observed transmission, where K(x) is the observed optical density. Limited to two terms for small $\Delta\nu_e$, by means of uncomplicated conversions we obtain

$$K(x)=k(x)-\left\{[k'(x)]^2-k''(x)\right\}\frac{\Delta\nu_e^2}{12}. \tag{11}$$

From formula (11) very general approximations are obtained of the correlation between the true and observed values of the maximum intensity, the half-width of the absorption bands, and also the integral absorption of the substance.

1. We designate by x_m and k_m the abscissa and the ordinate of the true maximum of the absorption curve. Then $k'(x_m)=0$, and for contours even though approximately symmetrical (i.e., for those whose curves also have extremes in the neighborhood of $x=x_m$) it is possible to assume that the maximum of the observed curve (K_m) also holds at $x=x_m$. Hence

$$K_m=k_m+\frac{k''(x_m)}{12}\Delta\nu_e^2 \tag{12}$$

for $k''(x_m)<0$.

2. Let the true half-width of the symmetrical absorption band equal b_0, i.e.,

$$\left(\pm\frac{b_0}{2}\right)=\frac{k(0)}{2}.$$

The observed half-width b is determined from the condition

$$K\left(\pm\frac{b}{2}\right)=\frac{K(0)}{2}.$$

Having considered K(x) as a function of x^2 and transformed it into a progressive series of the difference $x^2 - (b_0/2)^2$, we have for $x = b/2$

$$K\left(\frac{b}{2}\right)=K\left(\frac{b_0}{2}\right)+K'\left(\frac{b_0}{2}\right)\frac{b^2-b_0^2}{4b_0}.$$

$x = b_0/2$ is substituted into (11) and $K'(b_0/2)$ is calculated by differentiating (11), and having preserved terms not higher than the second order with respect to b and $\Delta\nu_s$, we obtain

$$K\left(\frac{b}{2}\right)=k\left(\frac{b_0}{2}\right)-\left\{\left[k'\left(\frac{b_0}{2}\right)\right]^2-k''\left(\frac{b_0}{2}\right)\right\}\frac{\Delta\nu_s^2}{12}+k'\left(\frac{b_0}{2}\right)\frac{b^2-b_0^2}{4b_0}.$$

Since $x_m = 0$ for symmetrical bands, by equality (12) gives

$$K\left(\frac{b}{2}\right)=k\left(\frac{b_0}{2}\right)+k''(0)\frac{\Delta\nu_s^2}{24}.$$

Hence

$$b^2=b_0^2+\frac{k''(0)+2\left\{\left[k'\left(\frac{b_0}{2}\right)\right]^2-k''\left(\frac{b_0}{2}\right)\right\}}{k'\left(\frac{b_0}{2}\right)}\cdot\frac{b_0\Delta\nu_s^2}{6}. \quad (13)$$

It follows that one may expect that the correlation of form (13) holds also for slightly assymmetrical bands.

3. Having calculated the observed integral absorption

$$I=\int_{-\infty}^{\infty}K(x)\,dx$$

by like terms, by integrating (11) we obtain

$$I=I_0-\frac{\Delta\nu_s^2}{12}\int_{-\infty}^{\infty}[k'(x)]^2\,dx, \quad (14)$$

where

$$I_0=\int_{-\infty}^{\infty}k(x)\,dx$$

is the true integral absorption. Formulas (12) and (13), suitable for narrow slits and the case of symmetrical or almost symmetrical bands, can be rewritten for practical purposes in more convenient form

$$k_m=K_m+c_1\Delta\nu_s^2, \quad (15)$$

$$b_0^2=b^2-c_2\Delta\nu_s^2. \quad (16)$$

Coefficients c_1 and c_2 depend on the true shape of the band and consequently remain constant at measurements with a given sample substance. Having measured K_m and b for several significant slit widths, k_m and b_0 can be determined by means of linear extrapolation of dependents K_m and b^2 from $\Delta\nu_s^2$ to $\Delta\nu_s = 0$.

Having assumed $k(x) = k_m\phi(x)$, where $\phi(x_m) = 1$, (14) can be rewritten in the form

$$I=I_0-\frac{I_0k_m\Delta\nu_s^2}{12}\cdot\frac{\int_{-\infty}^{\infty}[\varphi'(x)]^2\,dx}{\int_{-\infty}^{\infty}\varphi(x)\,dx},$$

i.e.,

$$I_0=I+c_3k_m\Delta\nu_s^2. \quad (17)$$

In this way, the linear dependence of the observed integral absorption I on the maximum optical density k_m, established by Ramsay[4] for dispersion band forms, must be fulfilled for any approximately symmetrical bands.

It is advantageous to determine the true significances of spectral parameters with respect to their observed significances at a constant spectral slit width. Also the measurements require less time and can be carried out at the most favorable value of $\Delta\nu_s$. For the solution of this problem in general form expression (10) may be used. With the same degree of accuracy as before, and by those same procedures, we obtain

$$k(x)=K(x)+\{[K'(x)]^2-K''(x)\}\frac{\Delta\nu_s^2}{12}. \quad (18)$$

For the true half-width of the band, we have the expression

$$b_0^2=b^2-\frac{K''(0)-2\left\{\left[K'\left(\frac{b}{2}\right)\right]^2-K''\left(\frac{b}{2}\right)\right\}}{K'\left(\frac{b}{2}\right)}\cdot\frac{b}{6}\Delta\nu_s^2, \quad (19)$$

and for the true integral absorption

$$I_0=I+\frac{\Delta\nu_s^2}{12}\int_{-\infty}^{\infty}[K'(x)]^2\,dx. \quad (20)$$

Formulas (18)-(20) differ from the corresponding formulas (12)-(14) only by what goes into them of significance derived from K(x) but not from k(x), and the results of the calculations with respect to that and the other group of formulae differ by the values of the fourth order with respect to $\Delta\nu_s$. These formulas are not applicable to narrow slits but for $\Delta\nu_s < b/2$, they permit the obtaining of simple quantitative relationships between the true and observed values and explain the influence of the shape of the absorption curve on distortion values, brought into the results of the measurements by the monochromator's optics.

In these cases, when the shape of the contour of the absorption band is known, these general formulas can be made specific and utilized for the determination of the true significances of k_m, b_0, and I_0 with respect to their observed significances by one quantity $\Delta\nu_s$. Thus, for a band whose contour is expressed by the dispersion curve

$$K(x)=\frac{A}{x^2+\left(\frac{b}{2}\right)^2}$$

formulas (18) and (20) give

$$k_m=K_m\left(1+\frac{2}{3}\frac{\Delta\nu_s^2}{b^2}\right) \quad (21)$$

and

$$b_0^2=b^2-\left(2-\frac{K_m}{3}\right)\Delta\nu_s^2. \quad (22)$$

Expressions (21) and (22) determine the significances of absorption in the maximum and the half-width of the band with accuracy not less than 2-3% at $\Delta\nu \leqslant 0.4b$ and $K_m \leqslant 2$. Results of the calculations with respect to these formulas agree well with the data obtained by other authors[4,5] using a more complicated method.

For the value of the true integral absorption of a substance, formula (20) gives

$$I_0=I\left(1+\frac{K_m\Delta\nu_s^2}{12b^2}\right). \quad (23)$$

In agreement with the results given in references

4 and 5, the error in the determination of the integral absorption of the band is considerably less than the errors in the determination of absorption in the maximum and the half-width.

As calculations showed,[1] formulas (21)-(23) are suitable also in the case of the contour having the form of a slightly asymmetrical dispersion curve. In a series of experimental works (see, for example, the work of Russel and Thompson[2]) it was shown that the approximation of the distribution of optical density in simple infrared bands by the dispersion formula of Lorenz reflects their properties well. From this it follows that the simple formulas (21)-(23) can be used with success in the determination of the true significances of spectral parameters.

Difficulties in the determination of true integral absorption have another source and appear for the most part on account of the slow decline of the band to zero. Frequently the integral absorption of the band is distorted by the imposition of other combining bands amplified as a result of Fermi resonance, etc. In formulas (21)-(23), evidently, the dependence of the amount of correction on the observed parameters entered from the relation of the effective slit width to the observed half-width of the band. Such dependence, limiting the use of our calculations to the case of isolated bands, does not bear upon the principal character, and the method of determination of the true significance of spectral parameters can be otherwise constructed.

That is all the more important since the characteristic of the absorption spectrum is necessary for the true distribution of the optical density (or of the coefficient of absorption) in those cases, also, when the spectrum consists of poorly resolved continuous bands or of extra maxima and minima on the background of continuous absorption.*

*It is understood that the determination of the null line in these cases requires the taking of spectral measurements.

For the determination of the true optical density in the maxima or minima of the absorption curve, where $K'(x) = 0$, formula (18), which in the given case takes the form (24), can be used.

$$k(x_m) = K(x_m) - \frac{K''(x_m)\,\Delta\nu_x^2}{12}. \qquad (24)$$

The second derivative at the point $x = x_m$ can be determined approximately with respect to the significants K(x) for three equidistant significants x

$$K''(x_m) = \frac{1}{h^2}\,|K(x_m + h) + K(x_m - h) - 2K(x_m)|.$$

which after substitution into (18) gives

$$k(x_m) = K(x_m) + \left[K(x_m) - \frac{K(x_m + h) + K(x_m - h)}{2}\right]\frac{\Delta\nu_x^2}{6h^2}. \qquad (25)$$

It follows that the significants $K(x_m)$ and $K(x_m \pm h)$ may be taken around the maximum or minimum of the experimental curve's distribution of intensity.

REFERENCES

1. I. V. Peisakhson. Vestnik LGU, No. 5, 129 (1955).
2. R. A. Russel and H. W. Thompson. Spectrochim. Acta, 9, 133 (1957).
3. S. G. Rautian. Kand. diss., Fiz. Inst. Akad. Nauk, SSSR, (1957).
4. D. A. Ramsay. J. Am. Chem. Soc., 74, 72 (1952).
5. "Methods of Investigation of Petroleum and Petroleum Products," p. 235, Gostoptekhizdat, Moscow, 1955.

THE LOW TEMPERATURE LUMINESCENCE OF ZINC OXIDE IN THE RED REGION OF THE SPECTRUM

V. V. Osiko

Received 4 April 1958

The low temperature luminescence characteristics of pure and manganiferous zinc oxide in the red region of the spectrum are described.

A large number of papers have been devoted to the photo- and cathodoluminescence of pure zinc oxide. It has been observed that, depending on the conditions of preparation, the zinc oxide luminesces either in the ultraviolet region,[1,2] or in the visible region,[3-5] or in both regions of the spectrum.[6]

By heating zinc oxide at a temperature above 1100° in air or oxygen we obtained specimens which, when excited by light of wavelength 365 mμ at room temperature, gave a weak yellowish luminescence. On lowering the temperature, the brightness increased sharply and the color of the luminescence changed. Figure 1 shows the corresponding spectra of the luminescence at 195 and 78°K. The spectrum of zinc oxide with the usual green luminescence (prepared in air at 900°) is given for comparison. The spectra were recorded with the aid of a UM-2 monochromator and a FEU-27 photomultiplier which is sensitive in the red region of the spectrum. The points of interest are the complexity of the spectrum, its weakly defined structure, and the changes in the short wavelength region as the temperature is lowered. The observed luminescence depends on the conditions of preparation, on the temperature and atmosphere at which the specimen is fired, and also to a considerable degree on the previous history, or "biography," of the specimen. This is seen from the following experiments. When zinc oxide of the "for luminophores" grade, (produced by the "Red Chemist" plant) is fired in oxygen at temperatures above 1100-1200°, the specimens obtained possess low temperature red luminescence (green luminescence absent). At temperatures below these, the specimens obtained are inhomogeneous in their luminescence. The same picture is observed on firing in air.

In a reducing atmosphere (ammonia, carbon monoxide) it is possible to obtain a luminophore with only the green luminescence. If specimens originally fired in an oxidizing atmosphere (producing low temperature red luminescence) are briefly exposed to the action of a reducing atmosphere, the red luminescence vanishes and is replaced by a green luminescence with a maximum at about 505 mμ.

We conducted similar experiments with pure zinc

oxide obtained by burning luminophore-grade zinc sulphide in a stream of oxygen at 900°. The specimens of zinc oxide obtained possessed a bright uniform green luminescence (maximum around 505 mμ). Firing this preparation in an atmosphere of oxygen or air at successively increased temperatures leads at first to a diminution of the intensity of the green luminescence (1000-1100°), then to the appearance of red low temperature luminescence and to a complete vanishing of the green luminescence (1100-1200°). As in the preceding case, the effect of a reducing atmosphere was to destroy the red luminescence and to cause the appearance of a weak green luminescence.

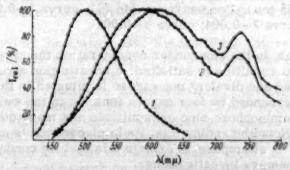

Fig. 1. Spectra of the photoluminescence of pure zinc oxide ($\lambda_{exc.}$ = 365 mμ). Conditions of preparation of specimens (firing temperature and atmosphere) and test temperature: curve 1—(900°, air), 291°K; curve 2—(1200°, air), 195°K; curve 3—(1200°, air), 79°K.

An entirely different picture is observed in the case of zinc oxide specimens similarly obtained by igniting the sulphide in a slow stream of oxygen, but at a temperature of 1200°. An interesting feature of this method is the fact that the zinc oxide is obtained in the form of concretions of single crystals, many of which attained dimensions of 5mm in length and 0.5 mm in thickness. The crystals had the shape of six-sided prisms with pointed ends, and were perfectly transparent and colorless. In this case, in contrast to that described above, the luminescence is green, rather than red. It deserves to be noted that the green luminescence of single crystals, which is weak at room temperature, increases considerably in brightness as the temperature is lowered.

On grinding single crystals in a mortar, the luminescence completely disappeared, but after the ground powder had been fired under the same conditions as were used for the sulphide (1200°, stream of oxygen, in presence of zinc sulphide specially placed in a separate combustion boat) the luminescence appeared. This time, however, it was not green, as for single crystals, but low temperature red. The behavior of these specimens toward a reducing atmosphere is the same as for the previous specimens: the red luminescence disappears and a green one appears.

Thus, the above-described low temperature red luminescence of zinc oxide is phenomenologically connected with the oxidizing atmosphere and high temperature of the firing, but the appearance of any particular band depends not only on the temperature and firing atmosphere but also on the history of each specimen. In order to check the possibility that the red luminescence of zinc oxide was a surface phenomenon, we placed prepared luminophores in solutions of ammonium salts and in dilute solutions of mineral acids. It was found that the brightness of luminescence of the residue after partial dissolution of the luminophore is the same as before dissolution. The luminescence centers are therefore situated within the crystallites.

In reference 3, the yellow luminescence of zinc oxide (amorphous band with λ_{max} = 600 mμ), observed at room temperature on specimens fired in oxygen, is associated with an excess of oxygen in the zinc oxide lattice. The present low temperature luminescence is also evidently connected with a stoichiometric excess of oxygen, notwithstanding the fact that in our case the luminescence spectrum is more complex.

In 1939, in a review presented at the Oxford Conference on Luminescence, Randall mentioned the luminophore ZnO-Mn and presented a photograph of its luminescence spectrum at 85°K. The spectrum was situated in the yellow-orange region of the spectrum. No details were given concerning the preparation of the luminophore[8]. Neither Randall himself nor other authors have subsequently confirmed the activating effect of manganese on zinc oxide. On the contrary, manganese has been listed among the quenchers of the luminescence of zinc oxide.[4,7] The similarity of the luminescence spectra and the fact that bright luminescence is observed only at low temperature suggested that the luminescence we observed was identical with that described by Randall. In connection with this, suspicions arose as to whether the initial zinc oxide which we used might not have had a manganese impurity. The zinc oside "for use as a luminophore" was analyzed by us for manganese;* its Mn content was found to be 0.0008% by weight (0.8×10^{-6} gm/gm). Such a concentration may in principle be sufficient for activation. The zinc oxide obtained by igniting the sulphide was considerably purer. Analysis for manganese gave a value less than 10^{-6} gm/gm. Nevertheless, the intensity of the red luminescence did not differ from its intensity in the other specimens of pure zinc oxide. Figure 2 shows the intensity of red luminescence as a function of manganese content.* The intensity was measured at −100°C with the aid of an FM photometer. The intensity of luminescence increases with decreasing manganese content and reaches a maximum value for a concentration of 10^{-5} gm/gm. With further decrease of the manganese concentration, however, the intensity does not decrease but remains approximately constant. For comparison, intensity values have been plotted at the left for the red luminescence of various specimens of zinc oxide prepared at 1200°, in which the manganese was not introduced purposely. Within the errors of measurement, these values agree with the value for zinc oxide containing manganese up to a concentration 10^{-5} gm/gm. This fact, as well as the above-mentioned strong dependence of the luminescence on the history of the specimens, makes it necessary to reject the idea of its origin as due to the manganese. The low

*The manganese was determined colorimetrically by the persulphate method.

*The specimens were prepared at 1200° in air (in a quartz test tube).

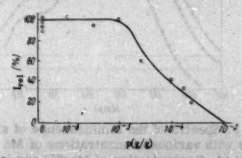

Fig. 2. Dependence of the intensity of luminescence of zinc oxide on the Mn concentration ρ at 173°K (λ_{exc} = 365 mμ). The specimens were fired at 1200° in an oxygen atmosphere.

temperature luminescence observed by us must therefore be ascribed to (chemically) pure zinc oxide.

LUMINESCENCE OF ZINC OXIDE CONTAINING MANGANESE

In the opinion of Konstantinova-Shlezinger luminophores activated by bivalent manganese, from the crystallochemical point of view, represent substitution structures. A small proportion of the cations of the lattice is statistically replaced by bivalent manganese ions. The crystallochemical criteria for the formation of such structures are a similarity in ionic radius, valence, and coordination number between the displacing and displaced ions. Luminophores activated by divalent manganes are widely known, with compounds of calcium, zinc, and cadmium serving as bases. Thus a luminescence characteristic of manganese may also be expected in zinc oxide. The radii of the zinc and divalent manganese ions (0.83 A and 0.91 A respectively) are similar, and the fourfold coordination of zinc with respect to oxygen is also characteristic to a certain degree of manganese. Nevertheless, neither we nor other investigators have succeeded in observing the luminescence of manganese in zinc oxide. The question, which we consider as fundamental, is the following: what accounts for the absence of luminescence of manganese in the case considered—is it the fact that a solid solution is not formed under our conditions (i.e., a crystallochemical condition for the formation of a luminophore is not satisfied) or (if the manganese enters the zinc oxide phase), is the cause hidden in factors of a physical nature?

We were able to show that when zinc oxide containing a small amount of manganese oxides is fired at temperatures of the order of 1200–1300°, a solid substitution solution ($Zn_{1-x}Mn_xO$) is formed. Chemical analysis showed that all of the manganese introduced into the system is in the divalent state; x-ray phase analysis indicates the single phase character of the system. The interplanar distance of the zinc oxide lattice increases systematically with the introduction of the manganese ion, which is larger than the zinc ion.*

*A detailed description of the chemical and physical chemical properties of this system ZnO–MnO–O_2 will be given in a separate article.

These data agree with those of reference 8 on the paramagnetic resonance of Mn^{II} in zinc oxide.

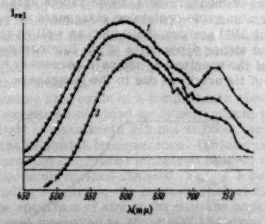

Fig. 3. Spectra of the luminescence of zinc oxide with various concentrations of Mn ($\lambda_{exc.}$ = 365 mμ). Concentration of Mn (%) and temperature of experiment: curve 1—0.0001, 195°K; curve 2—0.03, 195°K; curve 3—0.001, 78°K. Specimens were fired at 1200° in air.

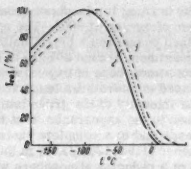

Fig. 4. Curves showing the intensity of photoluminescence of zinc oxides with various Mn contents as a function of temperature ($\lambda_{exc.}$ = 365 mμ). Concentration Mn (%): curve 1—0.01; curve 2—0.004; curve 3—0.001.

Thus, in the case under consideration the crystallochemical condition is satisfied: a substitution structure is formed and divalent manganese is situated in the same way, surrounded by four oxygen ions, as in the well-known luminophore zinc orthosilicate and many other bases. Notwithstanding this, its luminescence is not observed. In attempting to explain this fact we conducted supplementary investigations.

Figure 3 shows luminescence spectra of ZnO-Mn at low temperatures. On introducing manganese, the intensities of individual luminescence bands of pure zinc oxide are redistributed somewhat, but no new zones appear. Figure 4 shows the temperature dependence of the steady state intensity of luminescence for excitation by 365 mμ radiation. The introduction of the manganese shifts the curves in the direction of low temperatures.

The introduction of divalent manganese into zinc oxide produces a color which changes from yellow to dark red with increasing manganese content. Figure 5 shows the long wavelength end of the diffuse reflection spectra of zinc oxide powders with various manganese contents. It is seen that the absorption in the visible region systematically increases with increasing manganese content.

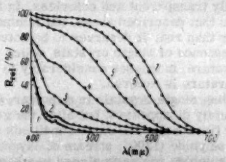

Fig. 5. Spectra of the diffuse reflection of zinc oxide with various Mn content. Mn concentration (%): curve 1—0; curve 2—0.0001; curve 3—0.001; curve 4—0.03; curve 5—0.3; curve 6—2; curve 7—0.92 ZnO · 0.08 MnO.

It is characteristic that the absorption spectrum of zinc oxide containing manganese does not depend on the firing atmosphere, and therefore cannot be connected with any stoichiometric defects. In working with pure monocrystalline zinc oxide, we observed the following peculiarity: when colorless single crystals are ground, intensely colored powders are obtained. Figure 6 shows the long wavelength end of the absorption spectrum of such powder. The corresponding curve for ZnO – 0.01 Mn is shown for comparison. It is characteristic that the curves agree in their general features. This indicates that the change of the absorption spectrum on introducing manganese is due not to absorption by the manganese ion but to absorption by the structural defects

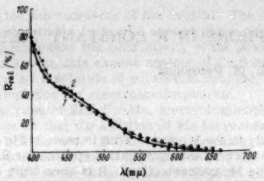

Fig. 6. Diffuse reflection spectra. Curve 1—powder obtained by grinding single crystals of pure ZnO; curve 2—powder of ZnO – 0.01Mn.

produced by the manganese. Evidently the nature of these defects is the same as that of the defects produced by grinding single crystals.

The introduction of small amounts of divalent manganese (<1%) into the zinc oxide lattice may produce a twofold effect: On the one hand discrete centers (structural defects) are formed (manganese ions surrounded by four oxygen ions plus certain adjoining layers of ions of a more distant order); on the other hand, a change in the energy state of the crystal as a whole occurs (width of forbidden band decreases). For small manganese contents the second effect is weaker than the first, but for high manganese contents there is no longer any meaning in speaking of centers, since the second effect—decrease of the width of the forbidden band of the crystal as a whole—then predominates. Curves 2-5 (Fig. 5) can thus be interpreted as the sum of the absorption of unactivated zinc oxide and the additional absorption of the centers produced by the manganese; curves 6 and 7 represent absorption spectra which have been displaced with respect to the curve for the unactivated oxide. The same displacement is observed, for example, on raising the temperature.[9] It is known that the absorption spectra of manganese-activated oxygen-containing luminophores, for example, zinc silicate with manganese, have discrete bands in the near ultraviolet which are associated with absorption by the divalent manganese ion, which is surrounded by four oxygen ions.[10] In the case of zinc oxide, these bands coincide with the continuous absorption spectrum of the lattice. This fact may be connected with the absence of manganese luminescence in zinc oxide.

In concluding, we consider it necessary to emphasize that conclusions in regard to the absence of manganese luminescence in zinc oxide (for example in reference 4) should be drawn only if: (1) the luminophore is analyzed for manganese, which is present in the specimens usually employed in quantities sufficient for activation, and (2) the phase composition of the specimens is investigated, it being shown that the conditions of firing produce a single phase and not a poly-phase system. In the latter case the manganese may be in the form of a separate phase consisting of one of its oxides, or in the form of a compound of manganese with zinc oxide (see, for example, reference 11).

RESULTS

1. The low temperature red luminescence of zinc oxide observed in specimens fired in an oxidizing atmosphere is described.

2. It is shown that the red luminescence is not caused by manganese impurities, but must be ascribed to the (chemically) pure zinc oxide.

3. The luminescence of zinc oxide is shown to depend strongly on the conditions of preparation and on the history of the specimen; e.g., the red luminescence is associated with a stoichiometric unbalance; i.e., with excess oxygen in the zinc oxide.

4. It is shown that even though the divalent manganese enters the lattice of the zinc oxide with the formation of a substitution structure, manganese luminescence does not occur.

The author expresses his gratitude to M. A. Konstantinova-Shlezinger for guidance in the work and to M. V. Fok for thoroughgoing discussions.

REFERENCES

1. R. E. Schrader and H. W. Leverenz. J. Opt. Soc. Am. **37**, 939 (1947).
2. H. W. Leverenz. "An Introduction to Luminescence of Solids." New York, 1950.
3. L. N. Shekhter, I. A. Myasnikov, and S. Y. Pshezhetskii. Mat. V. soveshch. po liuminests., Tartu, 1957. (Report of the Fifth Conference on Luminescence, Tartu, 1957.)
4. G. A. Konovalov. Trudy Sib. Fiz.-Tekh. Inst. No. 32, 35 (1953).
5. F. I. Vergunas and F. F. Gavrilov. Zhur. Eksp i Teoret. Fiz. **18**, 224 (1948).
6. J. T. Randall. Trans. Faraday Soc. **35**, 10 (1938).
7. A. V. Moskvin. "Katodoliuminestsentsiya." (Cathodoluminescence), GITTL, Moscow-Leningrad, 1949.
8. P. B. Dorain. Phys. Rev. Letters **1**, 385 (1958).
9. V. V. Kudryavtseva. Izvest. Akad. Nauk SSSR, Ser. Fiz. **13**, 115 (1949).
10. F. A. Kroeger. "Luminescence in Solids Containing Manganese." Amsterdam, 1940.
11. A. P. Rice. J. Electrochem. Soc. **96**, 114 (1949).

ELECTROLUMINESCENCE OF ZnS-Cu-Mn PHOSPHORS IN A CONSTANT FIELD

O. N. Kazankin, F. M. Pekerman, and L. M. Petoshina

Received 13 May 1959

It is known that the application of a constant electric field causes only a momentary flash of luminescence in an electroluminophore. This is explained by the fact that the internal field, which produces the acceleration of the electrons, decreases with time as a result of polarization. Thus, after even a relatively small time interval, the internal field is too weak to maintain electroluminescence, and the electroluminophores cease to emit light. It is found, however, that electroluminophores of the ZnS-Cu-Mn type prepared in a corresponding manner give bright electroluminescence in a constant field and possess special properties when excited in this manner.

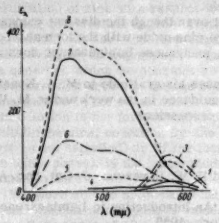

Fig. 1

Fig. 2

Fig. 1. Radiation spectra of ZnS-Cu (1%)-Mn luminophores excited by an alternating field of frequency 5000 cps. and 300 volts. Mn concentration (%): Curve 1—3, curve 2—2, curve 3—1, curve 4—0.5, curve 5—0.3, curve 6—0.1, curve 7—0.05, curve 8—0.02.

Fig. 2. Radiation spectra of ZnS-Cu (0.2%)-Mn luminophores excited by a constant field of 600 volts. Mn concentrations (%): Curve 1—3, curve 2—2, curve 3—1, curve 4—5, curve 5—0.3, curve 6—0.2.

The specimens of ZnS-Cu-Mn electroluminophores containing 0.05 to 0.3% Cu and 0 to 3.0% Mn were prepared in an atmosphere of H_2S + HCl by the method described in reference 1. The properties of these electroluminophores were investigated with the aid of a demountable condenser using a liquid dielectric (castor oil). The alternating field was obtained from an audio supply with a step-up transformer; the constant field from a VVS-1 high voltage stabilizer.

The electroluminophores prepared gave a bright luminescence in the alternating field, the optimal brightness being possessed by the specimens containing 0.2% Cu and 0.5-1.0% Mn. Depending on the concentration of Cu and Mn, it was possible to obtain luminophores with one, two, or three emission bands (the radiation spectra of these electroluminophores are shown in Fig. 1). On being placed in a constant field the ZnS-Cu-Mn electroluminophores begin to show persistent luminescence even at a Mn concentration of about 0.1%. The brightness of the radiation increases with increasing concentration of Cu and Mn up to a certain optimal value. The radiation occurs only in the Mn band. This is seen in Fig. 2 which shows the corresponding radiation spectra for 0.2% Cu and various Mn concentrations. It is seen from the same figure that for this series of electroluminophores the optimal brightness is possessed by specimens containing 0.5-1% Mn.

When the constant field is turned on, the radiation of the luminophores does not remain constant. Figure 3 shows the shape of the intensity vs. time curves for 2% Mn and various Cu concentrations. From these curves it follows that for small concentrations of Cu the brightness starts to drop immediately after the constant field is switched on. For large concentrations of Cu, however, the electroluminophore lights up in the same way as other electroluminophores. In several cases the luminescence may continue for several tens of minutes; the duration of luminescence apparently depends on the conditions under which the electroluminophores were prepared (this question is being investigated further). After a certain time, as is seen from Fig. 3, the luminescence ceases and the brightness starts to drop because of polarization. Investigation of the peculiarities of the behavior of this electroluminescence with time under dc excitation made it necessary to examine the variation of the initial current through the condenser. Table 1 presents data on the magnitude of the initial current passing through the condenser for specimens with various Cu and Mn contents and Fig. 4 shows the time variation curves of the current passing through the condenser. In examining these curves it is noticed first of all that the magnitude of the initial current increases with increasing concentration of Cu and Mn. The value of the initial current may reach several milliamperes and exceed by 2 orders of magnitude the current through the condenser obtained for the usual ZnS-Cu electroluminophores under the same conditions. The conductivity of the ZnS-Cu luminophores with high concentrations of Cu may attain considerable values since in firing this luminophore in an atmosphere of H_2S + HCl, of the 0.2% Cu introduced into the charge, approximately 0.05% penetrates the crystal lattice and re-

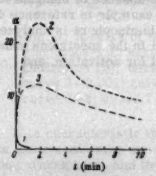

Fig. 3.

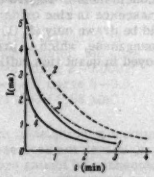

Fig. 4.

Fig. 3. Time variation of the brightness of ZnS-Cu-Mn (2%) luminophores excited by a constant 600 volt field. Cu concentration (%): Curve 1—0.1, curve 2—0.2, curve 3—0.3.

Fig. 4. Time variation of the current through the condenser for ZnS-Cu(0.2%)-Mn luminophores. Mn concentration (%): Curve 1—3, curve 2—2, curve 3—1, curve 4—0.5.

mains in the microdefects of the crystal. The rest of the Cu_2S remains in the form of a second phase and considerably increases the conductivity of the powder.

As is known, this excess amount of Cu_2S can be washed out by a solution of potassium cyanide, which is usually employed for electroluminophores.

In the case of ZnS-Cu-Mn, electroluminophores, Table 1 shows that the addition of Mn increases the conductivity still further. It was shown by analysis that this was due mainly to the appearance of a still greater quantity of Cu in the form of excess Cu_2S on adding Mn.

Table 1. Dependence of the Magnitude of the Initial Current (ma) on the Concentration of Cu and Mn

Mn (%) / Cu (%)	0	0.02	0.05	0.1	0.5	1.0	2.0	3.0
0	—	—	—	—	0.02	—	—	—
0.05	0.03	—	—	—	0.02	0.01	—	—
0.1	0.03	0.05	0.04	0.03	0.03	0.04	0.1	0.005
0.2	0.04	0.62	4.3	4.7	3.2	3.2	5.5	4.7
0.3	0.5	—	—	—	1.8	1.8	4.7	3.2

The phenomenon of continued and sufficiently bright luminescence in a constant field was found in further tests to be associated with the passage of a large current through the condenser, that is, with the presence of an excess amount of Cu_2S. After the ZnS-Cu-Mn luminophore specimens were washed with KCN they practically lost their capacity for luminescence in a constant field. The data are presented in Table 2.

Table 2. Brightness and Magnitude of Initial Current through the Condenser for ZnS-Cu(0.2%)-Mn Luminophores before and after Washing with KCN

Concentration of Mn (%)	Brightness (rel. units)		Initial current (ma)	
	Unwashed	Washed	Unwashed	Washed
0	—	—	0.24	0.013
0.5	74.0	0.8	4.5	0.032
1.0	88.0	4.0	5.6	0.01
2.0	46.0	0.3	5.9	0.02
3.0	40.0	0	5.0	0

Thus, a necessary condition for luminescence in a constant field is the presence of a large amount of excess copper, giving a relatively large current through the condenser. This condition is not sufficient, however, since if a large excess of Cu_2S (say 0.3% Cu) is introduced without Mn, there is no luminescence in a constant field, even though considerable current passes through the condenser. A second condition for the continued luminescence in a constant field, therefore, is the presence of Mn.

The next interesting property of ZnS-Cu-Mn electroluminophors is the increase in luminescence intensity which they exhibit when subjected to a preliminary application of a dc or ac field. Experiments aimed toward observation of this effect were performed in the following way: The electroluminophore was placed in a condenser containing a liquid dielectric (castor oil). An ac field was applied, and the intensity of luminescence measured. The ac field was switched off, and after 2-3 min, the dc field was switched on.

The dc field was now switched off, and the ac field once more switched on at the same voltage as before. The intensity of luminescence was measured. Experiment showed that in some cases the luminescence was as much as three times as bright as in the first case. It was found that this intensification depends on the concentration of Cu and Mn, and on the conditions of preparation of the luminophore. Table 3 gives data on the relationship between the intensification coefficient (ratio of intensity

Table 3. Magnitude of the Intensification for Luminophores with Various Cu and Mn Contents

Cu (%) / Mn (%)	0.5	1.0	2.0	3.0
0.05	1.0	1.1	1.0	—
0.1	1.1	1.2	1.7	1.5
0.2	1.5	2.0	4.4	4.3
0.3	2.3	3.2	3.6	3.4

after application of dc field to original intensity) and the Cu and Mn concentrations. It follows from this table that on increasing the concentration of Cu from 0.05 to 0.3% the intensification increases; an increasing concentration of Mn up to 2% likewise produces an increase in the intensification. The intensification effect is directly connected with the presence of excess Cu_2S. By washing with a potassium cyanide solution, the intensification effect can be almost completely nullified (see Table 4).

Table 4. Magnitude of the Intensification for ZnS-Cu(0.2%)-Mn Luminophores before and after Washing off Excess Cu_2S

Concentration of Mn (%)	Magnitude of intensification	
	Unwashed	Washed
0.5	252	119
1.0	256	113
3.0	292	107

It is natural to associate the intensification effect with residual phenomena occuring when crystallites of the luminophore are aligned in the direction of the field.[3,4] Under the action of the electric field the crystals form little bridges between the plates of the condenser; this can be observed under the microscope. By placing our electroluminophores in a condenser that was suitable for observation and photography under the microscope we were able to observe such little bridges under the action of alternating and constant fields. Considerable bridging takes place at field strengths of 2000 volts/cm and at concentrations of 0.2% Cu and 0.5% Mn, the intensification for which constitutes 252%. The same specimen with its excess Cu_2S washed out has only half the intensification, and bridging occurs at 1000 volts/cm.

After the field is switched off, a large proportion of the bridges do not break up. Thus, when the alternating field is switched on again, some of the crystallites are already oriented. This also leads to an increase in brightness when the field is switched on again.

Thus, under certain conditions of preparation, ZnS-Cu-Mn electroluminophores possess intense and prolonged luminescence in a constant electric field. This luminescence is caused by an increase in the conductivity of the electroluminophores, due to excess Cu_2S which does not enter the ZnS lattice, and to the activation by Mn.

At the same time, at certain Mn concentrations an intensification effect is observed after repeated application of a field, which sometimes amounts to as much as threefold.

REFERENCES

1. O. N. Kazankin, F. M. Pekerman, and L. N. Petoshina. Izvest. Akad. Nauk SSSR, Ser. Fiz. 21, 721 (1957).
2. S. A. R. Pearce. Brit. J. Appl. Phys. 5, 136 (1954).
3. W. Lehmann. J. Electrochem. Soc. 103, 24 (1956).

RESOLUTION OF A MONOCHROMATOR WITH PHOTOELECTRIC RECORDING

G. M. Malyshev, V. B. Skidan, E. E. Fradkin, and M. P. Chaika

Received 8 May 1959

The resolving power of a monochromator with photoelectric recording was investigated theoretically. The slit width of the entrance and exit slits of the spectrometer for which one obtains the best resolution of two monochromatic lines of the same intensity is determined, with specified values of the source brightness and characteristics of the optical and photoelectric parts of the monochromator.

An important characteristic of any spectral apparatus is its resolving power. For photoelectric recording of spectra, the resolution depends not only on the instrumental function of the monochromator, but also on the ratio of signal to noise of the detector at the exit; the latter in turn depends on the characteristics of the detector and on the magnitude of the flux passing through the monochromator. Both the instrumental function of the monochromator and the magnitude of the flux depend on the entrance and exit slit widths of the monochromator. In this paper, the slit widths, for which one obtains the best resolution of two monochromatic lines of the same intensity for a given source brightness and spectrometer characteristics, are determined.

1. Consider the case in which the illumination in the focal plane of the monochromator is determined by diffraction on a rectangular aperture stop of light waves coming from each infinitely narrow part of the entrance slit. Such a distribution in nearly pure form occurs in some spectral apparati (mainly in long focal length instruments), so that the case under consideration is of practical interest.

We shall assume that waves which come from different parts of the slit are incoherent.* Then the instrumental function of the monochromator is found by averaging the diffraction at the entrance slit[1] and subsequent integration over the exit slit, i.e.,

$$a(z, \zeta_1, \zeta_2) = \frac{1}{2\zeta_1 \pi} \int_{-\zeta_1}^{\zeta_1} \int_{-\zeta_2}^{\zeta_2} \frac{\sin^2(z + \xi_2 - \xi_1)}{(z + \xi_2 - \xi_1)^2} d\xi_1 d\xi_2$$

$$= \frac{1}{2\zeta_1 \pi} [m(z + \xi_2 - \xi_1)] \Big|_{-\zeta_1}^{+\zeta_1} \Big|_{-\zeta_2}^{+\zeta_2},$$

$$m(t) = t\,\mathrm{Si}(t) + \cos(t) + \mathrm{Ci}(t) - \ln(t), \qquad (1)$$

where z is the coordinate of the focal plane of the monochromator measured from the center of the image of the entrance slit and expressed in normalized slit units.

$$z = 2\pi \frac{x_2}{F_2} \Big/ \frac{\lambda_0}{X_1},$$

(where x_2 is the linear coordinate of the point; F_2 is the focal length of the exit collinator; X_1 is the width of the beam incident on the prism or the grating) and $2\zeta_1$ and $2\zeta_2$ are the widths of the entrance and exit slits in the same units.

Consider the spectral distribution from two monochromatic lines of the same intensity separated from each other by the distance Δz,

$$A(z, \zeta_1, \zeta_2) = a(z, \zeta_1, \zeta_2) + a(z - \Delta z, \zeta_1, \zeta_2). \qquad (2)$$

Let us determine the resolution Q of the monochromator as the ratio of the dip in the curve ΔA to the maximum of the spectral distribution (2) (Fig. 1).

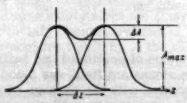

Fig. 1. Spectral distribution at the exit port of a monochromator for two monochromatic lines of equal intensity.

$$Q = \frac{\Delta A}{A} = \frac{A_{max} - A_{min}}{A_{max}} = 1 - \frac{A_{min}}{A_{max}}. \qquad (3)$$

Because the lines are monochromatic, it follows that

$$A_{min} = 2a\left(\frac{\Delta z}{2}, \zeta_1, \zeta_2\right); \quad A_{max} \simeq a(0, \zeta_1, \zeta_2) + a(\Delta z, \zeta_1, \zeta_2).*$$

Then

$$Q(\Delta z, \zeta_1, \zeta_2) = 1 - \frac{2a\left(\frac{\Delta z}{2}, \zeta_1, \zeta_2\right)}{a(0, \zeta_1, \zeta_2) + a(\Delta z, \zeta_1, \zeta_2)}.$$

Let us examine the dependence of the resolution on the relative widths of the entrance and exit slits. Let us find the maximum value of $Q(\Delta z, \zeta_1, \zeta_2)$ under the condition of a constant light flux. This is a typical problem of the conditional maximum. The quantities ζ_1 and ζ_2 are determined from the conditions

$$\left.\begin{aligned} Q(\Delta z, \zeta_1, \zeta_2) &= \max, \\ A_{max}(\Delta z, \zeta_1, \zeta_2) &= \text{const}. \end{aligned}\right\} \qquad (4)$$

As a result of calculation, the necessary condition of a conditional maximum reduces to the form

$$\Phi(\Delta z, \zeta_1 + \zeta_2) = \Phi(\Delta z, \zeta_1 - \zeta_2), \qquad (5)$$

where

$$\Phi(\Delta z, \eta) = \frac{2m'(\eta) + m_3(\Delta z + \eta) - m'(\Delta z - \eta)}{m'\left(\frac{\Delta z}{2} + \eta\right) - m'\left(\frac{\Delta z}{2} - \eta\right)},$$

$$m'(t) = \mathrm{Si}(t) + \frac{\cos(t)}{t} - \frac{1}{t}.$$

Equation (5) was evaluated numerically for the following values: $z = 2\pi, 3\pi, 4\pi, 6\pi$, and 8π. It turned out that in all

*The partially coherent waves, emitted by neighboring portions of the slit, do not introduce large distortions in the intensity distribution.

*The displacement of the maximum of $A(\Delta z, \zeta, \zeta_2)$ with respect to the maximum $a(z, \zeta_1, \zeta_2)$ is small; their magnitudes are nearly equal and the approximation used here does not introduce any marked errors in the final result.

cases of practical interest, the quantity Q has its largest value when the entrance and exit slits are equal ($\zeta_1 = \zeta_2$). The only exception is the case $\Delta z = 6\pi$ for which, at low light fluxes, the maximum value of Q occurs for unequal slits. In what follows we shall assume that the slits are of equal widths ($\zeta_1 = \zeta_2 = \zeta$). Since $Q = Q(\Delta z, \zeta)$ and $A_{max} = A_{max}(\Delta z, \zeta)$, then $Q = Q(\Delta z, A_{max})$. The separation of the lines Δz enters here as a parameter.

2. As is well known, photoelectric scanning introduces systematic and random distortions into the spectral distribution. In practice, one frequently works in such a region of values for the instrument parameters (the scanning speed and the time constant of the system τ) that one can neglect systematic scanning errors. It is, however, necessary to take random errors (noise in the detector) into account. It is precisely this case which is being considered here.

Let us define the total resolution R of the spectrometer with photoelectric recording as the difference between the resolution of the monochromator and the noise/signal ratio, taken for the maximum light flux (assume that the noise at the maximum of the light flux does not differ much from the noise at the minimum)

$$R = Q(\Delta z, A_{max}) - \frac{\sqrt{\overline{N_n^2}}}{N_s}(F_{max}), \qquad (6)$$

where $F_{max} = C2\zeta A$ is the light flux passing through the monochromator (the source brightness and monochromator parameters enter into the constant C); N_s and N_n are the magnitudes of the voltages corresponding to the signal and to the noise. In accordance with (6), we will consider that two lines are resolved if $R > 0$, i.e., if the dip in the curve between them is greater than the magnitude of the noise.

The ratio of the mean square noise voltage to the signal voltage is a function of the light flux. In the particular case of the photomultiplier[2] when the dark current can be ignored in comparison to the signal current, this relation has the form

$$\frac{\sqrt{\overline{N_n^2}}}{N_s} = \frac{B}{\sqrt{F}} = \frac{D}{\sqrt{2\zeta A}},$$

where $D = B/\sqrt{C}$ and B is determined by the parameters of the photoelectric recording apparatus.

Then the magnitude of the resolution will be

$$R(\Delta z, A_{max}) = \frac{\Delta A}{A_{max}} - \frac{D}{\sqrt{2\zeta A_{max}}}. \qquad (7)$$

The constant D is determined experimentally for a given pair of lines of the same intensity from the measured ratio of noise/signal for a definite entrance slit width $2\zeta_1$, and an exit slit which passes both lines.

The normalization of the instrument function was chosen by us in such a way that for these conditions $a_{max} = 1$, and consequently $A_{max} = 2$. Then

$$D = \frac{\sqrt{\overline{N_n^2}}}{N_s}\sqrt{2 \cdot 2\zeta_1},$$

where $2\zeta_1$, is expressed in normalized slit width units

$$2\zeta_1 = 2\pi \frac{l}{F} \cdot \frac{X_1}{\lambda_0}.$$

Here l is the linear width of the slit; X is the width of the beam falling on the prism or on the grating and λ_0 is the wavelength of the light in the line being studied.

3. The quantity $\Delta A/A_{max}$ was obtained by numerical integration for different separations Δz between the lines. On the graph (Fig. 2), it is shown as a function of $1/\sqrt{2\zeta A_{max}}$. This choice of argument is convenient because the dependence of the noise to signal ratio in the case under investigation turns out to be a straight line on this plot. In the case of other dependences of the noise to signal ratio on light flux the form of the argument can be changed in such a way as to preserve the linearity.

To construct the function $D/\sqrt{2\zeta A_{max}}$, it is sufficient to plot, for example, at the point $\sqrt{2\zeta_1 A_{max}} = 1$ the quantity D and to draw a straight line through this point and the center of coordinates.

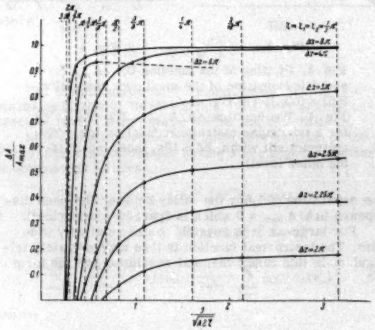

Fig. 2. Nomogram for determining the optimum slit width.

The difference between curves calculated for a given separation between lines Δz and a line drawn through experimental data gives the value of the resolution. Obviously, the resolution will be largest for those slit widths ζ for which the difference between the ordinate of the line and of the curve has the largest value (Fig. 3).

If all the curves lie below the line, this means that the pair of lines separated by a distance Δz cannot be resolved with the given spectrometer.

The limiting distance between lines which can still be resolved is determined from the condition R = 0. On the graph, it is found with the aid of the same family of curves (Fig. 2) for which the line $D/\sqrt{2\zeta A_{max}}$ is a tangent. In the linear approximation the dependence of the slit width (which gives the limiting resolution) on the separation between the lines has the form

$$\zeta_{lim} = \frac{5}{21}\Delta z - \frac{1}{24}\pi.$$

Such a value can be useful for investigation of the Zeeman effect where the brightness of the line stays constant (if the application of the magnetic field does not affect the character of the excitation), and the distance between the components depends on the magnitude of the magnetic field.

In the limiting case of very intense lines a large light intensity and a good detector, i.e., for small values of D the largest resolution, is conveniently attained by using very narrow slits. As the slit width is decreased, the instrument function $a(z, \zeta)$ approximates a diffraction distribution. Under these conditions, it is possible to resolve lines located closer together than lines resolved in accordance with the Rayleigh criterion, that is, $\Delta z < 2\pi$. Even in the complete absence of noise, however, it is not possible to reduce this distance by much, since even for a

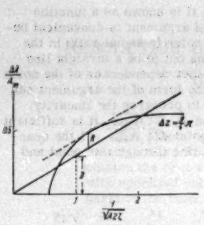

Fig. 3.

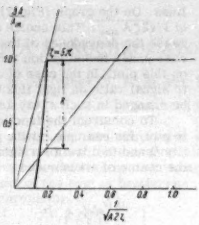

Fig. 4

Fig. 3. Plotting of the function $D/\sqrt{2A_{max}}\zeta$ and determination of the maximum resolution R(D = 0.3; R = 0.12).

Fig. 4. The function $\Delta A/A_{max} = f(1/\sqrt{2A_{max}}\zeta)$ for a triangular instrument function ($\Delta z = 20\pi$; optimum slit width, $2\zeta = 10\pi$, independent of the noise level).

line separation of 1.65π the valley between the lines disappears ($\Delta A/A_{max} = 0$ which is Sparrow's criterion[3]).

For large Δz it is possible to use relatively wide slits. The instrument function is then approximately triangular. In this case,[4] the total resolution has the form

$$\left.\begin{aligned} R(\Delta z,\ \zeta) &= 1-\frac{D}{\sqrt{2}\zeta}, \quad 2\zeta \leqslant \frac{\Delta z}{2}; \\ R(\Delta z,\ \zeta) &= \frac{\Delta z}{2\zeta}-1-\frac{D}{\sqrt{2}\zeta}, \quad \frac{\Delta z}{2} \leqslant 2\zeta \leqslant \Delta z. \end{aligned}\right\} \tag{8}$$

The maximum resolution occurs for a slit width equal to $2\zeta = \Delta z/2$. Thus, the choice of slit width to obtain the best resolution does not depend on the noise level. This is clearly seen in Fig. 4, which is constructed in the same coordinates for the triangular function. The smallest distance between lines of a given intensity, which can still be resolved, is determined by the value of D

$$\Delta z = \frac{2}{D}.$$

In this same case, when the slit width is nearly normal (in the region up to 10π), in order to find the optimum resolution conditions it is necessary to use the chart given above (Fig. 2).

The authors express their gratitude to S. E. Frish for fruitful discussions of this work.

REFERENCES

1. J. W. Parry. "Problems in Contemporary Optics." p. 265, 1956.
2. N. O. Chechik, S. M. Fainshtein, and T. M. Lifshits. "Electronic Amplifiers." (In Russian.)
3. C. M. Sparrow. Astrophys. J. 44, 76 (1916).
4. G. G. Petrash. Inzh.-fiz. Zhur. 1, 74 (1958).

APPARATUS FUNCTION OF A FABRY-PEROT SPECTROMETER WITH A RECTANGULAR APERTURE

R. I. Semenov, E. E. Fradkin, and M. P. Chaika

Received 19 June 1959

In optical measurements with the use of a Fabry-Perot spectrometer, it appears that it is necessary to take into consideration, or evaluate, the distortion caused by the presence of the aperture. Usually, for spectrometers making use of a circular aperture, the pattern produced by the interferometer is concentric. The performance of such an aperture, as shown by Chabbel,[1] is analagous to the effect on the distribution by an Airy slit having a spectral width $\Delta\nu$ and a constant separation $\chi = 1$

$$\Delta\nu = \frac{\nu}{2}\cdot\frac{R^2}{f^2}, \tag{1}$$

where ν is the frequency of the observed line in reciprocal centimeters, R is the radius of the aperture, and f is the focal length of the objective lens projecting the system of rings on the aperture.

The apparatus function of a Fabry-Perot spectrometer having a circular aperture, obtained as a convolution of Airy function with such a slit, is given by

$$f_A(z) = A\left\{\tan^{-1}\left[\sqrt{1+F}\tan\pi(z+a)\right] - \tan^{-1}\left[\sqrt{1+F}\tan\pi z\right]\right\}, \tag{2}$$

where

$$F = \frac{4r}{(1-r)^2}.$$

Here r is the coefficient of reflection of the plates of the interferometer, z is the order of the interference, a is the radius of the aperture in units of length, and A is a numerical coefficient. For this function the width can be obtained analytically as

$$2\delta = \frac{2}{\pi}\arcsin\sqrt{\frac{1}{F}+\sin^2\frac{a\pi}{2}} \tag{3}$$

and the contrast

$$\frac{f_{max}}{f_{min}} = \frac{\tan^{-1}\left(\sqrt{F+1}\cdot\tan\frac{a\pi}{2}\right)}{\frac{\pi}{2}-\tan^{-1}\left(\sqrt{F+1}\cdot\tan\frac{1-a}{2}\cdot\pi\right)}. \tag{4}$$

The maximum of energy passing through the aperture does not coincide with the maximum of illumination in the center of the interference pattern. The magnitude of such a displacement Δ likewise can be obtained analytically as

$$\Delta = \frac{a\pi}{2}. \tag{5}$$

After initial monochromatism, if the distance between lines is less than the size of the aperture, then a few lines will pass through the aperture. In such a case the line under investigation is separated by the slit. The aperture resulting from a combination of a circular opening with a slit (referred to in the discussion as a rectangular aperture) will transmit light of only the lines under investigation (Fig. 1).

In the present work a transmission function was ob-

tained for a rectangular aperture, and an apparatus function for the Fabry-Perot spectrometer having a rectangular aperture.

The rectangular aperture, as well as the circular aperture, is similar to a slit with the same spectral width $\Delta\nu$, but its transmission will discriminate different frequencies. We obtain the transmission of a rectangular aperture as a function of the distance R from its center, i.e., we find $\chi = \chi(R)$. For this we use a polar coordinate system, the center of which coincides with the center of the aperture (Fig. 1).

Let dE be the energy passing through the rectangular aperture in the interval R, R + dR, and dE_k be the energy passing through a circular aperture within the same interval. From Fig. 1 we obtain

$$dE = 4\vartheta d\Phi(R),$$

$$dE_k = 2\pi d\Phi(R),$$

$$d\Phi(R) = \int_R^{R+dR} I_\nu(r)\, r dr,$$

where $I_\nu(r)$ is the Airy function. Then

$$\chi(R) = \frac{dE}{dE_k} = \frac{2}{\pi}\cdot\vartheta.$$

For $R \leqslant R_1$, $\vartheta = \pi/2$ and $\chi = 1$, that is, the transmitting area coincides with the circular aperture. For $R > R_1$, $\vartheta = \arcsin R_1 R^{-1}$

Thus

$$\chi(R) = \begin{cases} 1 & R \leqslant R_1 \\ \frac{2}{\pi}\cdot\arcsin\frac{R_1}{R} & R_1 \leqslant R \leqslant R_2 \\ 0 & R > R_2 \end{cases} \qquad (6)$$

The transmission function for a rectangular aperture is given in Fig. 2.

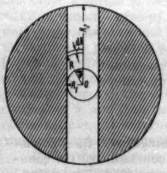

Fig. 1

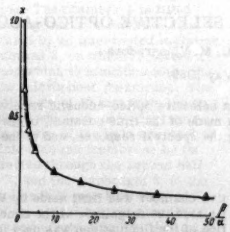

Fig. 2

Fig. 1. Rectangular aperture.
Fig. 2. Exact (continuous line) and approximate (dotted line) transmission function of a rectangular aperture.

In the course of the development of the solution of the apparatus function of the Fabry-Perot spectrometer with a rectangular aperture, two integrals appear

$$f_p(x) = \int_x^{x+\gamma} I(x)\,dx + \int_{x+a}^{x+b} I(x)\cdot\arcsin\sqrt{\frac{a}{x-z}}\,dx. \qquad (7)$$

The first term is the apparatus function of the Fabry-Perot spectrometer having a circular aperture of radius R_1. The second term can be obtained only as an approximation. The approximation consists of the replacement of arc sin R_1R^{-1} in the expression for transmission by the first term of its series expansion. Such a substitution does not introduce an appreciable difference in the degree of transmission of the aperture. The approximate transmission is given for comparison in Fig. 2.

In integrating the Airy function was expanded in a series of the dispersion functions.[2]

$$\frac{1}{1 + F\cdot\sin^2\pi x} = \frac{\delta_1}{\pi}\cdot\operatorname{th}\delta_1\pi\sum_{m=-\infty}^{\infty}\frac{1}{(x-m)^2+\delta_1^2} \qquad (8)$$

where

$$\delta_1 = \frac{1}{\pi}\cdot\operatorname{arc\,sh}\sqrt{\frac{1}{F}}.$$

For simplification of the calculations, δ_1 was replaced by δ, $\tanh\ \pi\delta$ by $\pi\delta$, which did not introduce an appreciable error with a large coefficient of reflection.

In our approximation, the apparatus function of the Fabry-Perot spectrometer having a rectangular aperture is obtained as follows

$$f_p(x) = \frac{1}{\pi\sqrt{F+1}}\cdot\{\tan^{-1}[\sqrt{F+1}\cdot\tan\pi\delta(x+a)] - \tan^{-1}[\sqrt{F+1}\cdot\tan\pi\delta x]\} + \frac{\delta}{\pi}\sqrt{2a}$$

$$\sum_{m=-\infty}^{\infty}\left[\frac{1}{2\gamma_m\alpha_m}\cdot\ln\varphi(x'_m) + \frac{1}{\gamma_m\beta_m}\cdot\sum_{k=1}^{4}\tan^{-1}\psi_k(x'_m)\right]. \qquad (9)$$

where

$$x = \frac{z}{b};\quad x'_m = x - m';\quad m' = m/b;\quad \gamma_m = \sqrt{x'^2_m + 1};$$

$$\alpha_m = \sqrt{\gamma_m - x'_m};\quad \beta_m = \sqrt{\gamma_m + x'_m};$$

$$\varphi(x'_m) = \frac{b + \alpha_m\sqrt{2b} + \gamma_m}{b - \alpha_m\sqrt{2b} + \gamma_m}\cdot\frac{a - \alpha_m\sqrt{2a} + \gamma_m}{a + \alpha_m\sqrt{2a} + \gamma_m},$$

$$\psi_1(x'_m) = \frac{\sqrt{2b} + \alpha_m}{\beta_m};\quad \psi_2(x'_m) = \frac{\sqrt{2b} - \alpha_m}{\beta_m};$$

$$\psi_3(x'_m) = -\frac{\sqrt{2a} + \alpha_m}{\beta_m};\quad \psi_4(x'_m) = -\frac{\sqrt{2a} - \alpha_m}{\beta_m}$$

(a = α/δ and α is the value of R_1 in units of length, b = β/δ and β is the dimension of R_2 in units of length.)

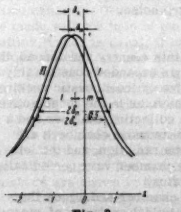

Fig. 3

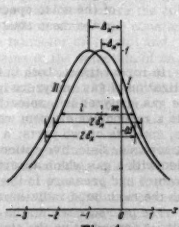

Fig. 4

Fig. 3. Apparatus function of a Fabry-Perot spectrometer with rectangular (I) and circular (II) aperture (b = 1, a = 0.04, R_2/R_1 = 5, 1/m = 1.1).
Fig. 4. Apparatus function of a Fabry-Perot spectrometer with rectangular (I) and circular (II) aperture (b = 2, a = 0.5, R_2/R_1 = 2, 1/m = 1.3).

The analytical determination of the parameters in such a function is very complicated. Therefore, the curve of the function (Figs. 3 and 4) was plotted by points calculated from formula (9), but the position of the maximum the width, and asymmetry were determined graphically. To calculate the points of the curve of the apparatus function near the maximum, only one term was taken with m = 0. For the determination of the contrast, the apparatus function was represented by a series of the form

$$I_p(x) = \sum_{m=-\infty}^{\infty} I_{Pm}(x). \qquad (10)$$

Next the sum

$$\sum_{m=0}^{\infty} \frac{(I_{Pm}(x) + I_{P-m+1}(x))_{min}}{I_p(x)_{max}}, \qquad (11)$$

was formed, the members of which were compared to terms of a series obtained by analogy from the apparatus function of the Fabry-Perot spectrometer having a circular aperture, the sum being known (Figs. 3 and 4).

The calculations were carried out for r = 0.84, 0.90, 0.95; b = 1, 2, 10, and b/a = 4, 25, 100.

In the treatment of the results, it became clear that the following rules were characteristic of the spectrometer with rectangular aperture.

1. The maxima are shifted in the same direction, but the magnitude of the shift is smaller than for the apparatus function of a spectrometer with a circular aperture.

2. The curves have an asymmetry, which for $b \leq 2$ is independent of the ratio R_1/R_2. With an increase in b, the asymmetry is increased.

3. The width of the curves for $b \leq 2$ coincides with the width obtained for the apparatus function of a spectrometer with a circular aperture. The ratio of the width of the curve to the width of the curve obtained for the spectrometer with a circular aperture decreases with increasing b.

4. The contrast for $b \leq 2$ is approximately equal to the contrast derived for the spectrometer with circular aperture. With increasing b, the contrast is decreased.

In the same manner, results were derived by numerical integration for the case b = 2, $R_2/R_1 = 7$, and r = 0.89.

The apparatus function of the Fabry-Perot spectrometer with a rectangular aperture was investigated by other workers.[3-5] In the work by Rank, an apparatus function was derived for a spectrometer having an infinitely narrow slit for low coefficients of reflection ($r < 0.6$) by numerical integration of terms similar to those in (7). At this time the results of calculations give satisfactory agreement with experiment.[4,5] Inasmuch as both the calculations and experiments were carried out for low coefficients of reflection and for very long slits (the aperture transmitting up to two orders of interference), the comparison of these results with ours may be only qualitative. Such a qualitative agreement of our calculations with the experimental data of Rank[4,5] does exist.

In conclusion, the authors express profound gratitude to N. I. Kaliteevski for his display of interest in the work and in the discussion of results.

REFERENCES

1. R. Chabbal. J. rech. Centre nat. rech. scient. **24**, 138 (1953).
2. S. G. Rautian. Uspekhi Fiz. Nauk **66**, 475 (1958).
3. J. H. Jaffe. J. Opt. Soc. Am. **43**, 1170 (1953).
4. D. H. Rank and J. M. Bennett. J. Opt. Soc. Am. **45**, (1955).
5. D. H. Rank, J. M. Bennett, and H. E. Bennett. J. Opt. Soc. Am. **46**, 477 (1956).

ON THE MAXIMUM POSSIBLE RESPONSE OF A SELECTIVE OPTICO-ACOUSTIC RECEIVER

N. A. Pankratov and L. M. Vinogradova

Received 5 May 1959

An account and results of an investigation of a selective optico-acoustic receiver with an optical microphone are presented. An estimate is made of the time constant, of the magnitude of the noise spectrum of the receiver determining the spectral response, and of the magnitude of the mean square noise.

In recent times, both in this country and abroad, the utilization of gas analyzers has expanded considerably.[1,2] The gas analyzer is a selective optico-acoustic receiver with a responsive element which, as in the nonselective one, consists of two parts: a collecting chamber and a microphone. Selective optico-acoustic chambers are filled with a gas which absorbs radiation, and the temperature and pressure in the chamber vary periodically with the modulated radiation flux.

The pressure within the chamber undergoes fluctuations dependent on the statistical exchange of energy between the gas and the walls of the cavity. The behavior of a noise signal, generated by the receiver by incident radiation, should not deteriorate with the use of any type of microphone (electrodynamic,[1] condenser,[2] or optical[3]) if the microphone is designed correctly. The sensitivity of the receiver is determined by the quality of the performance of the chamber and the applied microphone.

The theoretical analysis of the behavior of a selective chamber was first made by Veingerov.[4] He also estimated the magnitude of the time constant, but the question of the fluctuations was only formulated. The mathematical side of the problem for a cylindrical chamber with absolutely rigid walls and adiabatic ends was solved by El'yasevich. Stepanov and Girin[5] solved this problem more accurately. They developed the theory of the method of measuring the lifetime of the oscillatory excitation state of the molecules, based on the measurement of the magnitude of the phase shift between the radiation flux incident on the receiver and the formation of pressure increase in the chamber, which was proposed by Slobodskaya.[6]

Iofe, and somewhat later, but in greater detail, Sall' solved the problem of exciting sound waves with the calculation of the deflection of the microphone membrane. The analogous problem for the cavity of a selective receiver was solved by Mori[7] who investigated a flat cavity, not taking into account the dissipation of heat across the

lateral surfaces. Mori investigated the analytical expression for the response and its time constant. He showed in particular that the chamber time constant varies directly with the square of its depth. However, he did not consider the pressure fluctuations within the chamber and consequently the question of the threshold response of the receiver. Subsequently, the relation was established between the specific and the threshold response of a selective optico-acoustic receiver chamber and its time constant, which in its turn depends on the thermal loss and thermal capacity of the chamber. It was shown that having measured the time constant, it is possible to determine the magnitude of the thermal loss and, in principle, with this, to compute the specific and threshold response.[9] Experimental investigations are necessary for this determination but none have been conducted up to the present.

Sall' investigated the question of the threshold response of selective receivers and derived the expression for the threshold response and time constant with allowance for the loss from thermal conductivity.[10]

It should be noted that when a condenser or electrodynamic microphone is used in the receiver, some properties of the chamber, that is, its noise, time constant, and response dependence on frequency are incompletely manifested, since in measurement the properties of the microphone play a role. The use of the optical microphone[3, 11, 12] allowed the isolation of the properties of the chamber from the characteristics of the microphone in the investigation.

The optical microphone used in the experiments described below was used earlier in the development, by one of the authors, of a form of nonselective optico-acoustic receiver, now in commercial manufacture. Since the selective optico-acoustic cavity receiver and microphone were used in the series of experiments described below, we pause briefly here over its principle of operation.

The operating principle of the optico-acoustic receiver with optical microphone is illustrated in Fig. 1 and consists of the following: The chamber 1 is filled with a gas capable of absorbing infrared radiation. Its pressure pulsations generated by an interrupted radiation flux drive a celluloid membrane 2, on which is coated a mirror film of antimony and which is simultaneously the wall of the chamber and the microphone membrane. The membrane is placed at a distance of 15 mm from the objective 3, in the focal plane of which is located a transparent glass reticle 4. The image of the light source 6 is projected through the reticle onto the membrane by the condenser 5, and then reflected through the second half of the reticle, the mirror 7, and the diaphragm 8, to the single cascade photomultiplier 9 of type FEU-2.

Under the influence of the pulsating pressure the diaphragm vibrates, the result of which is that the image of the reticle is periodically displaced along the optical axis, and this causes fluctuations of the radiant flux which controls the secondary source for the multiplier. A cemented doublet objective of relative aperture f/20, focal length 100 mm, and half field 25 deg is used in the microphone. The condenser consists of two plano-convex lenses, one of which is parabolic; the condenser focus is 42.7 mm, the numerical aperture is 0.44 and the magnification 2.* The reticle lines were engraved on a glass disc of 50 mm diameter, and their width is 0.1 mm.

*The objective and condenser were computed by V. I. Lin'kova.

The cavity construction is illustrated in Fig. 2. The hollow space 1 serves as the working volume. The space 2 represents its trans-membrane volume or ballast, and has the form of an annular channel, 3 is the coupling channel, 4 is the submembrane annulus and membrane, 5 is the compensating canal, 6 is the entrance window, 7 is the safety window, and 8 is the body of the cavity.

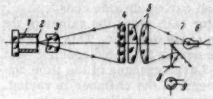

Fig. 1

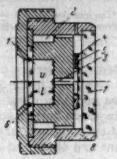

Fig. 2

To increase the absorption in the gas behind the wall of the working volume, which is indicated by the dotted line, it is polished and coated with a mirror film of aluminum, thus doubling the effective thickness of the absorbing layer of the gas.

THE TIME CONSTANT OF SELECTIVE OPTICO-ACOUSTIC CHAMBERS

For the measurement of the time constant of a chamber it is necessary to have a broad-band and adequately responsive microphone without attenuation in the low frequencies down to 5-7 cps. The width of the response bands of the microphones and amplifiers were accordingly designed to be approximately 2×10^4 and 4×10^3 cps.*

*The natural frequency of a chamber of volume 1 cm³ amounts to approximately 2×10^4 cps, and the natural frequency of the membrane owing to its small size and mass lies in the same neighborhood. The limitation on response on the low frequency side arises because of the presence of the compensating channel through which the gas is able to flow from the front to the rear side of the cavity and conversely, with a frequency of 3-5 cps.

In our investigation we made use of the sufficiently powerful lamp with a mica window developed by Maleev[13] (the incandescent area of the lamp is of very small size). In order to exclude the nonselective optico-acoustic effect arising from the walls of the chamber and which might change the picture, an interference filter transmitting radiation in the region 4.3-4.5μ was used before the collecting chamber. The determination of the time constant was made with the help of the taumeter of Tolstoi and Feofilov,[14] and, as usual, it came to the selection of an appropriate capacity and resistance in order to produce a straight line on the oscillograph screen. The interference filter served here simultaneously as a beam-splitting mirror for the receipt of two optical signals in the adapted taumeter.

The time constant was measured for chambers which varied with the magnitude of their working volume and the type of filling gas. The results of measurements for two chambers are shown in the table. The depth was chosen to conform with the gas analyzers.* The chamber was

*The maximum depth of the chamber was 1 cm, since the lag of the sound signal incident on the membrane from the gas volume situated near the window and from the volume at the rear of the chamber wall, on account of the finite velocity of sound, amounts to approximately 3×10^{-5} sec, which becomes the limiting factor in the accuracy of measurement and cannot influence the results of measurement.

No.	Dimension of entrance window	Depth of working volume (mm)	τ (sec.)	
			N_2O	CO_2
1	ø 9.4 (circular window)	10*	0.04	0.03
2	6×7 (rectangular window)	3	0.003	0.003

*The rear chamber wall was coated with a reflecting aluminum film, and the optical depth was twice the geometrical depth.

filled with nitrous oxide and carbon dioxide consecutively.

As seen in the Table, for both gases the values of the time constant obtained are close together. This is reasonable since both gases have nearly the same specific heat and thermal conductivity. Large changes of the time constant are observed if the depth of the chamber is varied. Thus, when the depth of the chamber differs by only three times, the time constant differs approximately ten times. This is explained by the fact that increasing the depth of the chamber not only increases the thermal capacity of the gas contained in it, but also decreases proportionately the heat emission. The calculated values of the time constants differ from the earlier computations in reference 4. For a long cylindrical chamber of diameter 1 cm filled with carbon dioxide gas, a time constant of approximately 0.5 sec is found on the basis of the indicated computations, which exceeds our observed values. The discrepancy is explained by not taking into account in the calculation the loss across the front surface of the chamber, since the depth of the chamber was assumed considerably larger than its diameter, and moreover it was not taken into account that more heat is lost near the window, the greater the depth of the chamber.

The values obtained by us allow the computation of the general thermal loss in the chambers, which will be used below for the estimate of the specific and the threshold response.

NOISE OF SELECTIVE CHAMBERS AND OPTICAL MICROPHONES

Gas pressure fluctuations in the chamber act on the membrane, and through the optical microphone are introduced into the amplifier circuit. In addition to this noise, there exists noise in the input circuit originating from other causes: the shot effect of the photocurrent, the fluctuations in the light flux, the noise from charge resistance, and in the case of use in the optical microphone of a semiconductor light receiver, and semiconductor noise.

It is therefore necessary to use a microphone of such response that under the action of the pressure fluctuations noise would be generated in the input circuit substantially exceeding the noise from the other sources.

As was shown in reference 15, in nonselective receivers in which the radiation is absorbed in very thin aluminum layers and the cavity is filled with xenon, the noise generated by pressure fluctuations in the regions of low frequencies may be considerably stronger, since since the response of the optical microphone may be made sufficiently high without particular trouble. In the high frequencies, on the other hand, the pressure fluctuations are lost in the general noise. The extent to which this is correct for selective receivers has not been evaluated till now, either theoretically or experimentally.

In so far as the transferred noise is different throughout the spectrum, it will be distributed through the region from 10 to 1000 cps.

The scheme of the equipment on which the measurements were made is shown in Fig. 3. The signals from the receiver 1 amplified by the broad-band amplifier 2, were fed to the input of the noise analyzer 3. The signals from the noise analyzer were amplified by the power amplifier 4, detected by the thermal bridge (LT-2) 5, and recorded with the help of the electronic potentiometer 6 (type EPP-09). Simultaneously, the output from the analyzer switched on the lamp voltmeter 7 and the electronic oscillograph 8, with which it was possible to make a quick choice of the necessary amplification and to tune the equipment.

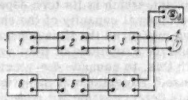

Fig. 3

In this equipment the analyzer proposed by Davydov and Voishvillo was used, based on the heterodyne principle of selection which permits the separation of frequency bands of fixed widths in the whole spectrum from 5 cps to 10 kcps. The width of the separated bands and the lower bounds of the measured frequencies were determined by the use of detuning in the analyzer quartz crystals, and amounted to 4 cps. The sound generator ZG-2 was used as an auxiliary generator.

The time constants of the recording equipment, consisting of the thermal bridge, power amplifier, and electronic potentiometer, amounted to about 40 sec, and was fixed principally by the time constant of the thermal bridge. Thanks to this large time constant the accuracy of the equipment was adequately high. The use of the thermal bridge allowed the measurement of the noise power, and by reading the electronic potentiometer, the determination of the mean square value of the noise voltage in the output of the analyzer. The accuracy of measurement was considerably increased also beyond that computed in that the record of noise in each frequency was produced over a long period (approximately 5-10 min), and then was averaged in addition.

The noise record in the frequencies 60, 90, 140, 190, 400, and 600 cps is shown in Fig. 4. The straight lines separate the several frequency regions, and the ordinates correspond to the noise magnitude.

Fig. 4

The results of measurement (with an optical microphone) of noise distribution in the chamber (of 3 mm depth) as a function of frequency are represented in Fig.

5, in which the abscissae are logarithmic frequencies in cycles/second, and the ordinates are the mean square noise values in microvolts. Curve 1 represents the overall cavity and microphone noise. This curve was obtained by direct measurement of the noise in the output of the receiver. Curve 2 represents the total noise without the chamber, since this noise was measured when a plane mirror was placed before the microphone instead of the chamber. Under these circumstances the illumination threshold of the photomultiplier was the same as that of the chamber (approximately 0.0121 lumen). Curve 3 represents the amplifier noise (the optical microphone lamp was switched off), and curve 4 represents the natural chamber noise ($\tau = 3 \times 10^{-3}$ sec).

From these graphs it is seen that the receiver noise and the photomultiplier circuit noise decreases with increasing frequency when the chamber is replaced by a fixed mirror. In the low frequencies (10-60 cps) receiver noise considerably exceeds the noise in the photomultiplier circuit; in the high frequencies (100-1000 cps) on the other hand, it is barely greater, and in this region the noise in practice does not depend on the frequency. The dependence appears to be on the shot effect and the fluctuations in the light flux from the auxiliary light source. Thus, in the low frequencies the receiver noise is established principally by chamber noise. Then in the 10 cps frequency the chamber noise exceeds the rest of the noise in the photomultiplier circuit by about 2.5 times. With increase in frequency the part of the noise dependent on pressure fluctuations decreases with the general noise. This is seen in curve 4 which represents the chamber noise. Its ordinates are the square roots of the difference of the squares of the ordinates of curves 1 and 2.

The rise of curve 2 in the low frequencies, i.e., the noise increase in the vacuum single cascade photomultiplier in the low frequencies should be controlled independently. This effect was not found in the case of the photomultiplier, but for vacuum photocells it is now new[17] and is seemingly dependent on the semiconductor effect of the cesium-antimony photocathode in a glass envelope.[18,19] These results were obtained by us with the standard photomultiplier FEU-2 with the normal potential between electrodes (170 and 70 volts). The usual procedure, from the viewpoint of noise, to find the most favorable conditions was not investigated.

In Fig. 6, curve 1 represents the noise of cavity No. 2, which was represented in Fig. 5, curve 4, and curve 2 represents the noise of cavity No. 1. The time constants of these two cavities are compared in the Table. Curve 3 serves for the comparison of the frequency dependence of noise of both cavities. It is found by reducing the ordinates of curve 2 at the frequency of 10 cps by the ordinate of curve 1 at the same frequency. From these curves it is evident that the noise of cavity No. 1 falls faster with frequency than the noise in cavity No. 2, which follows of course since the time constant of cavity No. 1 is 10 times larger than the time constant of cavity No. 2. Both curves are satisfactorily represented by the law $1/\sqrt{1 + (\omega\tau)^2}$.

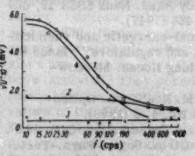

Fig. 5

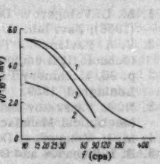

Fig. 6

Curve 1 deviates somewhat from this law in the region of high frequencies where, however, the measurement of noise is of poor accuracy. Curve 2, on the on the other hand departs from this law at the high frequencies. The deviation is apparently explained by inaccuracte measurements.

In the region of low frequencies (10-20 cps) curve 2 lies substantially lower than curve 1, although the heat loss of chamber No. 1, determined from the results of measurement of the time constant, amounts to 0.93×10^{-2} cal/sec, and for chamber No. 2 correspondingly 1.67×10^{-2} cal/sec, that is, 1.8 times larger. The heat capacity of the chambers amounts to 0.05×10^{-3} cal/deg, and 0.28×10^{-3} cal/deg, respectively; that is, they differ by a factor of 5.6.

From the computation of the response and the noise of the chamber it follows that the noise is inversely proportional to the square root of the heat loss. Consequently the pressure fluctuations in chamber No. 1 in the low frequencies (10-15 cps), where the thermal inertia does not play an essential role, should be 1.35 times larger than the pressure fluctuations in chamber No. 2. (The square root of the ratio of the thermal losses is equal to 1.35). Furthermore, chamber No. 1 has a volume 5.6 times larger than chamber No. 2. Consequently, its elasticity is that much greater.[15,20] Then, if the elasticity of the membranes in the chambers is greater than the elasticity of the chambers themselves, the noise of chamber No. 1 would be 1.35×5.6 times larger than the noise of the second chamber. This comparison should be correct under the circumstances that the reflectivities of the membranes of the chambers being compared and the properly weighted microphone would be the same in both cases. But experience, despite adhering to the specified conditions, brings contrary results. In the 10 cps frequency the noise in chamber No. 2 is twice as large as large as the noise in chamber No. 1. It seems that this is explained by the fact that chamber No. 1 has a much less flexible membrane; thus its noise and its specific response are reduced. In fairness to this conclusion, we are satisfied with the comparison of the chamber noise power, which will be the question considered in the following section.

SPECTRAL AND THRESHOLD RESPONSE OF SELECTIVE OPTICO-ACOUSTIC RECEIVERS

The spectral response of a selective optico-acoustic receiver is determined chiefly by the absorption of the gas filling its chamber. Expressly, the selectivity of a receiver provides the high selectivity of the optico-acoustic gas analyzers, which are adjusted for the determination of some component or another of the gas mixture. It is important in these cases that the receiver should not absorb radiation outside the absorption band of the gas, for example, by the walls of the chamber. In the other case, the nascent nonselective optico-acoustic effect may produce a false signal in the receiver and gas analyzer. In the chambers studied the nonselective optico-acoustic effect was reduced to a minimum in that the back wall of the chamber was polished and coated with a reflecting film of aluminum. The spectral response of such a chamber filled with CO_2 is shown in Fig. 7.

For the estimation of the threshold response corresponding to the mean square value of the noise of a selective chamber, a Hefner candle was used as the standard radiation source, the emission of which is selective. The part of the energy absorbed in the chamber was evaluated by placing an irradiated cell filled with gas before a nonselective receiver and a Hefner candle

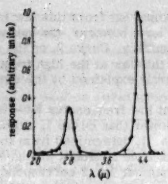

Fig. 7

at a distance of 1 meter. For this, the cell length was made equal to the optical length of the chamber. In this way the absorption of the radiation from this source by the gas in the cell was determined, and consequently that of the gas in the chamber.

From the results of the measurement it was established that in a chamber of 10 mm depth (optical length 20 mm) the part of the radiated energy of the candle absorbed amounts to only 13%; in another chamber (depth 3 mm) it is 6%. Thus with an increase of cavity depth by a factor of 3.3, the absorption increases only 2.2 times.

The measurement of the mean square noise, and consequently the threshold response was made in the following way. The radiation flux from a Hefner candle placed at a distance of 1 meter from the window of the receiver was chopped at a frequency of 10 cps. A diaphragm of diameter 5 mm was placed before the receiver so that a flux equal approximately to 2×10^{-8} watts passed through the chamber of the receiver. The signals from the receiver were amplified by a broad band amplifier and observed with the help of an oscillograph. Then, with the help of a filter with reverse coupling having a pass band width 0 to 0.15 cps, the peak noise was determined visually for a protracted period. Considering the mean square noise, it is known from experimental data that its magnitude is approximately a fifth of the peak noise.[21] The mean square noise, expressed in watts was computed from known data: (1) the signal expressed in instrument scale units, (2) the radiation flux generating this signal expressed in watts, and (3) the mean square noise expressed in instrument scale units. Then the radiation of the Hefner candle passing through the receiver chamber was taken into account.

It was established by the results of the measurement that in the computation of the radiation absorption of chamber No. 1 (greater depth), having the larger absorption coefficient and somewhat smaller thermal loss, it has a mean square noise corresponding to a signal caused by a flux equal to 3×10^{-9} watts in the spectral region of response. The second cavity appeared to be approximately 2.5 times noisier. This discrepancy of the response at the limiting accuracy of measurement is in harmony with the determination of the higher absorption and thermal loss. If the mean square noise is computed on the basis of the values found here for the thermal losses, and the absorption coefficients by formula (4) of reference 9, then we find correspondingly 4×10^{-9} and 1×10^{-8} watts in the 0.15 cps wide observation band. Thus the results of the earlier calculations are in satisfactory agreement with experiment.

CONCLUSIONS

An investigation of selective optico-acoustic receivers with optical microphones was conducted. The investigation was made on two chambers filled with carbon dioxide gas and of differing dimensions. One chamber had a depth of 10 mm, diameter 9.4 mm; the other was rectangular 6 mm × 7 mm and of depth, 3 mm. The first chamber had a time constant 0.03 sec, the second, 0.003 sec.

The radiation absorbed from a Hefner candle amounted to 13% and 6% in the chambers. The mean square noise at the frequency of 10 cps in the first case corresponded to a radiation flux of 3×10^{-9} watts and in the second case to 8×10^{-9} watts for a pass band amplifier of width 0.15 cps.

Noise decreases with increasing frequency. In the low frequency range the noise of the receiver is determined by the noise of the chamber. In the region of low frequencies the semiconductor noise of vacuum photomultipliers is observed in the same way, which exceeds the shot effect and constitutes a substantial part of the general noise. In the high frequencies the noise of the receiver is determined by the shot effect and fluctuations of the light flux in the auxiliary source, but not by chamber noise.

Thus in the low frequencies (in the region 10-15 cps) optical microphones allow the complete realization of the threshold response of optico-acoustic chambers, i.e., the noise of all receivers is determined in their entirety only by the chamber noise.

Chambers with large depth have better sensitivity threshold at the expense of small thermal losses and larger absorption, but significantly larger time constants. The thermal losses are chiefly determined by the thermal conductivity, radiation for such chamber constructions amounting to only a small portion of the general losses.

Further increase of response by increase of the dimensions of the chamber would entail further increase of the time constant. However, a more acceptable means is planned. It appears possible to improve substantially the response of a chamber by increasing its dimensions, filling with a gas at lower pressure, and using radiation in multiple paths. Then the absorbed radiation will be the same as in the usual chamber, but the specific response should be higher. The heat loss, dependent on the thermal conductivity, will be smaller because of the increased dimensions of the chamber, but the part of the loss from radiation will be increased, and might become commensurate with the thermal conductivity dependent loss. This is very important, as it has been shown[12] that the optimal construction of the nonselective chamber is achieved when the thermal conductivity loss is approximately equal to the radiation loss. We think that this is correct for selective cavities. By means of such systems it is possible, it appears, to approach the realization of high sensitivity dependent on the degree of enhancement of the selective receiver.[22]

The authors of the paper express their appreciation to Professor M. L. Veingerov for his constant interest and guidance in this work.

REFERENCES

1. M. L. Veingerov. Doklady Akad. Nauk SSSR 19, 687 (1938); Zav. lab. No. 4, 426 (1947).
2. V. A. Pavlenko. "Thermal-energetic and chemico-technological equipment and regulators." Issue 6, p. 96, Machinery Publishing House, Moscow-Leningrad, 1959.
3. N. A. Pankratov and L. M. Nechaeva. Optico-Mechanical Manufacture No. 4, 8 (1958).
4. M. L. Veingerov. Doctoral Dissertation, GOI, 1940.
5. B. I. Stepanov and O. P. Girin. Soviet Phys.-Tech. Phys. (translation of Zhur. Tech. Fiz.) 20, 10, 1950.

6. P. V. Slobodskaya. Izvest. Akad. Nauk SSSR, Ser. Fiz. **12**, 656 (1948).
7. A. O. Sall', Soviet Phys.-Tech. Phys. **26**, 157 (1956).
8. K. Mori. J. Sci. Res. Inst. **1**, 290, 407, 414 (1955).
9. N. A. Pankratov. Opt. i Spektr. **2**, 662 (1957).
10. A. O. Sall'. Opt. i Spektr. **6**, 219, 556 (1959).
11. M. Golay. Rev. Sci. Instr. **18**, 347 (1947).
12. M. Golay. Rev. Sci. Instr. **20**, 816 (1949).
13. E. N. Maleev. Opt. i Spektr **4**, 121 (1958).
14. N. A. Tolstoi and P. P. Feofilov. Doklady Akad. Nauk SSSR **58**, 389 (1947).
15. N. A. Pankratov. Optico-Mechanical Manufacture No. 3, 7 (1957).
16. V. S. Davydov and G. V. Voishvillo. Prib. i Tekh. Eksp. **6**, 82 (1958).
17. H. J. I. Zijlstra and C. T. J. Alkemade. J. Appl. Phys. **27**, 656 (1956).
18. P. I. Lukirskii and N. N. Lusheva. Soviet Phys.-Tech. Phys. **7**, 1900 (1937).
19. S. Yu. Luk'yanov, N. N. Lusheva, and I. S. Mazover. Soviet Phys.-Tech. Phys. **9**, 1808 (1938).
20. V. V. Furduev. "Elektroakustika." GTI, 1948.
21. S. Gol'dman. "Harmonic Analysis, Modulation, and Noise." IL, Moscow, 1951.
22. P. B. Fellget. J. Opt. Soc. Am. **39**, 970 (1949).

DETERMINATION OF ABSORPTION SPECTRA OF CRYSTALLINE PHOSPHORS BY MEANS OF DIFFUSE REFLECTION SPECTRA

I. P. Shapiro

Received 5 March 1959

We studied the absorption and diffuse reflection spectra in the visible and near ultraviolet for a series of powdered materials (Se, CdI_2, PbI_2) and sulfide phosphors.

We have shown that the values of the absorption coefficients determined by diffuse reflection and directly by means of sublimated films, respectively, are in good agreement. They thus permit determination of the contour of the absorption bands of dispersed materials.

1. In studying the luminescence of powdered materials, including crystalline phosphors, it is necessary to know the absorption spectrum of the luminor. It is difficult, however, to obtain the absorption spectra of the majority of crystalline phosphors due to the strong scattering of light in finely crystalline powders.

Attempts to obtain the absorption spectra of tiny crystals which are based on Brumberg's method[1] are not successful in the case of a finely dispersed medium. More reliable data on the absorption spectra can be obtained only for phosphors grown in the form of single crystals, which is not always possible. Direct determination of the absorption spectrum from the diffuse reflection spectrum leads only to a qualitative idea concerning the absorption spectrum, since it is not always possible to identify the absorption spectrum with the diffuse reflection spectrum.[2] An attempt at such an identification led to the incorrect determination of the width of the forbidden band in a number of semiconductors and insulators.[3] The reflection spectra of dispersed materials depend not only on the optical constants of the basic substance but also on several other factors.[4] The methods for computing diffuse reflection coefficients proposed by Gurevich[5] and other authors[6] do not take particle size into account. This leads to results which do not agree with experimental data.[3,7,8] Bodo[9] has proposed a method for taking particle size into account. His relations, however, are cumbersome and inconvenient for actual computation. Girin and Stepanov[2,10] have developed a general theory of diffuse reflection based on the idealized Bodo model. This theory is also applicable for less highly dispersed and strongly reflecting materials. Their expressions are much simpler than the Bodo formulas and have been tabulated. They permit easy and convenient determination of the absorption coefficients from the experimental values of the diffuse reflection coefficients. Antonov-Romanovskii[11] took the fact that the phosphor layer consists of small crystals into account, and studied the type of scattering produced by crystals of different shapes. He thus obtained particularly simple relations which permit a quantitative estimate of the absorption coefficients from the diffuse reflection spectra.

The present paper gives additional experimental data which confirm the correctness of the diffuse reflection theory developed by Stepanov and Antonov-Romanovskii. It also gives the absorption curves of a series of sulfide phosphors from their diffuse reflection spectra.

2. For a preliminary investigation, we chose easily sublimed substances whose absorption spectra could be measured directly with an SF-4 spectrophotometer and a UM-2 monochromator. The first experiments on the measurement of the absorption spectrum $K(\lambda)$ of amorphous selenium were carried out by two independent methods—the method of Stepanov and Antonov-Romanovskii and absorption by thin films. Figure 1 shows the curves $R_\infty(\lambda)$ for the diffuse reflection spectra of amorphous selenium powders with average grain sizes of 90, 175, and 265 μ. It also presents the curve $K(\lambda)$ calculated from the diffuse reflection spectra, using Stepanov's formulas and Chekalinskii's[3] Tables. Figure 1 shows that the calculated points of all three of the diffuse reflection spectra investigated fall rather well on the curve $K(\lambda)$.

The selenium films were obtained by evaporation in vacuo. The thicknesses of the films (2.4 and 4.2 μ) were determined by accurate weighing. These films were used to measure the true value of $K(\lambda)$ by means of the monochromator UM-2. Table 1 contains the values—for several frequencies—of the absorption coefficient $K(\lambda)$ computed from the diffuse reflection spectrum and found experimentally.

Table 1

Wavelength λ (mμ)	K(λ) computed (cm^{-1})	K(λ) experimental (cm^{-1})
640	131	123.7
650	130	128.8
665	122	112
670	100	105
678	82	86.4
687	69	71.4

The values given in Table 1 indicate that by using the method of Stepanov and Antonov-Romanovskii we can obtain the correct order of magnitude for the quantity K and the correct dependence of K on λ.

We also performed experiments to determine the low frequency absorption edge of $CdI_2 \cdot PbI_2$ phosphors. The measurement of K(λ) was also carried out by two independent methods—the method of diffuse reflection and absorption by thin films.

In this case, films of specified thickness and activator concentration were obtained as follows: A flat platinum heater was mounted inside a bell jar connected to a vacuum pump. (See Fig. 2.) An electromagnetic arrangement permitted porcelain crucibles containing CdI_2 or PbI_2, respectively, to be brought the heated surface. The heated powders were sublimed onto the surface of a cover glass placed on a disc, which could rotate at a prescribed speed. The heating rate and the vacuum system remained constant throughout the evaporation process. Assuming that the molecular beam of the substance being evaporated is propagated rectilinearly and also that the rate of deposition does not change in the course of evaporation, we may consider (with a certain degree of approximation) that the mass of the deposit is proportional to the evaporation time. Knowing the speed of rotation of the disc and weighing the deposit after a given number of revolutions, we may subsequently determine the weight of the deposit from the total number of revolutions. Thus there is no difficulty in obtaining CdI_2 and PbI_2 films and also films of the $CdI_2 \cdot PbI_2$ phosphor with a given activator concentration.

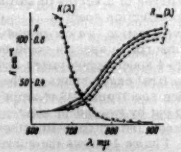

Fig. 1

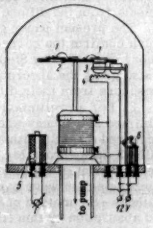

Fig. 2

Fig. 1. The absorption spectra K(λ) and the diffuse reflection spectra $R_\infty(\lambda)$ of amorphous selenium powders of different grain sizes. Curve 1—90, curve 2—175, curve 3—265 μ.
Fig. 2. Diagram of arrangement for obtaining sublimed phosphors. 1—sample, 2—disc, 3—porcelain crucible, 4—platinum heater, 5—indicator of number of revolutions, 6—rotating arrangement.

Figure 3 shows the absorption curves of pure CdI_2 (curve a) and pure PbI_2 (curve b) obtained with an SF-4 spectrophotometer in the 330-800 mμ region. No measurements were performed below 330 mμ. From cheesman's data[12] we can obtain the long wavelength edge of the absorption band of the substances studied by extrapolating the straight portion of the curve to the abscissa axis. Figure 3 shows that the long wavelength edge of the CdI_2 absorption band corresponds to a frequency of 26,000 cm^{-1}, and that of PbI_2 to 19,000 cm^{-1}. An analogous situation is observed when we analyze the absorption spectra obtained from the diffuse reflection spectra of CdI_2 and fuse reflection spectra of CdI_2 and PbI_2 powders.

The right-hand portion of Fig. 3 shows the diffuse reflection curves and the corresponding calculated absorption curves for pure CdI_2 (curves 1, 1′) and PbI_2 (curves 2, 2′). The curves show that the long wavelength edge of the absorption bands for CdI_2 and PbI_2 also correspond to the frequencies ~26,000 and 19,000 cm^{-1} respectively. The absorption curves of the $CdI_2 \cdot PbI_2$ phosphors obtained with an SF-4 also correspond to the calculated absorption curves obtained by diffuse reflection methods.*

*Such a correspondence indicates not only the applicability of the method of diffuse reflection but also the fact that the fine crystalline and the sublimed layers have the same structure.

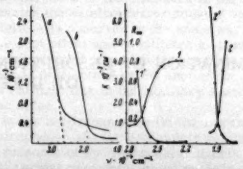

Fig. 3. Absorption curves (a, b), diffuse reflection curves (1, 2), and the corresponding calculated absorption curves (1′, 2′) for pure CdI_2 and PbI_2. Curves a, 1, 1′—CdI_2; curves b, 2, 2′—PbI_2.

We must note in estimating the absorption coefficient by the diffuse reflection method that marked deviations from true values obtained by direct measurement are highly probable. This is due to the fact that the latter values depend on particle size as well as on film thickness. We were unable to use homogeneous classes of grain size in the experiments described. (The size of the grains used ranged from 5 to 15 μ.)

The occurrence of multiple reflection in thin films can also lead to different values of the absorption coefficient, depending on the relative thickness of the sample being studied. An error of a factor of two is therefore highly probable in extimating the magnitude of the absorption coefficient. It is possible, nevertheless, to use the method of Stepanov and Antonov-Romanovskii for obtaining the correct order of magnitude for K and for determining the envelope of the absorption bands of dispersed substances. This includes the majority of the technically important crystalline phosphors.

3. In addition, we used the diffuse reflection method to obtain the absorption spectra of a number of sulfide phosphors. Figure 4 shows the diffuse reflection curves and the corresponding calculated absorption curves for sulfide phosphors of the following brands: Fk-106; L-15; FKP-03[1]; ZJ-9; FK-102. We determined the long wavelength edge of the absorption band and the width of the forbidden band from the absorption spectra.

The results of the investigations are tabulated in Table 2.

Table 2

Phosphor brand	Long wavelength edge of absorption band (mμ)	Width of forbidden band (eV)
FK –106	385	3.11
FKP– 03[1]	407	2.94
L – 15	411	2.91
ZJ – 9	411	2.91
K – 49	432	2.7
FK –102	450	2.66

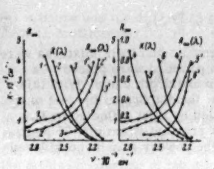

Fig. 4

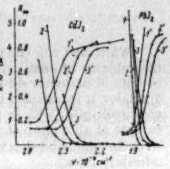

Fig. 5

Fig. 4. Absorption curves K(λ) and diffuse reflection curves $R_\infty(\lambda)$ for Phosphors of different brands. Curves 1, 1′—FKP-03[k]; curves 2, 2′—ZJ-9; curve 3, 3′—FK-102; curves 4, 4′—FK-106; curves 5, 5′—L-15; curves 6, 6′—K-49. Fig. 5. Diffuse reflection curves (1′, 2′, 3′) and corresponding calculated absorption curves (1, 2, 3) for CdI_2 and PbI_2 at different temperatures.

We also carried out experiments on obtaining the diffuse reflection spectra of hot CdI_2 and PbI_2 powders. Figure 5 shows the diffuse reflection curves and the corresponding calculated absorption curves for these powders at temperatures from 100 to 200°C. We deduce from the curves that heating displaces the long wavelength edge by about 0.9 A/deg for CdI_2. Cheesman[12] found that for CdS the absorption edge is displaced upon heating, by about 0.7 A/deg. This displacement is apparently connected with a decrease in the width of the forbidden band caused by a broadening of the fundamental bands of the heated lattice.

I express my deep appreciation to B. I. Stepanov for valuable comments in discussing the results of this work.

REFERENCES

1. E. M. Brumberg and F. M. Pekerman. Izvest. Akad. Nauk SSSR, Ser. Fiz. **13**, 218 (1949).
2. O. P. Girin and B. I. Stepanov. Zhur. Eksp. i Teoret. Fiz. **4**, 10 (1954).
3. I. P. Shapiro. Opt. i Spektr. **4**, 256 (1958).
4. B. I. Stepanov, Iu Chekalinskii, and O. P. Girin. Trudy Inst. Fiz. i Mat. Akad. Nauk BSSR **1**, (1952).
5. M. M. Gurevich. Trudy GOI, **6**, no. 57 (1931).
6. P. Kubelka and F. Munk. Z. tech. Physik **12**, 593 (1931);
G. Kortüm and M. Kortüm-Seiter. Naturforsch. **2a**, 652 (1947).
7. Z. V. Zhidkov. Zhur. Eksp. i Teoret. Fiz. **27**, 458 (1954).
8. G. Kortüm and P. Hang. Z. Naturforsch. **8a**, 372 (1953).
9. L. Bodo. Acta Phys. Acad. Sci. Hung. **1**, 135 (1950).
10. B. I. Stepanov. Izvest. Akad. Nauk SSSR, Ser. Fiz. **21**, 11 (1957).
11. V. V. Antonov-Romanovskii. Zhur. Eksp. i Teoret. Fiz. **26**, 459 (1954).
12. J. C. Cheesman. Department of Mathematics, Imperial College, London, 1951.

STUDY OF DIFFUSE REFLECTION FROM POWDERS UNDER DIFFUSE ILLUMINATION

A. S. Toporets

Received 13 April 1959

Diffuse reflection by powders of white and colored pigments, and their mixtures, under diffuse illumination was studied with the help of a special spectrophotometric apparatus. It is shown that there is a linear relationship in the interval of observation angle from 0 to 70 deg between the concentration of the absorptive pigment in the mixture and the difference of the functions of the coefficients of brightness.

The results are examined and the observed phenomena are interpreted.

1. In certain theoretical works which consider the passage of light through diffusing media, it is assumed that the structure of the light beam is maintained even within the medium. Such an assumption greatly eases the study, and leads to comparatively simple laws.[1,2] In practice, however, it is necessary to deal with beams of changing structure, since most often directed beams are used for illumination of the objects under study. Such a beam, passing through a light-scattering layer, gradually loses its directedness and becomes diffuse; its structure changes with depth of penetration, and mathematical description of such a beam leads to exceedingly complex expressions which it is not feasible to use.[3]

In our own preceding researches[4] we have produced diffuse illumination by the method of dilution, which consists of mixing the strongly absorptive powder under study with one of weak absorption.

In the present work we have applied diffuse illumination, having built a special spectrophotometric apparatus for the purpose. The apparatus consists of the following: a light source, condenser lens, monochromator, a diffuse illuminator, and an amplifier-receiver device.

The structure of the diffuse amplifier is shown schematically in Fig. 1. Its basic part is sphere 1 of diameter 200 mm, coated inside with barium sulphate. Light from the monochromator slip passes into the interior of the sphere through milk-glass 2 (transmission coefficient about 50%), is diffused in the sphere, and gives a uniform illumination on its walls.

There sphere has pivots 3, about which it can rotate. Samples to be measured are held in a horizontal plane which passes through the axis of rotation of the sphere, and introduced into the sphere through window 4. Samples are placed in holder 5, which can be moved from the center of the sphere to the wall and back by means of spindle 6. The spindle passes through the tube 7, to the end of which is soldered the spherical segment opposite window 4. For setting up the sample, the tube together with the spindle is moved to the left as far as possible.

When the sample is at the center of the sphere, it is illuminated by light reflected from the upper hemi-

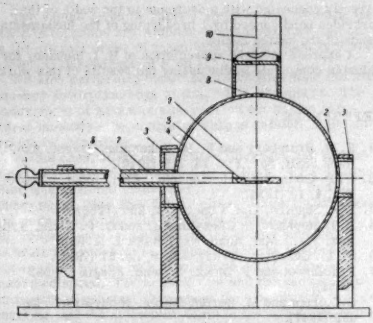

Fig. 1. Sketch of the diffuse illuminator.

sphere, and since the brightness of the walls is everywhere the same, the illumination of the sample is perfectly diffuse. The light reflected by the sample, passing through diaphragms 8 and 9, falls on the photocathode of the receiver in the box 10. Turning the sphere on its bearings, one can measure the angular distribution of the reflected light flux within the limits of two quadrants.

2. With the help of the apparatus just described one can measure the absolute coefficient of brightness. Let us place at the center of the sphere a nonabsorbing sample which diffuses according to Lambert's law. We will find its brightness. If a light flux Φ enters the sphere (the radius of the sphere is 1, the coefficient of reflection of the wall of the sphere is ρ_c), then the illumination on the wall of the sphere is

$$E_c = \frac{\Phi}{4\pi l^2} \frac{\rho_c}{1-\rho_c},$$

and the brightness of the wall of the sphere

$$B_c = \rho_c \frac{E_c}{\pi}.$$

In such a case the illumination on the sample is expressed by

$$E_0 = \pi B_c,$$

the brightness of the sample by

$$B_0 = r \frac{E_0}{\pi} = B_c,$$

since $r = 1$.

Thus the brightness of a nonabsorbing ideally diffusing sample is equal to the brightness of the wall of the sphere diffusely illuminating the sample. Consequently, measuring the brightness of any sample placed at the center of the sphere relative to the brightness of the wall of the sphere, it is possible to find the absolute coefficient of brightness of the sample.

3. Measurements of the coefficient of brightness under diffuse illumination were performed in the following manner. By means of spindle 6, the sample to be studied was moved toward the wall of the sphere. The light reflected by the wall of the sphere $\Delta\Phi_c$ then fell upon the photomultiplier. The sample was then put at the center of the sphere, and the magnitude of light flux $\Delta\Phi_c$ reflected by it was measured. It is easy to show that

$$\frac{\Delta\Phi_0}{\Delta\Phi_c} = \frac{B_0}{B_c} = \rho. \qquad (2)$$

White and colored pigments and their mixtures were the subjects of study. The powders were placed in a cuvette of diameter 42 mm and depth 5 mm. With this diamater it is assured that the diaphragm in front of the photomultiplier will be filled by light reflected by the sample at all angles of observation (from 0 to 75 deg). With the indicated depth, the powder may be considered infinitely thick.

Some results of the measurements are given in the figures. In Fig. 2 the dependence of the coefficient of brightness is shown. Curve 1 is for magnesium oxide. Here we see a systematic increase in the coefficient of brightness with increase in the angle of observation. It is true that the increase is slight—at an angle of 75 deg the coefficients of brightness has grown only by 4%, but for an object of pronounced absorption, the increase of the coefficient of brightness with angle of observation is significantly greater. Curves 2, 3, and 4 are for mixtures of magnesium oxide and ultramarine. It is clear from the figure that the larger the absorption in the layer, the larger the change of the coefficient of brightness. Thus, in changing the angle of observation from 0 to 75 deg for a mixture with 2% content of ultramarine, the coefficient of brightness changes by 28%; for a 5% mixture by 41%; for a 10% mixture by 50%; and for pure ultramarine by 60%.

Figure 3 illustrates the change of the coefficient of brightness for the same objects, but for another, lesser absorbed wavelength. Here the relative changes of the coefficient of brightness are significantly smaller than in the preceding case.

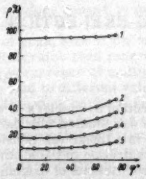

Fig. 2

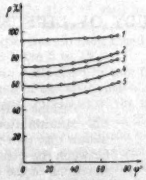

Fig. 3

Fig. 2. Coefficients of brightness of various powders at varying angles of observation $\phi(\lambda = 580 m\mu)$. Curve 1—magnesium oxide; curves 2, 3, and 4—mixtures of magnesium oxide with ultramarine (concentrations of ultramarine respectively: 2, 5, and 10%); curve 5—pure ultramarine.

Fig. 3. Coefficients of brightness of various powders at varying angle of observation ($\lambda = 450$ mμ). For indices see Fig. 2.

It is seen from the given data that the greatest change of the coefficient of brightness takes place with small concentrations of absorbing pigment. In Fig. 4 is shown the dependence of the relative change of coefficient of brightness $(\rho_\infty - \rho_0)/\rho_0$ upon the concentration of ultramarine in the mixture. The curve expressing this dependence has two regions: in the first, which is very small, the coefficient of brightness changes quite rapidly, and the curve is steep; in the second region the curve becomes almost flat.

In a preceding work[4] we established a dependence of the following form between the pigment concentration in

the mixture and the difference of the functions of the reflection coefficients:

$$\frac{a_p}{s_b} c \cong \frac{(1-R_{CM})^2}{2R_{CM}} - \frac{(1-R_b)^2}{2R_b}(1-c), \qquad (3)$$

where c is the concentration of absorbing pigment in the mixture, R_{CM} and R_b are, respectively, the coefficients of reflection of the mixture and the diluting pigment a_p is the absorption constant of the absorbing pigment, s_b is the diffusion constant of the diluting pigment.

We have attempted to apply this formula to the results of the present work. The coefficient of brightness was substituted for the coefficient of reflection in the formula. Figure 5 shows the dependence of the difference of the functions of formula (3) in the concentration of ultramarine in a mixture with magnesium oxide. The following conclusions can be drawn from the figure: (a) There is a linear relationship between the concentration of absorbing pigment in the mixture and the difference of the functions of coefficients of brightness. (b) This law holds for coefficients of brightness corresponding to various angles of observation (from 0 to 70 deg). (c) The slope of the lines expressing this law is a function of the angle of observation: the greatest slope is for normal coefficient of brightness; the slope of the line varies inversely as the angle of observation.

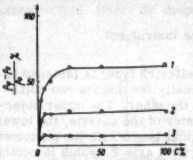

Fig. 4

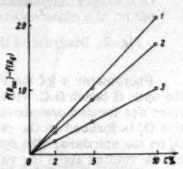

Fig. 5

Fig. 4. Dependence of the relative change of the coefficient of brightness on the concentration of absorbing pigment in the mixture at various angles of incidence (λ = 580 mμ). Angle of incidence: Curve 1—75 deg; curve 2—60 deg; curve 3—40 deg.

Fig. 5. Dependence of the difference of the functions of the coefficients of brightness upon concentration of the absorbing pigment in the mixture at various angles of incidence. (λ - 580 mμ). Angle of incidence: Curve 1—0 deg; curve 2—40 deg; curve 3—70 deg.

4. We will now discuss the results obtained. We will first examine the question of the increase of the coefficient of brightness with increase in the angle of observation. It seems to us that this phenomenon may be explained as follows. It is known that the indicatrices of light scattering particles are strongly drawn forward so that the quantity of light reflected by a layer depends on the angle of incidence of the light. With normal incidence, the indicatrix is necessarily also normal, and a comparatively small portion of the incident light is reflected. With increase in the angle of incidence, the quantity of reflected light begins to grow, and this growth proceeds in directions at large angles. Under our conditions the sample is illuminated by a hemisphere, i.e., by rays falling on the sample with angles of incidence from 0 to to 90 deg.

The light flux issuing from the diffusing layer may be considered as consisting of two components—a perfectly diffused part, caused chiefly by deep layers of particles, and a directed portion corresponding to the elementary layers situated near the surface. In weakly absorbing substances, for example magnesium oxide, the fraction of the directed dispersed light in the total reflection is small, so that the magnitude of the coefficient of brightness at large angles of observation is insignificant. In the presence of absorption the deep layers, corresponding to the diffuse component, became more or less negligible and the fraction of the directed dispersed light grows, becoming larger with greater absorption. From this it follows that the brightness of absorbing light scattering objects under diffuse light must increase with increased angles of observation.

We will turn now to consideration of Fig. 4. The presence in the curve of two portions—a steep and a flattened part—we are inclined to explain in the following manner. On the steep part of the curve we are concerned with both components, diffuse and directed. With increase in concentration the fraction of the diffuse component falls until that concentration is reached at which the reflected flux consists entirely of once-dispersed rays. In this case the fraction of the directed component almost reaches a maximum, and hardly changes with further increase in concentration. This region of concentrations corresponds to the flattened portion of the curve of Fig. 4. Thus the two portions of the curve are related to different mechanisms of dispersion.

Attention is drawn to the fact that change of the coefficient is finished in a comparatively narrow region of concentration, the width of this region being different for fluxes dispersed at different angles: a 5% concentration is sufficient for an angle of 40 deg; 10% for an angle of 60 deg, and 25% for an angle of 75 deg. It follows from this that rays incident at different angles are differently attenuated in reflection: the greatest attenuation is experienced by a normally incident ray, and the least by a ray incident at an angle approaching 90 deg. From this one can draw the conclusion that for differently inclined rays the concept of the "infinitely thick film" has differing meaning. For rays incident at large angles "infinitely thick" is a thinner layer than for rays incident at smaller angles.

The existence of a linear dependence between the difference of functions of the coefficients of brightness and the concentration of the absorbing pigment in the mixture (Fig. 5) attests that this law is correct not only for the entire reflected flux, but also for the elementary fluxes diffused within the limits of the solid angle $\Delta\omega$. This conclusion follows from the fact that under diffuse illumination the coefficient of brightness may be considered as the ratio of flux reflected within the solid angle $\Delta\omega$ to the flux incident within the same solid angle.

REFERENCES

1. P. Kubelka and F. Munk. Z. techn. Physik 12, 593 (1931).
2. M. M. Gurevich. Physik. Z. 31, 753 (1930); Trudy GOI, 4, No. 57 (1931).
3. S. Q. Duntley. J. Opt. Soc. Am. 32, 61 (1942); J. Opt. Soc. Am. 33, 252 (1943).
4. A. S. Toporets. Opt. i Spektr. 4, 494 (1958).

A VISUAL NEPHELOMETER

V. N. Tsvetkov and V. S. Skazka

Received 19 March 1959

A visual nepholometer for study of the index of diffusion of light by solutions of high-molecular compounds is described. The experimental methods are briefly examined. As an example the article gives the data of measurements of two fractions of polystyrene in benzene. Results are found in good agreement with data in the literature.

INTRODUCTION

The application of the method of light diffusion for the determination of molecular weight and dimensions in solution is generally known.[1-3] To this end, for example, one can measure Rayleigh's ratio for the solution, R_{90}, at an angle $\theta = 90°$ in the direction of the incident light, and the asymmetry of the diffusion index 1, defined as the ratio of the intensities of light dispersed at two angles, symmetrical with respect to $\theta = 90°$ (for example, 45° and 135°).

However. for more precise determination of the molecular weight and dimensions in solution, knowledge of the entire index of diffusion is necessary,[4,5] which may yield additional information about the polymer.[6-8]

At the present time many instruments exist, in this country and abroad, which allow measurement of the diffusion index in the interval of angles 30-150 deg.[5,9,10] In all of them the receiver of diffused light is a photomultiplier, which considerably complicates them. With the goal of simplification of construction and experimental method, we have built an analogous visual instrument in which a photometer of the Pulfreich type is used.

STRUCTURE OF THE NEPHELOMETER

The scheme of the nephelometer is shown in Fig. 1 (projected on a horizontal plane XY) and Fig. 2. Light from the source S (mercury lamp SVDSh-250) is focused by the condenser O_1 (f = 3 cm) on the slit D (1 × 2 mm), an image of which is projected by objective O_2 (f = 18 cm) to the center of the cuvette K. A green filter F is situated in the optical path, as is a polaroid filter separating the vertically polarized component of the light (the Z-component). A portion of the primary light is separated by the thin glass plate P, situated at an angle of 45 deg to the direction of the optical axis. This second beam is twice turned by glass mirrors Z_1 and Z_2 (Fig. 2) and is directed upward at the cylinder E (or turbid glass, diameter 1.5 cm height 1 cm); it represents a source of standard diffuse light. Observation of the light diffused by the standard is always made at an angle of 90 deg to the direction of the light beam incident upon it. The standard is illuminated by circularly polarized light the device for which is shown in the diagram by a Frank-Ritter prism P_2 and a quarter-wave plate, properly oriented. This assures uniformity of light dispersed by the standard in all directions normal to the Z-axis.

Fig. 1. Diagram of the instrument in the XY plane.

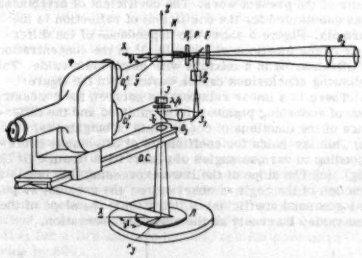

Fig. 2. Diagram of the instrument.

Photometer Φ (of the Pulfreich type) is fastened to the optical bench O.C. vertically, so that its two objectives are located one above the other. The upper objective O_1' is focused on the center of the cuvette, the lower O_2' on the standard. The optical bench with the photometer can be rotated about the vertical axis Z, which is coincident with the axis of the cuvette. The angle of rotation of the bench is defined by the base L, rigidly connected with it. The operating interval of angles is from 30 to 140 deg.

THE CUVETTE

The liquid under study (solution, solvent, or a standard liquid for calibration) is poured into the operating cuvette K. The cuvette is a glass cylinder, machined from a block of optical glass, and polished inside and outside. The exterior diameter of the cylinder is 50 mm, the interior 40 mm, and the height from 30 to 60 mm. In the lower portion of the cylinder there are two apertures of diameter 10 mm for entry and exit of the light beam. An optical glass rod of length 40 mm is cemented to the input aperture, to space the air-glass boundary from the solution. Simiarly, a rod of black absorbing glass (marblite) is cemented to the output aperture. Light reflection from the glass-solution boundary is negligibly small. The rear wall of the cuvette is coated with an antihalation lacquer. The cuvette is fastened to a special base, and placed in the instrument in a position which is fixed with respect to the incident light beam.

CALCULATION OF RAYLEIGH'S NUMBER FOR A SOLUTION FROM EXPERIMENTAL DATA

The turbidity of the glass standard is chosen to be so great that the intensity of light diffused by the standard

is at all events greater than the intensity of the light diffused by the solution. Therefore, the possibility exists of operating with the diaphragm of objective O_1' of the photometer fully open over the entire operating interval of dispersion angles. Light metering is performed by changing the diaphragm of the lower objective O_2'. The indication of the drum of the diaphragm of this objective, when the two fields of the photometer are equally illuminated, is proportional to the intensity of the light dispersed by the solution (or other liquid) placed in the cuvette.

The given measurements of dispersion of light by a solution at various angles must be normalized with respect to volume of liquid. The diffusing volume V_θ observed in the photometer changes as a function of the angle of observation according to the following law:

$$\frac{V_\theta}{V_{90}} = \frac{1}{\sin\theta}. \qquad (1)$$

where V_{90} is the dispersing volume at $\theta = 90°$. The inclinations yielded by this theoretical formula are theoretically possible. As has been shown by measurement of dispersion by a solution not having an asymmetric index of dispersion (a solution of low-molecular polystyrene in tetrachlormethane, and also benzene), for our instrument the change in volume as a function of the angle of observation confirms, with an adequate degree of accuracy, the theoretical formula (1). Figure 3 illustrates this. Here, the dispersion angle θ is on the

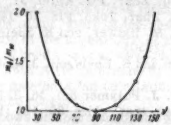

Fig. 3. Dependence of the dispersing volume as a function of angle of dispersion. The curve was calculated on the basis of Eq. (1); the points are the experimental results.

abcissa, and the ratio m_θ/m_{90} on the ordinate; m_θ is the drum reading at observation angle of θ, and m_{90} is that at observation angle of 90 deg, for the same dispersing substance. Since $m_\theta \sim I_\theta$, where I_θ is the light intensity dispersed at an angle θ, and $I_\theta \sim V_\theta$, then

$$\frac{m_\theta}{m_{90}} = \frac{I_\theta}{I_{90}} = \frac{V_\theta}{V_{90}}.$$

With an accuracy within a factor, the value of the Rayleigh ratio for the solution R_θ is obtained by multiplying the reading of the lower drum m_θ by the corresponding value of sin θ.

To obtain the absolute value of Rayleigh's ratio for the solution, we can compare it with a standard of dispersion, for which benzene can be chosen. In this, two cases should be distinguished.

1. The fracture index of the solution under study (practically speaking, of the solute) n_s coincides with that of the standard liquid (benzene) n_0. In this case the ratio of the quantity $m_\theta \sin\theta$ to the drum reading m_{90}^0 in the photomeasurement of benzene at an angle of 90 deg is equal to the quotient of the Rayleigh ratios for the solution R_θ and benzene R_0.

$$\frac{R_\theta}{R_0} = \frac{m_\theta \cdot \sin\theta}{m_{90}^0}. \qquad (2)$$

The absolute value of R_θ for the solution is found from Eq. (2), using the known value of R_0 for benzene.

2. The fracture index of the sample n_s differs from that of the standard. In this case, it is necessary to introduce into Eq. (2) the correction factor $(n_s/n_0)^2$, [11] and to define the quantity R_θ by the relationship

$$R_\theta = R_0 \frac{m_\theta \cdot \sin\theta}{m_{90}^0} \left(\frac{n_s}{n_0}\right)^2. \qquad (3)$$

Special attention should be given to quantity R_0 for benzene. The value $R_0 = 16.3 \times 10^{-6}$ cm^{-1} [12] is obtained for the case in which the dispersing substance (benzene) is illuminated by nonpolarized light. In working with polarized light, it is necessary to consider the extent of depolarization Δ of the scattered light. It follows from the theory that the magnitudes of Rayleigh's ratio for one and the same dispersing sample, under illumination by vertically polarized ($R_{pol.}$) and nonpolarized ($R_{nonpol.}$) light, and observed at an angle $\theta = 90°$, satisfy the following relationship:

$$\frac{R_{pol.}}{R_{nonpol.}} = \frac{2}{1+\Delta},$$

where Δ is the degree of depolarization of the substance for natural light. A test of this formula by comparison of the dispersion of benzene ($\Delta = 0.412$) with the dispersion of a solution of the low-molecular fraction of polystyrene in C Cl_4 ($\Delta = 0.03$) showed good agreement between it and experiment.

It is easy to show that in work with polarized light (which takes place in our instrument—polaroid P_1 in Figs. 1 and 2), it is necessary to introduce into formula (3) the correction factor $(1 + \Delta_0)$ and to use the formula

$$R_\theta = R_0 \frac{m_\theta \cdot \sin\theta}{m_{90}^0} \left(\frac{n_s}{n_0}\right)^2 (1+\Delta_0). \qquad (4)$$

Here the symbols are the same as in formula (3). R_0 is the Rayleigh ratio for the standard liquid in natural light (for benzene $R_0 = 16.3 \quad 10^{-6}$ cm^{-1}), and Δ_0 is the degree of depolarization of the standard liquid for natural incident light (for benzene $\Delta_0 = 0.412$).

The theory of light dispersion by solutions of high molecular compounds requires knowledge of the excess dispersion of the solution R_θ', caused by the presence in the solution of macromolecules. Here Rayleigh's number for the solute is determined by a method analogous to that described above, which is subtracted from R_θ of the solution. The difference is R_θ'.

PURIFICATION OF SOLUTIONS

Purification of solutions by means of filtration through the densest glass filters is frequently inadequate. The separation of dust from solutions should be done with a centrifuge, using a field of not less than 4000 g. Such purification has given completely satisfactory results in the measurements described below.

DETERMINATION OF THE MOLECULAR WEIGHT AND DIMENSIONS

The data is processed in order to obtain the average molecular weight M_w of the polymer being studied, and the mean-square distance between the ends of its macromolecules $(\overline{h^2})^{1/2}$ according to the method proposed by Zimm.[3] In this method a graph is constructed showing the dependence of C/R_θ' (C is the concentration of the solution in gm/cm^3, R_θ' is the excess dispersion of the

solution over the dispersion of the solute) upon

$$\sin^2 \frac{\theta}{2} + 100C$$

(see Figs. 4 and 5). Upon extrapolation of the obtained family of curves to C = 0 and θ = 0, the ordinate intercept gives the molecular weight, the initial slope of the curve at C = 0 is proportional to $(\overline{h^2})^{1/2}$, and the slope of the curve at θ = 0 is equal to twice the second virial coefficient A_2 of the osmotic equation.

As an example of the application of the described instrument, similar graphs are introduced (Figs. 4 and 5), obtained in the study of the two fractions of polystyrene in benzene.

The results obtained in the processing of the curves given in Fig. 4 and Fig. 5, are shown in the table.

Fraction	$M_w \times 10^{-4}$	$A_2 \times 10^4$	$(\overline{h^2})^{1/2}/A$	$(\overline{h^2})^{1/2}/\overline{h^2}_f{}^{1/2}$	$[\eta]$	$M_\eta \times 10^{-4}$
1	1.0	3.24	870	2.7	2.05	1.1
1a	3.4	3.46	1820	3.26	4.0	2.8

Note: $\overline{h^2}_f$ is the mean-square measure of unexcited molecular chains in assumed free rotation around the valence bonds.

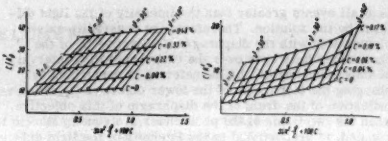

Fig. 4

Fig. 5

Fig. 4. An extrapolation according to Zimm for a solution of the polystyrene fraction of $M_w = 1 \times 10^6$, in benzene.
Fig. 5. The same as Fig. 4 for the fraction of $M_m = 3.4 \times 10^6$.

In the last column of the table are given the values of M_η for the same fractions, computed by their characteristic viscosity $[\eta]$ in benzene by use of the formula obtained by Kunst.[13]

$$[\eta] = 0.52 \cdot 10^{-4} M^{0.78}. \qquad (5)$$

The values of M_w and M_η are in sufficiently close agreement.

REFERENCES

1. P. Debye. J. Appl. Phys. **15**, 338 (1944).
2. E. V. Frisman and K. G. Kiseleva. Doklady Akad. Nauk SSSR **74**, 221 (1950).
3. V. N. Tsbetkov, K. Z. Fattakhov, and O. V. Kallistov. Zhur. Eksp. i Teoret. Fiz. **26**, 345 (1954).
4. P. Debye. J. Phys. Coll. Chem. **51**, 18 (1947).
5. B. H. Zimm. J. Chem. Phys. **16**, 1093, 1099 (1948).
6. H. Benoit. J. Polymer Sci. **11**, 507 (1953).
7. H. Benoit, H. A. Holtzer, and P. Doty. J. Phys. Chem. **58**, 635 (1954).
8. O. B. Ptitsyn. Zhur. Fiz. Khim. **31**, 1091 (1957).
9. V. E. Eskin. Zhur. Tekh. Fiz. **28**, 1459 (1958).
10. B. A. Brice, M. Halwer, and K. Speiser. J. Opt. Soc. Am. **40**, 768 (1950).
11. J. J. Herman and S. Levinson. J. Opt. Soc. Am. **41**, 460 (1951).
12. B. H. Zimm. J. Polymer Sci. **16**, 351 (1953).
13. K. Kunst. Rec. trav. chim. **69**, 125 (1950).

SHORT COMMUNICATIONS

INFLUENCE OF TEMPERATURE ON THE ABSORPTION SPECTRUM OF NITRIC OXIDE

V. N. Ivanov

Received 16 March 1959

Several articles have been devoted to a study of the nature of the absorption of light by nitric oxide.[1-4] In the present work the methods of absorption spectroscopy were used to investigate the absorption spectrum of NO in the temperature range from 20 to 1020°C.

The spectra were photographed with the help of an ISP-22 spectrograph. The light source was an LV-2 hydrogen lamp. Nitric oxide was prepared according to the laboratory method described in reference 5. The purification of the nitrogen dioxide was accomplished by passage through a solution of NaOH, and then drying by KOH. The cuvette used was a quartz tube 65 cm long which was connected at the middle to a vacuum apparatus and a heater for degassing. Before filling, the nitric oxide was liquefied, and the vapors from the boiling nitric oxide filled the tube to the required pressure. At the moment of unsoldering (disconnecting) the tube from the vacuum apparatus the nitric oxide was frozen in liquid nitrogen. The tube was heated in a tube furnace with quartz windows. Temperature was measured with a platinum-platinum-rhodium thermocouple. The spectra were photographed on "Spectral, Type I" photographic plates with identical exposures and with a constant schedule of burning of the hydrogen lamp.

The influence of temperature on the absorption in the γ-band system of NO is described in the following.

1. Bands of the γ-system appear in the highest original quantum state. Increasing the temperature from 20 to 1020°C leads to the successive appearance of the (0,1), (0,2), (0,3), and (0,4) bands of the γ-system. Qualitatively this agrees with the prediction of the Boltzmann distribution of molecules according to vibrational state.

2. Temperature has an effect on the band intensity. Heating nitric oxide to 420°C causes an increase in the intensity of the (0,1) band, resulting in a merging of the electronic-rotational structure with the sharp band edge.

To detect the possibility of dissociation in the temperature interval from 20 to 420°C we carried out a long heating (10-12 hr) and illumination with the hydrogen lamp (2-3 hr). In individual experiments we used as indicators drops of mercury found in the unheated part of the quartz tube. Mercury reacts very readily with nitrogen dioxide, losing its characteristic metallic luster in the process. There was absolutely no evidence of decomposition of NO,

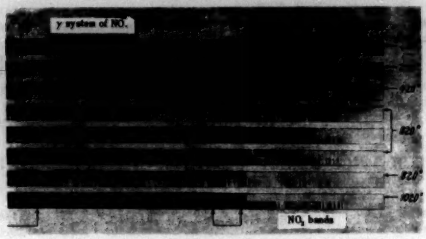

Fig. 1

either from absorption spectra or from the appearance of the mercury indicator; i.e., the dissociation of NO does not occur to any significant extent under these conditions.

At 620°C there appears in the absorption spectrum a yellow-green continuous region with diffuse bands, a sharp band edge at 2491.4 A, and other bands characteristic of nitrogen dioxide. Heating to 820°C causes an increase in the intensity of the ultraviolet and the yellow-green continua up to almost complete absorption of the light from the hydrogen lamp. At 1020°C the absorption diminishes, although at this temperature the spectrum in all wavelength regions is considerably less intense.

Changing the temperature of the absorption tube permits the detection of the appearance of sharp absorption bands of NO_2 with band edges at wavelengths of 2541, 2576, 2629, and 2665 A (in reference 6) there is an indication of their existence but no citation of the wavelengths of the band edges).

Figure 1 shows photographs of the absorption spectra of NO at various temperatures, at a concentration of NO equal to 1.81×10^{19} molecules/cm³, and at constant volume. The spectra were photographed after keeping the vapors at the specified temperature for several hours. As a general practice at 620°C three photographs were taken during this time. The formation of nitrogen dioxide at a temperature of 620°C was an indication of the decomposition of nitric oxide. To determine the role of illumination from the hydrogen lamp during the photographing of the spectra, nitric oxide was heated at 620-800°C without illumination. After cooling down the tube it was possible to observe directly the appearance of the brownish-red color indicating nitrogen dioxide. In this way the decomposition was shown to have a thermal origin.

It was determined, furthermore, that the speed of the decomposition of nitric oxide is affected greatly by the presence of small amounts of water vapor. Figure 2 shows photographs of absorption spectra of nitric oxide at a concentration of 1.81×10^{19} molecules/cm³, after drying with KOH and no other treatment. A comparison of Figs. 1 and 2 shows that, in the latter case, the absorption is appreciably more intense. This is an indication of the increased rate of decomposition of NO. In all probability there is a catalytic effect exerted either by the water molecules of by the products of their decomposition. The presence in the absorption spectra, at temperatures of 620-1020°C, of absorption bands which indicate the presence of NO_2 is a further indication of the high stability of the molecules of nitrogen dioxide under these conditions. This fact does not agree with the findings of Wise and Frech,[7] who postulated a mechanism for the oxidation of nitric oxide at temperatures from 872 to 1275°C which does not involve the possibility of the formation of molecules of nitrogen dioxide nor of their influence on the kinetics of the decomposition of NO.

CONCLUSIONS

1. Heating nitric oxide to 420°C and absorption in (0,v) bands of the γ-system do not cause dissociation of the NO molecule.
2. The dissociation of NO at temperatures $T > 420°C$ is thermal in origin and is probably catalyzed by small quantities of H_2O.
3. The presence of absorption bands of NO_2 in the spectrum at 620-1020°C shows the appreciable stability of the NO_2 molecule under the experimental conditions.

REFERENCES

1. M. Lambrey. Ann. phys. 14, 95 (1930).
2. V. Kondratjew and L. Polak. Soviet Physics 4, 764 (1933).
3. O. Wulf. Phys. Rev. 46, 316 (1934).

Fig. 2

4. A. G. Gaydon. "Dissociation Energies and Spectra of Diatomic Molecules." IL. Moscow; and Dover. New York. 1949.
5. Yu. V. Karyakin and I. I. Angelov. "Pure Chemical Reagents." G. Kh. I.. Moscow. 1955.
6. R. W. B. Pearce and A. G. Gaydon. "Identification of Molecular Spectra." IL. Moscow. 1949; and Chapman and Hall. London. 1949.
7. H. Wise and M. F. Frech. J. Chem. Phys. 20. 1724 (1952).

THE SEMICONDUCTOR MECHANISM OF SURFACE-RECOMBINATION LUMINESCENCE

A. N. Gorban and V. A. Sokolov

Receiver 11 April 1959

To explain the candoluminescence of crystalline phosphors, a surface-recombination mechanism was proposed[1] according to which the luminescence of phosphors in flames is caused by recombination of atoms and radicals of the flame into molecules on the surface of the phosphor. Experimental justification for such a mechanism has been reported by us.[2] In connection with this, there arose the question of a semiconductor model for the excitation of candoluminescence in crystalline phosphors.

In considering this problem we used the ideas of F. F. Vol'kenshtein, V. V. Voevodskii, and N. N. Semenov[3-6] on the connection between the recombination processes of atoms and radicals on surfaces of solids and their semiconducting properties. Using the energy band representation of the luminescence of crystalline phosphors, we have attempted to describe the separate stages of the recombination process of atoms and radicals on the surface of a phosphor which result in luminescence. As an example, the recombination of atomic hydrogen is considered (see Figure).

Figure 1 shows the energy band diagram of a crystalline phosphor with the corresponding model of the crystal lattice. When a hydrogen atom is adsorbed producing a "weak" (one-electron) homopolar bond 5 (Fig. 2), the bonding electron may, in effect, become a trapping center which is represented in the energy diagram of the crystal as an acceptor level 6. An electron may arrive at this level by the following two routes: either an electron jumps into this level from the valency band (Fig. 3), or a free electron drops into it from the conduction band (Fig. 4). This corresponds to the appearance of a "strong" (electron-pair) homopolar bond 7.

When an electron jumps into level 6 from the valency band, a hole 8 appears in the latter. This makes possible an exothermic ionization of the luminescence center 9. Such a process may lead to the recombination of an electron from the conduction band with an ionized center of luminescence (10, Fig. 6).

An electron may appear in the conduction band as a result of recombination of hydrogen atoms into a molecule after an adsorbed hydrogen atom has been struck by another hydrogen atom phase

$$(x)_{ads.} + x \rightarrow (x_2)_{ads.}.$$

Energy is then released, and the molecule desorbed. Because of the recombination energy a trapped electron may be ejected into the conduction band (Fig. 7).* In the case of similar processes which take place directly on an activator atom, a direct ionization of the luminescence center is possible.

*The possibility of a similar release of an electron from a trapping center was shown by F. F. Vol'kenshtein in his work.[7]

Clearly, when an atom of the gas is adsorbed on an activator atom, then a shift of the level may take place (Fig. 8) which is analogous to the production of a trapping level (Fig. 2). This will cause the energy required to eject an electron into the conduction band (Fig. 9) to be smaller than the quantum energy of luminescence. The latter remains the same as in other cases, since after recombination of the atoms and desorbtion of the molecule the activator level will be found in the usual position. Therefore, when atoms are adsorbed on the activator the luminescence may be due to the recombination of atoms (or radicals), the binding energy of which is smaller than the quantum energy of the luminescence (anti-Stokes luminescence).

Consequently, when atoms or radicals are adsorbed on the ions of the lattice, the energy released in recombination migrates to the centers of luminescence, using the electron-hole mechanism described above; however,

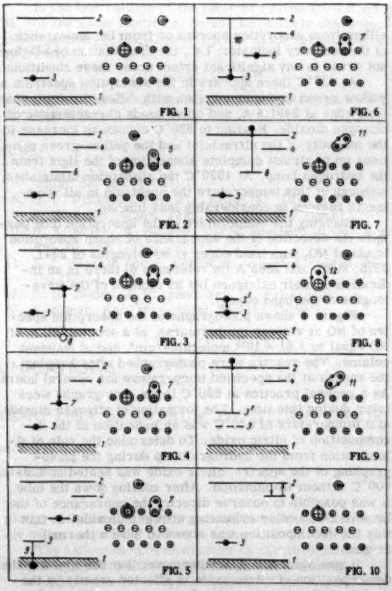

the adsorption of the gas atoms on the activator results in direct ionization of the emission centers and aids the anti-Stokes chemiluminescence.

Figure 10 shows the transitions of an electron from the conduction band to the trapping levels and conversely.

Thus, all stages of the recombination process which lead to the luminescence of crystalline phosphors find a satisfactory explanation in the band diagram of phosphor luminescence.

REFERENCES

1. V. A. Sokolov. Opt. i Spektr. 1, 411 (1958).
2. A. N. Gorban and V. A. Sokolov. Opt. i Spektr. 7, 573 (1950).
3. F. F. Vol'kenshtein. Sb. "Geterogennyi kataliz v khimicheskoi promyshlennosti." (Heterogenous Catalysis in Chemical Industry), p. 213, GKhI, Moscow, 1955.
4. N. N. Semenov and V. V. Voevodskii. Sb. "Geterogennyi kataliz v khimicheskoi promyshlennosti." (Heterogeneous Catalysis in Chemical Industry), p. 233, GKhI, Moscow. 1955.
5. V. V. Voevodskii, F. F. Vol'kenshtein, and N. N. Semenov. Sb. "Voprosy khimicheskoi kinetiki, kataliza i reaktsionnoi sposobnosti." (Problems on Chemical Kinetics, Catalysis, and Reactive Capability), p. 423, Moscow, 1955.
6. F. F. Volkenshtein. Uspekhi Khim. **27**, 1304 (1958).
7. F. F. Vol'kenshtein. Izvest. Akad. Nauk SSSR, Ser. Khim. **2**, 143 (1957).

ON THE HYDROGEN BOND IN ACETYLENIC AMINES

A. A. Petrov and T. V. Yakovleva

Received 14 April 1959

Hydrocarbons with a terminal acetylene group, as is known, quite readily substitute the hydrogen atom with a metal atom, i.e., they behave to some degree as acids.[1] It is possible to expect that a terminal acetylenic group is also capable of forming complexes with amines.

With the purpose of clarifying this question, we investigated the infrared spectra of a series of tertiary acetylenic amines with the general formula $R_2N-(CH_2)_n-C\equiv C-H$ with n = 1, 2, and 3. The spectra were obtained using an IKS-14 with LiF and NaCl prisms. The substances were prepared using methods described in references 4-6.

In all cases, next to the band, characteristic for the stretching vibration of the acetylenic hydrogen (3300 cm^{-1}), an overlapping band at about 3210 cm^{-1} was discovered (cf. the Figure, curves 1-5). We assign this band to the stretching vibration of the acetylenic hydrogen, hydrogen-bonded to the nitrogen of the amino group.

$$HC\equiv C-(CH_2)_n-N\begin{matrix}R\\R\end{matrix} \quad . \quad . \quad . \quad . \quad . \quad H-C\equiv C-(CH_2)_n-NR_2.$$

The following facts support this proposal:

1. The frequency 3210 cm^{-1} is absent in the spectra of 2% solutions of the investigated amines in CCl_4 and appears in 5% solutions (cell thickness 500μ). In the spectrum of the liquid amine (10μ thickness) equivalent to the first solution, the 3210 cm^{-1} frequency is present.

2. In the spectra of amines, in which the unpaired electrons of the nitrogen are partially conjugated (e.g., the amine $(C_2H_5)_2N-CH=CH-C\equiv CH$), the 3210 cm^{-1} frequency is absent (curve 6).

3. The frequency considered also appears in the spectra of solutions of acetylenic hydrocarbons in tertiary amines (e.g., in solutions of tertiary butyl acetylene and of vinyl acetylene in triethylamine).

Thus, the origin of the band at about 3200 cm^{-1} is not doubtful.

The shift of the stretching vibration band of the acetylenic hydrogen in the case of the acetylene amines is about 90 cm^{-1}. The same degree of shift is observed as a result of hydrogen-bonding also in the spectra of primary and secondary amines.[2] In the case of solutions

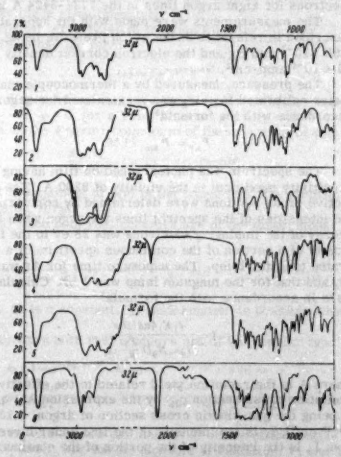

The infrared transmission spectra of the acetylenic amines. 1—dimethylaminobutyne-3; 2—diethylaminobutyne-3; 3—diethylaminopentyne-4; 4—piperidinobutyne-3; 5—piperidinopentyne-4; 6—diethylaminobutene-1-yne-3.

of tertiary butyl acetylene and vinyl acetylene in triethylamine, the magnitude of the shift attains 125 cm^{-1} and 140 cm^{-1}, respectively.

Far from all of the amine molecules take part in the hydrogen bonding since in the spectra the band of the stretching CH vibration of the free group $C\equiv C-H$ is always more intense than that of the bonded.

It should be noted that between molecules of some other acetylenic compounds with a terminal acetylenic group, also, a hydrogen bond arises. This is found, for example, in vinyl acetylenic ketones. At the same time, in the spectra of propargyl aldehyde and of butyneone the shift of the 3300 cm^{-1} band is not observed.[3]

A hydrogen bond occurs also between molecules of amino alcohols. In the infrared spectra of the latter with a tertiary amino group (e.g., in the spectrum of ethanol diethyl amine) a strong broadening of the absorption band, characteristic of the O—H bond, on the low-frequency side, is observed.

REFERENCES

1. A. I. Shatenshtein. Uspekhi Khim. **24**, 377 (1955).
2. L. Bellamy. "Infrakrasnie Spektry." (Infrared Spectra), IL, Moscow, 1957.
3. A. A. Petrov and G. I. Semenov. Zhur. Obshchei Khim. **27**, 2947 (1957).
4. V. Wolf. Lieb. Ann., **576**, 35 (1952).
5. A. A. Petrov and I. A. Maretina, Zhur. Obshchei Khim. **29**, 2458 (1959).
6. A. A. Petrov and V. A. Kormer. Doklady Akad. Nauk SSSR **126**, 1278.(1959).

EFFECTIVE EXCITATION CROSS SECTIONS OF CERTAIN SPECIAL LINES OF ARGON

L. M. Volkova and A. M. Devyatov

Received 4 May 1959

The effective excitation cross sections of argon were determined by Herrmann[1] for wavelengths up to 7724 A. In the present study we measure the relation between effective cross sections and the velocity of the impinging electrons for eight argon lines in the 7724–8424 A interval.

The measurements were made with the apparatus described in reference 2, the argon pressure being $4.68 \cdot 10^{-3}$ mm Hg and the electron current density 56×10^{-4} amp/cm^2.

The pressure, measured by a thermocouple manometer calibrated for air, was recalculated for argon in accordance with the formula[5]

$$P_{Ar} = P_{air} \cdot 1.56.$$

The spectrum was photographed on film having its sensitivity maximum in the vicinity of 8200 A. The effective cross sections were determined by comparing the intensities of the spectral lines for argon when the energy of the impinging electrons was 28 ev to the intensity of a portion of the continuous spectrum of a calibrated tungsten lamp. The exposure time for Ar was 3 hr, and that for the tungsten lamp was 1 hr. Calculations were in accordance with the formula[4]

$$A = \frac{I_\lambda K_\lambda 4\pi d \lambda s t w}{I_w h c N_0 D \frac{F_1}{F_2} \tau t_\lambda},$$

where A is the radiation yield related to the effective excitation cross section q_{1k} by the expression $A = q_{1k}/q$ (q being the gas-kinetic cross section of argon, 6.15×10^{-16} cm^2); I_λ is the intensity of the line under investigation; I_w is the intensity of the portion of the continuous spectrum of a tungsten lamp in the vicinity of the line under study; K_λ is the radiant emittance of the tungsten lamp; d is the beam diameter; λ is the mean free path of an electron; s is the width of the spectrograph slit in photographing the spectrum of the tungsten lamp, t_w is the tungsten lamp spectrum exposure time; t_λ is the argon spectrum exposure time; N_0 is the number of electrons passing through the impact region per second; D is the linear dispersion of the spectrograph; F_1, F_2 are, respectively, the focal lengths of the collimating lens and the spectrograph camera; and τ is the attenuation of tungsten lamp emission by a neutral filter.

In order to compare our results with the literature data, a calculation was made of the radiation yield for the 7723–7724 A argon line previously measured by Herrmann.[1] At the maximum of the excitation function, Herrmann found $A = 14.6 \times 10^{-4}$; our measurements yielded the value $A = 15.0 \times 10^{-4}$.

Wavelength λ	Electron configuration of atom before and after the transition	q_{1k} 10^{-20} cm^2 at 28 ev	q_{1k} 10^{-20} cm^2 at max
7514.6	—	5.4	7.5
7948.2	$3p^5(^2P^0_{3/2})4p - 3p^5(^2P^0_{3/2})4s$, $j=1 \to j=0$	5.5	7.7
8006—8014.8	$3p^5(^2P^0_{3/2})4p - 3p^5(^2P^0_{3/2})4s$, $j=2 \to j=1$	4.9	7.4
8115.3	$3p^5(^2P^0_{3/2})4p - 3p^5(^2P^0_{3/2})4s$, $j=3 \to j=2$	7.4	11
8264.5	$3p^5(^2P^0_{1/2})4p - 3p^5(^2P^0_{1/2})4s$, $j=1 \to j=1$	6.0	8.4
8408.2	$3p^5(^2P^0_{1/2})4p - 3p^5(^2P^0_{1/2})4s$, $j=2 \to j=1$	12.9	19.1
8424.6	$3p^5(^2P^0_{1/2})4p - 3p^5(^2P^0_{1/2})4s$, $j=1 \to j=0$	17.8	23.2

The table presents the effective excitation cross sections of the lines investigated, and Figs. 1 and 2 present their dependence upon the energy of the impinging electrons. The data on the electronic configuration of the argon atom before and after the transition are from reference 5.

The authors wish to express their gratitude to N. A. Kaptsov for his interest in their work.

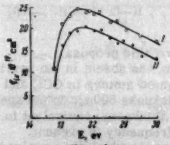

Fig. 1

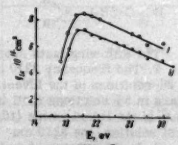

Fig. 2

Fig. 1. Effective excitation cross sections of 8424 A (I) and 8408 A (II) lines versus the energies of the exciting electrons.
Fig. 2. Effective excitation cross sections of 8264 A (I) and 8006 A (II) lines versus the energies of the exciting electrons.

REFERENCES

1. O. Herrmann. Ann. Physik **5**, 143 (1936).
2. L. M. Volkova. Opt. i Spektr. **6**, 273 (1959).
3. B. I. Korolev. "Osnovy Vakuumnoi Tekhniki." (Fundamentals of Vacuum Engineering), Gosenergoizdat, M.-L., 1957.
4. O. Fischer. Z. Physik, **86**, 646 (1933).
5. C. Moore. "Atomic Energy Levels, I." 1949.

METHOD OF TRANSFORMATION OF SPECTRAL LINE CONTOURS AND ITS APPLICATION FOR MEASURING THE TEMPERATURE AND OTHER PARAMETERS OF A LIGHT SOURCE

M. P. Chaika and E. E. Fradkin

Received 8 May 1959

In many cases, in the study of the contour of a line, the apparatus function of the spectrometer is unknown. Nevertheless, if the form of the true contour at the input of the spectrometer can be considered known, in certain cases it turns out to be possible to determine the parameters of this contour, using the proposed method of contour transformation. The method consists of the fact that from the actual contour of one line and the assumed relationship of the true contours of two lines, one can define the actual contour which is obtained with the help of the same instrument with which the other line is studied (the frequency of the lines must be nearly the same, in order that the apparatus function for both lines may be considered identical). The actual contour can best be approximated by means of the details of the relationship between the true contours. Then, from the value of the parameter, which serves for determination of the optimal calculated value of the contour, the value of the physical constant is found which characterizes the true contour in the source.

We will represent the actual contours of two spectral lines by g_1 and g_2; their true contours by k_1 and k_2; the apparatus function by f. Then

$$g_1(\nu)=\int_{-\infty}^{\infty} f(\nu-x)\,k_1(x)\,dx,$$
$$g_2(\nu)=\int_{-\infty}^{\infty} f(\nu-x)\,k_2(x)\,dx. \qquad (1)$$

For the corresponding Fourier components we obtain the equation

$$G_1(u)=F(u)\,K_1(u),$$
$$G_2(u)=F(u)\,K_2(u).$$

whence

$$G_2(u)=\frac{K_2(u)}{K_1(u)}\,G_1(u) \qquad (2)$$

and

$$g_2(\nu)=\frac{1}{2\pi}\int_{-\infty}^{\infty} G_2(u)\,e^{-i\nu u}du=\frac{1}{2\pi}\int_{-\infty}^{\infty} G_1(u)\frac{K_2(u)}{K_1(u)}\,e^{-i\nu u}du. \qquad (3)$$

In this case, when $K_2(u)/K_1(u)$ are the Fourier components of a certain function $\phi(\nu)$

$$\varphi(\nu)=\frac{1}{2\pi}\int_{-\infty}^{\infty}\frac{K_2(u)}{K_1(u)}\,e^{-i\nu u}du,$$

then substituting the expression for the Fourier components in (3), and changing the order of integration,* we obtain

$$g_2(\nu)=\int_{-\infty}^{\infty} g_1(x)\,\varphi(\nu-x)\,dx. \qquad (4)$$

*Change of the order of integration is possible only in the case of transformation from a narrow contour to a wide one.

The scale of the contours is quite arbitrary. It is most convenient for the sake of comparison to normalize all contours with respect to units of the maximum value.

The contours of spectral radiation lines are usually of three types: dispersion, doppler, and those of the form of the Voigt function, which represents a beam of dispersion and doppler distribution

$$k(\nu)=C\int_{-\infty}^{\infty}\frac{e^{-\beta x^2}dx}{(\nu-x)^2+\gamma^2}.$$

A line contour has the latter form if natural decay (decay as a result of collisions) and doppler broadening all take place simultaneously.

For all three types of function $k(\nu)$, the Fourier transform has the form

$$K(u)=Ce^{-\gamma|u|-\alpha u^2}$$

(for a dispersion contour $\gamma \neq 0$, $\chi = 0$; for a doppler contour $\gamma = 0$, $\chi = 0$; for a Voigt function $\gamma \neq 0$, $\chi = 0$). We obtain as the Fourier transform of the argument of $\phi(\nu)$

$$\frac{K_2(u)}{K_1(u)}=Ce^{-(\gamma_2-\gamma_1)|u|-(\alpha_2-\alpha_1)u^2}.$$

The argument of $\phi(\nu)$ in the transformation formula (4) has the form:

(a) when both real contours are of the dispersional type

$$k_1(\nu)=\frac{1}{\nu^2+\gamma_1^2};\quad k_2(\nu)=\frac{1}{\nu^2+\gamma_2^2};\quad \varphi(\nu)=C\frac{1}{\nu^2+(\gamma_2-\gamma_1)^2},$$

where C is a constant. Transformation is possible when $\gamma_2 > \gamma_1$.

(b) when both real contours are of the doppler type

$$k_1(\nu)=e^{-\beta_1(\nu-\nu_1)^2};\quad k_2(\nu)=e^{-\beta_2(\nu-\nu_2)^2};\quad \varphi(\nu)=Ce^{-\alpha\nu^2};$$
$$\beta_i=\frac{m_i c^2}{2kT_i\nu_i^2}\ (i=1,2);\quad \alpha=\frac{c^2}{2k}\cdot\frac{m_1m_2}{m_1T_2\nu_2^2-m_2T_1\nu_1^2},$$

where m_1 and m_2 are the masses of atoms of the radiators, ν_1 and ν_2 are the frequencies of radiation, T_1 and T_2 are the temperatures of the corresponding sources. Transformation is possible when $\beta_2 < \beta_1$.

(c) when both real contours are represented by the Voigt function

$$k_1(\nu)=\int_{-\infty}^{\infty}\frac{e^{-\beta_1x^2}dx}{(\nu-x)^2+\gamma_1^2};\quad k_2(\nu)=\int_{-\infty}^{\infty}\frac{e^{-\beta_2x^2}dx}{(\nu-x)^2+\gamma_2^2};$$
$$\varphi(\nu)=C\int_{-\infty}^{\infty}\frac{e^{-\alpha x^2}dx}{(\nu-x)^2+\delta^2},$$

where $\delta=\gamma_2-\gamma_1$. Transformation is possible when $\beta_2 < \beta_1$, $\gamma_2 > \gamma_1$. When the real contours of $k_2(\nu)$ are Voigt functions and those of $k_1(\nu)$ are dispersional or doppler

type, the argument of $\phi(\nu)$ will have an analogous form. Only the expressions for the parameters σ and δ are changed. Thus, for the case in which the contour for $k_1(\nu)$ is of the doppler type, σ has the previous form and $\delta = \gamma_2$. Transformation is possible when $\beta_2 < \beta_1$. In the case in which the contour of $k_1(\nu)$ has a dispersional form, $\alpha = \beta_2$, $\delta = \gamma_2 - \gamma_1$. Transformation is possible when $\gamma_2 > \gamma_1$.

Those parameters of the source which enter into the argument, that is, σ and γ, can also be found by the method of transformation. The temperature of the source can be determined from the magnitude of σ; from the magnitude of γ the mean free time can be found, or the constant of the linear Stark effect (natural decay, barring special cases, can be ignored). In the determination of each of these quantities, one can choose the most convenient lines with contours $g_1(\nu)$ and $g_2(\nu)$. Thus, for example, the source temperature can be simply determined if lines of elements of different atomic weights are present in the radiation, and if it is possible to assume (a) thermal equilibrium between the vapors of these elements and (b) absence of broadening effects other than the doppler. The recorded contour and the computed contour (calling $g_1(\nu)$ the contour of the line of the heavy element) coincide if the value of temperature in the calculations is taken correctly. The temperature is determined in the same manner if there is the possibility of recording the contour of one and the same line in the source under study and in a source of lower, and known, temperature. The determination of temperature is also possible with other variants in the recording method. Inasmuch as the apparatus function is unknown, the function $g_1(\nu)$ is given point-by-point, and function $g_2(\nu)$ can be found, also only point-by-point, by means of numerical integration. The operation of numerical integration introduces a certain amount of error into the result, but it can always be made smaller than the error in the recording accuracy. Thus, the error in the determination of the parameters is determined by the precision in recording the contour.

As the characteristic of the accuracy of determination of temperature with the aid of the described transformation, we will introduce examples of the change of temperature with increase of the strength of the current through the discharge tube with a bare cathode. The table gives the ordinates of the curve of recorded points (averages of several curves) for the line UI λ5027 A with a current of 30ma (the center column). The record of the same line at a current of 10ma is used as the $g_1(\nu)$ function. Columns 2 and 6 give values, calculated by formula (4), of the ordinates of the contours under the assumption that the temperature difference for the two regimes is 100° and 110°, respectively. The intervening columns give the differences (Δ) of these ordinates which allow judgment regarding the accuracy of the coincidence of the recorded and computed contours.*

Frequency calculated for the center of the line* (mk)	Ordinates of the computed contour with a temperature difference ΔT=100°	Δ	Ordinates of the measured contour with a current strength of 30 ma	Δ	Ordinates of the computed contour with a temperature difference ΔT=110°
−29.4	63	−1	62 ± 3	−2	64
−14.7	372	−1	371	−7	379
−11.8	517	17	534	9	523
− 7.3	784	10	774	6	768
0	1000	—	1000	—	1000
7.3	791	1	792 ± 5	−2	794
11.8	551	5	556	−1	557
14.7	405	11	416	5	411
22.0	172	5	177	1	176

*1 mk = 0.001 cm^{-1}

*In performing the numerical integration of formula (4) the number of points taken is such that σh^2 does not exceed 1.5×10^{-2}, where h is an interval of the approximate integration.

It is seen from the table that the temperature difference corresponding to the two regimes of the source is about 110°, with a tolerance of 10%. Thus, with registration of a contour with small errors, the proposed method makes possible the determination of the parameters of the source with satisfactory accuracy.

The authors express their gratitude to S. E. Frish for his interest in the work, to V. I. Perel for much valuable advice, and to N. I. Kaliteevsky for his discussion of the results.

ON DIFFRACTION AT THE EXIT OF OPTICAL WAVEGUIDE

B. S. Skorobogatov

Received 11 May 1959

D. Heinze and C. Schmelzer[1] have investigated the diffraction of light in "deep slit" under different angles of incidence and have carried out a qualitative comparison of the experimental results with the calculation of the diffraction at the exit of the plane wave guide of Barrow and Green. On the basis of these comparisons Heinze and Schmelzer draw a conclusion regarding the field distribution inside the slit. The optical scheme of their setup is shown in Fig. 1a.

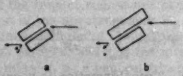

Fig. 1

While investigating under similar conditions, but with white light, the author discovered the periodic dark lines[2] in the spectra of the principal maxima. This phenominon was investigated in detail in reference 2, and explained on the basis of the following consideration:

If the geometrical path of the rays is examined in a deep slit (or in a so-called optical wave guide), then it is obvious that the ray, after undergoing an even number of reflections, emerges from a waveguide parallel to the beam of light which is incidental upon the entrance ($\phi = 0$) and with an odd number of reflections, with an angle $\phi = 2\theta$. In order that the light emerges simultaneously in both directions, it is sufficient to have a small dispersal of the angles with which the wave is excited in the wave guide. Such dispersal always exists as a result of the diffraction at the entrance. However, it is known that the wave with the given length can propagate at the angles which satisfy the condition,

$$2a \sin\theta = m\lambda \quad (m = 1, 2, 3 \ldots)$$

from whence it follows that waves with different lengths emerge either at the angle $\phi = 0$ or $\phi = 2\theta$. This is what

leads to the appearance of the principal maximum of the mutually supplementing dark lines in the spectra.

From these considerations it follows that with such "nonsymmetrical" excitation, the diffraction pattern depends upon the length of the wave guide and, generally speaking, is nonsymmetrical. This conclusion contradicts the results obtained by Heinze and Schmelzer,[1] as this conclusion shows that with nonsymmetrical excitation the field distribution inside the slit (wave guide) does not correspond to a definite mode.

In connection with the above, the author conducted the additional investigation of the diffraction, using monochromatic light, with nonsymmetrical and symmetrical excitations.

For nonsymmetrical excitation the optical scheme of the setup was the same as in Fig. 1a. For the realization of the symmetrical excitation at the entrance of the waveguide, it was necessary to direct two symmetrical parallel coherent beams of light incident on the entrance at angles which are equal to ϑ and $-\vartheta$. It is possible to realize this with the help of the receiver as shown in Fig. 1b. A portion of the parallel beam of light incident on the entrance is reflected from the elongated side, creating the second beam, which is symmetrical to the first.

With the nonsymmetrical excitation (Fig. 2, a-c) it was established that the diffraction pattern depends on the length of the waveguide and will become symmetrical only at a certain length (Fig. 2a). However, with this condition the intensity of the minima is not equal to zero.

With the symmetrical excitation (Fig. 2d) the diffraction pattern does not depend on the length of the wave guide, whereupon, by observing the diffraction with white light the periodic lines in spectra of principal maxima disappear.

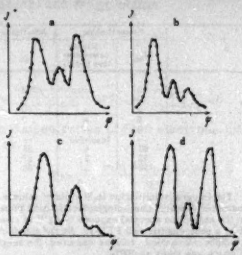

Fig. 2

In conclusion I express deep gratitude to K. D. Sinel'nikov for continuous attention to the work.

REFERENCES

1. D. Heinze and C. Schmelzer. Z. Physik **142**, 133 (1955).
2. B. C. Skorobogatov. Opt. i Spektr. **3**, 272 (1957).

THE RELATION BETWEEN THE CHEMICAL STRUCTURE AND SCINTILLATION EFFICIENCY OF 1, 3, 4-OXADIAZOLE DERIVATIVES

O. P. Shvaika and A. P. Grekov

Received 19 May 1959

In order to search for new scintillation materials it is extremely important to know the dependence of the scintillation efficiency on the structure of the material. Attempts to clarify the connection between scintillation compounds and their structure have been performed on samples of plastic and crystalline scintillators.[1-3] We have some knowledge about the role of certain structural factors for primary scintilation solutes dissolved in toluene. From this work,[4] it appears that a necessary condition for the scintillation of liquid luminophors is the presence of continuous conjugation of bonds throughout the molecule. However, this condition seems insufficient, since in diarylpolyenes of condensed aromatic hydrocarbons and also in compounds of the Ar-Ar' type such conjugation is present. Nevertheless, they have a low efficiency in solutions,[4,5] similar to substances in which two aryl radicals are separated by an isolating or weakly-transmitting bridge coupling, such as methylene,[5,6] oxygen,[5] or metal.[7] Therefore, an additional requirement appears necessary: the molecule should contain a linear chain of certain aromatic rings (as in m-terphenyl, 2, 5-diphenyl-pyrol, etc.) among which the presence of sulfur-containing groups or rings with clearly expressed acceptor character (for example, pyrazine, pyridine, quinoline, tetrazole, etc.[4,6]) is undesirable.

The introduction of certain functional groups in a luminophore showed that substituents can substantially influence the pulse height of scintilation.[4,5] However, this question was not studied systematically.

In this communication the influence of a broad range of para-substituents on the scintillation efficiency of 2-phenyl- and 2, 5-diphenyl-1, 3, 4-oxadiazoles is examined. The molecules of the latter consist of linear chains of three aromatic rings and surpass in efficiency the derivatives of the 2-phenyl-1, 3, 4-oxadiazoles which are of the Ar-Ar' type. But on the other hand, in series which are unlike in structure and efficiency, we discovered a parallel influence of the substituents on the scintillation yield. From the data presented in the Tables we see that electron-donating substituents tend to increase the scintillation efficiency, as distinct from electron-acceptors which decrease it or reduce it to zero. Analysis of literature data shows that a similar influence of functional groups is also observed in other cases, not only for para-substituents.[4] Therefore, it seemed possible to us to assume that this is true, in general, for many types of primary liquid solutes. It is necessary to discuss separately the variations observed when substituents contain the heavy elements, S, Br, I. Their suppressing effect, of which Sangster and Irwin gave an extensive explanation,[8] was noted in many of the organic compounds.

Since in other cases it was shown that the presence of oxygen in the scintillation solution significantly reduces the efficiency,[9-11] it seemed expedient to observe whether the influence of the substituents was the same in samples flushed by an inert gas. In spite of the significant, al-

Table 1. Integral Scintillation Efficiency, $I_{sc.}$, of Para-Derivatives of 2-phenyl-1, 3, 4-oxadiazole

X	Without flushing		After flushing with nitrogen	
	$I_{sc.}$	Optimum concentration (gm/l)	$I_{sc.}$	Optimum concentration (gm/l)
NO_2	0	—	0	—
$COOC_6H_5$	0	—	0	—
Br	0	—	0	—
H	0	—	0	—
CH_3	0	—	0	—
NH_2	—	Insoluble	—	—
$N(CH_3)_2$	67	4	98	2
OCH_3	22	3	27	1
C_6H_5	79	5	89	3

Note: The integral scintillation light yield of toluene solutions of these substances (purified chromatographically until there was no change in the absorption spectra) exposed to Ag^{110} of about 0.1 mC was measured by a photoelectric cell FEU-19. As the standard a solution of 3 gm/l 2,5-diphenyloxazole in toluene was used, the scintillation efficiency of which was taken as 100%.

though not identical, increases of yield (see Tables 1 and 2), the character of the influence of the substituents did not change. It is interesting that for almost all the investigated derivatives of the oxadiazole the optimum concentrations are smaller for the oxygen-free samples.

A discussion of the photoluminescence characteristics of the scintillators described by us will be given in a later paper.

Table 2. Integral Scintillation Efficiency, $I_{sc.}$, of Para-Derivatives of 2. 5- diphenyl-1, 3, 4-oxadiazole

X	Without flushing		After flushing with nitrogen	
	I_{sc}	Optimum concentration (gm/l)	I_{sc}	Optimum concentration (gm/l)
NO_2	0	—	0	—
$COOC_6H_5$	83	5	88	5
SCH_3	81	3	100	1
H	96	1	117	5
I	0	—	0	—
Br	50	5	52	3
Cl	112	6	130	5
F	106	7	118	5
CH_3	113	5	144	5
OH	<10	low solubility	—	—
$OCOCH_3$	<10	the same	—	—
OCH_3	112	5	140	3
NH_2	<10	low solubility	—	—
$NCOCH_3$	10	0.14 saturated solution	10	0.14
$N(CH_3)_2$	102	3	123	5
C_6H_5	135	5	153	5

Note: See Note to Table 1.

REFERENCES

1. N. A. Adrova, M. M. Koton, and F. S. Florinskii. Doklady Akad. Nauk SSSR, **114**, 311 (1957).
2. A. S. Cherkasov, G. A. Tishchenko, and K. G. Voldaikina. Opt. i Spektr. **4**, 345 (1958).
3. R. Sangster and J. Irwin. Phys. Rev. **83**, 241 (1951).
4. F. N. Hayes, D. G. Ott, F. N. Kerr, and B. S. Rogers. Nucleonics **13**, Dec., p. 38 (1955).
5. H. Gilman, E. A. Weipert, J. J. Dietrich, and F. N. Hayes. J. Org. Chem. **23**, 361 (1958).
6. H. Gilman, E. Weipert, T. Soddy, and F. N. Hayes. J. Org. Chem., **22**, 1169 (1957).
7. H. Gilman, E. A. Weipert, and F. N. Hayes. J. Org. Chem. **23**, 760 (1958).
8. R. C. Sangster and I. W. Irwin. J. Chem. Phys. **24**, 670 (1956).
9. R. W. Pringle, L. D. Black, B. L. Funt, and S. Sobering. Phys. Rev. **92**, 1582 (1953).
10. Kh. V. Protopopov, Kh. A. Arslanov, S. B. Butomo, and T. V. Timofeeva. Prib. i Tekh. Eksp. **2**, 24 (1958).
11. D. Ott, F. N. Hayes, I. E. Hammel, and I. E. Kepharct. Nucleonics **13**, 62 (1955).
12. A. P. Grekov, O. P. Shvaika, and L. M. Europova. Zhur. Obshchei Khim. **29**, 2027 (1959); A. P. Grekov, L. N. Kulakova, and O. P. Shvaika. Zhur. Obshchei Khim **29**, (1959).

THE SUPERLINEAR INCREASE OF PHOSPHOR CONDUCTIVITY IN THE INITIAL STAGES OF EXCITATION

V. V. Antonov-Romanovskii

Received 2 January 1959

Tolstoi[1] was the first to devote serious attention to the difficulties encountered in applying the usual band picture to the kinetics of phosphorescence, in particular when trying to explain the superlinear increase in photoconductivity at the start of excitation. These difficulties led Tolstoi to develop an original "two-step" theory of phosphorescence applicable at the instant of action of the exciting light. The gist of the theory is that each recombination requires a minimum of two quanta of exciting light. The mechanism of luminescence is outlined as follows:

In the first step the exciting light raises the electrons to some intermediate level. The electrons do not recombine hereby but are merely accumulated at this intermediate level. Luminescence becomes possible only as a result of their subsequent release by light (photostimulation[2]).

This phenomenological theory encountered a number of difficulties, the first being a value in excess of ½ for the quantum yield of phosphorescence, which is sometimes observed experimentally.[3] According to the two-step theory in its pure form (i.e., without additional assumptions), this yield cannot exceed ½, since the emission of one quantum of luminescence requires at least two quanta of the exciting light. To avoid this difficulty it became necessary to admit the possibility of thermal release of localized electrons.

However, the introduction of thermal release gave rise to another difficulty in connection with the fact that superlinear photoconductivity usually begins above room temperature. It was necessary to assume that stimulation increases more strongly with heating than the thermal ejection of electrons, i.e., that stimulation requires an activation energy in excess of the energetic depth of

the trap. In this case the probability of optical release should, at high temperature, exceed the probability of thermal release.

There are still other difficulties, which we shall not discuss.

Frerichs, and later, Rose[4] also devoted their attention to the superlinear increase in photoconductivity as well as to other nonlinear effects (though primarily for ordinary semiconductors rather than phosphors). In contrast to Tolstoi, they concluded that all of this is caused by a saturation effect, i.e., by almost complete filling of the levels. This naturally should bring about an increase in the average lifetime of the free charges and a superlinear rate of growth of photoconductivity at a certain stage of this increase.

There are thus two theories which can interpret the initial superlinear increase of photoconductivity. First of all we note that the saturation theory is inapplicable to phosphors. The fact is that due to photostimulation by the exciting light, both electron and hole traps are only partly filled at—and even below—room temperature. This has been shown by a number of experiments for a variety of phosphors.[3] Since an increase in temperature can only increase the probability of thermal release of localized charges, it can only result in a still further decrease in their concentration. It is well known that a phosphor's capacity for light sum storage decreases markedly with heating.

As mentioned above, the other (two-step) theory is phenomenological in nature and encounters a number of difficulties. As a result, it left one feeling unsatisfied. However, it was very difficult to object to it, since it seemed impossible to resolve the situation within the framework of usual ideas concerning the kinetics of phosphorescence.

The purpose of the present communication is to show that there is such a solution, at least with regard to the initial superlinear growth of photoconductivity.

Let us consider the band model (shown in Fig. 1) of a crystalline phosphor with two kinds of electron traps C_1 and C_2 of different depths ε_1 and ε_2. We assume for concreteness that $\varepsilon_2 > \varepsilon_1$.

Let us assume that the exciting light causes only a transfer of electrons from the lower filled band Q to the C_2 levels; i.e., causes the optical transition $Q \to C_2$. We consider the optical transitions $Q \to C_1$ and $Q \to P$ to be very weak. Then the thermal conductivity in P depends only on the thermal transfer of electrons from C_2. We can neglect hole conductivity if the concentration ν and depth of the hole traps C are sufficiently large.

In view of the absence of saturation (see above) we may set

$$n_1 \ll \nu_1 \text{ and } n_2 \ll \nu_2, \tag{1}$$

where ν_1 and ν_2 are the concentrations of the shallow and deep traps respectively and n_1 and n_2 are the corresponding concentrations of electrons in them.

We thus obtain the following differential equation for n_1 in the very initial stages when recombination may be neglected

$$\frac{dn_1}{dt} = -w_1 n_1 + \frac{\sigma_1 \nu_1}{\sigma_1 \nu_1 + \sigma_2 \nu_2}(w_1 n_1 + w_2 n_2), \tag{2}$$

where w_1 and w_2 are the probabilities of thermal ejection of electrons from C_1 and C_2; σ_1 and σ_2 are the effective capture cross sections for electrons in C_1 and C_2; and t is the time. There is no sense in writing a differential equation for n_2, since by neglecting recombination again we have the obvious relation

$$n_1 + n_2 = \varkappa_2 E t, \tag{3}$$

where χ_2 is proportional to the absorption coefficient corresponding to the transition $Q \to C_2$, and E is the intensity of the exciting light.

From Eqs. (2) and (3) we obtain

$$n_1 = \frac{\mu}{\lambda}\left[t - \frac{1}{\lambda}(1 - e^{-\lambda t})\right] = \frac{1}{2}\mu\lambda t^2 - \frac{1}{6}\mu\lambda^2 t^3 + \ldots, \tag{4}$$

where

$$\lambda = \frac{\sigma_1\nu_1 w_2 + \sigma_2\nu_2 w_1}{\sigma_1\nu_1 + \sigma_2\nu_2} \text{ and } \mu = \frac{\sigma_1\nu_1 w_2}{\sigma_1\nu_1 + \sigma_2\nu_2}\varkappa_2 E. \tag{5}$$

Since the concentration of free electrons (of velocity u) is written as

$$N = \frac{1}{u} \cdot \frac{w_1 n_1 + w_2 n_2}{\sigma_1\nu_1 + \sigma_2\nu_2} \tag{6}$$

and $w_1 \gg w_2$, we obtain from Eqs. (3) and (4)

$$N = \frac{1}{u} \cdot \frac{w_2 \varkappa_2 E}{u\sigma_1\nu_1 + \sigma_2\nu_2}\left[t + \frac{1}{2}\frac{\sigma_1\nu_1}{\sigma_1\nu_1 + \sigma_2\nu_2} w_1 t^2\right], \tag{7}$$

for small values of t when $0 \leqslant t \ll 1/\lambda$.

For large values of t when $1/\lambda \ll t \ll 1/w_2$, assuming $\sigma_1\nu_1 \sim \sigma_2\nu_2$ (a "reasonable" case) we find

$$N = \frac{1}{u} \cdot \frac{w_2 \varkappa_2 E}{\sigma_2\nu_2}\left[t - \frac{\sigma_1\nu_1}{\sigma_1\nu_1 + \sigma_2\nu_2} \cdot \frac{1}{w_1}\right]. \tag{8}$$

It follows from Eqs. (7) and (8) that N, and hence also the photoconductivity, first increases linearly with the slope $k_1 = w_2\chi_2 E/(\sigma_1\nu_1 + \sigma_2\nu_2)$ and later with $k_2 = w_2\chi_2 E/\sigma_2\nu_2$. This is shown schematically in Fig. 2. The ratio

$$\frac{k_2}{k_1} = 1 + \frac{\sigma_1\nu_1}{\sigma_2\nu_2} \tag{9}$$

can in principle be very large.

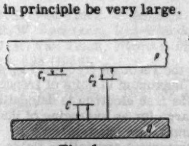

Fig. 1

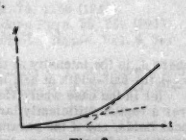

Fig. 2

It is thus possible to explain the initial superlinear increase in photoconductivity within the framework of the usual band scheme. Photostimulation by the exciting light is not essential, since the result is independent of the mode of release of the charges, whether by heat or by light. It is only important that $w_1 \gg w_2$, that is, to have, for example, much weaker photostimulation for the levels to which the electrons are raised initially.

If w_1 and w_2 are of a thermal character, it is easy to explain why superlinearity is more pronounced at high temperatures (see above). The fact is that in addition to the transitions $Q \to C_2$ (see Fig. 1) we may also have the transitions $Q \to C_1$ and $Q \to P$, though these are very weak. The $Q \to C_1$ transitions cause a linear increase in photoconductivity, the $Q \to P$ transitions a certain constant component of the photoconductivity. Since $\varepsilon_2 > \varepsilon_1$, the superlinear part of the photoconductivity will decrease much faster on cooling than the linear one, not to mention the constant component which apparently does not require activation energy.

Hence the interesting fact noted by Tolstoi (that superlinearity requires greater activation than the other processes) is a natural consequence of the scheme shown in Fig. 1.

It is also perfectly obvious that the scheme proposed above for the explanation of superlinearity does not contradict the possibility of a luminescence yield close to 1.

REFERENCES

1. N. A. Tolstoi. Zhur. Eksp. i Teoret. Fiz. 30, 171 (1956);
N. A. Tolstoi and A. V. Shatilov. Opt. i Spektr. 1, 216 (1956); Opt. i Spektr. 5, 590 (1958); Opt. i Spektr. 6, 665 (1959).
2. V. V. Antonov-Romanovskii. Izv. Akad. Nauk SSSR, Ser. Fiz. 15, 637 (1951);
Z. L. Morgenshtern. Doklady Akad. Nauk SSSR, 58, 783 (1947);
Z. A. Trapeznikov. Doklady Akad. Nauk SSSR 58, 791 (1947);
E. S. Krylov. Doklady Akad. Nauk SSSR 64, 495 (1949);
L. I. Anikina. Trudy Fiz. Inst. Akad. Nauk 7, 5 (1956).
3. V. V. Antonov-Romanovskii and M. I. Epshtein. Doklady Akad. Nauk SSSR 64, 483 (1949);
M. N. Alentsev. Opt. i Spektr, 1, 240 (1956).
4. R. Frerichs. Phys. Rev. 76, 1869 (1949);
A. Rose. Phys. Rev. 97, 252 (1955).

A METHOD OF ANALYSIS OF THE LINE SHAPE IN ELECTRON PARAMAGNETIC RESONANCE

N. N. Tikhomirova and V. V. Voevodskii

Received 27 April 1959

The goal of line-shape analysis in electron paramagnetic resonance (EPR) (i.e., the establishment of the dependence of J on ω in the neighborhood of the resonance frequency ω_0) is the elucidation of the nature of the bonding of the unpaired electron with the atoms around it. From many theoretical investigations (see, for example, references 1 and 2) it is known that:

(a) In the case of pure spin-spin interaction the line shape is described by a Gaussian function

$$J(\omega) = J_0 e^{-\frac{(\omega-\omega_0)^2}{1.45\omega_G^2}}, \qquad (1)$$

where J_0 is the intensity at the resonant frequency ω_0 and ω_G is the half-width at half maximum in units of frequency.

(b) In the case where the free electron is delocalized over a region sufficiently large for an averaging of the local fields, and if the paramagnetic particles are all identical and there are no important crystalline fields, the line is narrowed in the center and broadened in the wings, and obeys a Lorentzian relation

$$J(\omega) = J_0 \cdot \frac{1}{1+\frac{(\omega-\omega_0)^2}{\omega_L^2}}. \qquad (2)$$

This narrowing is connected with the fact that the line width in this case $\omega_L = \omega_s^2/\omega_e$,[2] and the delocalization frequency of the electron ω_e is significantly greater than ω_G, where ω_G is the line width produced only by spin-spin interaction in the absence of exchange coupling.

(c) If the paramagnetic particles are not fully identical, or if there are crystalline fields which orient different particles differently in the external constant field, the resultant spectrum represents a superposition of a number of sharp lines describable by Eq. (2). If the difference in g-factors of these lines is sufficiently great, the resultant line will be described by Eq. (1).

(d) If, in the last case, there is an exchange of electrons between different regions of delocalization with frequency ω_e' (usually much smaller than the delocalization frequency ω_e), then, as Van Vleck pointed out,[3] the central part of the line ($\Delta\omega \ll \omega_e'$) will follow a Lorentz curve with parameter $\omega_L' = \omega_s^2/\omega_e'$. The tails of the line will be described by Eq. (1) as before.

The difficulties attending a detailed analysis of a complex line of this type have usually led investigators to limit the determination of the line shape to the central part, and thus to the parameter ω_L'. However, it is clear from what has been said that the determination of the parameters ω_L' and ω_G' is much more important in order to establish the nature of the interaction of the electron with its surrounding medium. A rather simple method for determining these parameters from experimental data is presented below. It requires that Eqs. (1) and (2) be written in such a form that combinations of the experimentally measurable quantities J and $(\omega - \omega_0)$ will lead to linear relations.*

*Since the resonance frequency is usually held constant in EPR measurements and the uniform field H varied, we will speak from now on of the dependence of J on H.

Since, in experiments, we are ordinarily concerned with the first derivative of the absorption line, we should carry out this operation not with Eqs. (1) and (2) themselves, but with the relations

$$J' = \frac{dJ}{dH} = 2J_0 b^2 y e^{-b^2y^2}, \qquad (3)$$

where $b^2 = 1/1.45\Delta H_G^2$, $y = H - H_0$, and

$$J' = \frac{dJ}{dH} = J_0 \frac{2b^2 y}{(1+b^2y^2)^2}, \qquad (4)$$

where $b^2 = 1/\Delta H_L^2$, $y = H - H_0$. With the aid of simple rearrangements, these equations may be made linear in terms of the coordinates

$$\lg\left(\frac{y}{J'}\right) = \frac{b^2y^2}{2.3} + \lg\left(\frac{0.427}{J'_{max}\cdot b}\right), \qquad (5)$$

$$\sqrt{\frac{y}{J'}} = \frac{0.57}{\sqrt{bJ'_{max}}} + 0.57\sqrt{b}\,y^2. \qquad (6)$$

Analysis of a line shape consists in plotting $\log(y/J')$ and $\sqrt{y/J'}$, obtainable from the experimental curve, as functions of y^2. In the region of applicability of (6) the dependence of $\sqrt{y/J'}$ on y^2 must be linear, except for deviations from linearity in the neighborhood of $\Delta H \cong \Delta H_e'$. The dependence of $\log(y/J')$ on y^2 must be nonlinear for $\Delta H \leq \Delta H_e'$ and linear for $\Delta H > \Delta H_e'$. It is a simple matter to determine $\Delta H_L'$ and $\Delta H_G'$ from the linear portions of the two curves. The value of ΔH corresponding to the transition region between (5) and (6), for example, is $\Delta H_e'$. As a criterion for the validity of such an analysis one can use the fact that the three independently determined parameters $\Delta H_e'$, $\Delta H_G'$, and $\Delta H_L'$ must satisfy the

simple relationship $\Delta H_L' = \Delta H_G'^2/\Delta H_*'$, pointed out above.

Let us examine the EPR line of coke prepared from polyvinyl chloride (PVC) as an example of the application of the above method. As we have shown previously, such cokes have intense paramagnetic resonance signals.[4] The derivative of the EPR line of coke, obtained at 700°C, is shown in Fig. 1. The linearized form of this curve is given in Fig. 2. It is evident from Fig. 2 that the points in a plot of $\sqrt{y/J'}$ vs. y^2 lie satisfactorily on a straight line up to $y^2 = 400$ (corresponding to $\Delta H \approx 3$ gauss). It is also clear that for higher values of y^2 the experimental points follow a linear relation between $\log(y/J')$ and y^2. This means that the EPR line investigated is Lorentzian in the center, but Gaussian beyond $\Delta H \approx 3$ gauss. We have studied in exactly the same manner the EPR lines of cokes obtained at temperatures of 400°, 500°, and 600°C. The values of $\Delta H_G'$, $\Delta H_L'$, and $\Delta H_*'$ are given in the table. Values of $\Delta H_G'^2/\Delta H_L'\Delta H_*'$ are given in the last column. The small deviations from unity indicate that the analysis is valid.

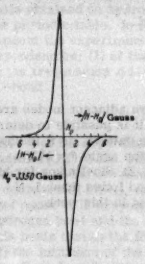

Fig. 1

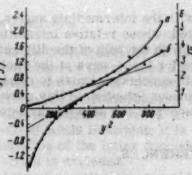

Fig. 2

Fig. 1. EPR derivative curve of a coke obtained by heating polyvinyl chloride at 700°C. Fig. 2. Linearized form of the coke EPR curve. Curve a—in coordinates corresponding to a Lorentz relation; curve b—in coordinates corresponding to a Gaussian relation. Abscissa—y^2 in arbitrary units (10 units = 1.4 gauss).

Coking temperature °C	$\Delta H_*'$ from experimental curve (gauss)	$\Delta H_L'$ (gauss)	$\Delta H_G'$ (gauss)	$\frac{\Delta H_G'^2}{\Delta H_L'\Delta H_*'}$
400	13	5.0	7.8	0.95
500	12	3.8	6.3	0.9
600	4.2	1.2	2.3	1.05
700	3	0.93	1.7	1.0

The results obtained can be compared with our knowledge of the structural changes of cokes when the coking temperature is raised. Thus it is well known that raising the coking temperature increases the number of aromatic rings, which should lead to an enlargement of the regions over which electrons are delocalized. This should manifest itself in a decreased value of $\Delta H_G'$. On the other hand, the increase in number of rings at high temperatures of carbonization takes place at the expense of the side chains, which clearly contribute to the existence of exchange interaction. We are therefore entitled to expect a simultaneous decrease of $\Delta H_*'$ and $\Delta H_G'$. It is clear from the table that both these expectations are fulfilled in the data we have obtained.

REFERENCES

1. J. H. Van Vleck. Phys. Rev. **74**, 1168 (1948).
2. P. W. Anderson. Revs. Modern Phys. **25**, 269 (1953).
3. J. H. Van Vleck. Nuovo Cimento, Supple. Vol. **6**, Ser 10, 993 (1956).
4. N. N. Tikhomirova, B. V. Lukin, L. L. Rasumova, and V. V. Voevodskii. Doklady Akad. Nauk SSSR **122**, 264 (1958).

FIELD DISTRIBUTION IN OPTICAL WAVEGUIDES

B. S. Skorobogatov

Received 1 June 1959

In the study of the wave propagation in the optical wave guide,[1] the wave guide was excited by the source which was located outside and at a great distance from the wave guide. With this method of excitation there arose a series of peculiarities in the wave propagation. Phenomena observed in reference 1 were explained by noting that in exciting the wave guide with a parallel beam of light, incident at the entrance, it is possible, by selecting a definite angle of incidence, subject to the relation $\cos\theta = c/v_p$ (v_p is the wave phase velocity of a given mode), to excite the waves with the different modes separately. But at the angles not satisfying the given equality, waves with two adjacent modes are excited simultaneously.

In reference 2 it was indicated that only with a "symmetrical excitation" does the diffraction pattern at the exit of wave guide not depend on its length, and the field distribution in the wave guide corresponds to the theoretically calculated distribution for the waves of the assumed modes. Using the Fourier transformation and the Kirchhoff method for the diffraction calculation, it is possible to reconstruct the field distribution inside the wave guide as a function of the angular distribution of the intensities in the diffraction pattern.

The experimental arrangement used, represents the usual set-up for observation of the Fraunhoffer diffraction. The diffraction patterns have been photographed and then measured with a photometer.

Figure 1 shows the angular distribution of the relative intensity at the exit of the wave guide (the width $2a$ = 25 mμ) for the H-waves (light polarization is along the slit) with the angles of excitation $\theta = 30'$ (a), 50' (b), 1°40' (c), 1°20' (d); and for the E-wave (the polarization is perpendicular to the slit) with $\theta = 30'$ (e).

Figure 2 shows the dependence of the magnitude of the transverse electric vector E_t (as calculated from the diffraction pattern) as a function of the x- coordinate (x-axis perpendicular to the guiding surface of the wave guide). The uniform lines show the theoretical curves,

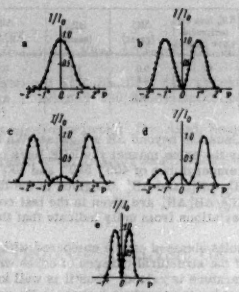

Fig. 1

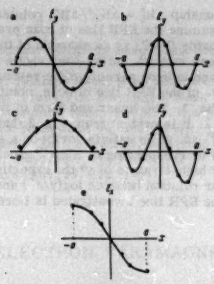

Fig. 2

as calculated by formulas[1] corresponding to the field distribution for H_z, H_y, H_x, and E_x waves (correspondingly a, b, c, and e). The curve in Fig. 2d is plotted using experimental points.

Using the harmonic analysis of this curve, it resolves to $E_y = 0.4 \sin \frac{\pi x}{a} + \cos \frac{3\pi x}{2a}$, i.e., the intensities of H_z and H_y waves are related, in this case, as 1:0.16.

Thus, it is shown that with those excitation angles for which the field distribution of one mode was assumed, the field distribution corresponds very exactly to the theoretical calculation for the wave of the expected mode; but with the intermediate angles, two adjacent modes are excited, whose relative intensities it is possible to determine with the help of the diffraction pattern, as it is shown above for the H-wave at the excitation angle $\theta = 1°20'$.

In conclusion I wish to thank K. D. Sinel'nikov for his continuous attention to this work, and I also thank I. N. Shklapevskii for showing his interest in this work.

REFERENCES

1. B. S. Skorobogatov. Opt. i Spektr 3, 272 (1957).
2. B. S. Skorobogatov. Opt. i Spektr 7, 823 (1959).

THE DEFORMATION VIBRATIONS δ(OH) FOR STRONG HYDROGEN BONDS

Ya. I. Ryskin and G. P. Stavitskaya

Received 30 June 1959

The formation of the complex RXOH...O'R', in which the molecules RXOH and O'R' are joined by a hydrogen bond (H-bond), is connected with an increase of the equilibrium length to (O—H) of the bond O—H. Even before the experimental verification of this fact,[1] it was shown theoretically[2] that a fundamental spectral manifestation of H-bonds—the decrease of the frequency of the stretching vibration νOH—can be explained only on the basis of an assumption about the lengthening of the O—H bond, an increase of the excess charge of the H atom, and a redistribution of the electron density of the O' atom in the process of formation of the hydrogen bridge.

From an analysis of the systems in which H-bonds are very strong [R(O...O) ≤ 2.7 A, νOH ≤ 2900 cm^{-1}], it follows that for the formation of such bonds a partial shift of the electron cloud of the hydrogen atom beyond the OH bond is essential.[3] This process leads to a strong decrease of the covalent contribution in the O—H bond and, accordingly, must have a lowering influence on the frequency of the deformation vibration δ(OH), an influence possibly less strong than on the frequency of the stretching vibration νOH. It is interesting to trace the change of the "weight" of the "decreasing" factor studied, in its dependence on the strength of the hydrogen bond.

Beginning in 1948,[4] many attempts have been made to identify the deformation vibrations δOH of isolated and

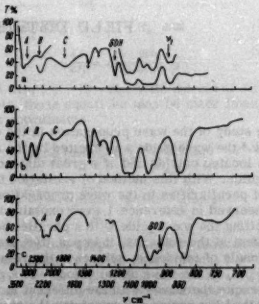

The absorption spectra of powdered samples of disubstituted potassium phosphates. a—$K_2HPO_4 \cdot 3H_2O$; b—K_2HPO_4; c—K_2DPO_4. The absorption bands of the paraffinic mulling agent are indicated by +. The short wavelength part of the spectrum was obtained with samples mixed with a fluorinated medium.

associated molecules of alcohols and of phenols. However, in spite of the carefulness and systematic approach of some of the investigations (e.g. reference 5), they were not successful in achieving completely definite results. This is explained by an insufficient characterization of the δOH vibration in the compounds investigated. Nevertheless, in the literature there has been established a proposition, according to which the H—bond in alcohols and phenols increases the frequency δOH; and the relative change of the latter is approximately equal (or even exceeds) the change of the frequency of the stretching vibration.[5,6]

A greater degree of certainty characterizes the results obtained on hydroxides of the first three groups of the periodic table. In this work[7] an attempt was made to present the experimental data in the form of two linear dependencies: (1) of the dependence between the changes in the frequencies $\Delta\delta$OH and $\Delta\nu$OH, resulting from the H—bond

$$\Delta\delta\text{OH} = -0.66\Delta\nu\text{OH} \ldots$$

and (2) of the dependence of the δOH frequency on the radius r(OH) of the OH^- ion, taken by the authors as a measure of the covalent character of the X—O bond (with a decrease of r(OH), the frequency δOH increases). In this paper it is supposed that interaction between the hydrogen bond and the X—O—H bonds is absent; it is on this basis that in the formulation of the latter dependence (2) the influence of the H—bond is excluded.

In an investigation[8] of the absorption spectra of basic copper salts, significant deviations from dependence (1) are observed—in the region of stronger H—bonds, formula (1) gives a high value of the frequency δOH (with νOH = 3000 cm^{-1} the experimental value of δOH is 75 cm^{-1} lower than the calculated value).

Among compounds with strong H—bonds, the carboxylic acids have been exposed to systematic investigations. However, in molecules of these compounds there is a very strong interaction of the νCO and δOH vibrations,[9] but, in certain cases an approximate assignment of the measured absorption bands to the δOH vibrations has proved possible. These bands are located in the interval 1200–1380 cm^{-1}, and with the transition from the monomeric acids to the dimers (in the vapor phase), the δOH frequency increases 50–150 cm^{-1}.[9] At the same time, the decrease of the νOH frequency exceeds 1000 cm^{-1} and, accordingly, the ratio $\Delta\delta\text{OH}/\Delta\nu\text{OH} = -0.15$ instead of −0.66 for H-bonds of intermediate strength.

With the purpose of obtaining better defined data, we carried out an investigation of the absorption spectra of some acid salts in the crystalline (finely dispersed) state. The frequencies νOH and δOH of some of the compounds investigated by us are gathered in the table.

Description of the band / Compound	Frequencies of the stretching vibrations νOH (cm^{-1})					Frequencies of the deformation vibrations δOH (cm^{-1})
		A		B	C	D
$Ca_2[HSiO_4]OH$[2, 10]	3532	2847	2594	2450		1282
$Ca_2[DSiO_4]OD$	2607	2115	1910	1790		910
$k = \frac{\nu OH}{\nu OD} : \frac{\delta OH}{\delta OD}$	1.35	1.35	1.36	1.38		1.40
K_2HPO_4		2940		2400	1910	1289; 1275
K_2DPO_4		2210; 2105		1825	?	934
$k = \frac{\nu OH}{\nu OD} : \frac{\delta OH}{\delta OD}$		1.36		1.36		1.39
$K_2HPO_4 \cdot 3H_2O$	~3325	~2950		2285	1740	1214
γ-$Al(OH)_3$[11]	3617	3510	3428	3380		1020; 960; 918
γ-$Al(OD)_3$	2672	2602	2558	2505		
$k = \frac{\nu OH}{\nu OD} : \frac{\delta OH}{\delta OD}$	1.35	1.35	2548 1.35	1.35		

The substances investigated are characterized by an independence of the δOH vibration on other vibrations of the anion. This is proved by the close value of the coefficient of the isotopic shift to the value appropriate to the harmonic oscillator O—H (k = 1.39–1.40), and also by the extremely small width of the absorption bands δOH and δOD. Besides, it was shown that the values of δOH in K_2HPO_4 and $Ca_2(HSiO_4)OH$ are practically identical and exceed by only 260 cm^{-1} the maximum frequency of δOH in crystalline γ-$Al(OH)_3$. At the same time, if the dependence (1) was possibly applicable in systems with strong H-bonds, then the δOH frequency in the crystals K_2HPO_4 and $Ca_2(HSiO_4)OH$ would differ greatly from the analogous frequency in γ-$Al(OH)_3$ (and would exceed 1600 cm^{-1}). Thus, Eq. (1), expressing, in substance, the independence of the bonds O—H and H...O, is not valid for strong H-bonds. It possibly explains only the decrease of the covalent and weakening of the directional characteristics of the O—H bond in the process of formation of the complex RXOH...O'R', since in the case of the substances considered it is impossible to attribute a low value of the δOH frequency to a lack of characteristic nature of this vibration.

The effect of the factor of decreasing δOH appears particularly clear on a comparison of the spectra of K_2HPO_4 and $K_2HPO_4 \cdot 3H_2O$.

In the crystal $K_2HPO_4 \cdot 3H_2O$ the hydrogen bonds are stronger than in the K_2HPO_4 crystal, since two of its νOH absorption bands are shifted in the direction of lower frequency: 2490 – 2285, 1910 – 1740 cm^{-1} (cf. the figure). At the same time, the δOH frequency in the spectrum of the trihydrate is 68 cm^{-1} lower than in the spectrum of the anhydrous salt. Hence, for strong hydrogen bonds, the influence of the decreasing factor can increase faster than the influence of the imposition of an external bond.

Not long ago it was shown[12] that bonds of the type A, B, and C (cf. the table) are characteristic of compounds containing the group X(:O)OH, where X = P, As, S, Se, and, sometimes, C. The authors of this work, not taking account of the weakening factor, were disposed to a mistaken conclusion about the correspondence of band C to a δOH vibration. KH_2AsO_4 appears as the only substance, the spectrum of which in this work[12] was compared with that of its deuterium analog. In this case a band due to a hydroxyl vibration at 1300 cm^{-1} is also observed, which is close to the values of δOH in the substances investigated by us. The attempt to write in one group the bands 1300 cm^{-1} (D) and 1650 cm^{-1} (C) and to assign both of these bands to a vibration of the δOH type (12) is not proved, since the properties of the bands indicated (the width, intensity, and the sensitivity of the frequency to hydrogen bonding) are very different.

We must note that the assignment of the band C to a pure stretching hydroxyl vibration is not as definite as that for the A and B bands, since in our spectrum of K_2DPO_4 the band of type C so far has not been discovered, and in the spectra of $Ca_2(HSiO_4)OH$ and $Ca_2(DSiO_4)OD$ it is definitely absent.

Let us summarize the preceding discussion.

The character of the influence of the hydrogen bond on the δOH vibration radically changes on the transition from long to short H-bonds. The latter influence relatively slightly the degree of anharmonicity and the frequency, δOH, of the deformation vibration.

The noted phenomena are explained in a natural manner on the basis of the donor-acceptor theory of the H-bond.

We express our thanks to Member-Correspondent of the Academy of Sciences of the U.S.S.R., E. F. Gross, for his constant attention to our work and discussion of the results obtained.

REFERENCES

1. H. K. Welsh. J. Chem. Phys. 26, 710 (1957).
2. H. D. Sokolov. Zhur. Eksp. i Teoret. Fiz. 23, 392 (1952); Uspheki Fiz. Nauk 57, 205 (1955).
3. Ya. I. Ryskin. Opt. i Spektr. 7, 278 (1959).
4. M. Davies. J. Chem. Phys. 16, 267 (1948).
5. A. V. Stuart and G. B. B. M. Sutherland. J. Chem. Phys. 24, 559 (1956).
6. C. G. Cannon. Spectrochim. Acta 10, 341 (1958).
7. E. Hartert and O. Glemser, Z. Elektrochem. 60, 746 (1956).
8. P. Tarte. Spectrochim. Acta 13, 107 (1958).
9. D. Hadzi and M. Pintar, Spectrochim. Acta 12, 162 (1958).
10. L. Heller. Acta Cryst. 5, 724 (1952).
11. V. A. Kolesova and Ya. I. Ryskin. Opt. i Spektr. 7, 261 (1959).
12. I. T. Braunholtz, G. E. Hall, F. G. Mann, and N. Sheppard. J. Chem. Soc. 868 (1959).

ON THE SPECTRAL DETERMINATION OF THE ISOTOPIC COMPOSITION OF STRONTIUM

A. G. Zhiglinskii and G. G. Kund

Received 8 July 1959

Strontium possesses four stable isotopes with atomic weights of 84, 86, 87, and 88. Sr^{87} is formed as a result of the β-decay of Rb^{87}; consequently the concentration of this isotope in strontium is related to the Rb/Sr ratio and the geological age of the rock from which the sample was obtained. Determination of the ratio of the concentration of Sr^{87} to the sum of the concentrations of even isotopes of strontium thus serves as one of the methods for studying the age of rocks.[1]

The isotopic shift in the spectral lines of strontium is so small that the lines of the even isotopes overlap, but the line of the isotope Sr^{87}, whose nucleus possesses angular momentum I = 9/2, has a fairly well resolved hyperfine structure.[2] This affords the possibility of measuring the ratio of the intensity of the line belonging to the even isotopes to the component due to the isotope Sr^{87}, and thus determining the relative content of odd and even isotopes.

We used a photoelectric device for recording the hyperfine structure (h.f.s.); this apparatus is described in our paper on the isotopic analysis of lead.[3] For this analysis we chose the line Sr II 4078 A, corresponding to the transition $^2S_{1/2} - {}^2P_{3/2}$. The h.f.s. of this line is essentially determined by the splitting of the $^2S_{1/2}$ term,[2] which is 0.158 cm^{-1}. The structure of this line is shown in Fig. 1.

The value of the etalon constant was chosen so as to cause components A and B from adjacent orders to be superimposed on one another. The corresponding distance between mirrors of the etalon was 31.8 mm (we selected the nearest ring from the standard set—32 mm).

A sample pattern showing the structure of Sr II 4078 A for a Sr^{87} concentration of 40% is given in Fig. 2. The effective coefficient of reflection of the mirror of the etalon was 80%. The partial superposition of the lines of even and odd isotopes is due to the inadequate resolving power of the etalon and the Doppler broadening of the line; the latter played a decisive role under our conditions.

For analysis we therefore used a curve constructed from standards carefully measured by means of a mass spectrometer. The curve deviated noticeably from linearity, particularly in the region where the Sr^{87} content

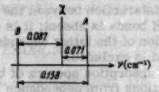

Fig. 1

Fig. 2

Fig. 1. Structure of the 4078 A line of Sr II. Component lines: A—Sr^{87}, B—Sr^{87}, χ—Sr^{88} + Sr^{86} + Sr^{84}.

Fig. 2. Record of the structure of the 4078 A line of Sr II for a concentration of 40% Sr^{87}.

was approximately 7% (7% is the lowest concentration of Sr^{87} in natural strontium).

A graph was constructed for the concentration range 7.0-52.6% Sr^{87}, for which we used 6 standards with different Sr^{87} contents (7.03, 15.0, 20.0, 30.0, 52.6%). An estimate of the error leads to a relative error of 2-3% for concentrations of 15-50% Sr^{87}, and 5-7% for concentrations of 7-15% Sr^{87}. This does not appear to be the best accuracy possible by this method.

The authors express deep gratitude to A. N. Zaidel for his constant interest in the work and discussion of the results, and to I. E. Starik and V. S. Zolotarev for making the necessary separated isotopes of strontium available.

REFERENCES

1. O. O. Rankama. "Isotopes in Geology." 1956.
2. M. Heyden and H. Kopfermann. Z. Physik 108, 3 (1938).
3. A. N. Zaidel, A. G. Zhiglinskii, and Iu. Chaiko. Czechoslov. J. Phys. 8, 530 (1958).

THE INTERFEROMETRIC DETERMINATION OF GAS DENSITY AND ELECTRON CONCENTRATION IN A DISCHARGE

A. M. Shukhtin

Received 26 June 1959

It is well known that changes in gas density, ionization, and excitation are connected with a change in the refractive index of a gas. These properties are widely used in the dynamics of gases for the determination of the density of the gas in flowing streams.[1] In references 2 and 3 these same principles were exploited for the determination of gas density and electron concentration in open arcs and sparks. We have attempted to determine the variation in gas density along the axis of a straight tube during a pulsed discharge in argon by measuring the change of refractive index using a Rozhdestvenskii two-beam interferometer.

The discharge tube under investigation is placed in the path of one of the interfering parallel beams of light; a compensator is placed in the other beam. The interferometer is crossed with a spectrograph. The system is illuminated by means of a light source emitting a continuous spectrum; an undistorted interference pattern is observed in the focal plane of the spectrograph. The perturbation of the gas is accompanied by a change in the interference pattern, namely, by a displacement of the interference fringes.

Consider that only a change of density of magnitude $\Delta\rho$ occurs when the gas is perturbed. We shall assume the following equation for the dispersion of the gas:

$$n - 1 = A\rho, \tag{1}$$

The displacement of the pattern K, expressed in wavelengths, can be written in the form

$$\frac{AL\Delta\rho}{\lambda} = K, \tag{2}$$

where L is the length of the column of gas being examined.

For some definite λ values, the displacement will be equal to a whole number of wavelengths; for others it will be equal to an odd number of half wavelengths. We shall record the undisturbed and the perturbed interference patterns by superimposing them on the same area of the photographic film. For wavelengths corresponding to a displacement of a whole number of fringes, the maxima of different orders of the two patterns will coincide; this means that we obtain on the film a section with a sharp fringe pattern. For light frequencies corresponding to a displacement of the pattern by an odd number of half wavelengths, the maxima of one pattern coincide with the minima of the other; this means that the pattern on the film will be indistinct.

Thus, photographing over a wide spectral range, we obtain an interference pattern with a succession of sharp and indistinct portions. For two indistinct patterns, one may write the following system of equations:

$$\left.\begin{aligned} AL\Delta\rho &= (2K_1 + 1)\frac{\lambda_1}{2}; \\ AL\Delta\rho &= (2K_2 + 1)\frac{\lambda_2}{2}; \\ K_2 &= K_1 + i. \end{aligned}\right\} \tag{3}$$

λ_1 and λ_2 are determined with the aid of a comparison spectrum; i is the number of sharp portions in the pattern between the two indistinct portions under consideration, as determined from the spectrogram. The unknowns $\Delta\rho_1$, K_1, and K_2 can easily be determined from Eq. (3).

If the change in the refractive index was caused by ionization, the change in the concentration of electrons can be determined in exactly the same way by applying the equation for the dispersion of an electron gas. Considerable concentrations of electrons are necessary for an observable displacement of the pattern. Such concentrations should occur, for instance, at the moment of compression of the plasma in strong pulsed discharges. According to data[4] on experiments carried out with straight tubes 100 cm long, electron concentrations occur at the moment of compression, which should cause a displacement of the pattern of approximately 25 fringes at λ = 6000 A. The use of short exposures synchronized with the pulses being investigated, and the use of a narrow beam of light passing through various portions of the tube under study should enable us to observe the change in electron concentration with time and location along the tube.

If the changes in gas density and electron concentration take place simultaneously, it is easy to set up a system of equations analogous to Eq. (3), connecting the magnitude of the displacement of the fringes with the change in the electron concentration ΔN_e and the change in density $\Delta\rho$. For example, having determined the wavelengths of three indistinct regions, one can separately determine the quantities ΔN_e and $\Delta\rho$.

At the image plane of the spectrograph, one may replace the film by one or two photomultipliers connected to oscilloscopes. Each photomulipliер should be provided with a slit parallel to the interference fringes; the interference pattern is focused in the planes of the slits. If as a result of the process under study there occurs a change in the refractive index of the gas, the illumination of the photomultiplier slit will change periodically. A trace will appear on the screen of the oscilloscope which will permit the determination of the magnitude of the displacement of the interference fringes at any desired moment. In a number of cases this method may make it possible to observe the change of the refractive index of the medium continuously during the whole duration of the process under study.

The photographic method was used in our experiment. A straight discharge tube of approximately 100 cm long and 6 cm in diameter was placed in the path of one of the light beams. At the ends of the tube, which were provided with plane parallel windows, were placed diaphragms with round openings of 6 mm in diameter, which isolated the axial part of the tube. The tube was filled with argon. The discharge was accomplished with the aid of an artificial transmission line giving an approximately rectangular

Spectrograms of an electrical discharge in argon. a) Superposition of two unretouched photographs; b) Retouched photograph superimposed on the retouched one.

[4](Ed. note: the incorrect figure was published in the Russian issue 6 but it has been possible to substitute the correct one in this English edition-)

current pulse whose flat part had a duration of approximately 200μ sec and an amplitude of about 600 amp. A pulsed capillary discharge tube with a flash duration of about 3μ sec served as a source of continous radiation. The flash of the capillary tube could be synchronized with the flash of the tube being examined, but it could also be fired independently. In this way we were able to obtain interference patterns corresponding to various stages of the discharge under study and to superimpose them on an unperturbed pattern. The spectral apparatus employed was a prism spectrograph with quartz optics. The periodically alternating sharp and indistinct interference fringes did actually appear in the spectrogram (see Figure). The distribution and number of indistinct fringe groups in a given spectral region varied for the various stages of the pulse. It was found that at some stages of the discharge the change in the density of the gas reached quite considerable values. For instance, with an initial argon pressure of 6 mm Hg, some spectrograms were obtained which showed an almost complete escape of the gas from the axis of the tube. On the basis of these spectrograms, one can apparently say that the density along the axis during this stage of the discharge does not exceed 10% of the initial density.

Finally I would like to express my thanks to S. E. Frish, Member-Correspondent of the USSR Academy of Sciences, for discussions and his interest in this work.

REFERENCES

1. "Fizicheskie izmereniya v gazovoi dinamike i pri gorenii." (Physical Measurements in Gaseous Dynamics and During Burning), IL, Moscow, 1957.
2. G. G. Dolgov and S. L. Mandel'shtam. Zhur. Eksp i Teoret. Fiz. 24, 6, 691 (1958).
3. G. G. Dolgov and G. D. Petrov. Materialy, X Vsesoiuzn. Soveshch. po. spektr. (Proceedings of the Tenth National Conference on Spectroscopy), Vol. 2, p. 68., L'vov University, 1958.
4. L. A. Archimovich. Uspekhi Fiz. Nauk 56, 4, 454 (1958).

LUMINESCENCE SPECTRA OF TRIVALENT URANIUM IONS

L. N. Galkin and P. P. Feofilov

Received 2 July 1959

In 1957 we described briefly the characteristic absorption spectra and infrared luminescence spectra of trivalent uranium ions that had been introduced into synthetic single crystals of calcium fluoride, strontium fluoride, and barium fluoride.[1] More detailed data on the luminescence spectra of these crystals at room temperature and cooled to −150°C are presented in this note.

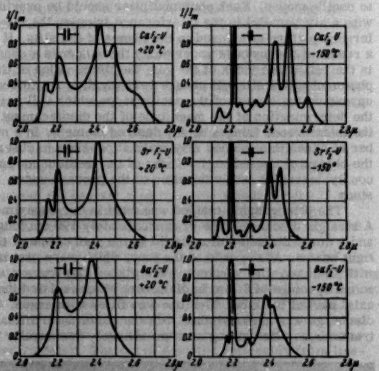

Luminescence spectra of $MF_2 - U^{+3}$ at + 20° and −150°C.

The crystals were grown from fusion in a vacuum by I. V. Stepanov and M. A. Vasil'ev, using the method developed under I. V. Stepanov's leadership.[2] The strongly reducing conditions required to obtain uranium ions with low valences were produced by introducing graphite powder into the mixture. The uranium concentration in the crystals was 0.1 to 0.3%. The method of studying the luminescence spectra was the same as that used previously. The luminescence was excited with light from an "SVD-Sh-250" mercury lamp. This light was passed through a water cell and heat-shielding glass to eliminate infrared radiation from the exciting beam. The exciting light was modulated with a frequency of 300 cps. A mirror monochromator with a diffraction grating (300 lines per mm) was used for the spectral analysis of the luminescence. A cooled lead sulfide photoconductive cell served as the detector. The signals were amplified and recorded with an "EPP-09" potentiometer. The comparatively high sensitivity of the apparatus makes it possible to operate with a slit sufficiently narrow to show fine structure in the luminescence spectra of the cooled crystals (the spectral width of the slit is 10-30 cm^{-1} in the region of 2.5μ). It should be noted that the luminescence intensity is increased 2 to 3 times* on cooling the crystals to −150°C. This allows one to use even narrower slits.

*The temperature quenching curves of $MF_2(U^{+3})$ luminescence that we measured show that it takes place in a rather broad temperature interval (from −100°C to + 100°C) and depends little on the cation in the host material lattice. In contrast to this we find in the case of hexavalent uranium luminescence in the same crystals that the ranges of temperature quenching are substantially different for M = Ca, Sr, or Ba.

The main results obtained from the luminescence spectra studies are presented in the figure. The spectral position and general characteristics of the emission bands are changed relatively little by switching from $CaF_2(U)$ to $BaF_2(U)$. This, as we noted in reference 1, is associated with screening of the 5f shell, within the limits of which there occur transitions determining the absorption and emission of trivalent uranium ions. As can be seen from the figure, cooling enhances the development of distinct structure and makes it possible for

Wavelengths (in μ) Corresponding to Maxima of $MF_3(U^{+3})$ Luminescence Bands (t = −150°C)

CaF_3-U	SrF_3-U	BaF_3-U
2.14	2.14	2.17
2.22	2.20	2.19
2.25	2.24	—
2.33	2.30	2.28
2.43	2.40	2.38
2.50	2.45	2.41
2.60	—	—

one to trace in greater detail the effects of crystal lattice parameters on the spectra. The locations of maxima of individual bands in the luminescence spectra are shown in the table.

The presence of an extremely narrow and intense band (corresponding to the wavelengths printed in heavy type in the table) that monotonically shifts toward the short wavelength side in association with the switching from $CaF_3(U)$ to $BaF_3(U)$ is characteristic of the spectra of all the crystals studied. A number of broader bands are located on both sides of this band, and their displacement from the narrow band is systematically reduced in proportion to the enlargement of the host material lattice. On one hand this shifting can be considered as the result of a change in the intracrystalline, electric field intensity, giving rise to a separation of ion energy levels as a consequence of the internal Stark effect. On the other hand, the possibility that the structure of the luminescence spectra has, even if only partially, a vibrational nature is not excluded. In that case the change in the interval between bands should be treated as a change in vibrating frequencies of "modulating" electron transitions as a consequence of the change in mass of the vibrating atoms and the distance between them. At present we do not have data available which would make it possible to interpret the structure of the luminescence spectra uniquely.

As already noted in our previous paper,[1] we are inclined to identify the infrared luminescence of trivalent uranium ions that we detected with forced electron transitions within the limits of the 5f shell, namely $^4I_{11/2} - {}^4I_{9/2}$ transitions. According to Jørgensen,[3] the spacing between these levels is 4100 cm^{-1} (2.44 μ), which agrees satisfactorily well with our data on the U^{+3} ion absorption spectrum in MF_3 crystals.

REFERENCES

1. L. N. Galkin and P. P. Feofilov. Doklady Akad. Nauk SSSR 114, 745 (1957).
2. I. V. Stepanov and P. P. Feofilov. Iskusstvennyi fluorit. V sbornik: "Rost kristallov." (Synthetic Fluorite. In the collection of papers entitled "Crystal Growth"), Izd. Akad Nauk SSSR, Moscow, 1957; I. V. Stepanov, I. A. Siniukova, and E. G. Chernevskaya. Opt. i Spektr. 4, 272 (1958).
3. Chr. K. Jørgensen. Kgl. Danske Videnskab. Selskab, Mat.-fys. Medd. 29, No. 11 (1955).

ORIENTATION OF LUMINESCENCE CENTERS IN URANIUM ACTIVATED LITHIUM FLUORIDE CRYSTALS

P. P. Feofilov

Received 20 June 1959

The bright green luminescence of uranium-activated lithium fluoride has been known for a long time.[1] Though there is no doubt that the luminescence centers in this luminophor include hexavalent uranium ions and that oxygen plays an essential role in their formation, it appears that up to the present time no direct experiments to establish the structure of the centers have been conducted.

The luminescence-polarization method which we developed to determine the nature of luminescence center orientations in crystals of cubic syngony[2] makes it possible to suggest plausible models of the centers in a number of cases. The application of this method to the study of LiF(U) luminescence centers becomes possible because Belyaev and his co-workers[3] have recently grown sufficiently large single crystals which, when excited, luminesce brightly over a broad spectral range.*

*We take this opportunity to express our gratitude to L. M. Belyaev and Z. B. Perekalina for their kind donation of the single crystal LiF(U) samples.

The samples investigated were plates cleaved from the crystal parallel to the (100) plane of the cube. The luminescence of the crystals which was excited by linearly polarized light, and observed in spectrally unresolved light, turned out to be partially polarized. The degree of polarization (P) displayed a clearly expressed azimuthal dependence (see reference 2), and also a strong dependence on the wavelength of the exciting light (the polarization spectrum). At room temperature and $\lambda_{excit.}$ = 405 mμ, P is negative; i.e., the direction of the main vibration in the luminescence is perpendicular to its direction in the exciting light. With $\lambda_{excit.}$ = 365 mμ, the luminescence is not polarized. At $\lambda_{excit.}$ = 313 mμ, negative polarization is again observed, but its absolute magnitude is decreased. It appears that one can expect positive polarization in association with excitation in the long wavelength absorption bands which are resonance-coupled with emission bands; in this situation, however, the observations would be greatly complicated by the necessity of accurate matching of the crossed light filters. For this reason during the study of the azimuthal dependence of the luminescence polarization we confined ourselves to the region of negative P values and excited the luminescence with radiations, at λ = 405 and 313 mμ, that had been isolated from the spectrum of an "SVD-Sh-350" mercury lamp. Measurement of the degree of polarization was done visually using a polarimeter with Savart plates and compensating stops.

Our preliminary experiments showed that the degree of polarization is different for different lines in the luminescence spectra of cooled crystals. However, since in this instance the only point which interested us was the determination of the orientation of centers, with the purpose of establishing a geometrical model for them, a large part of the measurements were conducted in spectrally unresolved light. In this case what was observed

was a value of the polarization averaged over the spectrum; however, this should not affect the character of the azimuthal dependences. A detailed study of the polarization state of individual lines in the emission spectrum and the multipolarity of the corresponding transitions will have to be made later.

The azimuthal dependences obtained are depicted in Fig. 1. A comparison of these with the calculated[3] values unequivocally indicates orientation of centers along the fourfold axis of symmetry (C_4).

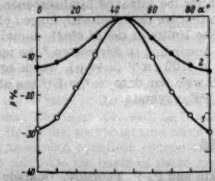

Fig. 1. Azimuthal dependence of the polarization of luminescence of LiF(U) crystals. $\lambda_{excit.}$: curve 1—405 mμ; curve 2—313 mμ.

Proceeding from this fact and the principle of localized charge compensation, one can propose a model of the LiF(U) luminescence center (Fig. 2). The hexavalent uranium ion (U^{+6}) isomorphously replaces a lithium ion (Li^+). The excess positive charge (+5) arising from this substitution is compensated by the isomorphous substitution of oxygen ions (O^{-2}) for 5 out of 6 of the fluoride ions (F^-) that surround the U^{+6} ions. It is easily seen that associated with this luminescence center there will be an anisotropic formation with the distinct direction oriented along one of the C_4 axes. The possibility of isomorphous substitution of O^{-2} for F^- is assured by the similarity of the radii of these ions. The fact that oxygen is essential for the production of hexavalent uranium luminescence in crystals was shown by us for $CaF_2(U)$[4], by Runciman[5] for NaF(U), and by Shapiro[6] for a number of uranium-activated alkali halide salts.

It should be noted that the model proposed by Runciman[5] for the luminescence center in the luminophor NaF(U) is apparently perfectly analogous to the LiF(U) luminophor that we investigated. Runciman's model proposes the substitution of oxygen for all 6 fluoride ions and compensation of the charge by an anion vacancy in the second coordination sphere. It is easy to satisfy oneself that a model like this suggests the presence of a distinct direction—a threefold axis (C_3). As we have seen, this property of the center that follows from Runciman's model is in contradiction with our experimental data.

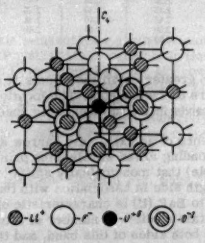

Fig. 2. A model of the luminescence center in LiF(U) crystals.

REFERENCES

1. M. K. Slattery. J. Opt. Soc. Am. 19, 175 (1929).
2. P. P. Feofilov. Zhur. Eksp. i Teoret. Fiz. 26, 609 (1959); "Polyarizovannaya liuminestsentsiya atomov, molekul i kristallov." (The Polarized Luminescence of Atoms, Molecules, and Crystals), Fizmatgizdat, Moscow, 1959.
3. L. M. Belyaev et al. Tezisy dokladov no soveshchanii po fizike shchelochno-galoidnykh kristallov. (Thesis reported at the Conference on the Physics of Alkali Halide Crystals), Tartu, 1959.
4. P. P. Feofilov. Mat. V Soveshch. po liuminestsentsii. (Transactions of the 5th Conference on Luminescence), p. 3, Izd. Akad. Nauk ESSR, Tartu, 1957.
5. W. A. Runciman, Nature 175, 1082 (1955); Proc. Roy. Soc. 237A, 39 (1956); J. phys radium 17, 645 (1956).
6. I. P. Shapiro. Opt. i Spektr. 7, 126 (1959).

ON THE VIBRATION FREQUENCY OF THE THALLIUM IODIDE MOLECULE

K. S. Krasnov

Received 8 June 1959

Two values are given in the literature for the value of the vibration frequency of the thallium iodide molecule: $\omega_e = 150\ cm^{-1}$,[1] and $\omega_e = 120\ cm^{-1}$.[2,3] We should like to bring forward arguments in support of the first of these two values.

1. The magnitude ω_e might be used for computing the repulsion coefficient ρ and the energy of repulsion $Ae^{-r/\rho}$ in diatomic molecules, the energy of which is found by a computation based on the ionic model.[4]

The values computed by us are presented in the Table.

For $\omega_e = 150\ cm^{-1}$, the energy of repulsion of thallium iodide is less than in the other thallium halides, as one should expect; for $\omega_e = 120\ cm^{-1}$, we obtain for the energy of repulsion in thallium iodide, a value that is greater than in thallium chloride. This is impossible since the distance between the atoms in thallium iodide is considerably more than that in thallium chloride.

Energies of Repulsion $Ae^{-r/\rho}$, Coefficients of Repulsion ρ, and Frequencies of Oscillation of Thallium Halogenides

Molecule	$Ae^{-r/\rho}$ (erg × 10^{12})	ρ (Å)	Deviation of ω_e computed according to (1) from experiment (%)
TlF	3.582	0.259	1
TlCl	3.180	0.304	5
TlBr	3.052	0.318	5
TlJ ($\omega = 150\ cm^{-1}$)	2.853	0.338	1
TlJ ($\omega = 120\ cm^{-1}$)	3.320	0.395	25

In analogous fashion, the quantity ρ in the first case for all four halogenides is strictly linear with respect to the equilibrium interatomic distance; in the second case, an abnormally large value of ρ is observed for thallium iodide.

2. For the value $\omega_e = 150$ cm^{-1}, for all the thallium halides, there is a linear dependence of ω_e on $1/\mu$, specifically

$$\omega_e = 58.17 + 7147.22 \cdot \frac{1}{\mu}, \quad (1)$$

where μ is the reduced mass. An analogous dependence is observed also in other series of diatomic molecules.[5] For the value $\omega_e = 120$ cm^{-1} this dependence is sharply different, and not linear.

From the considerations considered above (particularly 1), it is necessary to conclude that the proper value of ω_e of the thallium iodide molecule is 150 cm^{-1} as determined by Butkov.[1]

REFERENCES

1. K. Butkov. Z. Physik **58**, 232 (1929).
2. R. T. Rao and K. R. Rao. Current Sci. (India) **17**, 121 (1948).
3. G. Hertzberg. "Spectra and Structure of Diatomic Molecules." IL. Moscow. 1949.
4. E. S. Rittner. J. Chem. Phys. **19**, 1030 (1951).
5. J. P. Varshni. J. Chem. Phys. **28**, 1078 (1958).

FREQUENCIES OF THE NORMAL VIBRATIONS OF THE LEAD HALOGENIDES

A. M. Aleksandrovskaya, I. V. Rigina, and I. N. Godnev

Received 19 June 1959

Methods used by us for the prediction of the frequencies of zirconium halogenides[1] might be used also in a number of other cases. This is a report of the prediction of the frequencies of the normal vibrations of the lead halogenides, for which only the frequencies of $PbCl_4$,[2] are known, and only a single interatomic distance Pb-Cl, equal to 2.43 A.[3]

The rest of the distances were determined from the curve $r = f(Z_{halog.})$, drawn through the point from r = 2.43 A, corresponding to $PbCl_4$ (see reference 1). The values of r obtained are shown in Table 1, where they are compared with the values computed as the sum of the covalent radii[4] with the correction a = −0.10 A. The latter was obtained from the data for $SnCl_4$, $SnBr_4$, and SnI_4; the value of r for $PbCl_4$ calculated in this manner agrees well with experiment, which is the method for determining the magnitude of the correction.

In Table 2 are shown the values of the reduced potential coefficients k^*_{ij} and the reduced kinetic coefficients k_{ij} which were determined according to the curves $k^*_{ij} = f(A_{tensor})$ and $k_{ij} = f(A_{tensor})$, constructed for elements of the fourth group with electron configurations s^2p^2 (C, Si, Ge, Sn).

The frequencies of the normal vibrations of the lead halogenides were computed (see references 1 and 5) according to the values of k^*_{ij} and k_{ij}, and the average was taken (see Table 3). Both methods gave similar results. Evaluation of the errors in the computation of the frequency leads to values of the order indicated in reference 1, although in the case of PbX_4 it is impossible to avoid an extrapolation. For this reason, we could not determine all the frequencies of PbF_4.

The computed frequencies of $PbCl_4$ were in excellent agreement with the experimental data (see Table 4); a comparison of the frequencies of $PbBr_4$ with those of the isoelectronic molecule $TlBr_4^-$ [6] shows that the former appears to be larger (see Table 4), as would be expected on the basis of a comparison of the frequencies of molecules of an isoelectronic series.

Table 1. Interatomic Distances $r_{(Pb\text{-}X)}$ (in A)

Molecule	$r = f(Z_{halog})$	$r = r_{Pb} + r_X - 0.10$
PbF_4	2.02	2.08
$PbCl_4$	2.43 *	2.43
$PbBr_4$	2.57	2.58
PbI_4	2.76	2.77

*Experimental value.[3]

Table 2. Reduced Potential Coefficients (k*) and Reduced Force Constants (k)

Molecule	k* (× 10^{-5} cm^2)					k (× 10^5 cm^{-2})				
	k^*_1	k^*_2	k^*_{34}	k^*_{56}	k^*_{12}	k_1	k_2	k_{34}	k_{56}	k_{12}
PbF_4	0.175	?	0.19	−0.018	?	5.40	0.50 (?)	5.00	0.30	0.80 (?)
$PbCl_4$	0.29	2.44	0.31	−0.015	1.57	3.50	0.34	2.98	0.10	0.56
$PbBr_4$	0.32	2.18	0.34	−0.09	1.88	3.30	0.50	2.30	0.20	0.70
PbI_4	0.44	2.62	0.52	−0.21	2.14	2.10	0.30	1.70	0.08	0.42

Table 3. Frequencies of the Normal Vibrations of PbX_4 (in cm^{-1})

Frequencies	PbF_4			$PbCl_4$			$PbBr_4$			PbI_4		
	A	B	Average	A	B	Average	A	B	Average	A	B	Average
$\nu_1(A_1)$	572	558	584	325	327	326	206	208	207	139	134	137
$\nu_2(E)$	?	158 (?)	—	87	79	83	58	60	59	39	35	37
$\nu_3(F_2)$	581	560	570	348	333	341	246	215	231	173	162	168
$\nu_4(F_2)$	?	180 (?)	—	100	97	99	70	76	73	50	46	48

Note: A was computed according to the reduced potential coefficients; B was computed according to the reduced kinetic coefficients.

Table 4. Comparison of the Frequencies of $PbCl_4$, $PbBr_4$, and $TlBr_4^-$

Frequencies	$PbCl_4$		$TlBr_4^-$	$PbBr_4$
	Computed	Experimental	Computed	Experimental
$\nu_1(A_1)$	326	327	207	190
$\nu_2(E)$	83	90 (85)	59	54
$\nu_3(F_2)$	341	348	231	209
$\nu_4(F_2)$	99	90 (93)	73	64

1. I. N. Godnev, A. M. Aleksandrovskaya, and I. V. Rigina. Opt. i Spektr. **7**, 272 (1959).
2. J. T. Neu and W. D. Gwinn. J. Am. Chem. Soc. **70**, 3463 (1948).
3. M. W. Lister and L. E. Sutton. Trans. Faraday Soc. **37**, 393 (1941).
4. L. Pauling. J. Am. Chem. Soc. **69**, 542 (1947).
5. N. I. Ushanova, I. N. Godnev, and I. V. Orlova. Opt. i Spektr. **5**, 567 (1958).
6. M. L. Delwaulle. Compt. rend. **238**, 2522 (1954).

ON THE COLORS OF WRINKLED TRANSPARENT FILMS ON METAL SURFACES

K. D. Sinel'nikov, I. N. Shkliarevsky, and I. V. Gladkova

Received 15 June 1959

More than half a century ago Wood[1,2] described a curious type of interference in a thin layer of collodion applied to the reflecting surface of silver. The collodion is diluted by five or six parts of ether, to which a small amount of alcohol is added, and then poured out on a tilted glass plate previously coated with silver. After the plate is dry its surface wrinkles. The wrinkling of the film increases when one breathes on it. The size of the wrinkles is so small that they were observed by Wood only with the aid of a very strong microscope.

A thin transparent film deposited on an ideal reflecting surface in normally incident light does not produce interference colors. The wrinkled plate of collodion behaves quite differently. If the film deposited on silver is illuminated by white light normal to its surface, then bright colors are visible in the angular region 70-90 deg. The brightness of the colors increases when observed through a Nicol prism oriented in a particular way. Turning the Nicol prism 90 deg changes the colors into the complementary ones, i.e., it appears that half the spectrum is polarized in one plane and the other half in a perpendicular one. For the same light normally incident on the film, however, the scattered light observed in the angular region 10-30 deg is not polarized. We notice that for large angles of incidence (70-85 deg) the same rich (but more intense) colors and the same polarization are observed in rays reflected from the mirror. The collodion film does not produce colors when deposited on glass.

Wood convincingly demonstrated the interference nature of the colors under investigation; however, he was not able to explain the saturation of the color and the polarization effects. The aim of this short paper is to clarify these puzzling phenomena.

The saturation of the interference colors and the polarization effects may be accounted for in the following way. Light scattered by the wrinkles undergoes reflection and refraction in the wrinkle-free parts of the film. When the wrinkles are undulating, the light scattered by them impinges upon the wrinkle-free parts of the film mainly at large angles of incidence. These angles of incidence may be greater than Brewster's angle (56 deg). It is well-known that the reflection coefficient of a dielectric film increases with the angle of incidence. For large angles of incidence it may become equal to the coefficient of reflection at the boundary of the film (the silver). Thus the intensity of rays reflected from the surface of the film may be of the same order as the intensity of rays which have entered the film, been reflected from the silver, and then left the film. The interference of such rays naturally yields rich colors.

On this basis the polarization effects become explicable. For reflections from a dielectric film at angles greater than Brewster's angle, there is a phase difference of 180 deg between p- and s-components. Rays entering the film and refracted by it fall on the surface of the silver at relatively small angles. Thus, light incident on the film at 70 and 85 deg falls on the surface of the silver after refraction at corresponding angles of the order of 39 and 42 deg. The phase difference between p- and s-components caused by reflection is insignificant in this case, so that the total phase displacement is close to 180 deg. Thus, the optical path length for one of the components is almost a half-wave longer than for the other, which explains the change in the film's colors to the complementary ones when the Nicol prism is turned through 90 deg.

Figure 1 shows photographs of the interference from a wrinkled colloidal film with monochromatic light reflected from the mirror at 80 deg. The lower part of the film was coated with a semitransparent layer of silver. Photographs were taken in natural light (a), in light polarized perpendicularly to the plane of incidence (b), and in light polarized in the plane of incidence (c). As seen from the photographs, the sharpness of the interference patterns occurring in the silver-film-air system is just the same as in the silver-film-silver system.

The photographs show the different interferences of the mutually perpendicularly polarized components in the collodion film at an air boundary. In the film bounded on both sides by silver, the polarization effects are exhibited to a considerably smaller degree. We note that although the photographs of Fig. 1 were taken for obliquely incident light, their appearance when taken in light reflected from the film at this same angle is objectively the same as when taken in grazing reflection when the incidence of light on the film is normal. Because in the latter case the intensity is considerably smaller, the pictures were taken as indicated above.

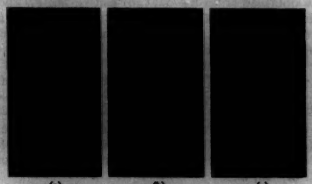

(a) (b) (c)

Fig. 1

The following experiment was then carried out. A wedge-shaped layer of dielectric film was deposited on a silver-coated glass plate in vacuum. A part of the film along the slope was coated with a layer of silver having a coefficient of reflection of the order of 60-70%. With normally incident light an interference pattern could be observed only on the part of film silvered on both sides. As the angle of incidence increased, the interference pattern in the reflected light started to appear on the wedge with an air boundary. As Brewster's angle was passed through, the interference bands in the system silver-dielectric-air split up sharply and displaced relative to each other by almost half the distance between lines of the adjacent series. The line-splitting in the system silver-dielectric-silver increased uniformly with increasing angle of incidence, corresponding to the gradually increasing phase difference upon reflection at the film-silver boundary. This splitting was much less prominent.

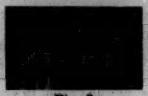

Fig. 2

Figure 2 shows photographs of the interference patterns for the model described above when the angle of light incidence was of the order of 80 deg. The lower strip of the photograph, the p-components of the interference, corresponds to the system silver-dielectric-silver. The middle and upper strips correspond, respectively, to the p- and s-components in the system silver-dielectric-air. It is evident that the lines of these two components are displaced relative to one another by almost half an order. These interference lines are no less sharp than the lines in the lower part of the Figure.

Thus the sharpness of the interference bands (the saturation of the colors) and the polarization effects in wrinkled films of collodion discovered by Wood have been obtained by us in a dielectric film with a reflecting surface deposited on silver. This experiment convincingly demonstrates the correctness of our proposed explanation.

REFERENCES

1. R. W. Wood. Phil. Mag. 7, 376 (1904).
2. R. Wood. "Fizicheskaya optika." (Physical Optics), ONTI, 1936.

INTRAMOLECULAR HYDROGEN BOND IN ISOPROPYL BENZENE HYDROPEROXIDE

V. V. Zharkov and N. K. Rudnevskii

Received 4 May 1959

In previous papers[1-3] it has been shown that aromatic hydrocarbons can act as weak electron donors in the formation of a hydrogen bond. The related intramolecular hydrogen bond is of considerable interest. A spectroscopic manifestation of such a bond has been observed for some aromatic alcohols[4-6] where it was supposed that the hydrogen bond was formed between the hydroxyl group and the π-electrons of the aromatic ring. In another work[7] a similar intramolecular hydrogen bond in alcohols of the type 2-allylphenol was discovered. This is treated as a bond between the phenolic OH-group and the π-electrons of the double bond of the substituent.

We have investigated the intramolecular hydrogen bond between the hydroxyl group and the π-electrons of the aromatic ring in isopropyl benzene (cumene) hydroperoxide. The infrared spectra of the cumene hydroperoxide were obtained with an IKS-2 spectrometer with a LiF prism. The spectral slit width was 13 cm^{-1} and the scanning speed 18 cm^{-1}/minute. The cumene hydroperoxide* was formed as the sodium salt, which was then washed with benzene and decomposed in an aqueous solution by bubbling with CO_2. The resulting hydroperoxide was distilled in vacuum and, by an iodometric analysis,[8] had a purity of 99-100%. Carbon tetrachloride, employed as a solvent, was dried over P_2O_5 and then distilled. For the particular measurements a solution of the cumene hydroperoxide in carbon tetrachloride with a concentration of hydroperoxide of 0.0035 M/liter was used. The cell of thickness 20 mm with KCl windows was thermostated for the recording of the spectra, with the temperature being maintained at ±0.2°C.

*The cumene hydroperoxide was kindly placed at our disposal by B. A. Redoshkiny.

The absorption band, due to the fundamental transition of the hydroxyl vibration in the cumene hydroperoxide, in sufficiently dilute solutions in CCl_4 ($C < 5 \times 10^{-3}$ M/liter) appears not as a sharp, single band, characteristic of a free –OH group, but as a doublet of two overlapping bands of almost identical intensity and width with frequencies of 3497 and 3530 cm^{-1} (Fig. 1). The ratio of the intensities of these bands does not depend on the concentration of the hydroperoxide, but does depend on the temperature. The band at 3530 cm^{-1} is due to the vibration of the free –OH group, and the band at 3497 cm^{-1} to the vibration of the bonded –OH group.

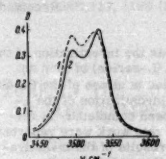

Fig. 1

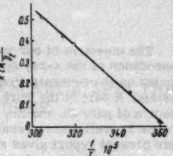

Fig. 2

Fig. 1. The absorption curves of cumene hydroperoxide for different temperatures. Curve 1—5°C; curve 2—45°C. Cell thickness = 20 mm; concentration = 0.0035 M/liter. Fig. 2. The graph of the dependence of $R\ln(D_1/D_2)$ on 1/T.

From the results of an investigation of the temperature dependence of the ratio of the intensities of the bands, corresponding to the free and bonded hydroxyl groups, we calculated the energy of the intramolecular hydrogen bond in cumene hydroperoxide.

It is not difficult to show that the equilibrium constant between the nonbonded and the intramolecularly bonded forms of the cumene hydroperoxide is given by the expression

$$K = \frac{\varepsilon_2}{\varepsilon_1} \cdot \frac{D_1}{D_2}, \qquad (1)$$

where ε_1 and ε_2 are the molar absorption coefficients and D_1 and D_2 the optical densities at the maxima of the absorption bands, corresponding to the free and bonded OH groups.

Application of the Vant-Hoff equation

$$\frac{d \ln K}{dT} = -\frac{Q}{RT^2} \qquad (2)$$

with the use of (1), together with the consideration that in the investigated temperature interval $\varepsilon_1/\varepsilon_2$ = const., we obtain

$$\ln \frac{D_1}{D_2} = \frac{Q}{RT} + \text{const}. \qquad (3)$$

From (3) it is possible graphically to calculate Q—the energy of the intramolecular bond—by studying the temperature dependence of $\ln(D_1/D_2)$.

In the determination of $\ln(D_1/D_2)$ the overlapping of the bands was neglected. For one of the temperatures a graphical separation of the absorption bands,[9] due to the free and bonded –OH groups, was carried out; in this the value of D_1/D_2 after the separation differed insignificantly from that before.

The results of the measurements for temperatures of 5, 16, 40, 45, and 55°C are represented graphically in Fig. 2. The energy of the intramolecular hydrogen bond, found from the slope of this graph, is equal to 0.90 ± 0.10 kcal/mole.

REFERENCES

1. H. B. Brown and J. D. Brady. J. Am. Chem. Soc. **74**, 3570 (1952).
2. R. M. Badger. J. Am. Chem. Soc. **73**, 3132 (1951).
3. M. Jamres. J. Am. Chem. Soc. **74**, 3375 (1952).
4. I. M. Goldman and R. O. Crisler. J. Organ. Chem. **23**, 751 (1958).
5. D. S. Trifan and J. L. Wieman. J. Am. Chem. Soc. **79**, 6566 (1957).
6. W. Lüttke and R. Mecke. Z. physik Chem. **196**, 56 (1950).
7. A. W. Baker and A. J. Shalgin. J. Am. Chem. Soc. **80**, 5358 (1958).
8. C. Wagner, R. Smith, and E. Peters. Anal. Chem. 19, 976 (1947).
9. S. E. Frish. "Tekhnika Spektroskopii." (Techniques of Spectroscopy), L.G.U. (1936).

INVESTIGATION OF THE L-SPECTRA OF Zn IN ALLOYS OF THE Cu-Zn SYSTEM

I. A. Rumyantsev and M. I. Korsunskii

Received 13 April 1959

The objective of our work was the investigation of the dependence of the x-ray spectra (L-series) of zinc and copper on the concentration of zinc in alloys of the Cu-Zn system. A part of the work, the investigation of the L-spectra of pure Cu and Zn, has been completed. In reference 1, preliminary results of this work were reported. This present report gives some results of the investigation of the L-spectra of zinc in alloys of the Cu-Zn system.

The x-ray spectral investigation was carried out by means of a fast tubular long wavelength x-ray spectrograph tube with the Jobann focussing arrangement. The radius of curvature of the mica crystal was 90 cm. The spectrograph is described in reference 2.

The x-ray tube chosen had interchangeable anodes, and was connected to the same vacuum system as the spectrograph. The primary method of excitation was used. While the tube was operating, a vacuum of the order of 1.5×10^{-5} mm Hg. was maintained in the spectrograph.

For investigation of alloys of the Cu-Zn system it was necessary to prepare the appropriate samples. The compositions were chosen so as to embrace all possible phases of the system under investigation, specifically: pure copper, α-brass (with 38% zinc), $\alpha + \beta'$(43%), β'(49%), $\beta' + \gamma$(55%), γ(63%), $\gamma + \varepsilon$(73%), ε(83%), $\varepsilon + \eta$(92%), and pure zinc.

The raw materials for preparation of the samples were L62 brass and granulated zinc. Some of the samples were prepared directly from melts of copper and zinc. Melting was carried out in quartz ampules, evacuated and sealed before heating. The composition of the samples was checked within each phase region to within an accuracy of 1%.

Cylinders 26 mm in diameter and 7-8 mm long were turned from the pigs of metal obtained. The samples were then placed in the cavity in the anode (made of steel) and soldered. After the sample had been soldered, the surface of the anode, including the sample, was cut off to form a 10 deg angle. The construction of the anode insured good cooling of the sample. Heat was removed from the sample by way of its soldered connection to the anode and the anode's thin wall (about 1 mm thick). The construction of the cathode was also different from that

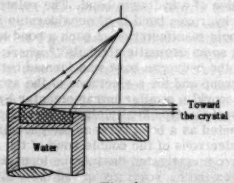

Fig. 1

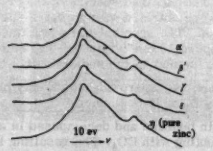

Fig. 2

used before. Since the direction of the cathode beam was opposite to that of the x-ray beam, (see Fig. 1), tungsten sputtered from the filament could not deposit on the working surface of the mica crystal.

The spectra were recorded photographically. Each sample was used to obtain 4 or 5 photographs of the L-series of zinc.

The conditions of the exposures were as follows: voltage, 5-8 kv; current, 20 ma; exposure, 2-6 hr. Thanks to the excellent cooling, the temperature of the anode during operation did not exceed 30-40°.

As reference lines, the $K\alpha_{1,2}$ and $K\beta_1$ lines of calcium were used in the fourth order, and the $K\alpha_{1,2}$ lines of vanadium in the fifth order. Calcium was applied to the anode in the form of chalk ($CaCO_3$), and vanadium in the form of a small thin plate stuck to the anode. The chalk and vanadium occupied only a small part of the anode surface, and no separate exposure was required to

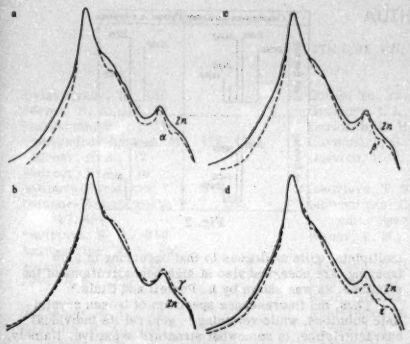

Fig. 3.

obtain the K-spectra of Ca and V since the lines of Ca and V were registered at the same time as the main photograph.

About 100 spectrograms were obtained of the L-series of zinc, with 13 anodes. Photometry was done using an MF-4 microphotometer. Figure 2 shows photomicrograms of plates of the L-series of zinc as obtained from samples of alloys of different concentrations.

Curves of relative intensity were constructed with the aid of an emulsion calibration curve. The curves analyzed in this fashion were averaged, several (not less than three) plates being used for each sample. It turned out that the differences between the curves used in striking an average were less than the differences between the averaged curves. The results of the experiment are shown in Fig. 3. In all cases the curve of the L-spectrum of pure zinc is shown (continuous line) for comparison with the curves for the L-spectra of zinc obtained from the alloys of different concentration (dotted line). As is evident from the figure, sharp differences are always observed between the averaged curves.

REFERENCES

1. I. A. Rumyantsev and M. I. Korsunskii. Izvest. Akad. Nauk SSSR, Ser. Fiz. 21, 1435 (1957).
2. G. P. Borovikova and M. I. Korsunskii. Doklady Akad. Nauk SSSR 114, 1192 (1957).

ON THE ORIGIN OF THE HYPERFINE STRUCTURE IN THE LUMINESCENCE SPECTRA OF AROMATIC HYDROCARBONS AT LOW TEMPERATURES

E. V. Shpolskii and L. A. Klimova

Received 13 October 1959

During recent years we have completed a number of investigations[1-8] dedicated to the study of emission spectra (fluorescence + phosphorescence) of the polyatomic aromatic hydrocarbons in paraffin solutions frozen at the temperature of boiling nitrogen (77.3°K). The possibility revealed in these studies of an extremely high resolution of the spectra of complex organic compounds, producing under normal conditions (as well as at low temperatures) continuous spectra or very broad bands, was confirmed and applied in further studies in other laboratories (by Bowen and Brocklehurst[9,10] and more recently by L. Pesteil, and Cials[9,12]. In our papers, the spectra of corynine, pyrene, and 3,4-benzopyrene were studied in detail in normal paraffins from pentane to decane which form, upon freezing, a small-grained snowlike mass. Under these conditions, on the whole, a complex picture was observed of resolved band spectra into groups of lines with a width up to 1-3 cm^{-1}. For instance, in the case of corynine in various paraffin solvents, sequences of sharp doublets were observed with a frequency difference that, for a given solvent, was the same throughout the spectrum; however, the frequency difference varied when solvents with a larger number of carbon atoms were used. On the other hand, in the spectra of solutions of pyrene and 3,4-benzopyrene, there was no definite connection between the increased mass of the solvent molecule, and the distance between the components of the doublet or the multiplet, but the number of components in each group was found to be different for different solvents and varied from 1 to 5.

The explanation of the nature of the described "multiplets" appeared to be difficult, because the usual causes of splitting (removal of degeneracy, Davydov-splitting, combination of the characteristic frequencies of the emitting molecule and those of the solvent molecule) in this case either did not take place, or were not sufficient to explain the observed details of the phenomena.[13]

It was an important step toward the interpretation of the nature of the "splittings" in question, when the fact was established[2-5] that in all cases of well-resolved spectra, the latter could be represented as a superposition of several line series of varying intensities, displaced relative to each other in an amount equal to the "splitting intervals."

Our recently conducted studies of the spectra of the same hydrocarbons at 20°K yielded a number of important new results. By lowering the temperature almost four times, certain changes in the spectra were produced. For instance, in the case of corynine, new lines appear, and the intensity distribution in the components of the "multiplets" is changed compared with the distribution at 77°K. Furthermore, the new lines produce the same vibrational series that are observed at the temperature of liquid nitrogen, which results in the increase of the corynine series up to five or six. Secondly, it was found that the intervals 86, 72, 38, (42), each of which was considered to be characteristic of the doublets in a given solvent, actually appear in the "multiplets" in all solvents, so that in hexane one can find not only the interval 86, but also 72, and in heptane—not only 72, but also 86, and so forth. Figure 1 illustrates this in the case of one of the "multiplets" of corynine in hexane and in heptane.

Similar results were obtained at 20°K for benzopyrene. Here also a number of series was observed which

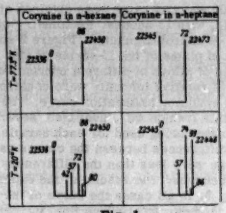

Fig. 1

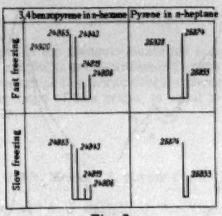

Fig. 2

corresponded to the number of the "multiplet" components. Furthermore, among the intervals between the components there were values that were either close to, or were coinciding with those between the series of corynine in different solvents (for instance, 54, 75, 85, 101). This shows that the number and the relative displacement of series is determined essentially by the properties of solvents, not by the properties of the emitting molecules. On the other hand, it was shown in the case of molecules, the vibrational levels of which were established by other methods (naphtalene,[5,6] anthracene,[1] acenaphtene[3]), that the components of this series themselves undoubtedly belong to the emitting molecules and are electronic-vibrational sequences of the ground state. Moreover, because the positions of very sharp lines in spectrum can be measured with a high precision, and because the frequencies obtained from several series can be compared, it is possible to establish very accurately the vibrational levels of such molecules the study of which by other means is either inconvenient or impossible.

In this connection, the previously established fact must be mentioned, that in the absorption spectra of the same hydrocarbons all lines of the head "multiplet" are in a resonance coincidence with the lines of the "multiplets" O′—O″ in the luminescence spectrum, that is, all vibrational series are resonance series. It should be remembered, however, that because the frequency difference between the extreme components of the "multiplet" is 130-150 cm^{-1}, there can be no equilibrium distribution of energy among the vibrational levels at the temperature of the solution ($kT = 14\ cm^{-1}$ at 20°K). It is obvious that the situation, appearing at first very complex, becomes clear if one assumes that the series forming the "multiplets" belong to different emitting molecules separated in space from each other. Then, the reason for the multiplicity of series and of the variability of the spectra in general may be the local differences of the crystal field in which the emitting molecules are located.

The following experiment lends strong support to the above suggested conception. The fluorescence spectrum of the solutions of benzopyrene and pyrene, frozen by two methods, were photographed: by the usual fast freezing, and by slow freezing. In the latter case, luminescence changed considerably as it was apparent to visual observation: at otherwise similar conditions, the luminescence became weaker, and its color changed somewhat. Figure 2 shows the changes occurring in the spectrum. It is apparent that at slow freezing the short wavelength components of the multiplets disappear, and the extreme long wavelength components are weakened considerably; the remaining central components are weaker, but retain their position. Visual observation of the frozen solutions shows that they differ in their external appearance from the pressed snow which forms at fast freezing. At slow freezing, "frost patterns" appear on the wall of the cell, indicating the formation of larger crystals.

It is of interest to note that the simplifications of the multiplets, quite analogous to that occurring at slow freezing, are observed also at high concentrations of the solutions, as was shown by L. Pesteil and Ciais.[12]

Thus, the fluorescence spectrum of frozen crystallinic solutions, while retaining in general its individual characteristics, is somewhat structure sensitive. Namely, the "multiplet" structure, as it is pointed out in the present communication, is a contribution to the spectrum produced to a large extent, if not entirely, by the microcrystalline structure of the solvent (defects of the lattice, surface effects, etc.). At the same time, the high resolution of the described spectra, obtainable already at the temperature of liquid nitrogen, and the weak interference in molecular crystals give an excellent opportunity of separating the complications produced by the properties of the crystallinic solvent from the spectrum belonging to the molecule in question.

The authors consider it their duty to express their sincere gratitude to the director of the Institute of Physical Problems AN SSSR, academician P. L. Kapitsa for the opportunity to make the study of spectra of complex molecules at extreme low temperatures.

REFERENCES

1. E. V. Shpolskii, A. A. Il'ina, and L. A. Klimova. Doklady Akad. Nauk SSSR, 87, 935 (1952).
2. E. V. Shpolskii and L. A. Klimova. Izvest. Akad. Nauk SSSR, Ser. Fiz. 20, 271 (1956).
3. E. V. Shpolskii, L. A. Klimova, and E. A. Girdzhiiauskaite. Trudy X Vses. soveshch. po spectr. (Transactions of the Tenth All-Union Conference on Spectroscopy), Vol. 1, "Molecularnaia spektroskopiia." (Molecular spectroscopy) p. 20, Lvov, 1956.
4. E. V. Shpolskii and L. A. Klimova. Doklady Akad. Nauk SSSR, 111, 1227 (1956).
5. E. V. Shpolskii and E. A. Girdzhiiauskaite. Opt. i Spektr. 4, 620 (1958).
6. T. N. Bolotnikova. Izvest. Akad. Nauk SSSR, Ser. Fiz. 23, 29 (1959).
7. E. Bowen and B. Brocklehurst. J. Chem. Soc. Nov. 3875 (1954).
8. E. Bowen and B. Brocklehurst. J. Chem. Soc. Dec. 4320 (1955).
9. A. Ciais and L. Pesteil. Compt. rend. 248, 1308 (1959).
10. P. Pesteil and A. Ciais. Compt. rend. 248, 1795 (1959).
11. A. Ciais and P. Pesteil. Compt. rend. 248, 2321 (1959).
12. L. Pesteil and A. Ciais. Compt. rend. 242, 528 (1959).
13. E. V. Shpolskii. "Sbornik posviashchennyi pamiati G. S. Landsberga." (Collection of Papers in Memory of G. S. Landsberg), p. 296, Akademiia Nauk, SSSR, Moscow, 1959.

AUTHOR LIST

VOLUME VII; JULY-DECEMBER

Abdusadykov, T., 158
Adrova, N. A., 16, 79
Aleksanian, V. T., 114
Aleksandrovskaia, A. M., 172, 495
Andreev, N. S., 72
Andreev, V. N., 79
Antinova-Karataeva, I. I., 167
Antonov-Romanowskii, V. V., 245, 327, 484
Anufrieva, E. V., 318
Apanasevich, P. A., 285
Aslanian, V. M., 132
Azen, R. S., 239

Bakhshiev, N. G., 29
Bazhulin, P. A., 123
Belousova, I. M., 7
Bresler, P. I., 371, 375
Biberman, L. M., 346
Bobovich, Ya. S., 163
Bogomolov, A. M., 444
Boitsov, E. N., 307
Bokut, B. V., 344
Bolotnikova, T. N., 24, 138
Borovinskii, L. A., 160, 358
Breido, I. Ya., 52
Brodin, M. S., 48, 82, 168
Broun, Zh. L., 271
Bubnov, N. N., 71
Bulanin, M. O., 119

Chaika, M. P., 460, 462, 481
Cheremisinov, V. P., 293
Cherkasov, A. S., 207, 211
Chizhikova, Z. A., 141, 176
Chulanovskii, V. M., 181, 451

Denisov, G. S., 119
Devyatov, A. M., 480
Dianov-Klokov, W. I., 377
Dolgov, G. G., 1

Egupova, L. M., 239
Erkovich, S. P., 346
Ermolaev, V. L., 399

Favorin, V. N., 420, 422
Fedorov, F. E., 344
Fedorova, L. M., 160
Fedotov, N. S., 389
Feofilov, P. P., 492, 493
Fetisov, E. P., 339
Finkel'shtein, A. I., 307, 393
Fok, M. V., 152
Fradkin, E. E., 460, 462, 481
Frishman, I. G., 354
Fugol, I. Ya., 19

Galkin, L. N., 492
Gasilevich, E. S., 58
Gavrilov, F. F., 185, 242
Gladkova, I. V., 496
Gorlovin, Ya. I., 63, 352
Grekov, A. P., 239, 483
Godnev, I. N., 172, 495
Gorban', A. N., 164, 350, 478
Gotlib, Yu. Ya., 191
Gromova, I. I., 80
Gurevich, D. B., 7
Gurinovich, G. P., 401
Gurvich, L. V., 70

Iakovleva, T. V., 170
International Commission on Molecular Spectroscopy 180
Ivanov, V. N., 476

Jaszczyn, P. B., 414

Kabachnik, M. I., 108
Khalinmonova, I. N., 386
Kaplyanskii, A. A., 406, 409
Kariakin, A. V., 75
Kazanskii, B. A., 114
Kazankin, O. N., 458
Krainov, E. P., 296
Krasnov, K. S., 494
Keirim-Markus, I. B., 250, 334
Khmelinin, B. A., 336
Kesler, Kh., 195
Kibalko, L. A., 71
Kilimov, A. P., 239
Kir'ionova, L. A., 163
Kislovskii, L. D., 201
Kizel', V. A., 35
Klimova, L. A., 499
Kliot-Dashinskii, M. I., 290
Kolesova, V. A., 165
Korsunskii, M. I., 498
Kormer, V. A., 170
Korolev, F. A., 429
Korosyleva, L. A., 89
Koton, M. M., 16, 79
Kovner, M. A., 309, 444
Koslov, B. A., 429
Kozina, G. S., 420
Kristofel', N. N., 45
Kudryavtseva, N. V., 357
Kulikov, S. A., 80
Kund, G. G., 490
Kuzyakov, Yu. Ya., 300

Lebedev, R. S., 104
Levshin, V. L., 149, 330
Liamichev, I. Ya., 258
Lindstrem, I. S., 228
Linnick, V. P., 84
Lisitsa, M. L., 305, 341, 383, 386
Lubchenko, A. F., 48, 215, 221
Lukina, M. Yu., 114

Maiants, L. S., 108
Malinko, V. N., 386
Mal'tsev, Yu. V., 76
Malyshev, G. M., 460
Mandel'shtam, S. L., 91
Markov, M. N., 228
Maslov, P. G., 232
Melankholin, N. M., 314, 396
Mikhailov, B. M., 389
Miloslavskii, V. K., 154
Mirumiants, S. O., 175
Morgenshtern, Z. L., 146
Morozov, V. P., 188
Musalev, N. S., 79

Neporent, B. S., 353
Nikitina, A. N., 389, 441
Novikov, M. M., 70

Odintsov, A. I., 429
Oranovskii, V. E., 336
Orlov, B. M., 330
Orlov, I. N., 258
Osiko, V. V., 454
Ovander, L. A., 383

Panov, Yu. N., 16, 79
Pankratov, N. A., 464
Parfianovich, I. A., 324
Penin, A., 195
Peisakhson, I. V., 451
Pekerman, F. M., 458
Petoshina, L. M., 458
Petrov, A. A., 170, 479
Pivovarov, V. M., 163
Pliavin', I. K., 41
Popov, E. M., 108
Popov, Yu. M., 417
Poskacheyeva, L. P., 422
Preobrazhenskii, N. G., 173
Prikhot'ko, A. F., 19, 82, 168
Prokof'ev, V. K., 7, 363
Pyatnitskii, B. A., 356

Rakov, A. V., 128
Rautian, S. G., 347
Razgovorova, T. V., 318
Razumtseva, G. P., 431
Rebane, V. N., 149
Rezaev, N. I., 72
Riazanov, A. N., 269
Rigina, I. V., 172, 495
Roev, L. M., 447
Rosenblat, M. G., 351
Rovinskii, R. E., 431
Rozenberg, G. V., 263
Rubinov, V. M., 35
Rudnevskii, N. K., 497
Rumyantsev, I. A., 498
Ryskin, Ya. I., 165, 177, 488

Safonova, I. L., 114
Sali', A. O., 162, 278, 355
Sarzhevskii, A. M., 401
Sasovskaia, I. I., 157
Savin, F. A., 435, 439
Scitashev, K. K., 399
Seman, O. E., 68
Semenov, R. I., 462
Sevchenko, A. N., 401
Shapiro, I. P., 78, 469
Shchepkin, D. N., 119, 451
Shimanskaya, N. P., 239
Shishova, L. N., 52
Shklyarevskii, I. N., 349, 496
Shliapintokh, V. Ya., 71
Shpolskii, E. V., 499
Shukhtin, A. M., 491

Shuraleva, E. I., 324
Shvaika, O. P., 483
Silin, V. P., 339
Sinel'nikov, K. D., 496
Skazka, V. S., 474
Skidan, V. B., 460
Skorniakov, G. P., 157
Skorobogatov, B. S., 483, 487
Slavnova, E. N., 396
Slobodskaia, P. V., 58, 63
Smirnov, V. N., 123, 302
Snegirev, B. N., 309
Snigirev, Yu. A., 7
Sobel'man I. I., 435, 439
Sokolov, V. A., 164, 350, 478
Soshnikov, V. N., 346
Soskin, M. S., 168
Speranskaya, N. I., 424
Stanevich, A. V., 162, 380
Stauer, E. V., 351
Stavitskaya, G. P., 488
Stepanov, B. I., 285
Sterin, Kh. E., 114
Striganova, G. A., 89
Strizhevskii, V. L., 305
Sukhorukov, B. I., 393
Sverdlov, L. M., 11, 97, 296, 363, 368

Tarkhov, G. N., 163
Tatevskii, V. M., 195, 300
Tekuchev, A. N., 55
Terenin, A. N., 447
Terpugova, A. F., 357, 359
Tikhomirova, N. N., 486
Tikhonova, L. K., 420
Toporets, A. S., 471
Treshchova, E. G., 195
Tsepalov, V. F., 71
Tsirlin, Yu. A., 52
Tskhai, N. S., 91
Tsvelykh, N. G., 341
Tsvetkov, V. N., 474
Turkin, Yu. I., 5
Vainshtein, L. A., 1
Van-Si-Fu, 339
Vasilevskii, K. P., 353
Vaver, V. N., 389
Vazykova, S. M., 433
Vember, T. M., 321
Vinogradova, L. M., 464
Vinokurov, L. A., 152
Vlasenko, N. A., 320
Voevodskii, V. V., 486
Vol'kenshtein, M. V., 132, 308
Volkova, L. M., 480

Yakhontova, V. E., 290
Yakovleva, T. V., 479
Yaroslavskii, N. G., 380

Zharkov, V. V., 497
Zhidkova, Z. V., 274
Zhiglinskii, A. G., 490

ERRATA IN VOLUME VII

Issue	Page	Line	Printed	Should be
2	92	14 from below LH col.	$(r_{i+2}^{\dagger} + r_i^{\dagger})^{1/2}\Delta_{ni}$	$(r_{i+1}^{\dagger} - r_i^{\dagger})^{1/2}\Delta_{ni}$
	94	Fig. 6	Curves 2 and 4 do not intersect but should closely approach each other.	

CONTENTS OF VOLUME VII

JULY-DECEMBER 1959

No. 1—JULY

L. A. Vainshtein and G. G. Dolgov: Effective Excitation Cross-sections of n^1P-Levels of He by Slow Electrons—1

Yu. I. Turkin: Anomalies in the Intensities of the Components of the Hyperfine Structure of Resonance Lines in Thallium—5

V. K. Prokof'ev, D. B. Gurevich, I. M. Belousova and Yu. A. Snigirev: On the Question of the Build-Up Time for Thermodynamic Equilibrium in the Plasma of an Arc Discharge—7

L. M. Sverdlov: Theory of the Intensities of the Infrared Spectra of Methane, Ethane and Hexadeuteroethane—11

Yu. N. Panov, N. A. Adrova and M. M. Koton: Optical Characteristics of Compounds of the Oxazole, Oxydiazol and Furan Series—16

A. F. Prikhot'ko and I. Ya. Fugol: Luminescence of Stilbene Crystals at 20°K—19

T. N. Bolotnikova: On the Question of the Interpretation of the Fluorescence Spectrum of Naphthalene—24

N. G. Bakhshiev: The Internal Field and the Position of Electronic Absorption and Emission Bands of Polyatomic Organic Molecules in Solution—29

V. A. Kizel' and V. M. Rubinov: The Optical Properties of Concentrated Solutions and Melts. I—35

I. K. Pliavin': On the Kinetics of Photo- and Gamma-Luminescence in Certain Thallium Activated Alkali-Halide Crystals—41

N. N. Kristofel': A Quantum Mechanical Calculation of the Luminescence Center in KCl-Tl—45

M. S. Brodin and A. F. Lubchenko: The Influence of Temperature on Electromagnetic Wave Propagation in Crystals in which Excitons Occur—48

I. Ya. Breido, Yu. A. Tsirlin and L. N. Shishova: Determination of the Luminescent Energy Yield of Plastic Scintillators Under the Action of Gamma Rays—52

A. N. Tekuchev: Absorption and Dispersion of Thin Gold Layers—55

P. V. Slobodskaia and E. S. Gasilevich: Development of a Method of Determining the Relaxation Time of the Vibratory State of Molecules Using a Spectrophone-I—58

Ya. I. Gerlovin and P. V. Slobodskaia: Enhancement of the Sensitivity of the Optic-Acoustic Method of Gas Analysis by Using Cells with the Multiple Passage of Radiation—63

O. E. Seman: On One Characteristic of Image Curvature in Short Focal-length Lenses of Electron Optics—68

L. V. Gurvich and M. M. Novikov: On the Valence Angle of Oxygen in the HoCl Molecule—70

N. N. Bubnov, L. A. Kibalko, V. F. Tsepalov and V. Ya. Shliapintokh: On the Nature of the Intermediate Product in the Photo-reduction of Eosine—71

N. I. Rezaev and N. S. Andreev: Investigation of the Temperature Dependence of the Intensity and Width of Raman Lines—72

A. V. Kariakin: On the Problem of the Chemiluminescence of Lucigenin and its Derivatives—75

Yu. V. Mal'tsev: On the Positions of the Extrema in the Light Scattering Function for Spherical Particles—76

I. P. Shapiro: Luminescence of Alkali Halides Containing Uranyl Salts—78

N. A. Androva, V. N. Andreev, M. M. Koton, Yu. N. Panov and N. S. Musalev: Optical and Scintillation Characteristics of Oxydiazolones—79

I. I. Gromova and S. A. Kulikov: Influence of Current Strength on the Intensity of the Spectrum of Hydrogen in the Region 2500-1200A—80

M. S. Brodin and A. F. Prikhotiko: Influence of the Thickness of Anthracene Crystals on their Absorption Curves at 20°K—82

V. P. Linnik: (The 70th anniversary of his birthday)—84

No. 2—AUGUST

L. A. Korosyleva and G. A. Striganova: Isotopic Shift in the Uranium Spectrum—89

N. S. Tskhai and S. L. Mandel'shtam: Influences on the Intensities of Spectral Lines in Flame Spectra—91

L. M. Sverdlov: Theory of Infrared Spectra Intensities of the Sulfur Dioxide, Ammonia and Phosphine Molecules IV—97

R. S. Lebedev and A. V. Serkachev: On the Question of Force Constants of the Cyclopentane Molecule—104

L. S. Maiants, E. M. Popov and M. I. Kabachnik: Investigation of the Characteristic Vibrations of Phosphorus Compounds II—108

V. T. Aleksanian, Kh. E. Sterin, M. Yu. Lukina, I. L. Safonova and B. A. Kazanskii: Spectroscopic Investigation of the Influence of the Mutual Orientation of Cyclopropane and Phenyl Rings upon their Conjugation—114

M. O. Bulanin, G. S. Denisov and D. N. Shchepkin: On the Study of Hydrogen Bonding Equilibria, Arising in Solutions by Infrared Absorption Spectra. Case of Unseparated Bands—119

V. N. Smirnov and P. A. Bazhulin: Investigation of the Temperature Dependence of the Intensity of Infrared Absorption Bands in Gases—123

A. V. Rakov: The Influence of the Intermolecular Interaction on Line Width in the Raman Spectra of Liquids—128

V. A. Aslanian and M. V. Vol'kenshtein: Optical Activity and Intermolecular Interaction—132

T. N. Bolotnikova: Spectroscopy of Certain Simple Aromatic Hydrocarbons in Frozen Crystalline Solutions—138

Z. A. Chizhikova: Luminescence and the Vavilov-Cherenkov Radiation in Solutions Bombarded by Gamma-Rays—141

Z. L. Morgenshtern: Luminescence of Unactivated CsI Monocrystals—146

V. L. Levshin and V. N. Rebane: Comparative Study of the Storage of Light Sums and the Temperature Quenching of the (ZnS:Ag) Phosphor Excited by the Beta-rays and Light—149

L. A. Vinokurov and M. V. Fok: On the Simultaneous Action of Photo and Electroexcitation on Electroluminophors—152

V. K. Miloslavskii: Infrared Absorption in Thin Films of Tin Dioxide—154

G. P. Skorniakov and I. I. Sasovskaia: On the Role of the Angle of Incidence in Observation of Ultraviolet Minimum of Silver Reflectance—157

T. Abdusadykov: Centers of Luminescence in Alkali-Halide Phosphors with Large Concentrations of the Activator and Microdefects of the Host Lattice—158

L. A. Borovinskii and L. M. Fedorova: A Comparison of the Energy Levels in a Three-dimensional and One-dimensional Metallic Model of the Benzene Molecule—160

A. O. Sall' and S. V. Stanevich: The Use of Selective

Radiation of Gas in Infrared Gas Analysers—162
V. M. Pivovarov, L. A. Kir'ionova, Ya. S. Bobovich and G. N. Tarkhov: Photoelectric Recording of Raman Spectra Excited by the 5875 A Line of a Helium Lamp —163
A. N. Gorban' and V. A. Sokolov: On the Question of Physico-Chemical Nature of Candoluminescence—164
V. A. Kolesova and Ya. I. Ryskin: Infrared Absorption Spectrum of Hydrargillite $Al(OH)_3$—165
I. I. Antinova-Karataeva: Investigation and Interpretation of Bands in the Absorption Spectra of Crystals Coloured by Chromium Ions—167
M. S. Brodin, A. F. Prikhot'ko and M. S. Soskin: On Certain Pecularities of the Dispersion of Strongly Absorbing Crystals—168
A. A. Petrov, T. V. Iakovleva and V. A. Kormer: Infrared Spectra of Some Disubstituted Allenic Hydrocarbons—170
I. N. Godnev, A. M. Aleksandrovskaia and I. V. Rigina: Normal Vibration Frequencies of Zirconium Halides —172
N. G. Preobrazhenskii: The Functional Description of Spectrum Line Profiles in Cowan-Dieke and Bartels Theories—173
S. O. Mirumiants: On the Question of the Effect of Light Gases on the Absorption of Vapors of Aromatic Compounds—175
Z. A. Chizhikova: Lummescent Energy Yield for Gamma-Scintillations in a Stilbene Crystal—176
Ya. I. Ryskin: On the Mechanism of Formation of a Strong Hydrogen Bond—177
Resolutions of the International Commission on Molecular Spectroscopy—179
The XIIIth Rozhdestvenskii Lecture—180
V. M. Chulanovskii (on his 70th birthday)—181

No. 3—SEPTEMBER

F. F. Gavrilov: Spectral Method of the Isotopic Analysis of Lithium—185
V. P. Morozov: Partial Frequencies (Modes) of Triatomic Hydrides and Deuterides of C_{2v} Symmetry—188
Yu. Ya. Gotlib: Theory of Vibrational Spectra of Polymers I—191
Kh. Kesler, Yu. A. Penin, E. G. Treshchova and V. M. Tatevskii: Investigation of Infrared Absorption Spectra of Hydrocarbons at Various Temperatures in the Liquid and Solid Phase—195
L. D. Kislovskii: Optical Characteristics of Water and Ice in the Infrared and Radiowave Region of the Spectrum —201
A. S. Cherkasov and T. M. Vember: On the Influence of p-Toluidine upon the Quantum Yields of Photo-oxidation and Photo-dimerization of Some Anthracene Derivatives—207
A. S. Cherkasov: Absorption and Fluorescence Spectra and the Fluorescence Quantum Yield of Certain Methyl and Methylmesoaryl Anthracenes—211
A. F. Lubchenko: Theory of the Faraday Effect in the Region of Exciton Absorption of Light by Molecular Crystals—215
A. F. Lubchenko: Theory of the Linear Kerr Effect in the Region of Exciton Light Absorption by Molecular Crystals—221
M. N. Markov and I. S. Lindstrem: Optical Properties of Sublimed Bismuth in the 3-15 Microns Region Spectral Range—228
P. G. Maslov: On the Use of the Additive-Statistical Method to the Study of Adsorption and Fluorescence Spectra—232
N. P. Shimanskaia, A. P. Kilimov, A. P. Grekov, L. M. Egupova and R. S. Azen: Plastic Scintillators with Admixtures of 1, 3, 4-Oxadiazol Arylderivatives—239
F. F. Gavrilov: Luminescence of Lithium Hydride—242
V. V. Antonov-Romanovskii: Initial Stages of Decay of Phosphors with Levels of Several Kinds—245
I. B. Keirim-Markus: Investigation of Light Sums in a SrS-Eu, Sm. Phosphor I—250
I. Ya. Lyamichev and I. N. Orlov: Influence of the Electrical Prehistory of an Electroluminophor on its Luminescence Characteristics Under Excitation by Short Voltage Pulses—258
G. V. Rozenberg: Luminous State in the Interior of a Medium with Rayleigh Scattering—263
A. N. Ryazanov: On the Possibility of Resolving Two Light Sources of Sharply Differing Intensities—269
Zh. L. Broun: On the Use of a Light-Measuring Sphere in the Differential Spectrophotometric Method—271
Z. V. Zhidkova: On the Influence of the Thickness of the Adsorbed Layer on the Diffuse Reflection Spectrum from Adsorbates—274
A. O. Sall: On the Threshold Sensitivity of an Optico-Acoustic Radiation Detector. III—278

No. 4—OCTOBER

B. I. Stepanov and P. A. Apanasevich: The Classification of Secondary Radiation—285
V. E. Yakhontova and M. I. Kliot-Dashinskii: The Pressure Dependence of the Intensity of Certain Helium Lines—290
V. P. Cheremisinov: Vibrational Spectrum and Structure of the Arsenic Trioxide Molecule—293
L. M. Sverdlov and E. P. Krainov: Calculation and Interpretation of Vibrational Spectra of Naphthenes. II. Methylcyclopropane and 1,1-Dimethylcyclopropane —296
Yu. Ya. Kuzyakov and V. M. Tatevskii: Rotational Structure of the (1-1) and (0-1) Bands in the Spectrum of the Carbon Monochloride Molecule—300
V. N. Smirnov: Study of the Temperature Dependence of the Intensity of Infrared Absorption Bands in Solutions—302
M. P. Lisitsa and V. L. Strizhevskii: On the Temperature Dependence of the Intensities of Vibrational Absorption Bands of Gases in the Case of Fermi Resonance —305
E. N. Boitsov and A. I. Finkel'shtein: Optical Investigation of the Molecular Structure of s-Triazine Derivatives.—307
M. A. Kovner and B. N. Snegirev: Intensities and Depolarization in Raman Spectra of Polymethylbenzenes. I. The General Theory. Toluene—309
N. M. Melankholin: Absorption Spectra of Crystals of Some Thiazine and Oxazine Dyes—314
E. V. Anufrieva, M. V. Vol'kenshtein and T. V. Razgovorova: Vitrification of Polymers and Luminescence—318
N. A. Vlasenko: A Study of the Intrinsic Absorption Spectrum of Zinc Sulfide—320
I. A. Parfianovich and E. I. Shuraleva: The Influence of an Activator on the Stability of F-Centers—324
V. V. Antonov-Romanovskii: Initial Stages of Luminescence Build-up in Phosphors with Levels of Several Kinds—327
V. L. Levshin and B. M. Orlov: Investigation of the Thermal Activation Energy of Photostimulated Flashes in ZnS:Cu:Pb Phosphors—330
I. B. Keirim-Markus: Study of Ligh Sums in the SrS Eu:Sm Phosphor. II—334
V. E. Oranovskii and B. A. Khmelinin: Study of the Electroluminescence of ZnS:Cu Single Crystals—336
Van-Si-Fu, V. P. Silin and E. P. Fetisov: Optical Proper-

ties of Metal Films in the Region of Anomalous Skin-Effect—339
M. P. Lisitsa and N. G. Tsvelykh: Thin Layer Optics V. Properties of Silicon—341
B. V. Bokut' and F. E. Fedorov: The Propagation of Light in Absorbing Magnetic Optically Active Isotropic Media and Cubic Crystals—344
L. M. Biberman, S. P. Erkovich and V. N. Soshnikov: The Transition Probability in the Schumann-Runge Band System of the O_2 Molecule—346
S. G. Rautian: On Echelette Theory—347
I. N. Shklyarevskii, E. T. Verkhovtseva and G. N. Polyakova: The Vernier Effect in the Interferometric Measurement of the Thickness of Thick Layers—349
A. N. Gorban' and V. A. Sokolov: Candoluminescence and Surface-Recombination Luminescence of Phosphors in an Activated Gas Atmosphere—350
E. V. Stauer and M. G. Rosenblat: Influence of Crushing on the Optical and Electrical Properties of Some ZnS Electroluminors—351
Ya. I. Gerlovin: An Optico-Acoustic Phenomenum in the Ultraviolet Region of the Spectrum—352
K. P. Vasilevskii and B. S. Neporent: Effect of Foreign Gases on the Absorption of Infrared Radiation by Water Vapors in the Region of an Individual Line in the Band 2.7μ—353
I. G. Frishman: Registration of Spectra of the Aurora Borealis by Means of a Photoelectric Spectrometer —354
A. O. Sall': Selective Modulation of Radiation by Periodic Variation of Gas Temperature—355
B. A. Pyatnitskii: On the Article by M. G. Kaminskii 'Contribution to the "Ballistic" Method of Investigation of the Decay of Phosphorescence'—356
N. V. Kudryavtseva and A. F. Terpugova: On the Article by L. A. Borovinskii—357
L. A. Borovinskii: Reply to N. V. Kudryavtseva and A. F. Terpugova—358

No. 5—NOVEMBER

A. F. Terpugova: Calculation of Some Parameters of Monosubstituted Benzene Molecules by the "Metal" Model Method—359
L. M. Sverdlov and N. I. Prokof'eva: Calculation and Interpretation of Vibrational Spectra of Naphthenes. III —363
L. M. Sverdlov: Theory of Intensities in the Infrared Spectra of Molecules CF_4 and C_2F_6—368
P. I. Bresler: Laws of the Absorption of Infrared Radiation in Thin Layers of Some Gases. I—371
P. I. Bresler: Laws of the Absorption of Infrared Radiation in Thin Layers of Some Gases. II—375
V. I. Dianov-Klokov: Absorption Spectrum of Liquid and Solid Oxygen Under Pressure (12,600-3000 Å)—377
N. G. Yaroslavskii and A. E. Stanevich: The Long-Wavelength Infrared Spectrum of H_2O Vapor and the Absorption of Atmosphere Air in the Region 20-2500 μ (500-4 cm^{-1})—380
M. P. Lisitsa and L. A. Ovander: Influence of Solvent on the Intensities of Resonating Intramolecular Vibrations of Carbon Tetrachloride—383
M. P. Lisitsa, V. N. Malinko and I. N. Khalinmonova: Influence of Temperature and of the State of Aggregation of the Intensity of Vibrational Absorption Bands of Carbon Tetrabromide—386
A. N. Nikitina, V. A. Vaver, N. S. Fedotov and B. M. Mikhailov: Spectra of Organo-Boron Compounds of the Aromatic Series—389
B. I. Sukhorukov and A. I. Finkel'shtein: Optical Investigation of the Molecular Structure of Cyanamide and its Derivatives. II—393
N. M. Melankholin and E. N. Slavnova: On Some Peculiarities of Absorption Spectra of Crystals and Solutions of Thionine Violet—396
V. L. Ermolaev and K. K Svitashev: Quantum Yields of Phosphorescence and Fluorescence of Some 1-Derivatives of Naphthalene in Solutions at –196°C —399
G. P. Gurinovich, A. M. Sarzhevskii and A. N. Sevchenko: On the Limiting Polarization of Luminescence of Complete Molecules—401
A. A. Kaplyanskii: Effect of Elastic Deformation by Uniaxial Compression and Elongation of Crystals on the Spectra of Local Anisotropic Centers in a Cubic Lattice I—406
A. A. Kaplyanskii: Effect of the Elastic Deformation by Uniaxial Compression and Elongation of Crystals on the Spectra of Local Anisotropic Centers in a Cubic Lattice II—409
P. B. Jaszczyn: On the Influence of Infrared Light on Luminescence of ZnS-Mn Phosphors—414
Yu. M. Popov: Influence of Fast Electrons on the Light-sum Stored in Cathodoluminescence—417
V. N. Favorin, G. S. Kozina and L. K. Tikhonova: Spectral Characteristics of Electroluminescence of Some Electroluminophors in the Case of the Simultaneous Action of Constant and Alternating Fields —420
V. N. Favorin and L. P. Poskacheyeva: Voltage Dependence of the Spectral Composition of the Radiation from Certain Electroluminophors in an Alternating Field—422
N. I. Speranskaya: Determination of Spectrum Color Coordinates for 27 Normal Observers—424

No. 6—DECEMBER

F. A. Korolev, B. A. Kozlov and A. I. Odintsov: Study of the Contour of the Cadmium Red Line Using an Atomic Beam—429
R. E. Rovinskii and G. P. Razumtseva: The Transparency of a Discharge in Xenon at Very High Pressures—431
S. M. Vazykova: Eigenvalues of Pi-Electrons in a Potential Box with an Even Number of n Barriers—433
F. A. Savin and I. I. Sobel'man: Intensities in Raman Spectra and the Metallic Model of the Molecule. I. Polyene Compounds—435
F. A. Savin and I. I. Sobel'man: Intensities in Raman Spectra and the Metallic Model of the Molecule. II Aromatic Compounds—439
E. E. Nikitin: Band Shape in the Induced Rotational and Vibrational Spectra of Dipoleless Molecules—441
M. A. Kovner and A. M. Bogomolov:Vibrational Spectra of Aromatic Compounds. VI. Calculation and Interpretation of Vibrational Spectra of o-Xylene—444
L. M. Roev and A. N. Terenin: Infrared Spectra of Nitric Oxide Adsorbed on Transition Metals, their Salts and Oxides—447
V. M. Chulanovskii, I. V. Peisakhson and D. N. Shchepkin: Determination of the Absolute Value of Parameters Characterizing Intensity in the Infrared Absorption Spectrum in the Cases of the Absence of Time Distortions I —451
V. V. Osiko: The Low-Temperature Luminescence of Zinc Oxide in the Red Region of the Spectrum—454
O. N. Kazankin, F. M. Pekerman and L. M. Petoshina: Electroluminescence of ZnS-Cu-Mn Phosphors in a Constant Field—458

G. M. Malyshev, V. B. Skidan, E. E. Fradkin and M. P. Chaika: Resolution of a Monochromator with Photoelectric Recording—460
R. I. Semenov, E. E. Fradkin and M. P. Chaika: Apparatus Function of a Fabry-Perot Spectrometer with a Rectangular Opening—462
N. A. Pankratov and L. M. Vinogradova: On the Maximum Possible Response of a Selective Optico-Acoustic Receiver—464
I. P. Shapiro: Determination of Absorption Spectra of Crystalline Phosphors by Means of Diffuse Reflection Spectra—469
A. S. Toporets: Study of Diffuse Reflection from Powders Under Illumination Powders—471
V. N. Tsvetkov and V. S. Shazka: A Visual Nephelometer —474
V. N. Ivanov: Influence of Temperature on the Absorption Spectrum of Nitric Oxide—476
A. N. Gorban and V. A. Sokolov: The Semiconductor Mechanism of Surface-Recombination Luminescence—478
A. A. Petrov and T. V. Yakovleva: On the Hydrogen Bond in Acetylenic Amines—479
L. M. Volkova and A. M. Devyatov: Effective Excitation Cross-Sections of Certain Spectral Lines of Argon—480
M. P. Chaika and E. E. Fradkin: Method of Transformation of Spectral Line Contours and its Application for Measuring the Temperature and other Parameters of a Light Source—481
B. S. Skorobogatov: On Diffraction at the Exit of Optical Waveguide—482
O. P. Shvaika and A. P. Grekov: The Relation between the Chemical Structure and Scintillation Efficiency of 1, 3, 4-Oxadiazole Derivatives—483
V. V. Antonov-Romanovskii: The Superlinear Increase of Phosphor Conductivity at the Initial Stages of Excitation—484
N. N. Tikhomirova and V. V. Voevodskii: A Method of Analysis of the Line Shape in Electron Paramagnetic Resonance—486
B. S. Skorobogatov: Field Distribution in Optical Waveguides—487
Ya. I. Ryskin and G. P. Stavitskaya: The Deformation Vibrations Delta (OH) for Strong Hydrogen Bonds—488
A. G. Zhiglinskii and G. G. Kund: On the Spectral Determination of the Isotopic Composition of Strontium —490
A. M. Shukhtin: The Interferometric Determination of the Gas Density and Electron Concentration in a Discharge—491
L. N. Galkin and P. P. Feofilov: Luminescence Spectra of Trivalent Uranium Ions—492
P. P. Feofilov: Orientation of Luminescence Centers in Uranium Activated Lithium Fluoride Crystals—493
K. S. Krasnov: On the Vibration Frequency of the Thallium Iodide Molecule—494
A. M. Aleksandrovskaya, I. V. Rigina and I. N. Godnev: Frequencies of the Normal Vibrations of the Lead Halogenides—495
K. D. Sinel'nikov, I. N. Shkliarevskii and I. V Gladkova: On the Colors of Wrinkled Transparent Films on Metal Surfaces—496
V. V. Zharkov and N. K. Rudnevskii: Intramolecular Hydrogen Bond in Isopropyl Benzene Hydroperoxide —497
I. A. Rumyantsev and M. I. Korsunskii: Study of L-Spectra of Zn in Alloys of the Cu-Zn System—498
E. V. Shpolskii and L. A. Klimova: On the Origin of the Hyperfine Structure in the Luminescence Spectra of Aromatic Hydrocarbons at Low Temperatures—499
Author Index—Vol. VII—501
Contents by Issue/Title, Vol. VII—503

TRANSLATION SERVICES OF THE NATIONAL RESEARCH COUNCIL OF CANADA

The National Research Council, through its Library's Translation Section, undertakes to provide the Council's scientific staff with translations of worthwhile foreign papers pertaining to their various fields of research. The present translation staff is able to deal with papers written in Russian, German, French, Italian, Spanish, Dutch, Swedish, and Norwegian. Papers written in such languages as Japanese, Chinese, and Finnish are also translated, but the work is farmed out to freelance translators.

When a N.R.C. scientist requests a translation, the first step is to determine whether or not a translation is already available. The chief tool for this search is the Canadian Index of Scientific Translations. If the search provides a negative answer, the papers is then assigned to the appropriate translator. While the translation is being prepared, the translator, when necessary, consults with the scientist who requested the translation and obtains advice regarding the interpretation of difficult or obscure concepts. A rough draft of the translation is prepared, and then submitted to a subject specialist (again usually the scientist who requested the translation) for criticisms and suggestions -- an arrangement which ensures technical accuracy. Further editing, from the point of view of readability, then takes place and the translation is ready for the final typing.

All N.R.C. translations are complete in that they include graphs, charts, illustrations, and bibliographies contained in the original paper. The charts and other illustrations are reproduced photographically, and translations of captions and headings superimposed upon the photograph. N.R.C. translations are published in the Council's Technical Translation series and are made available to the scientific community at large. One hundred copies of each translation are prepared and free copies sent to a prearranged list of Canadian scientists, to libraries of universities, and on a translation exchange basis to certain other organizations. With these exceptions, a small charge of 50¢ for each ten pages is normally made for each translation.

A list of the translations prepared by the Translations Section is available from the N.R.C. Library. The latest edition, published in May 1959, records 800 translations. A supplement to the list is published with the completion of each 100 additional translations, and this together with a cumulative author index is sent to holders of the original list. N.R.C. translations, as well as other Canadian translations, are also reported to the Commonwealth Index of Scientific Translations maintained by Aslib in London, and to the Office of Technical Services in Washington.

The Canadian Index of Scientific translations, mentioned above, records on 3" x 5" cards, and under authors, translations reported to the Library by the English-speaking countries of the world. The entries (50,000 at last count) comprise translations prepared in Canada, those reported by Aslib in London, and by O.T.S. in Washington.

Librarians are urged to check with the Index, either in person, or by phone or mail, regarding the existence and location of a needed translation. If the translation is recorded, information can always be provided as to its availability and, in many cases, a copy can be supplied from the Library's extensive file of translations.

AMERICAN METEOROLOGICAL SOCIETY TRANSLATION SERVICE

Background - The translation unit of the American Meteorological Society was established in 1952, the project being realized through a request by Air Force Cambridge Research Center that the American Meteorological Society undertake a translation program under its sponsorship. The translation unit has been in continuous operation under Air Force Cambridge Research Center sponsorship since then.

Scope - The material translated represents meteorology in its broadest sense, i.e., the study of atmospheric phenomena, their interaction with other media, such as the hydrosphere and the lithosphere, and the effect of external agents on the atmosphere (solar and cosmic forces). Thus, in addition to articles on synoptic and dynamic meteorology, climatology, atmospheric electricity, numerical forecasting, cloud physics and cloud chemistry, weather radar and unusual weather phenomena, the subject matter of the translations includes astrophysics, solar phenomena, meteoritics, colloidal studies, electronics (instrumentation), ice physics and ice drift, optics, photographic technique (cloud and underwater photography), oceanography, seismology, terrestrial magnetism, wave propagation, radio-activity, spectral analysis and others.

Complete translations, with graphs, tables, equations and bibliography constitute the main body of the American Meteorological Society translations, although recently another service has been introduced. The tables of contents of several Russian journals are now translated regularly as are many of the tables of contents of recent monographs and single copies of rare journals. In addition, a cumulative list of translations is issued annually. As Russian material became more accessible and references to it were more numerous (beginning about 1954), requests for translation of Russian articles increased. At present, 1959, about 65% of the requests are for Russian. Thus far, the translation unit of the American Meteorological Society has made more than 600 translations, of which 350 are from Russian, 185 from German and 35 from French.

Expansion - In 1959, the American Meteorological Society extended its translation activities. Under a grant from the National Science Foundation, it undertook the translation of selected Russian meteorological material. The first choice was the Transactions of the Main Geophysical Observatory (Trudy Glavnoi Geofizicheskoi Observatorii). The tables of contents of the most recent issues were translated by the American Meteorological Society translation unit and sent to officers of the Society, universities involved in meteorological research, and to meteorological research groups of the armed forces and industry. They were asked to indicate their preferences among the issues listed. This method of selection indicated a clear choice of two issues and translation of this material is in progress. The translations will be edited by specialists in each field and released for public distribution. It is hoped that this program will serve as a model for future selective translation programs.

RUSSIAN TRANSLATION PROGRAM AT THE MASSACHUSETTS INSTITUTE OF TECHNOLOGY

M.I.T. is the one University in a field of professional societies sponsoring the translation of journals from the Russian. In 1956 Dr. Paul E. Green, Jr., of Lincoln Laboratory, was impressed by the extent and quality of the published Russian work in electronics and by the few Americans who had any knowledge of it. He approached Professor W. N. Locke, Director of Libraries at M.I.T., with the proposal that a Committee be formed to apply for a grant from the National Science Foundation under which to translate two Russian journals, Radiotekhnika i Elektronika and Radiotekhnika. Professor Jerome B. Wiesner, Director of M.I.T.'s Research Laboratory of Electronics, and Professor Robert M. Fano, of the Department of Electrical Engineering, accepted to serve on a Committee with Professor Locke. A proposal was made to the National Science Foundation to translate these two and a third journal, Elektrosvyaz (Telecommunications), and, in August 1957, the National Science Foundation made a grant to M.I.T. for the translation of the 1957 issues of these three Russian journals, and a contract was let to the Pergamon Institute. The 1958 and 1959 issues of the three journals have been translated under the same arrangements. As of this writing 1959 issues are not yet finished. The 1960 issues will also be produced by the Pergamon Institute.

Another initiative of M.I.T. was to join the Instrument Society of America for the production in translation of Avtomatika I Telemekhanika (Automation and Remote Control), and, with the aid of the unexpended balance of the first-year National Science Foundation grant to M.I.T., the 1957 issues of this fourth journal were published.

Two major headaches have plagued M.I.T.'s Translation Program. The first is the time lag. The average delay in the appearance of the English editions of the 1957 Russian originals was seventeen months; for 1958 this was reduced to twelve months and for 1959 to somewhat less.

The second weakness has been quality control of translation, and an Editorial Advisory Committee of professors and research men in electronics at M.I.T. and Lincoln Laboratory now regularly read the articles in their fields.

The hope of the M.I.T. Committee and of the National Science Foundation is that a reduced time lag and improved quality may increase the number of subscriptions to the point where these three journals will be self-supporting.

Each of the three Russian journals sponsored in English editions by M.I.T. is devoted to electronics and electrical communications. The magazine Radiotekhnika i Elektronika is a publication of the Academy of Sciences of the USSR and tends to be devoted to more theoretical work. Radiotekhnika is the organ of the A. S. Popov Technical Society of Radio Engineering and Telecommunications, a professional society for electronics engineers. It covers much the same fields except that the treatment is not so theoretical as in the first journal. Electrosvyas is published by the USSR Ministry of Communications, and, unlike the other two journals, it is heavily oriented towards communication problems, including wire as well as radio communications.

AMERICAN ROCKET SOCIETY TRANSLATION PROGRAM

The American Rocket Society will, in the year ending in July, 1960 have published some 200 pages of Russian translations in the fields of rocketry and astronautics in one of its two monthly publications, the ARS Journal. The translation and publication program was undertaken under a $30,200 grant-in-aid made to the Society by the National Science Foundation, and is headed by J. George Adashko of the American Institute of Physics.

The Russian translations are published quarterly in the form of a special supplement bound in with the regular monthly issue of the Journal, the first supplement having appeared last October. Copies of the Journal are distributed free of charge to all 15,000 members of the Society, as well as to some 5,000 additional subscribers, with NSF underwriting the complete costs of translation and publication.

The ARS Russian translation program is a selective one, since at the present time there is no single Russian technical journal, or even a group of journals, specifically devoted to rocketry and astronautics. Consequently, selection of material for translation and publication is carried out through a process which involves the scanning of a large number of journals which frequently carry articles in these fields; sending abstracts of articles which appear to be of interest and facsimile copies of the articles themselves to reviewers; judging, on the basis of these reviews, whether the articles are worth translating and, if so, translating them and once again sending them out for final review and comment, prior to actual publication.

The program has attracted a good deal of favorable comment from ARS members, and it is hoped that it will be expanded in Fiscal 1961.

The Superlinear Increase of Phosphor Conductivity in the Initial Stages of Excitation . . . . . V. V. Antonov-Romanovskii 484
A Method of Analysis of the Line Shape in Electron Paramagnetic Resonance . . . . . N. N. Tikhomirova and V. V. Voevodskii 486
Field Distribution in Optical Waveguides . . . . . B. S. Skorobogatov 487
The Deformation Vibrations δ(OH) for Strong Hydrogen Bonds . . . . . Ya. I. Ryskin and G. P. Stavitskaya 488
On the Spectral Determination of the Isotopic Composition of Strontium . . . . . A. G. Zhiglinskii and G. G. Kund 490
The Interferometric Determination of Gas Density and Electron Concentration in a Discharge . . . . . A. M. Shukhtin 491
Luminescence Spectra of Trivalent Uranium Ions . . . . . L. N. Galkin and P. P. Feofilov 492
Orientation of Luminescence Centers in Uranium Activated Lithium Fluoride Crystals . . . . . P. P. Feofilov 493
On the Vibration Frequency of the Thallium Iodide Molecule . . . . . K. S. Krasnov 494
Frequencies of the Normal Vibrations of the Lead Halogenides . . . . . A. M. Aleksandrovskaya, I. V. Rigina, and I. N. Godnev 495
On the Colors of Wrinkled Transparent Films on Metal Surfaces . . . . . K. D. Sinel'nikov, I. N. Shkliarevsky, and I. V. Gladkova 496
Intramolecular Hydrogen Bond in Isopropyl Benzene Hydroperoxide . . . . . V. V. Zharkov and N. K. Rudnevskii 497
Investigation of the *L*-Spectra of Zn in Alloys of the Cu-Zn System . . . . . I. A. Rumyantsev and M. I. Korsunskii 498
On the Origin of the Hyperfine Structure in the Luminescence Spectra of Aromatic Hydrocarbons at Low Temperatures . . . . . E. V. Shpolskii and L. A. Klimova 499

EDITOR'S NOTE

Comments on the scientific content of the translated Russian articles published in OPTICS AND SPECTROSCOPY are invited. They should be addressed as a Letter to the Editor of the Journal of the Optical Society of America and forwarded to the Editor of that journal, Dr. W. R. Brode, National Bureau of Standards, Washington 25, D.C.

VOL. VII, NO. 6 OPTICS AND SPECTROSCOPY DECEMBER 1959

CONTENTS

Study of the Contour of the Cadmium Red Line Using an Atomic Beam . . . F. A. Korolev, B. A. Kozlov, and A. I. Odintsov 429
The Transparency of a Discharge in Xenon at Very High Pressures . . . R. E. Rovinskii and G. P. Razumtseva 431
Eigenvalues of π-Electrons in a Potential Box with an Even Number of n-Barriers . . . S. M. Vazykova 433
Intensities in Raman Spectra and the Metallic Model of the Molecule. I. Polyene Compounds . . . F. A. Savin and I. I. Sobel'man 435
Intensities in Raman Spectra and the Metallic Model of the Molecule. II. Aromatic Compounds . . . F. A. Savin and I. I. Sobel'man 439
Band Shape in the Induced Rotational and Vibrational Spectra of Dipoleless Molecules . . . E. E. Nikitin 441
Vibrational Spectra of Aromatic Compounds. VI. Calculation and Interpretation of the Vibrational Spectra of *o*-Xylene . . . M. A. Kovner and A. M. Bogomolov 444
Infrared Spectra of Nitric Oxide Adsorbed on Transition Metals, Their Salts and Oxides . . . L. M. Roev and A. N. Terenin 447
Determination of the Absolute Value of Parameters Characterizing Intensity in the Infrared Absorption Spectrum in the Cases of the Absence of Time Distortions. I . . V. M. Chulanovsky, L. V. Peisakhson, and D. N. Shchepkin 451
The Low Temperature Luminescence of Zinc Oxide in the Red Region of the Spectrum . . . V. V. Osiko 454
Electroluminescence of ZnS-Cu-Mn Phosphors in a Constant Field . . . O. N. Kazankin, F. M. Pekerman, and L. M. Petoshina 458
Resolution of a Monochromator with Photoelectric Recording . . . G. M. Malyshev, V. B. Skidan, E. E. Fradkin, and M. P. Chaika 460
Apparatus Function of a Fabry-Perot Spectrometer with a Rectangular Aperture . . . R. I. Semenov, E. E. Fradkin, and M. P. Chaika 462
On the Maximum Possible Response of a Selective Optice-Acoustic Receiver . . . N. A. Pankratov and L. M. Vinogradova 464
Determination of Absorption Spectra of Crystalline Phosphors by Means of Diffuse Reflection Spectra . . . I. P. Shapiro 469
Study of Diffuse Reflection from Powders under Diffuse Illumination . . . A. S. Toporets 471
A Visual Nephelometer . . . V. N. Tsvetkov and V. S. Skazka 474

SHORT COMMUNICATIONS

Influence of Temperature on the Absorption Spectrum of Nitric Oxide . . . V. N. Ivanov 476
The Semiconductor Mechanism of Surface-Recombination Luminescence . . . A. N. Gorban and V. A. Sokolov 478
On the Hydrogen Bond in Acetylenic Amines . . . A. A. Petrov and T. V. Yakovleva 479
Effective Excitation Cross Sections of Certain Spectral Lines of Argon . . . L. M. Volkova and A. M. Devyatov 480
Method of Transformation of Spectral Line Contours and its Application for Measuring the Temperature and Other Parameters of a Light Source . . . M. P. Chaika and E. E. Fradkin 481
On Diffraction at the Exit of Optical Waveguide . . . B. S. Skorobogatov 482
The Relation between the Chemical Structure and Scintillation Efficiency of 1, 3, 4-Oxadiazole Derivatives . . . O. P. Shvaika and A. P. Grekov 483

(Contents continued on inside back cover)